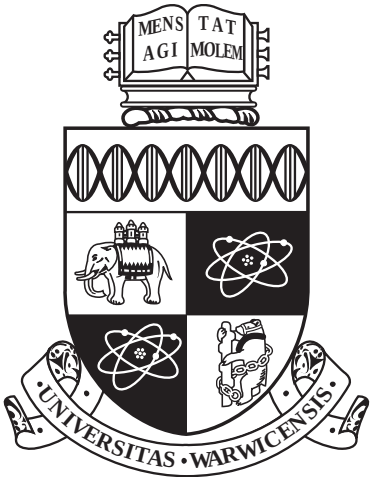

Large Deviations and Metastability in Condensing Stochastic Particle Systems

by

Paul Ian Chleboun

Thesis

Submitted to the University of Warwick

for the degree of

Doctor of Philosophy

Centre for Complexity Science and Mathematics Institute

October 2011

THE UNIVERSITY OF
WARWICK

Contents

Acknowledgements

I would like to express my warmest gratitude to my supervisor, Stefan Grosskinsky, for his continued guidance and support. It seems his door was always open, and he always found time for very useful discussions. He has always been happy to share his knowledge and insight, with enthusiasm and patience.

I would also like to thank all the other members of the DTC for making my time in the department so pleasurable. In particular my second supervisor Ellak Somfai. Also Robin Ball, for ensuring that the DTC was such a success and still finding time for very insightful discussions. I am very grateful for the many happy discussions I have had with colleagues in the department on this work, as well as many other things. Moreover I would like to thank Anthony Woolcock, Peter Jones and Steven Hill for their careful reading of this thesis.

Additional thanks go to the many people outside of the department with whom I have had the great pleasure of discussing my work, and who responded with helpful suggestions. I am very grateful to Michalis Loulakis and Inés Armendáriz for pointing out the particular local limit theorem for triangular arrays used in Chapter 3. Also thanks to Gunter Schütz, Hugo Touchette and Rosemary Harris for their support and advice.

Finally, I would like to thank my family for their constant support. I am especially grateful to Sarah Lloyd for her continuing support and affection, and for looking after me so generously in the last month or so of writing-up.

This work was supported by the Engineering and Physical Sciences Research Council as part of the University of Warwick Complexity Science Doctoral Training Centre.

Declarations

This work has been composed by myself and has not been submitted for any other degree or professional qualification.

- The work of Chapter 4 has largely been published in [25].
- Work from Chapter 3 and 6 will be submitted for publication.
- Chapter 5 extends results of Grosskinsky and Schütz [66], and significantly simplifies the analysis giving rise to the equivalence of ensembles. The analysis also extends the stationary results to give full large deviation properties of the maximum. This gives original insight into the dynamics of the condensate. This work is in preparation for publication.

Abstract

Condensation, or jamming transitions, are observed throughout the natural and social sciences as prevalent emergent phenomena in complex systems, from shaken granular gases to traffic congestion. The understanding of the critical behaviour in these systems is currently a major research topic, in particular a mathematically rigorous treatment of the associated metastable dynamics. In this thesis we study these phenomena in the context of interacting particle systems. In particular we focus on two generic models for condensation, the zero-range process, and the recently introduced inclusion process.

We firstly give a brief review of some relevant aspects of Markov processes, with a particular emphasis on interacting particle systems and a heuristic description of metastability. Subsequently, we present a general framework for studying the equivalence of ensembles, and the large deviations of the maximum site occupation, in interacting particle systems that exhibit product stationary measures. These original results are based on relative entropy methods and techniques from the theory of large deviations. They form the theoretical basis of this thesis, which enables us to find the relevant scales on which metastability is observed, and to derive refined results on the equivalence of ensembles.

The general approach is to first derive a large deviation principle for the density and maximum site occupation under a reference measure. This gives rise to the large deviations of the maximum in the thermodynamic limit, or a more refined scaling limit, which describe the metastable behaviour. Also it gives rise to equivalence of ensembles results, which are used to find the limiting expectation of important observables (such as the stationary current).

In the second part of the thesis we use these general results to give a detailed analysis of three cases. We derive the leading order finite size effects for a generic family of condensing zero-range process. At this scale we observe, and are able to characterise, metastable switching between fluid and condensed states. Secondly, we study a zero-range process with size-dependent rates, for which metastable effects are stabilised in the thermodynamic limit. Here we are able to describe two distinct mechanisms of condensate motion. Finally, we study condensation of a different origin in the inclusion process. In this case our general results can no longer be applied directly, since some of the regularity assumptions do not hold, however the guiding principles still apply. Following these we make formal calculations that give rise to the relevant stationary properties. We give a heuristic analysis of the dynamics which turn out to be very different from those in the zero-range process. Throughout the thesis theoretical results are supported by Monte Carlo simulations and numerical calculations where appropriate.

Our results contribute to a detailed understanding of the nature of finite size effects and metastable dynamics close to condensation and jamming transitions. This is vital in applications in complex systems such as granular media and traffic flow, which exhibit moderate system sizes and cannot be fully described by the usual thermodynamic limit.

Notation

(a_L)	Thermodynamic scale. Scale of the large deviation principle (p. 31)
(b_L)	Density (mass) scale (p. 30)
$\bar{A}$	Closure of the set A (p. 45)
$\bar{z}_{L,m}(\mu)$	Grand canonical partition function of the restricted ensembles (p. 34)
$\bar{\nu}_m^L$, $\bar{\nu}_{\mu,m}^L$	Restricted reference measure and restricted grand canonical measure with restriction m. (p. 33)
$\mathcal{B}$	The Borel σ-algebra generated by open sets (p. 5)
$\mathcal{D}_f$	Essential domain of the function f (p. 31)
$\mathbb{E}^\nu[F]$	Expectation corresponding to path measure $\mathbb{P}^\nu$ (p. 6)
η_x	Local configuration (particle number) on site x (p. 30)
$\nu(f)$	Expectation of f with respect to measure ν on the state space (p. 10)
$\boldsymbol{\eta} = (\eta_x)_{x\in\Lambda_L}$	Full configuration (p. 30)
$\mathbb{1}_A$	Indicator function of the set A, $\mathbb{1}_A(x) = 1$ if $x \in A$ and 0 otherwise (p. 35)
Λ_L	Lattice of L sites, connected subset of $\mathbb{Z}^d$ (p. 30)
$\lfloor x \rfloor$	The integer floor of a real number $x \in \mathbb{R}$ (p. 23)
$\ll$,$(\gg)$	Asymptotically much smaller (greater), $f_n \ll g_n \Leftrightarrow \lim \frac{f_n}{g_n} = 0$ (p. 45)
μ	Chemical potential (p. 31)
$\nu = \nu_L$	Reference single site marginal (p. 30)
ν^L	Reference measure (p. 30)
$\nu_\mu^L, \nu_{\mu,m}^L$	Grand canonical measure, and restricted grand canonical measure at system size L (p. 31)
$\mathbb{P}^\nu$	Path measure of a Markov process with initial distribution ν (p. 6)
$\pi \ll \nu$	Measure π is absolutely continuous with respect to ν (p. 152)
$\pi_\rho^L, \pi_{\rho,m}^L$	Canonical and restricted canonical measures at system size L (p. 35)
$\mathbb{R}$	The set of real numbers $(-\infty, \infty)$ (p. 30)

$\mathbb{R}_+$	Non-negative reals $[0, \infty)$ (p. 21)
s_{can}	Canonical entropy density (p. 39)
s_{cond}	Condensed entropy density contribution (p. 41)
s_{gcan}	Grand canonical entropy density (p. 40)
$\|X\|$	Cardinality of the set X (p. 30)
$\|\cdot\|_{T.V.}$	The total variation norm (p. 153)
$\wedge, \vee$	$a \wedge b = \min\{a, b\}$ and $a \vee b = \max\{a, b\}$ (p. 43)
$\xrightarrow{\pi}$	Convergence in probability w.r.t. probability measure π. (p. 23)
$\mathbb{Z}^d$	d-dimensional integer lattice (p. 5)
A°	Interior of the set A (p. 45)
A^c	Complement of the set A (p. 45)
C^b	Bounded continuous functions (p. 152)
C_0^b	Set of bounded cylinder functions (p. 37)
$D[0, \infty)$	Canonical path space of a Markov process (p. 6)
E	Local state space (p. 30)
$f(h) = o(h)$	$f(h)/h \to 0$ as $h \to 0$ (p. 6)
f^*	The Legendre-Fenchel transform of f (p. 157)
$f_n = O(n)$	$\|f_n\| \leq C\|n\|$ for some $C > 0$ and n sufficiently large (p. 45)
$f_n \sim g_n$	Asymptotically proportional $f_n = Cg_n + o(1)$ (p. 61)
$f_n \simeq g_n$	Asymptotically equivalent $f_n = g_n + o(1)$ (p. 61)
$I(\rho, m)$	Rate function for the joint density and maximum under the reference measure (p. 50)
$I_\rho(m)$	Rate function for the maximum under the canonical measures (p. 51)
M_L	Random variable on X_L giving the macroscopic maximum site occupation on scale (b_L) (p. 33)
$P_\rho^L \overset{a_L}{\longleftrightarrow} Q_\mu^L$	Measures P_ρ^L and Q_μ^L are equivalent, Definition 3.11 (p. 36)
S_L	Empirical density or rescaled density (p. 30)
x, y	Lattice sites (p. 30)
$X_L,\ X_{\rho_L}^L$	State space $X_L = \mathbb{N}^{\Lambda_L}$ and canonical state space $X_{\rho_L}^L = \{\boldsymbol{\eta} \in X_L \mid S_L(\boldsymbol{\eta}) = \rho_L\}$ (p. 34)

Chapter 1

Introduction

Statistical mechanics is fundamentally concerned with understanding the macroscopic behaviour of systems composed of many interacting microscopic components. Such systems are ubiquitous in nature, from states of matter comprising a huge number of particles (of the order $\sim 10^{23}$), through to granular media, traffic flow and crowd dynamics. In principle the microscopic dynamics often follow deterministic, albeit potentially complicated, equations of motion. However, typically it is not feasible or desirable to have a complete description of such systems on the level of the microscopic dynamics. We therefore approximate the system in terms of an effective probabilistic description. The origin of the apparent random fluctuations is often related to sensitive dependence on initial conditions and mixing properties of the microscopic dynamics. In practice a mathematically rigorous justification of this approximation is often very challenging. In many cases we cannot hope to accurately predict the microscopic dynamics, due to their complexity, such as predicting the behaviour of people in traffic flow. Due to the large number of individual components, however, it is often sufficient to approximate the microscopic behaviour in terms of postulated probability distributions, since the behaviour of the system on the macroscopic scale is robust with respect to the actually origin of the noise.

The probabilistic description gives rise to a characterization of the system in terms of the expected value of certain observables. Mathematically these correspond to measurable functions on the microscopic state space. It turns out that after some suitable equilibration time, in the large system size limit these observables are typically determined by a small number of macroscopic system parameters, such as the temperature or total density. Of particular interest is the dependence of certain observables on these parameters. Phase transitions occur when the system undergoes a qualitative change in the macroscopic behaviour as some parameter is varied. These are signalled by singularities in some thermodynamic functions and abrupt transitions of some macroscopic observables.

There is a very well developed general understanding of systems of many identical components which are in equilibrium with their surroundings. Such systems are described by a Hamiltonian, or energy function, and the dynamics are assumed to be ergodic and reversible with respect to associated stationary distributions. In this case,

in the long time and large system limit, the typical value of macroscopic observables are given by the expected values under the relevant stationary measure. Such systems have been extensively studied in the physical literature, since the seminal work of Boltzmann, and there is now a well developed mathematical theory [76, 111]. There is also a well developed mathematical understanding of phase transitions in such systems in terms of Gibbs measures [55].

There are two ways that the equilibrium scenario can breakdown. The system could be driven out of equilibrium, so that time reversibility is not satisfied, such as attaching a thermal system to two heat baths at different temperatures, or similarly, if we consider traffic on a uni-directional road. Secondly, dynamic aspects of the systems may be relevant on long time scales comparable with the typical observation times, such as slow relaxation times from certain initial conditions. In this case, a description of the system in terms of the long time stationary distributions for the process is no longer satisfactory. In both of these cases it is no longer clear that the equilibrium approach is still valid, and there currently exists no such general formalism. However, such systems are ubiquitous in nature, and of significant practical importance. The models discussed in this thesis will typically be non-equilibrium in the sense of at least one of these ways. Frequently, we consider the case of both non-reversibility and the existence of dynamics relevant on macroscopic time scales.

A system is said to exhibit metastability if given certain initial conditions it quickly relaxes to some apparently stable equilibrium, but on a much longer time scale a random fluctuation or external perturbation causes it to relax to a more stable state. The characterising feature is the existence of two or more well separated time scales. This phenomena is typically present at first order phase transitions. Metastability is well understood on a heuristic level, however a mathematical description is an active area of research in probability theory and statistical physics [17, 107].

To clarify ideas somewhat we describe the feature discussed above in more detail for the example of traffic modelling. We consider a single stretch of road, with two open boundaries, cars may enter at one end and move towards the exit. Any stochastic model of traffic on a uni-directional road (such as a motorway) clearly cannot be time reversible with respect to any stationary distribution since the system supports a non-zero current. As the total density of cars increases the flux initially increases until, at some critical density, a jam may form and the average flux then begins to decrease. A defining feature of such traffic models is that close to the jamming transition the system switches between metastable fluid and jammed states. Also the typical number of cars (single components) in traffic jams is typically only of order $\sim 10^3 - 10^4$. This is far fewer than the number of individual microscopic components in classical applications of statistical mechanics, which is of order $\sim 10^{23}$. Therefore, finite size effects are also significant in understanding the observed behaviour in applications. Each of these issues are addressed, for a system that can be applied as a simple model of traffic flow, in Chapter 4.

Although there is, as yet, fewer general principles that apply to non-equilibrium systems, considerable insight has been gained by studying interacting particle systems

[85, 94, 95]. These consist of particles that randomly jump on a lattice and whose dynamics are influenced by interactions with each other. Formally they are defined in terms of continuous time Markov process on a discrete state space (see Chapter 2). The specific dynamics can be chosen to represent the microscopic behaviour of some physical system of interest. These models have been widely applied in physics, biology and social sciences. The underlying process may naturally be defined in terms of discrete particles on some lattice, for example a system of coupled service queues, otherwise continuous degrees of freedom may be described by a coarse graining procedure, for example when modelling traffic. As usual we expect the phenomenology described by the models to be independent of certain details of the underlying microscopic system of interest. In this sense interacting particle systems can be interpreted as mesoscopic models that serve as an approximation of the true underlying microscopic dynamics. They continue to be of interest in the physics and mathematical literature due to their broad applications and the variety of non-trivial behaviour they can exhibit, such as phase transitions in only one dimension, whilst (in many cases) remaining reasonably tractable.

A particular interacting particle system, known as the zero-range process (introduced in [115]), serves as a generic model for condensation and jamming transitions and has various applications (see [42, 43, 113] and references there in). There is, a priori, no bound on the number of particles that can occupy each lattice site, and particles interact only with other particles on the same site (a zero-range of interaction). This process has received considerable research attention recently due to its non-trivial critical behaviour. This process, and the condensation transition, are the focus of Chapters 4 and 5. A description of the leading order finite size effects for a generic class of condensing zero-range processes is contained in Chapter 4.

A real space condensation transition analogous to that in the zero-range process has been observed experimentally in granular media [123]. In these experiments it has been found that the effective jump rates of particles can depend non trivially on the total system size [117]. In Chapter 5 we study a toy model in which size-dependent jump rates lead to an effective long range interaction, this stabilises metastability and non-equivalence of ensembles in the thermodynamic limit. Studying the thermodynamic limit in this model can therefore help to understand the behaviour of finite systems. This behaviour is analogous to the case of Kac potentials in equilibrium systems [107].

In the models we consider, the total number of particles (or total mass) is conserved by the dynamics. So, restricted to finite initial conditions the processes typically exhibit unique stationary measures. These stationary measures, called the canonical measures, describe the typical long time behaviour of the system. Calculating the expected value of relevant observables under these measures is often not practical. A much simpler description is often found by instead fixing only the mean of the conserved quantity, this gives rise to the grand canonical measures. One then hopes that in the limit of large system sizes these two descriptions give rise to the same predictions for all relevant observables. In this case the grand canonical measures give a sufficient description of the system. This is known as equivalence of ensembles, and is intimately related

to phases transitions [1, 55]. Although the systems we look at are non-equilibrium the stationary measures are essentially still Gibbs measures and many results from equilibrium statistical mechanics still hold [54].

In this thesis we develop a general approach, based on entropy and large deviation methods, for studying the stationary properties of a class of interacting particle systems that exhibit condensation transitions. These results belong to a wide class of large deviation and entropy methods in statistical mechanics [1, 40, 118]. We generalise recent methods such as relative entropy techniques, making use of refined local limit theorems. With regards to the equivalence of ensembles our results are closely related to the work of Lewis et al. [93]. However, the results here generalise to non-compact local state space and point-wise estimates of large deviation probabilities, which are relevant in the systems we study. The general framework we derive allows us to consider various scaling limits, and identify the relevant scale on which metastability is observed.

Broadly, the general approach is to derive a large deviation principle for the joint density (corresponding to the conserved quantity) and maximum site occupation under a fixed grand canonical measure [34]. This then gives rise to a large deviation principle for the density alone, which in turn gives rise to results on equivalence of ensembles, useful for calculating the expected value of certain observables. Also we are able to extract the canonical large deviations of the maximum site occupation, which give rise to an effective free energy landscape for the (scaled) maximum site occupation. The maximum site occupation turns out to be the relevant order parameter for describing metastability in the condensing systems we consider and we associate local minimum in the free energy landscape with metastable states. Phase transitions are observed when the nature of the global minimum changes. These results could be significant for a first rigorous analysis of metastability in such systems, as the system size diverges.

In Chapter 2 we define the models that are used in the thesis and summarise relevant results from existing literature on interacting particle systems and metastability. We outline our general approach to studying equivalence of ensembles and metastability, and summarise relevant technical results in Chapter 3. On first reading, the results of Section 3.4 may be omitted and used as a reference in later chapters. In Chapter 4 we apply these techniques to derive original results on the finite-size effects in a generic class of condensing zero-range processes, which give rise to metastability in the appropriate scaling limit. In Chapter 5 we study a system for which these effects are stabilised in the thermodynamic limit. Here we extend recent results on the stationary properties of the system, and gain further insight into the metastability and relocation dynamics of the condensate. The general framework of Chapter 3 also gives rise to a simpler analysis of this system than in previous studies [70]. Finally in Chapter 6, we discuss condensation in a different model, the recently introduced inclusion process [57, 69], where condensation in the canonical ensemble has not been studied before. We observe two distinct regimes which are dependent on an external parameter (namely the microscopic diffusivity), and describe the dynamics using non-rigorous approaches.

Chapter 2

Interacting particle systems

In this chapter we give a precise definition of the stochastic particle systems that are studied in this thesis, and summarise some relevant previous results related to these models. We introduce key concepts that will be treated throughout the thesis, such as equivalence of ensembles, condensation and metastability.

2.1 Definitions

In this section we give a precise description of stochastic particle systems largely following [95] and [86]. Relevant results for continuous time Markov chains can also be found in [106].

2.1.1 Dynamics: Generators and master equations

Interacting particle systems are a class of continuous-time Markov processes on discrete state spaces. States in the state space define particle configurations. The dynamics are usually specified by giving the infinitesimal rates at which transitions between states occur.

The **state space** X of the process is the set of all possible particle configurations. For interacting particle systems the state space is given by $X = E^{\Lambda}$ (formally given by the set of functions from Λ to E), where E is the (countable) local state space and Λ is a countable lattice. Throughout this thesis the lattice Λ is typically a finite connected subset of $\mathbb{Z}^d$, for example in the one dimensional case $\Lambda_L = \{1, 2, \ldots, L\}$. We restrict our attention to processes on the one dimensional, countable local state spaces $E = \mathbb{N} = \{0, 1, 2, \ldots\}$. We note that since the local state space E is not compact, X is itself not compact. We denote configurations of X by bold Greek letters, so that for each $x \in \Lambda$, η_x stands for the number of particles at lattice site x in the full configuration $\boldsymbol{\eta} = (\eta_x)_{x\in\Lambda} \in X$. The state space X is endowed with the product topology which is metrizable, with measurable structure given by the Borel σ-algebra, $\mathcal{B}$.

The time evolution is given by **sample paths** which are elements of the canonical

path space,

$$D[0,\infty) = \{\boldsymbol{\eta}(\cdot) : [0,\infty) \to X \mid \boldsymbol{\eta}(\cdot) \text{ is right continuous and has left limits}\} .$$

The occupation of site x at time t is given by $\eta_x(t)$. Let $\mathcal{F}$ be the smallest σ-algebra on $D[0,\infty)$ relative to which all the functions $\boldsymbol{\eta}(\cdot) \mapsto \boldsymbol{\eta}(s)$ for $s \geq 0$ are measurable. For $t \in [0,\infty)$, let $\mathcal{F}_t$ be the smallest σ-algebra on $D[0,\infty)$ relative to which all the mappings $\boldsymbol{\eta}(\cdot) \mapsto \boldsymbol{\eta}(s)$ for $0 \leq s \leq t$ are measurable. The filtered space $(D[0,\infty), \mathcal{F}, \mathcal{F}_t)$ serves as a generic choice for the probability space of the process.

Definition 2.1. A *Markov Process* on X is a collection $\{\mathbb{P}^{\boldsymbol{\eta}}, \boldsymbol{\eta} \in X\}$ of probability measures on $D[0,\infty)$ indexed by initial configuration in X with the following properties,

(a) $\mathbb{P}^{\boldsymbol{\eta}}[\boldsymbol{\zeta}(\cdot) \in D[0,\infty) : \boldsymbol{\zeta}(0) = \boldsymbol{\eta}] = 1$ for all $\boldsymbol{\eta} \in X$.

(b) $\mathbb{P}^{\boldsymbol{\eta}}[\boldsymbol{\zeta}(s+\cdot) \in A \mid \mathcal{F}_s] = \mathbb{P}^{\boldsymbol{\zeta}(s)}[A]$ a.s. for every $\boldsymbol{\eta} \in X$ and $A \in \mathcal{F}$.
(Markov property)

(c) The mapping $\boldsymbol{\eta} \mapsto \mathbb{P}^{\boldsymbol{\eta}}[A]$ is measurable for every $A \in \mathcal{F}$.

Property (a) states that $\mathbb{P}^{\boldsymbol{\eta}}$ is normalised on paths with initial condition $\boldsymbol{\eta}$. Property (b) is the Markov property and ensures that the probability of some future event occurring, conditioned on the history up to some time s, depends only on the configuration at time s (memoryless). Property (c) allows us to consider the process with arbitrary initial distribution ν on X, defined by,

$$\mathbb{P}^{\nu} = \int_X \mathbb{P}^{\boldsymbol{\eta}} \ \nu(d\boldsymbol{\eta}) \ . \tag{2.1}$$

For a Markov Process the expectation corresponding to $\mathbb{P}^{\boldsymbol{\eta}}$ will be denoted by $\mathbb{E}^{\boldsymbol{\eta}}$,

$$\mathbb{E}^{\boldsymbol{\eta}}[F] = \int_{D[0,\infty)} F \ d\mathbb{P}^{\boldsymbol{\eta}} \ , \tag{2.2}$$

for any measurable function F on $D[0,\infty)$ which is integrable with respect to $\mathbb{P}^{\boldsymbol{\eta}}$.

The dynamics are characterised by **transition rates** $c(\boldsymbol{\eta}, \boldsymbol{\eta}') \geq 0$ which, for all $\boldsymbol{\eta}, \boldsymbol{\eta}' \in X$, describe the rate at which the system changes from the current state $\boldsymbol{\eta}$ to the new state $\boldsymbol{\eta}'$. The intuitive meaning of the transition rates c is given by

$$\mathbb{P}^{\boldsymbol{\eta}}[\boldsymbol{\eta}(\delta t) = \boldsymbol{\eta}'] = c(\boldsymbol{\eta}, \boldsymbol{\eta}')\delta t + o(\delta t) \quad \text{as} \quad \delta t \searrow 0 \quad \text{for } \boldsymbol{\eta}' \neq \boldsymbol{\eta} \ . \tag{2.3}$$

So given the state is currently $\boldsymbol{\eta}$ then in a small time δt the probability of the system transitioning to state $\boldsymbol{\eta}'$ is approximately $c(\boldsymbol{\eta}, \boldsymbol{\eta}')\delta t$.

Throughout this thesis we focus on systems in which the number of particles is locally conserved, so-called driven diffusive systems (or lattice gases), in which particles move on the lattice without being created or annihilated. For compact local state spaces there is a general theory on how to construct interacting particle systems even on infinite lattices using continuous test functions and the Hille-Yosida theorem [95]. For non-compact

local state spaces which we consider in this thesis, constructions on infinite lattices can be done on a case by case basis and require more restrictive assumptions on possible test functions and jump rates, see for example [2] for a construction of zero-range processes. To extend this construction to inclusion processes with bilinear growth of jump rates is an interesting theoretical problem which has not been studied so far. We do not discuss such constructions here, since do not study processes on infinite lattices, but only scaling limits of large finite systems and their properties. On finite lattices or graphs the state space of our models is still non-compact but countable, and therefore we are effectively working with Markov chains and their construction is standard [95, 106].

Markov chains are well defined for all time if the process does not explode for each initial configuration (see e.g. Chapter 2 of [106]). This is trivially fulfilled in our case since the processes we consider conserve the total number of particles. Under every (reasonable) initial distribution we have $\nu[\eta_x < \infty] = 1$, so the total number of particles on a finite lattice is $\sum_{x\in\Lambda} \eta_x < \infty$ almost surely. Therefore, for every initial condition the time evolution of the process concentrates on a finite subset of the total state space characterized by the number of particles, and explosion is impossible.

Although we only consider Markov chains, we stick to the customary formulation using semigroups and generators in this thesis, and explain the connection to the master equation and other concepts for Markov chains in the following. Our state space X is a countable (not necessarily compact) metric space and we denote,

$$C^b = \{f : X \to \mathbb{R} \mid f \text{ is continuous and bounded}\} ,$$

regarded as a Banach space with respect to the uniform norm $\|f\|_\infty = \sup_{\boldsymbol{\eta}\in X} |f(\boldsymbol{\eta})|$. Functions in C^b are regarded as observables, and we define the dynamics firstly with respect to the time evolution of the expected value of all observables. In particular cases it is possible to consider a larger class of functions, however C^b is sufficient to uniquely characterize the distribution of the Markov chain as a consequence of the Riesz representation theorem (for example see [110], Theorem 2.14).

Definition 2.2. For a given process $\{\mathbb{P}^{\boldsymbol{\eta}}, \boldsymbol{\eta} \in X\}$, for each $t \geq 0$ we define the operator,

$$S(t) : C^b \to C^b \quad \text{by} \quad (S(t)f)(\boldsymbol{\eta}) = \mathbb{E}^{\boldsymbol{\eta}} \left[f\big(\boldsymbol{\eta}(t)\big) \right] . \tag{2.4}$$

In general $f \in C^b$ need not imply $S(t)f \in C^b$, however all the processes we consider do have this property and are known as Feller Processes.

These operators form a Markov semigroup in the following sense.

Definition 2.3. A *Markov semigroup* is a collection of linear operators $\{S(t), t \geq 0\}$ on C^b with the following properties:

(a) $S(0) = 1$, the identity operator on C^b.

(b) The mapping $t \mapsto S(t)f$ is right continuous for every $f \in C^b$.

(c) $S(t+s)f = S(t)S(s)f$ for all $f \in C^b$ and all $s, t \geq 0$.

(d) $S(t)1 = 1$ for all $t \geq 0$.

(e) $S(t)f \geq 0$ for all non-negative $f \in C^b$.

The importance of Markov semigroups lies in the fact that there is a one-to-one correspondence with Markov processes.

Theorem 2.1. *Suppose $\{\mathbb{P}^{\boldsymbol{\eta}}, \boldsymbol{\eta} \in X\}$ is a Feller Markov process on X, then $S(t)$ in Definition 2.2 is a Markov semigroup.*

Also the following converse of this theorem holds.

Theorem 2.2. *Suppose $\{S(t), t \geq 0\}$ is a Markov semigroup on C^b. Then there exists a unique Feller Markov process $\{\mathbb{P}^{\boldsymbol{\eta}}, \boldsymbol{\eta} \in X\}$ such that (2.4) holds for all $t \geq 0$.*

Proof. For proofs of these two theorems see for example [95] and [106]. □

The semigroup defined above describes the time evolution of expected values of observables $f \in C^b$ for a given Markov process. It provides a full representation of the Markov process, dual to the path measures $\{\mathbb{P}^{\boldsymbol{\eta}}, \boldsymbol{\eta} \in X\}$. Following (2.1) and (2.2) the expectation of observables at $t \geq 0$ with respect to initial distribution ν is given by,

$$\mathbb{E}^{\nu}\left[f\big(\boldsymbol{\eta}(t)\big)\right] = \int_X (S(t)f)(\boldsymbol{\zeta})\nu[d\boldsymbol{\zeta}] = \int_X S(t)f \; d\nu \quad \text{for all } f \in C^b \; .$$

We expect, from property (c) of the definition of the semigroup operator $S(t)$, that it is of an exponential form generated by the 'time derivative' of S at zero, $S'(0)$,

$$\text{“}S(t) = e^{tS'(0)} = I + S'(0)t + o(t)\text{”} \; .$$

This is made precise in the following.

Definition 2.4. The (infinitesimal) generator $\mathcal{L} : C^b \to C^b$ for the process $\{S(t), t \geq 0\}$ is given by,

$$\mathcal{L}f = \lim_{\delta t \searrow 0} \frac{S(\delta t)f - f}{\delta t} \quad \text{for } f \in C^b \; . \tag{2.5}$$

Theorem 2.3. *There is a one-to-one correspondence between Markov generators and semigroups on C^b, given by*

$$S(t)f = \lim_{n\to\infty} \left(I - \frac{t}{n}\mathcal{L}\right)^{-n} f \quad \textit{for } f \in C^b, \; t \geq 0 \; .$$

For $f \in C^b$ also $S(t)f \in C^b$ for all $t \geq 0$ and,

$$\frac{\mathrm{d}}{\mathrm{d}t} S(t)f = S(t)\mathcal{L}f = \mathcal{L}S(t)f \; , \tag{2.6}$$

called the forward *and* backward equation*, respectively. Formally we write $S(t) = e^{t\mathcal{L}}$ in analogy with scalar exponentials.*

With jump rates $c(\boldsymbol{\eta}, \boldsymbol{\eta}')$ the generator can be computed directly from (2.3), for small $\delta t \searrow 0$,

$$\begin{aligned} S(\delta t) f(\boldsymbol{\eta}) = \mathbb{E}^{\boldsymbol{\eta}} \left[f\big(\boldsymbol{\eta}(\delta t)\big) \right] &= \sum_{\boldsymbol{\eta}' \in X} f(\boldsymbol{\eta}') \mathbb{P}^{\boldsymbol{\eta}}[\boldsymbol{\eta}(\delta t) = \boldsymbol{\eta}'] \\ &= \sum_{\boldsymbol{\eta}' \neq \boldsymbol{\eta}} c(\boldsymbol{\eta}, \boldsymbol{\eta}') f(\boldsymbol{\eta}') \delta t + f(\boldsymbol{\eta}) \left(1 - \sum_{\boldsymbol{\eta}' \neq \boldsymbol{\eta}} c(\boldsymbol{\eta}, \boldsymbol{\eta}') \delta t \right) + o(\delta t) \ . \end{aligned} \tag{2.7}$$

With the definition 2.4 of the generator, above, this implies,

$$\mathcal{L} f(\boldsymbol{\eta}) = \sum_{\boldsymbol{\eta}' \in X} c(\boldsymbol{\eta}, \boldsymbol{\eta}') \big(f(\boldsymbol{\eta}') - f(\boldsymbol{\eta}) \big) \ .$$

where we use the convention that $c(\boldsymbol{\eta}, \boldsymbol{\eta}) = 0$ for all $\boldsymbol{\eta} \in X$.

The description above, for Markov chains, is equivalent to a description in terms of the **master equation** as follows. The indicator functions $\mathbb{1}_{\boldsymbol{\eta}} : X \to \{0, 1\}$ defined by,

$$\mathbb{1}_{\boldsymbol{\eta}}(\boldsymbol{\zeta}) = \begin{cases} 1 & \text{if } \boldsymbol{\zeta} = \boldsymbol{\eta} \\ 0 & \text{otherwise,} \end{cases}$$

are bounded and form a basis of C^b. We denote the probability distribution on X at time t starting from initial distribution ν by,

$$p_t[\boldsymbol{\eta}] = \int_X S(t) \mathbb{1}_{\boldsymbol{\eta}} \, d\nu \ . \tag{2.8}$$

Since we have countable state space, we can identify measures on X with their probability mass functions and use the same symbol to avoid overloading the notation. Substituting into the forwards equation from Theorem 2.3, for all $\boldsymbol{\eta} \in X$,

$$\begin{aligned} \frac{\mathrm{d}}{\mathrm{d}t} p_t[\boldsymbol{\eta}] = \int_X S(t) \mathcal{L} \mathbb{1}_{\boldsymbol{\eta}} \, d\nu &= \sum_{\boldsymbol{\zeta} \in X} p_t[\boldsymbol{\zeta}] \sum_{\boldsymbol{\zeta}' \in X} c(\boldsymbol{\zeta}, \boldsymbol{\zeta}') \big(\mathbb{1}_{\boldsymbol{\eta}}(\boldsymbol{\zeta}') - \mathbb{1}_{\boldsymbol{\eta}}(\boldsymbol{\zeta}) \big) \\ &= \sum_{\boldsymbol{\zeta} \in X} p_t[\boldsymbol{\zeta}] c(\boldsymbol{\zeta}, \boldsymbol{\eta}) - p_t[\boldsymbol{\eta}] \sum_{\boldsymbol{\zeta}' \in X} c(\boldsymbol{\eta}, \boldsymbol{\zeta}') \ . \end{aligned}$$

This gives rise to the **master equation**,

$$\frac{\mathrm{d}}{\mathrm{d}t} p_t[\boldsymbol{\eta}] = \sum_{\boldsymbol{\zeta} \in X} \big(p_t[\boldsymbol{\zeta}] c(\boldsymbol{\zeta}, \boldsymbol{\eta}) - p_t[\boldsymbol{\eta}] c(\boldsymbol{\eta}, \boldsymbol{\zeta}) \big) \tag{2.9}$$

with intuitive gain and loss terms on the right-hand side. For Markov chains this is equivalent to the forward equation (2.6), since the indicator functions form a basis of C^b.

2.1.2 Stationary measures

A stationary distribution for the process is a probability distribution which is invariant under the dynamics.

Definition 2.5. A measure ν on X is stationary if

$$\nu\left(S(t)f\right) = \nu\left(f\right) \quad \text{for all } f \in C^b \ .$$

Throughout the thesis we use the notation $\nu\left(f\right) = \int_X f \ d\nu$ for the expected value with respect to measures on the state space.

If ν is a stationary measure then,

$$\mathbb{P}^\nu[\boldsymbol{\eta}(\cdot) \in A] = \mathbb{P}^\nu[\boldsymbol{\eta}(t+\cdot) \in A] \quad \text{for all } t \geq 0, A \in \mathcal{F} \ .$$

Equivalently, using the master equation notation (2.8), if ν is stationary and $p_0 = \nu$, then $p_t = \nu$ for all $t \geq 0$.

Proposition 2.4. *A measure ν on X is stationary if and only if,*

$$\nu\left(\mathcal{L}f\right) = 0 \quad \textit{for all } f \in C^b \ .$$

Proof. See for example Liggett [95] Proposition 2.13. □

Since the indicator functions used to construct the master equation form a basis of C^b this can be stated equivalently in terms of the master equation as; ν is stationary if and only if it solves the system of differential equations,

$$\frac{\mathrm{d}}{\mathrm{d}t}\nu[\boldsymbol{\eta}] = \sum_{\boldsymbol{\zeta} \in X} \left(\nu[\boldsymbol{\zeta}]c(\boldsymbol{\zeta}, \boldsymbol{\eta}) - \nu[\boldsymbol{\eta}]c(\boldsymbol{\eta}, \boldsymbol{\zeta})\right) = 0 \quad \text{for all } \boldsymbol{\eta} \in X \ .$$

Definition 2.6. A Markov process with semigroup $\{S(t), t \geq 0\}$ is *ergodic* if there exists a unique stationary distribution π and,

$$\lim_{t \to \infty} p_t = \pi \quad \text{for all initial distributions } p_0 \ ,$$

where p_t is the distribution at time t, as given by (2.8).

Not every Markov chain has a stationary distribution. However, existence of at least one stationary distribution is guaranteed if the state space X is finite.

Definition 2.7. A Markov process $\{\mathbb{P}^{\boldsymbol{\eta}} : \boldsymbol{\eta} \in X\}$ is called *irreducible*, if for all $\boldsymbol{\eta}, \boldsymbol{\eta}' \in X$,

$$P^{\boldsymbol{\eta}}[\boldsymbol{\eta}(t) = \boldsymbol{\eta}'] > 0 \quad \text{for some } t \geq 0 \ .$$

An irreducible Markov process can sample the entire state space, from any initial condition. This implies that there is at most one stationary distribution (see [106], Sec-

tion 3.5). The processes we focus on in this thesis are typically ergodic when restricted to a fixed finite number of particles on a finite lattice, due to the following theorem.

Theorem 2.5. *An irreducible Markov process with finite state space X is ergodic.*

Proof. The proof is a direct result of the Perron-Frobenius theorem ([64] Theorem 6.6.1). The generator of the process for finite state space is a real matrix $c(\boldsymbol{\eta}, \boldsymbol{\eta}')$, which has unique eigenvalue 0, and the corresponding unique eigenvector corresponds to the unique stationary distribution. □

2.1.3 Reversibility

Definition 2.8. A measure ν is called *reversible* for the process with semigroup $\{S(t) : t \geq 0\}$ if,

$$\nu\left(fS(t)g\right) = \nu\left(gS(t)f\right) \quad \text{for all } f, g \in C^b \ .$$

For Feller processes the definition is equivalent to,

$$\nu\left(f\mathcal{L}g\right) = \nu\left(g\mathcal{L}f\right) \quad \text{for all } f, g \in C^b \ .$$

Choosing $g = 1$ in the definition of reversible we see that every reversible measure is stationary. Under the stationary distribution the process can be extended to negative times on the path space $D(-\infty, \infty)$. If the measure ν is reversible then the forward process, with initial condition ν, has the same joint distributions as the time reversed process.

By inserting indicator functions into the definition 2.8 we arrive at the following characterisation on countable state spaces.

Proposition 2.6. *A measure ν on countable state space X is reversible for the process with transition rates $c(\cdot\,, \cdot)$ if and only if it fulfils the* ***detailed balance conditions***

$$\nu[\boldsymbol{\eta}]\, c(\boldsymbol{\eta}, \boldsymbol{\zeta}) = \nu[\boldsymbol{\zeta}]\, c(\boldsymbol{\zeta}, \boldsymbol{\eta}) \quad \textit{for all } \boldsymbol{\eta}, \boldsymbol{\zeta} \in X \ .$$

2.2 Models

2.2.1 Zero-range process

The zero-range process (ZRP) is a stochastic particle system with no restriction on the number of particles per site and with jump rates that depend only on the occupation of the departure site. The process was originally introduced by Spitzer [115]. The simple zero-range interaction leads to a product structure of the stationary distributions [2, 115]. These processes have been a focus of recent research interest since they can exhibit a condensation transition (described in Section 2.3.2). Findings for the zero-range process can be applied to understand condensation phenomena in a variety of nonequilibrium systems (see [43] and references therein), as well as providing a generic model of domain wall dynamics and a criterion for phase separation using a mapping to one-dimensional

exclusion systems [81] (see Section 2.2.2 for more details). The process continues to be of interest; recent work on variations of the model includes mechanisms leading to more than one condensate [84, 114, 116], or the effects of memory in the dynamics [74].

Definition

There is a-priori no restriction on the number of particles on each site, in this sense the zero-range process is a bosonic lattice gas. The local state space will therefore be $\mathbb{N} = \{0, 1, \ldots\}$. We focus on finite translation invariant lattices with periodic boundary conditions. Denote by $\mathbb{T}_n = \mathbb{Z}/n\mathbb{Z} = \{1, 2, \ldots, n\}$ the one dimensional integer torus. We consider the zero-range process defined on the d dimensional torus, $\Lambda_L = (T_n)^d$, of $L = (n^d)$ sites. For example in the one dimensional case $\Lambda_L = \{1, 2, \ldots, L\}$ with periodic boundary conditions. The state of the system is described by $\boldsymbol{\eta} = (\eta_x)_{x\in\Lambda_L}$ belonging to the state space of all particle configurations

$$X_L = \{\boldsymbol{\eta} = (\eta_x)_{x\in\Lambda_L} : \eta_x \in \mathbb{N}\} = \mathbb{N}^{\Lambda_L} \ .$$

Particles jump on the lattice at a rate that depends only on the occupation number of the departure site (zero-range). A particle jumps off site $x \in \Lambda_L$ after an exponential waiting time with rate $g(\eta_x)$ and moves to a target site y according to the probability distribution $p(x, y)$. We restrict our analysis to the case of homogeneous jump distributions,

$$p(x, y) = q(y - x) \quad \text{for all } x, y \in \Lambda_L \ .$$

Further, we assume that $q(0) = 0$, q is normalised, and is of finite range,

$$\sum_{y\in\Lambda_L} q(y) = 1 \quad \text{and} \quad q(z) = 0 \ \text{ if } |z| > R \text{ for some } R > 0 \ ,$$

where R is independent of the system size L. Also p is irreducible on Λ_L so that every particle can reach any site with positive probability. The transition rates, from configuration $\boldsymbol{\eta}$ to configuration $\boldsymbol{\zeta}$, are given by,

$$c(\boldsymbol{\eta}, \boldsymbol{\zeta}) = \begin{cases} g(\eta_x)q(y - x) & \text{if } \boldsymbol{\zeta} = \boldsymbol{\eta}^{x\to y} \\ 0 & \text{otherwise,} \end{cases} \tag{2.10}$$

where $\eta_z^{x\to y} = \eta_z - \delta(z, x) + \delta(z, y)$ and δ is the Kronecker delta. We assume that the jump rates are strictly positive on the positive integers and have bounded variation,

$$\sup_{k\in\mathbb{N}} |g(k + 1) - g(k)| < \infty \quad \text{and} \quad g(k) = 0 \iff k = 0 \ . \tag{2.11}$$

The infinitesimal generator of the process acting on suitable functions f is given by

$$(\mathcal{L}_L f)(\boldsymbol{\eta}) = \sum_{x,y\in\Lambda_L} g(\eta_x)q(y - x) \left(f(\boldsymbol{\eta}^{x\to y}) - f(\boldsymbol{\eta})\right) \ , \tag{2.12}$$

for $f \in C^b(X_L)$ [2, 96]. In general the jump rates may also depend on the size of the system (see Chapter 5), in this case we explicitly included the size dependence by including a subscript L, $g_L(\eta_x)$. This defines the Markov process on the countable state space X_L as described in the previous section. The process can also be defined on an infinite lattice under certain constraints, for details see [2, 75].

For example, if $g(k) = k$ for all k then the zero-range process reduces to the superposition of independent random walkers on Λ_L. If $g(k) = 1$ for all $k > 0$ then the zero-range process reduces to a system of L queues with mean-one exponential random times of service.

Stationary Measures

The following summarises well known results on stationary measures of the zero-range process, for details see [2, 42, 115]. The zero-range process with generator (2.12), on a periodic lattice, has a family of stationary homogeneous product measures on X_L which we refer to as the **grand canonical ensemble**. These measures are parametrized by a chemical potential $\mu \in \mathbb{R}$ and are of the form,

$$\nu_\mu^L[\boldsymbol{\eta}] = \prod_{x \in \Lambda_L} \nu_\mu[\eta_x] \quad \text{where} \quad \nu_\mu[n] = \frac{1}{z(\mu)} w(n) e^{n\mu}. \tag{2.13}$$

These exist for all $\mu \in [0, \mu_c)$ where μ_c is the logarithmic radius of convergence of the (single site) partition function

$$z(\mu) = \sum_{k=0}^{\infty} w(k) e^{\mu k}. \tag{2.14}$$

The stationary weights w are given by $w(0) = 1$ and

$$w(n) = \prod_{k=1}^{n} g(k)^{-1}, \quad n > 0. \tag{2.15}$$

Throughout the thesis the expect value of a function f with respect to a measure ν is denoted by $\nu(f)$ with round brackets. The grand canonical expected particle density is a function of μ and is given by

$$R(\mu) := \nu_\mu(\eta_1) = \sum_{k=0}^{\infty} k \nu_\mu[k] = \partial_\mu \log z(\mu) \ , \tag{2.16}$$

which is strictly increasing and $\lim_{\mu \to -\infty} R(\mu) = 0$. The critical density is defined by $\rho_c = \lim_{\mu \nearrow \mu_c} R(\mu) \in (0, \infty]$, and condensation occurs if $\rho_c < \infty$, as described in Section 2.3.

It follows from the form of the stationary weights (2.15) that the expected rate of particles leaving any site under the grand canonical measures is given by the exponential

of the chemical potential,

$$\nu_\mu\left(g(\eta_x)\right) = \sum_{k=0}^{\infty} g(k)\nu_\mu[k] = e^\mu \ .$$

The expected jump rate off a site is proportional to the average stationary current, or, in the case that the first moment $\sum_z z\, q(z)$ vanishes, to the diffusivity. Therefore for simplicity, in the rest of this thesis, **current** will refer to the average jump rate off a site, which is clearly site independent under a homogeneous stationary distribution. In the grand canonical ensemble the current is therefore simply given by

$$j^{\mathrm{gc}}(\mu) = \nu_\mu\left(g(\eta_x)\right) = e^\mu \ . \tag{2.17}$$

The zero-range process is reversible if and only if the dynamics are symmetric $q(z) = q(-z)$.

The process conserves the total number of particles in the system, so X_L can be partitioned into invariant subsets,

$$X_{L,N} = \{\boldsymbol{\eta} \in \Omega_L \mid \sum_{x\in\Lambda_L} \eta_x = N\} \ , \tag{2.18}$$

on which the zero-range process is a finite state irreducible Markov process. So for fixed system size L and total number of particles N the process restricted to $X_{L,N}$ is ergodic, the corresponding unique stationary measures belong to the **canonical ensemble** and are given by

$$\pi_N^L\left[\boldsymbol{\eta}\right] := \nu_\mu[\boldsymbol{\eta} \mid \sum_{x\in\Lambda_L} \eta_x = N] \ . \tag{2.19}$$

These measures are independent of μ and are given explicitly by

$$\pi_N^L\left[\boldsymbol{\eta}\right] = \frac{1}{Z(L,N)} \prod_{x\in\Lambda_L} w(\eta_x)\, \delta\big(\sum_{x\in\Lambda} \eta_x - N\big) \ ,$$

where the canonical partition function is the finite sum

$$Z(L,N) = \sum_{\boldsymbol{\eta}\in X_{L,N}} \prod_{x\in\Lambda_L} w(\eta_x) \ . \tag{2.20}$$

In the canonical ensemble the form of the stationary weights, Eq. (2.15), implies that the average current is given by a ratio of partition functions,

$$j_L^{\mathrm{can}}(N/L) := \pi_N^L\left(g(\eta_x)\right) = \frac{Z(L,N-1)}{Z(L,N)}. \tag{2.21}$$

The canonical partition functions can be calculated iteratively,

$$Z(L,N) = \sum_{k=0}^{N} w(k) Z(L-1, N-k) \ . \tag{2.22}$$

Similarly we can calculate the canonical distribution of the maximum site occupation. To this end we define the cut-off canonical partition function which counts configurations for which the maximum site occupation is less than or equal to M,

$$Q(L,N,M) = \sum_{k=0}^{\min\{M,N\}} w(k) Q(L-1, N-k, M) \ . \tag{2.23}$$

This gives rise to the cumulative distribution for the maximum under the canonical measures, and allows us to calculate

$$\pi_N^L \left[\max_{x \in \Lambda_L} \eta_x = M \right] = \frac{Q(L,N,M) - Q(L,N,M-1)}{Z(L,N)} \ . \tag{2.24}$$

For more details see Appendix D.1.

2.2.2 Mapping to the exclusion process

The one dimensional zero-range process, on translation invariant lattices with nearest-neighbour jumps, can be mapped onto a simple exclusion process (a model in which each site can contain at most one particle). From the point of view of a tagged particle in the exclusion process the systems are equivalent. This was first noticed in [50, 85], and has been applied to the study of jamming transitions in simple traffic models [22, 53, 83].

In the simple exclusion process the local state space is $E = \{0, 1\}$ where $\eta_x = 1$ is interpreted as the presence of a particle at site $x \in \Lambda$, and $\eta_x = 0$ an empty site. Particles are allowed to jump to neighbouring sites on the lattice only if the target site is empty. We consider a generalised version of the exclusion process originally introduced in [115], where the rate that particles jump on the lattices is allowed to depend on the entire configuration (we restrict our attention again to finite lattices). The generator of the process is given by,

$$\mathcal{L}f(\boldsymbol{\eta}) = \sum_{x \in \Lambda} \big(p_x(\boldsymbol{\eta}) \eta_x (1 - \eta_{x+1}) + q_{x+1}(\boldsymbol{\eta}) \eta_{x+1} (1 - \eta_x) \big) \big(f(\boldsymbol{\eta}^{x \leftrightarrow y}) - f(\boldsymbol{\eta}) \big) \ .$$

where,

$$\eta_z^{x \leftrightarrow y} = \begin{cases} \eta_y & \text{if } z = x \\ \eta_x & \text{if } z = y \\ \eta_z & \text{otherwise,} \end{cases}$$

$p_x(\boldsymbol{\eta}) > 0$, is the rate at which a particle at site x jumps to site $x+1$, given the current configuration is $\boldsymbol{\eta}$, similarly, $q_x(\boldsymbol{\eta})$, is the rate at which a particle jumps to the left. The

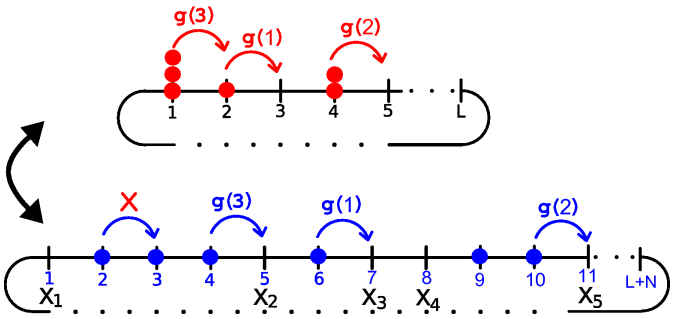

Figure 2.1: Equivalence between a totally asymmetric zero-range process and an exclusion process. The zero-range process is shown at the top, and the corresponding exclusion dynamics are shown below. The position of holes x_i in the exclusion process corresponds to the lattice sites in the zero-range process as explained in the text.

case most relevant for applications is that of totally asymmetric dynamics on a ring, for which $q_x(\boldsymbol{\eta}) = 0$ for all configurations $\boldsymbol{\eta}$ and $x \in \Lambda$.

The mapping between the zero-range and the exclusion processes, for totally asymmetric dynamics, is shown in Figure 2.1. Lattice sites in the zero-range process are associated with empty sites in the exclusion process, and the number of particles on a site in the zero-range process corresponds to the number of particles adjacent to each other in the exclusion process ('block sizes'). More precisely the mapping is constructed as follows. We consider a totally asymmetric zero-range process on $\{1, 2, \ldots, L\}$ with periodic boundary conditions and fix the total number of particles to N. This corresponds to a totally asymmetric exclusion process of N particles, on the lattice $\{1, 2, \ldots, L+N\}$. Let $x_i \in \{1, 2, \ldots, L+N\}$ be the position of the i-th hole in the exclusion process, such that $x_1 < x_2 < \ldots < x_L$. We fix a reference frame by tagging the first hole, so that initially $x_1 = 1$. The order of the particle holes is preserved by the dynamics, since particles can not pass each other. The x_i are associated with lattice sites in the zero-range process, whose occupation number is given by the number of particles to the right of x_i in the exclusion process, that is $\eta_i = x_{i+1} - x_i - 1$. The dynamics in the exclusion process are inferred from the zero-range process. Particles in the exclusion process jump to the right at a rate that depends on the number of particles adjacent to the left (distance to the previous hole to the left). This corresponds to particles exiting a 'jam' of n particles at rate $g(n)$ (see Figure 2.1). This means that depending on the form of the jump rates, $g(n)$, in the zero-range process, there may be long-range interactions between particles in the exclusion process. With this interpretation zero-range processes can be used as simple models of traffic flow [83]. It has further been observed in [81], that condensing zero-range process can serve as effective models for domain wall dynamics in a two-species exclusion model.

2.2.3 Inclusion process

In this section we introduce an interacting particles system called the Inclusion Process. This is a system of random walkers on a lattice which interact by attracting each other. The symmetric inclusion process (SIP) was introduced in [56, 57]. It was originally introduced as a dual process (in the sense of Definition 3.1 in [95]) to the so-called Brownian energy process. Correlation inequalities in the SIP and the asymmetric inclusion process (ASIP) were analysed in [58]. The existence of product stationary measures under general conditions was shown in [70]. It was also shown that if the rate of particle diffusion decreases quickly enough with system size that a condensation phenomenon can occur under the grand canonical measures.

Definition

We consider a connected, translation invariant, lattice of L sites Λ_L (as defined for the zero-range process). Typically we have in mind the one dimensional case $\Lambda_L = \{1, 2, \ldots, L\}$ with periodic boundary conditions. The local state space for the process is the same as for the zero-range process, namely $\mathbb{N}$, so that the full state space on a system of size L is $X_L = \mathbb{N}^{\Lambda_L}$. As with the zero-range process we denote states of the system by bold $\boldsymbol{\eta} = (\eta_x)_{x\in\Lambda_L} \in X_L$ where η_x is the number of particles residing on site x. Particles diffuse on the lattice independently (performing independent random walks) with diffusion constant d which could depend on the size of the system. As well as the diffusion dynamics particles also attract each other, every particle at site x attracts all particles at site y with rate $p(x, y)$. This is the so-called 'inclusion' attraction. The dynamics on a finite lattice Λ_L are defined by the generator acting on bounded test functions $f : X_L \to \mathbb{R}$,

$$\mathcal{L}_L f(\boldsymbol{\eta}) = \sum_{x,y\in\Lambda_L} \eta_x(d_L + \eta_y)p(x, y) \left(f(\boldsymbol{\eta}^{x\to y}) - f(\boldsymbol{\eta})\right) \ . \tag{2.25}$$

As before, the $p(x, y)$ are transition probabilities of a finite range irreducible random walk on the lattice such that $p(x, x) = 0$. The diffusion parameter d_L determines the relative strength of the diffusion (random walk) compared to the attraction. Large d corresponds to strong diffusion and weak attraction, and small d vice versa. If $p(x, y) = p(y, x)$ the process is called the symmetric inclusion process (SIP), otherwise it is referred to as the asymmetric inclusion process (ASIP). Note that a construction of the dynamics on infinite lattices is not covered by previous results on zero-range processes due to the quadratic term in the jump rates.

Stationary Measures

For the symmetric case (SIP), stationary product measures were found in [58]. These results were generalised in [70] to the existence of product stationary measures under the conditions;

(a) The random walk $p(x, y)$ is doubly stochastic,

$$\sum_{j \in \Lambda_L} (p(i,j) - p(j,k)) = 0 \quad \text{for all } i, k \in \Lambda_L \ . \tag{2.26}$$

(b) The random walk $p(x, y)$ is reversible with respect to some measure $\lambda(i)$,

$$\lambda(i)p(i,j) = \lambda(j)p(j,i) \quad \text{for all } i, j \in \Lambda_L \ . \tag{2.27}$$

As before we focus on finite translation invariant lattices Λ_L which are subsets of $\mathbb{Z}^d$ with periodic boundary conditions. We also restrict the dynamics to having a homogeneous, irreducible jump distribution,

$$p(x, y) = q(y - x) \quad \text{for } q : \Lambda_L \to \mathbb{R}_+ \text{ with bounded support} \ ,$$

and $\sum_{z \in \Lambda_L} q(z) = 1$. Then the condition in (2.26) implies that there exists a family of homogeneous product stationary measures, referred to as the **grand canonical ensemble**. These measures are products of the single site marginals, which can be expressed in terms of the single site weights, and are parametrized by a chemical potential $\mu \in \mathbb{R}$,

$$\nu_\mu^L [\boldsymbol{\eta}] = \prod_{x \in \Lambda_L} \nu_\mu [\eta_x] \quad \text{where} \quad \nu_\mu [n] = \frac{1}{z(\mu)} w(n) e^{n\mu}. \tag{2.28}$$

These exist for all $\mu \in [0, \mu_c)$ where μ_c is the logarithmic radius of convergence of the (single site) partition function

$$z(\mu) = \sum_{k=0}^{\infty} w(k) e^{\mu k}. \tag{2.29}$$

The stationary weights w are given by,

$$w(n) = \frac{\Gamma(d_L + n)}{n! \Gamma(d_L)} \ . \tag{2.30}$$

It follows from the properties of the gamma function that the single site weights obey the following recursion relation,

$$w(n+1) = \frac{d_L + n}{n+1} w(n) \ . \tag{2.31}$$

As observed for the zero-range process the average particle density under the grand canonical measures is a function of the chemical potential, and is given in the usual way as,

$$R(\mu) := \nu_\mu (\eta_1) = \sum_{k=0}^{\infty} k \nu_\mu [k] = \partial_\mu \log z(\mu) \ , \tag{2.32}$$

Just as for the zero-range process the average jump rate off a site is proportional to the average current (or diffusivity for symmetric dynamics). By convention we call the average jump rate off a site the **current**, and under the grand canonical measures this is given by,

$$j^{\mathrm{gc}}(\mu) = \nu_\mu \left(\eta_x \sum_{y \in \Lambda_L} (d_L + \eta_y) q(y - x) \right) = R(\mu) \left(R(\mu) + d_L \right) \ . \tag{2.33}$$

The inclusion process clearly conserves the total number of particles, as the zero-range process does. By assumption, the underlying random walk the particles perform is irreducible, and by construction, the rate of particles exiting a site is zero if and only if the number of particles on the site is zero. So the dynamics restricted to initial conditions with N particles are irreducible on the finite canonical state space given by (2.18), and therefore ergodic. The unique stationary distributions are, again, called the **canonical measures** and are given by the conditioned reference measures (see Section 2.2.1),

$$\begin{aligned} \pi_N^L[\boldsymbol{\eta}] &= \nu_\mu^L[\boldsymbol{\eta} \mid \sum_{x \in \Lambda_L} \eta_x = N] \\ &= \frac{1}{Z(L,N)} \prod_{x \in \Lambda_L} w(\eta_x) \, \delta\big(\sum_{x \in \Lambda} \eta_x - N \big) \ , \end{aligned}$$

where the canonical partition function has the same form as (2.20).

As discussed in Section 2.2.1 the canonical partition function, and the truncated version, can both be calculated efficiently using an iterative procedure (see Appendix D.1). However, unlike the zero-range process, there is no simple relation between the average current under the canonical measures and the partition function. The canonical current is given by,

$$j^{\mathrm{can}}(N/L) = \pi_N^L \left(\eta_x \sum_{y \in \Lambda_L} (d_L + \eta_y) q(x - y) \right) \ . \tag{2.34}$$

Since stationary measures conditioned on a fixed number of particles are not product measures this quantity is difficult to calculate.

2.2.4 Generalisations

In this section we summarize generalisations of the above systems which could in principle be analysed by the same methods developed in this thesis.

Several particle species

Interacting particle systems with several conservation laws can show very rich critical behaviour (see [46, 113] and references therein). In view of this the zero-range process has been generalised to a model with two conserved particle species [65, 72]. These have several applications, including in shaken granular media with several particle sizes, and

in growing and re-wiring networks with directed edges. The dynamics are defined such that jump rates of each particle off a site depend on the occupation numbers of each of the species on that site. Due to this interaction a condensation in one particle species can be induced by another particles species.

Although the focus of this thesis is on a single particle species for each model, the methods described in Chapter 3 could be extended to several particle species, in the case that there exist stationary product distributions. Fortunately, provided the dynamics satisfy certain constraints, there exist product measures for the multiple species zero-range process. For the case of two particle species the local state space becomes $\mathbb{N}^2$, and the state at site $x \in \Lambda$ is given by $\eta_x = (\eta_x^1, \eta_x^2)$, where η_x^1 is the number of 'type 1' particles on site x and η_x^2 the number of 'type 2'. It has been shown [46, 67], that the zero-range process has product stationary measures if the jump rates of the type 1 particles, g_1, and type 2, g_2, satisfy

$$g_1\left((\eta_x^1, \eta_x^2)\right) g_2\left((\eta_x^1, \eta_x^2 - 1)\right) = g_2\left((\eta_x^1, \eta_x^2)\right) g_1\left((\eta_x^1 - 1, \eta_x^2)\right) \ .$$

Mass transport processes

A natural extension of the zero-range process is to allow the jump rates to depend on the occupancy of more than a single site. In the physics literature, such models, which have dynamics that conserve the total number of particles on the lattice, are referred to as 'urn models', as reviewed in [62]. These models are typically defined by an energy function which is the sum of local contributions, and the dynamics are assumed to satisfy detailed balance with respect to a corresponding stationary measure. A more direct generalisation of the zero-range dynamics is to allow the jump rates to depend on both the occupancy of the departure site and the target site. Such a class of processes was introduced in the mathematical literature as 'Misanthrope' processes [26]. They still exhibit product stationary measures, provided the jump rates satisfy certain constraints. On a translation invariant subset of $\mathbb{Z}^d$, in which particles jump from site x to site y at rate $g(\eta_x, \eta_{x+y})\, q(y-x)$, sufficient conditions for product stationary measures are given by,

$$\begin{aligned}
&\frac{g(i,j)}{g(j+1,i-1)} = \frac{g(i,0)g(1,j)}{g(j+1,0)g(1,i-1)} \quad \text{for } i \geq 1,\, j \geq 0 \\
&\text{and} \quad p(z) = p(-z) \quad \text{for all } z \in \mathbb{Z}^d; \\
&\text{or} \quad g(i,j) - g(j,i) = g(i,0) - g(j,0) \quad \text{for } i,j \geq 0 \ .
\end{aligned}$$

Note that the inclusion process is in fact part of this family.

Another natural extension of the zero-range process is to allow for the movement of more than a single particle in each transition. Evans et al. [48] proposed such a generalisation of the zero-range process, called a 'Mass Transport Model'. The model includes the case of continuous local state space, where $\eta_x \in \mathbb{R}_+$ is associated with the mass on site x. The dynamics are defined by a probability distribution, $\varphi(m|\eta_x)$,

on the mass m that leaves a site given the current occupation is η_x. Necessary and sufficient conditions for the existence of product stationary measures in these processes have been investigated [49, 63, 132]. It turns out the system still exhibits product stationary measures, provided the jump rates satisfy certain constraints. For the totally asymmetric case in one dimension and with discrete mass, where a mass m jumps from site x to site $x+1$ with rate $g(m|\eta_x)$, a necessary and sufficient condition for the existence of product stationary measures is given by,

$$g(m|\eta_x) = \frac{f(m)w(\eta_x - m)}{w(\eta_x)} \ ,$$

where f and w are non-negative functions (it turns out that the w are the corresponding single site weights). This result has been generalised to higher dimensions in [63] and to continuous mass in [49, 132].

Another class of continuous mass models, with unbounded local state space, is given by a system of interacting diffusions called the Brownian energy process and the related Brownian Momentum process [57]. These are lattice systems with local state space give by $\mathbb{R}_+$. It turns out that the Brownian energy process is dual (in the sense of Liggett [95] Definition 3.1) to the inclusion process defined in Section 2.2.3. It has been observed that these systems can also exhibit a condensation transition [70]. The generator of the Brownian energy process is given by

$$\mathcal{L}_L f(\boldsymbol{\eta}) = \sum_{x,y\in\Lambda_L} p(x,y)\eta_x\eta_y \left(\frac{\partial}{\partial\eta_x} - \frac{\partial}{\partial\eta_y}\right)^2 - d_L p(x,y)(\eta_x - \eta_y)\left(\frac{\partial}{\partial\eta_x} - \frac{\partial}{\partial\eta_y}\right) \ ,$$

for $\boldsymbol{\eta} \in \mathbb{R}_+^{\Lambda_L}$ and d_L and p as in Section 2.2.3.

2.3 Equivalence of ensembles and condensation

A **condensation transition** is said to occur when a non-zero fraction of all the particles typically accumulate on a single lattice site (or vanishing volume fraction). This phenomenon has been the subject of recent research interest, as an interesting class of phase transitions that can occur even in one dimensional systems. As suggested in Section 2.2.2, condensation transitions in particle systems with unbounded local state space can be interpreted as 'jamming' transitions in exclusion models with long-range interactions. To be more specific we discuss details of the transition in the context of the homogeneous zero-range process, however this class of transitions is not restricted to this model (as is observed in Chapter 6). Condensation due to spatial inhomogeneities has been studied for zero-range processes in [9, 45], in relation to jamming in exclusion models [87], and in models with a single defect site [3].

Condensation can occur in a homogeneous zero-range process if the jump rates $g(n)$ asymptotically decay with the number of particles n. In terms of the exclusion process representation in Section 2.2.2 this would correspond to long range dependence of the

jump rates. A prototypical model with rates

$$g(n) = 1 + \frac{b}{n^\gamma} \quad \text{for } n = 1, 2, \dots \tag{2.35}$$

has been introduced in [42], where condensation occurs for parameter values $\gamma \in (0, 1)$, $b > 0$ or $\gamma = 1$, and $b > 2$. If the particle density ρ exceeds a critical value ρ_c, the system phase separates into a homogeneous background (fluid phase) with density ρ_c and a condensate (condensed phase), where the excess particles accumulate on a single randomly located lattice site. This transition has been established on a rigorous level in a series of papers [4, 5, 69, 80] for the thermodynamic limit, as well as on a finite system as the total number of particles diverges [52]. Dynamic aspects of the transition such as equilibration and coarsening [59, 69] and the stationary dynamics of the condensate [61] are well understood heuristically. For the latter first rigorous results have been achieved recently [8]. In this work it was shown that on a finite system as the particle number diverges the time dependent location of the condensate converges to an effective Markov process, and they were able to calculate the transition rates in the case of reversible dynamics.

2.3.1 Equivalence of ensembles

By choice of the jump rates (2.35) the grand canonical single site partition function $z(\mu)$ (see (2.14)) turns out to converge on the boundary of its domain, and its first derivative is finite. This implies that the average density under the grand canonical measures is increasing on $(-\infty, \mu_c]$ and $\rho_c = R(\mu_c) < \infty$ (see (2.16)). So the grand canonical measures exist only for densities up to (and including) ρ_c, and product stationary distributions do not exist with higher average density. The grand canonical measure with average density ρ_c is referred to as the 'critical measure', and the critical single site marginals decay sub-exponentially,

$$\lim_{n\to\infty} \frac{1}{n} \log \nu_{\mu_c}[n] = 0 \ .$$

Since $R(\mu)$ is strictly increasing on $(-\infty, \mu_c]$ it is invertible, and we denote the inverse by $\mu(\rho)$ (with slight abuse of notation). In this way we can parametrise the grand canonical measures by densities $\rho \in [0, \rho_c]$. We extend this function to higher densities by fixing the chemical potential constant at μ_c,

$$\bar{\mu}(\rho) = \begin{cases} \mu(\rho) & \text{for } \rho \le \rho_c \\ \mu_c & \text{for } \rho > \rho_c \ . \end{cases} \tag{2.36}$$

The first rigorous results on the equivalence of ensembles were given in [69]. This can be stated in terms of the relative entropy (see Appendix A) as in the following theorem.

Theorem 2.7. *Let $\bar{\mu}$ be defined as in (2.36). Then the specific relative entropy between $\pi^L_{\lfloor \rho L \rfloor}$ and $\nu^L_{\bar{\mu}(\rho)}$ asymptotically vanishes,*

$$\lim_{L\to\infty} \frac{1}{L} H(\pi^L_{\lfloor \rho L \rfloor} \mid \nu^L_{\bar{\mu}(\rho)}) = 0 \ .$$

For $x \in \mathbb{R}_+$ we denote the largest integer less than x by $\lfloor x \rfloor$ (the integer floor).

Proof. See proof of Theorem 1 in [69]. □

Convergence in relative entropy implies weak convergence of the canonical measures to the grand canonical measure on finitely many lattice sites. We generalise this concept of equivalence of ensembles in Chapter 3 in order to deal with more refined scaling limits and generalized models with size-dependent parameters. This result implies that below ρ_c the canonical measures converge locally to the grand canonical measures. Above the critical density the canonical measures converge locally to a product of the critical grand canonical marginals, with density ρ_c, and the excess mass accumulates on a vanishing volume fraction.

2.3.2 Condensation

Further to the equivalence of ensembles and phase separation, it has been proved that the condensed phase occupies only a single lattice site [69] which is located uniformly at random on the lattice and typically contains all of the excess mass. The result can be stated in terms of the normalised maximum site occupation which satisfies a weak law of large numbers,

$$M_L := \frac{1}{L} \max_{x\in\Lambda_L} \eta_x \xrightarrow{\pi^L_{\lfloor \rho L \rfloor}} (\rho - \rho_c) \quad \text{as } L \to \infty \ ,$$

where $\xrightarrow{\pi^L_{\lfloor \rho L \rfloor}}$ denotes convergence in probability, i.e.

$$\pi^L_{\lfloor \rho L \rfloor} \left[|M_L - (\rho - \rho_c)| > \epsilon \right] \to 0 \quad \text{as } L \to \infty \ .$$

The equivalence of ensembles in the case of supercritical densities $\rho > \rho_c$, for the bulk of the system after removing the maximum component was strengthened by Armendáriz and Loulakis [4] (with partial results already in [80]). Here it was shown that, after removing the condensate, the canonical measure converges in total variation to the critical grand canonical measures on the rest of the system. This result was first shown for a fixed number of sites as the total number of particles diverges [52]. To state the result we define the cut operator that removes the maximum occupied site, $C : X_L \to$

X_{L-1},

$$(C(\boldsymbol{\eta}))_x = \begin{cases} \eta_x & \text{if } x < i(\boldsymbol{\eta}), \\ \eta_{x+1} & \text{if } x \geq i(\boldsymbol{\eta}) \ , \end{cases} \tag{2.37}$$

where $i(\boldsymbol{\eta})$ is the (smallest) index of the lattice site containing the maximum. Then the strong form of equivalence of ensembles above the critical density can be stated as,

$$\text{For each } \rho > \rho_c, \qquad \left\| \pi^L_{\lfloor \rho L \rfloor} \circ C^{-1} - \nu^{L-1}_{\mu_c} \right\|_{\text{T.V.}} \to 0 \quad \text{as } L \to \infty \ ,$$

where $\|\cdot\|_{\text{T.V.}}$ is the total variation norm, defined in (A.4). This gives rise to fluctuations of the maximum, which have already been studied in [80], heuristically in [59], and using saddle point calculations in [47]. It has been shown that in the condensed regime $\rho > \rho_c$, if the critical grand canonical measure has finite variance, the fluctuations of the maximum are Gaussian, otherwise they are given by a completely asymmetric stable law. For $\rho \leq \rho_c$ the fluctuations are given by standard extreme value statistics for maxima of independent random variables [47], and the transition between different distributions at the critical point has been studied recently in [5].

2.4 Metastability

Metastability is a generic dynamic phenomenon that is typically observed in the presence of first order phase transitions. Classical examples being the existence of supersaturated vapour at the liquid-gas transition of water, and magnetic systems with magnetization opposite to the external field. Metastability is rather well understood on a heuristic level, however a mathematically rigorous description is an active field in modern probability theory and mathematical physics. Several different approaches are summarized in [107], Chapter 4 and [17, 36]. Metastability is characterised by the existence of two or more well separated time scales. On a fast time scale the system relaxes to an apparently stable state and appears to be in equilibrium, but in fact only explores a significantly restricted portion of the phase space. On a much longer time scale, a spontaneous fluctuation or external perturbation, causes the system to escape from the restricted state space and quickly relax to another stable state. In the models we study the origin of the perturbation that triggers the transition is the randomness in the underlying dynamics.

We are typically interested in the limiting behaviour of finite state irreducible Markov processes as the system size grows. In this case we have unique stationary measures for each canonical system. However, we observe that for suitable initial conditions, the system may behave as if it were described by another stationary distribution, until on the larger time scale it tunnels to a globally stable state. There are, therefore, two aspects of the metastability phenomena that are relevant. Firstly, the concentration points of the stationary measure and corresponding bottle necks that give rise to the metastable states. We characterize these rigorously in terms of local minima (and maxima) of large

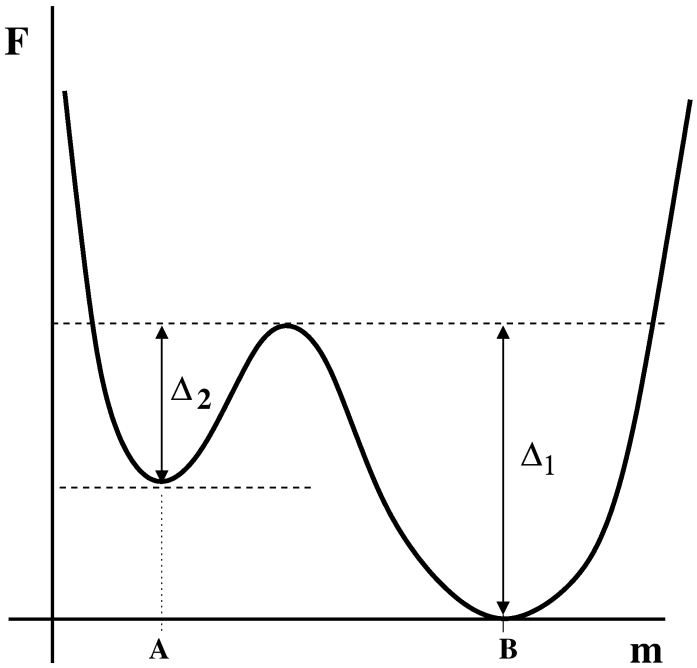

Figure 2.2: Free energy landscape with a double well.

deviation rate functions for the relevant observable, which in case of condensation is the maximum site occupation M_L. This large deviation rate function has the interpretation of the usual free energy function in equilibrium statistical mechanics, such as in van der Walls-Maxwell theory (see for example [107, 109]). Secondly, the dynamics that describe the metastable switching on the reduced state space of local minima. This is in general a much more challenging problem to treat rigorously, and here we make heuristic arguments to derive the relevant time scales and typical paths for transitions between metastable states. We outline our approach below.

In this thesis we define metastable states by local minima of the free energy function (large deviation rate functions defined in Section 3), and observe the following characterizing features:

1. The lifetime is very large in the sense that a system that starts in this minimum will take a long time to escape.

2. The decay from metastable states (local, non-global minima) to the globally stable states is irreversible in the sense that the scale of the return time is larger than the decay time.

3. The (normalised) escape time from the metastable states is asymptotically exponentially distributed so the coarse grained system (the dynamics on the metastable states) is asymptotically Markovian.

This is in direct analogy with metastability in equilibrium systems, in particular those with long range interactions, where metastable states are associated with local minima of the free energy (see Chapter 4 in [107]).

The relevant time scales associated with the metastable states can be predicted heuristically in terms of an Arrhenius law [82]. Based on a simple diffusion approximation in the potential given by the free energy landscape, one finds that the escape rate out of a valley grows exponentially with the system size, with rate given by the height of the barrier. For example in Fig. 2.2 the expected time to escape from valley A grows with system size L as,

$$\mathbb{E}[\tau_L] \sim e^{L\Delta_2} \ .$$

This is essentially the result of a Laplace approximation, and a detailed calculation is given in Section 4.5. This long time scale diverges with the system size, and the asymptotic rescaled transition times are found to be exponential random variables. Heuristically, one can argue that the exit times will be exponentially distributed based on a simple renewal argument. Starting in the valley with minimum A, the relaxation time scale inside the valley is much smaller than the time scale associated with the escape from the valley. Therefore the mean time to escape is independent of the initial starting point in the valley, and the process will return to the minimum of the valley many times before it finally exits. So the return times to the point A are independent identically distributed (i.i.d.) random variables, and the probability of escaping between each return is constant. The eventual escape from the valley is therefore happening after a geometric number of independent 'trials', and the scaled exit time will therefore be exponential,

$$\frac{\tau_L}{\mathbb{E}[\tau_L]} \sim Exp(1) \ .$$

This leads to an effective Markovian description of the system on a highly reduced state space, defined by the points of local minima of the free energy function (or large deviation rate function).

We may also predict the typical path that the process takes conditioned on escaping from a metastable state, based on similar scaling arguments that give rise to the Arrhenius law. We assume that relevant observables, such as the macroscopic size of the maximum site occupation M_L, change by a microscopic amount (an amount that is decreasing with the system size) when a single particle moves, and that the stationary large deviations are described by a free energy landscape F. Then, the dynamics of such an observable on the large (tunneling) time scale τ_L are approximated by a diffusive process in a potential that is given by F. We may write this approximation in differential form as

$$dM_L(t/\tau_L) = -\nabla F(M_L(t/\tau_L))dt + \epsilon_L dB_t \ . \tag{2.38}$$

Here ϵ_L is a small parameter that results from taking a diffusive scaling limit, as the system size and large time scale diverge, and B_t is a Brownian motion (or white noise). The large deviations in such a system, around the deterministic solution (without the white noise), are well understood since the pioneering work of Freidlin and Wentzell on metastability in dynamical systems with small random perturbations [100]. In this

context they were able to derive a large deviation principles on path space. It was shown that the measure on path space induced by this process satisfies a large deviation principle with speed ϵ_L^{-2} and rate function (or 'action'),

$$A(\psi) = \frac{1}{2}\int_0^T \left|\dot{\psi}(s) - \nabla F(\psi(s))\right| \, \mathrm{d}s \ .$$

This defines a minimum action principle for the probability of observing a certain path $M_L(t/\tau_L) = \psi(t)$ between metastable states. Roughly speaking this result states that the most likely exit path from one metastable state to another is given by the steepest accent/decent path over the lowest saddle point between the two states. This result gives rise to the typical path observed in Section 5.4. A rigorous path-wise treatment of metastability in stochastic particle systems was also introduced in [23] which is based on an analysis of empirical averages along typical trajectories.

We introduce a class of restricted ensembles as a tool to calculate non convex rate functions in Section 3 (for a review of methods of calculating non convex rate functions, including by restricted ensembles, see [119]). These also give rise to generalisations of thermodynamic functions such as the grand canonical pressure, which in many cases correspond to the analytic extension of such functions. These in turn can be associated with metastable states in the canonical system. It is natural to consider the stationary measures restricted to the valleys that define the metastable states. A analogous approach by Penrose and Lebowitz [109],[108] gives rise to rigorous results in the case of van der Waals-Maxwell theory. The restricted ensembles also have a dynamical interpretation, in that on the time scale that the system remains in a metastable state it behaves (asymptotically on a large system) as if the stationary measures were given by the grand canonical measures restricted to that valley. In this way we may identify metastable distributions to the valleys in terms of restricted measures.

This is one of the simplest choices to associate measures with metastable states and is sufficient for our heuristic approach. Recently, so-called quasi stationary distributions have been connected with metastable states in a rigorous approach [10]. These distributions are stationary for a process which is conditioned on not leaving the metastable state. This dynamic definition on path space makes quasi-stationary distributions hard to compute explicitly, but they have a few nice properties which are advantageous in rigorous approaches (see e.g. [51]).

Our large deviation estimates and insight into the dynamics could help to formulate a rigorous treatment of dynamic aspects of metastability in these systems. Currently the most promising methods for a rigorous treatment, in the case of reversible systems, is provided by a potential theoretic approach developed in [18, 19], using systematically the concept of capacities to prove sharp estimates on transition times between metastable states. This has been applied to describe metastability in disordered spin systems or kinetic Ising models (see [20] and references therein). Recently, the metastable dynamics of the condensate in zero-range condensation restricted to finite lattices has been addressed using these technique [7, 8].

Chapter 3

Entropy methods and equivalence of ensembles

3.1 Introduction

In this chapter we introduce a general approach for understanding the role of finite size effects and metastability in interacting particle systems that exhibit a condensation transition. We use techniques from large deviation theory to prove results on equivalence of ensembles as well as finding the saddle point landscape that describes the distribution of the maximum site occupation. This landscape allows us to calculate the relevant time scales, of the metastable motion of the condensate, and the switching between fluid and condensed states. We apply these techniques to three examples in the following chapters; finite-size effects in the standard condensing zero-range process [25], a size-dependent zero-range process introduced in [66] and the recently introduced inclusion process [70].

We adopt a large deviation and entropy approach to the equivalence of ensembles similar to that of the work by Lewis, Pfister and Sullivan [90, 91, 92, 93]. However, we consider canonical (conditioned) measures for which we condition on the density being a specific value rather than conditioning on density 'shells'. We focus on such point-wise conditioning because these correspond physically to the asymptotic long time behaviour of a finite system prepared with a fixed number of particles, rather than fixing the number of particles to be in some range. This is also a more natural restriction for simulating the process. Due to the point-wise nature of the condition, we use local limit results to strengthen the large deviation estimates.

We also extend the equivalence of ensembles results to cover equivalence between the canonical measures and restricted grand canonical measures. The restricted ensemble shares the advantages of the grand canonical ensembles to be of product form, so that it is much easier to analyse than the canonical measures themselves. Restricted ensembles have been introduced previously, for example in [108, 109], as a tool to calculate the analytic extension of thermodynamic functions related to metastable decay rates. They have also been used as a tool to study thermodynamic properties of glassy systems [37] and metastable dynamics [107]. We show that the restricted ensemble is intimately

related to the large deviations of the maximum. It turns out that the rate functions associated with the large deviations of the maximum site occupation are straightforward to calculate given this relationship with the restricted ensembles. The full canonical entropy density can then be calculated by a contraction principle. This leads to a full description of the equivalence of ensembles.

We observe that for high particle densities the canonical entropy density is given by the sum of a contribution due to a homogeneous background (fluid phase) and a contribution due to a single site carrying a macroscopic proportion of the total mass (condensed phase), which is attributed to the phase separation explained in Section 2.3.2. These results are in many ways analogous to droplet formation in spin systems such as the Ising model [11, 12]. However, in that case there are boundary terms associated with the typical geometry of the droplet (known as the Wulff-shape [38]), whereas due to the product nature of the stationary measures there is no interface contribution to the entropy density in our models.

The results in this chapter generalise previous work on the equivalence and non-equivalence of ensembles, using entropy methods, in systems with product stationary measures such as in [69]. We also extend previous results by finding the full potential landscape for the maximum under the canonical measures, which is important in condensing systems and characterises the metastable behaviour (for example see Chapter 5). The results also cover scaling regimes, different from the thermodynamic limit, so allowing for a systematic analysis of finite-size effects (see Chapter 4).

The large deviation and entropy methods in statistical mechanics are typically applied to models with compact state space, for example $\{-1, 1\}$, however we focus on a unbounded (hence non-compact) local state space $\mathbb{N} = \{0, 1, \ldots\}$. This gives rise to the possibility of non-concave canonical entropy densities that are not equal to the necessarily concave grand canonical entropy densities. The method we adopt for calculating the non-concave entropies, namely contracting on the maximum site occupation, is particularly suited to these systems because the breakdown of equivalence of ensembles is associated with a macroscopic number of particles accumulating on a single lattice site. This fits into a general class of methods for calculating non-concave entropies, known as the micro-canonical contraction [119]. Another method, which can also give rise to the full canonical entropy density, is to introduce a *generalised* grand canonical distribution [28, 29, 30]. However, this is much less suited to the case of condensation discussed here, and does not give rise to the free energy landscape of the maximum under the canonical measures.

3.2 Definitions

3.2.1 State space and reference measures

In this section we set some more specific notation that will be used in the rest of thesis with a particular emphasis on a flexible notion of scales which will be different for the particular applications in later Chapters.

We consider systems whose local state space $E = \mathbb{N}$, which we endow with the Borel σ-algebra. The results of this chapter can also be extended to systems with continuous local state space $\mathbb{R}_+$ with only a small amount of extra work, see the discussion in Section 3.6. We consider an increasing sequence of lattices Λ_L of $\mathbb{Z}^d$ such that $|\Lambda_L| = L$. For example in applications we often consider the one dimensional lattice of L sites $\Lambda_L = \{1, 2, \dots, L\} \subset \mathbb{Z}$. The product space X_L is then endowed with the standard product σ-algebra $\mathcal{F}_{\Lambda_L}$. As before, for a given site $x \in \Lambda_L$ we interpret an element of the local state space $\eta_x \in X_x$ as the number of particles on site x and a full configuration on Λ_L is given by $\boldsymbol{\eta} = (\eta_x)_{x\in\Lambda_L} \in X_L$.

We assume that there exists a sequence of reference probability measures such that $(X_L, \mathcal{F}_{\Lambda_L}, \nu^L)$ is a probability space. In general ν^L is a stationary measure of the process of interest defined on X_L, however this section is presented independently of any dynamics and we see in the following chapters how these results can be applied to various interacting particle systems. We assume throughout that the reference measure is product and permutation invariant, and we may therefore express ν^L as a product of single site marginals,

$$\nu^L[\boldsymbol{\eta}] = \prod_{x\in\Lambda_L} \nu[\eta_x] \ , \quad \forall \boldsymbol{\eta} \in X_L \ . \tag{3.1}$$

These marginals may still depend on the size of the system, and in this case we stress the dependence with a subscript L, $\nu = \nu_L$.

Let $S_L : X_L \to \mathbb{R}_+$ be a sequence of random variables corresponding to the empirical density of a state or the empirical rescaled density. We equip $\mathbb{R}_+$ with the standard Borel σ-algebra so that all test functions we consider, including S_L, are measurable functions. The density is defined on a scale $b_L \to \infty$ as $L \to \infty$.

Definition 3.1 (Empirical density)**.** $S_L : X_L \to \mathbb{R}_+$ is the empirical density on a scale (b_L), such that $b_L \to \infty$ as $L \to \infty$,

$$S_L(\boldsymbol{\eta}) = \frac{1}{b_L} \sum_{x\in\Lambda_L} \eta_x \ .$$

(b_L) represents the rate at which we consider the total mass in the system $\sum_{x\in\Lambda_L} \eta_x$ to be increasing with the system size L. In the normal thermodynamic limit $b_L = L$ and S_L is the total number of particles divided by the system size. However, the methods in this chapter apply to rather general b_L and also to re-centred (not necessarily positive)

versions of S_L. This is discussed at the end of this chapter 3.6 and applied to the scaling limit studied in Chapter 4.

3.2.2 Grand canonical (tilted) measures

In this section we introduce the exponentially tilted measures which remain of product form and are normally referred to as the *grand canonical measures*. Under the grand canonical measures the average of S_L is fixed by a conjugate parameter μ called the *chemical potential*. We define the pressure in terms of the Laplace transform of the random variable S_L.

Let (a_L) be a sequence of positive real numbers diverging to $+\infty$ as $L \to \infty$. We refer to (a_L) as the *thermodynamic scale*, it is the scale on which we find large deviations of the density S_L under the reference measure, which gives rise to the canonical entropy density (see Section 3.2.4). In the usual thermodynamic limit this scale is given by the total volume of the system, $a_L = L$. It turns out that $a_L \ll L$ may give rise to more refined results on the equivalence of ensembles (see Section 3.3 for more details).

Definition 3.2 (Grand canonical pressure)**.** At the *thermodynamic scale* (a_L) the grand canonical pressure $p : \mathbb{R} \to \mathbb{R} \cup \{-\infty, \infty\}$ is given by the scaled generating function,

$$p(\mu) = \lim_{L\to\infty} \frac{1}{a_L} \log \nu^L \left(e^{a_L \mu S_L}\right) \tag{3.2}$$

$$= \lim_{L\to\infty} \frac{1}{a_L} \log \sum_{\boldsymbol{\eta}\in X_L} e^{a_L \mu S_L(\boldsymbol{\eta})} \nu^L[\boldsymbol{\eta}] \ . \tag{3.3}$$

The extended real valued function p is assumed to always exist, but is not necessarily finite. The *essential domain* of p is given by,

$$\mathcal{D}_p = \{\mu \in \mathbb{R} : p(\mu) \in \mathbb{R}\} \ . \tag{3.4}$$

For all $\mu \in \mathcal{D}_p$, we have

$$0 < \nu^L \left(e^{a_L \mu S_L}\right) < \infty$$

for all L sufficiently large. For these values of the chemical potential we define the grand canonical measures.

Definition 3.3 (Grand canonical measures)**.** For $\mu \in \mathcal{D}_p$,

$$\nu_\mu^L[\boldsymbol{\eta}] = \frac{e^{a_L \mu S_L(\boldsymbol{\eta})}}{\nu^L \left(e^{a_L \mu S_L}\right)} \nu^L[\boldsymbol{\eta}] \ . \tag{3.5}$$

The grand canonical measures are absolutely continuous with respect to the reference measures and their density is given by,

$$\frac{\mathrm{d}\nu_\mu^L}{\mathrm{d}\nu^L}(\boldsymbol{\eta}) = \frac{e^{a_L \mu S_L(\boldsymbol{\eta})}}{\nu^L \left(e^{\mu a_L S_L}\right)} \ . \tag{3.6}$$

The grand canonical measures share the product nature of the reference measures, and their marginals are the same for all sites. So we can write them in terms of their single site marginals such that $\nu^L = \prod_{x\in\Lambda_L} \nu_{L,\mu}$ where,

$$\nu_{L,\mu}[\eta_x] = \frac{e^{(a_L b_L^{-1}\mu)\eta_x}}{\nu_L\left(e^{(a_L b_L^{-1}\mu)\eta_1}\right)}\nu_L[\eta_x] \ . \tag{3.7}$$

The normalisation in Definition 3.3 is called the *grand canonical partition function* and the normalisation for the single site marginals is called the single site grand canonical partition function.

Definition 3.4 (Grand canonical partition function)**.** For $\mu \in \mathcal{D}_p$,

$$\mathcal{Z}(L,\mu) = \nu^L\left(e^{a_L\mu S_L}\right) \tag{3.8}$$

$$= (z_L(\mu))^L \tag{3.9}$$

where the single site grand canonical partition function is given by the exponential moment

$$z_L(\mu) = \nu_L\left(e^{(a_L b_L^{-1}\mu)\eta_1}\right) \ . \tag{3.10}$$

Notice that for the standard results on equivalence ensembles in the thermodynamic limit we have $a_L = L$ and $b_L = L$ and these two terms cancel in the previous definition of the single site partition function. The grand canonical pressure can be rewritten in terms of the grand canonical partition functions,

$$p(\mu) = \lim_{L\to\infty} \frac{L}{a_L}\log z_L(\mu) \ .$$

We denote the pressure on a finite system as

$$p_L(\mu) = \frac{L}{a_L}\log z_L(\mu) \ . \tag{3.11}$$

Notice that the expected value of the empirical density S_L under the grand canonical measures is given by the first derivative of the pressure, $\partial_\mu p_L(\mu) = \nu_\mu^L(S_L)$.

In applications S_L is conserved by the microscopic dynamics. It follows that if the reference measures are stationary then so are the grand canonical measures, since they have density with respect to reference measures that is only a function of S_L.

3.2.3 Restricted grand canonical measures

In this section we introduce the restricted ensembles which are given by conditioning the grand canonical measures on a certain local restriction. The conditioning is done in such a way as to preserve the product nature of the measures, however these measures are in general not stationary for the underlying microscopic dynamics in applications.

The idea of restricted ensembles in the study of metastability was first discussed in the rigorous treatment of metastable states in van der Waals-Maxwell theory [109]. They have also been applied to finding the analytic continuation of thermodynamic functions, as they relate to metastability, in [108]. More recently the idea has been applied to the study of the equations of state for a model of glass [37].

We find that it is natural to restrict the grand canonical measures to configurations for which the maximum site occupation is less than some cut-off value. This restriction is always made on the same scale as we defined the empirical density, namely (b_L). We therefore introduce the following random variable that gives the macroscopic size of the maximum single site occupation number.

Definition 3.5. On the same scale (b_L) as in Definition 3.1 we let,

$$M_L(\boldsymbol{\eta}) = \frac{1}{b_L} \max_{x \in \Lambda_L} \eta_x \ . \tag{3.12}$$

We define the restricted grand canonical pressures as the scaled cumulant generating function of S_L under $\nu^L[\boldsymbol{\eta} \mid M_L \leq m_L]$. It turns out that these are analytic extensions of the grand canonical pressures, see Corollary 3.9.

Definition 3.6 (Restricted pressure)**.** Fix a sequence m_L such that $m_L \to m \in \mathbb{R}$. At the thermodynamic scale (a_L) the restricted grand canonical pressure $p_m : \mathbb{R} \to \mathbb{R} \cup \{-\infty, \infty\}$ is given by the scaled cumulant generating function,

$$p_m(\mu) = \lim_{L \to \infty} \frac{1}{a_L} \log \nu^L \left(e^{a_L \mu S_L} \mathbb{1}_{M_L \leq m_L} \right) \tag{3.13}$$

It turns out that under fairly weak assumptions the limit is independent of details of the sequence $m_L \to m$ and depends only on m (see assumptions in Section 3.4.1). We may now define the restricted grand canonical measures.

Definition 3.7 (Restricted ensemble)**.** For a sequence $m_L \to m$ and for $\mu \in \mathcal{D}_{p_m}$,

$$\begin{aligned} \bar{\nu}^L_{\mu,m}[\boldsymbol{\eta}] &= \nu^L_\mu[\boldsymbol{\eta} \mid M_L \leq m_L] \\ &= \frac{e^{a_L \mu S_L(\boldsymbol{\eta})} \mathbb{1}_{\{M_L \leq m_L\}}(\boldsymbol{\eta})}{\nu^L \left(e^{a_L \mu S_L} \mathbb{1}_{\{M_L \leq m_L\}} \right)} \nu^L[\boldsymbol{\eta}] \\ &= \prod_{x \in \Lambda_L} \frac{\nu_L[\eta_x] e^{(a_L b_L^{-1})\eta_x}}{\bar{z}_{L,m}(\mu)} \mathbb{1}_{\{\eta_x \leq m_L b_L\}}(\eta_x) \ , \end{aligned} \tag{3.14}$$

where the single site normalisation is given by $\bar{z}_{L,m}(\mu) = \nu_L \left(e^{(a_L b_L^{-1})\eta_1} \mathbb{1}_{\{\eta_x \leq m_L b_L\}}(\eta_1) \right)$. We write,

$$\bar{\nu}^L_m = \bar{\nu}^L_{0,m} \ .$$

Equation (3.14) shows that $\bar{\nu}^L_{\mu,m}$ is absolutely continuous with respect to both the reference measures and the grand canonical measure. Note that the restriction on the maximum being less than $m_L b_L$ is equivalent to restricting each site to contain no more

than $m_L b_L$ particles, which is a local restriction, so the measures remain of product form. It follows that the partition function for the restricted ensemble is simply given by the product of the single L site normalisations

$$\bar{z}_m^L(\mu) = \nu^L\left(e^{a_L\mu S_L}\mathbb{1}_{\{M_L\leq m_L\}}\right) = (\bar{z}_{L,m}(\mu))^L \quad \text{where,}$$
$$\bar{z}_{L,m}(\mu) = \sum_{k=0}^{m_L b_L} \nu_L[k]e^{(a_L b_L^{-1})k} \ . \tag{3.15}$$

The expected value of the density under the restricted grand canonical measures is given by the first derivative of the restricted pressure on a finite system,

$$\frac{1}{a_L}\partial_\mu \log \bar{z}_m^L(\mu) = \frac{L}{a_L}\partial_\mu \log \bar{z}_{L,m}(\mu) = \bar{\nu}_{\mu,m}^L(S_L) \ .$$

3.2.4 Canonical (conditioned) measures

In applications we choose S_L such that it is conserved by the microscopic dynamics. In this case the state space decomposes into non-communicating subsets on which S_L is constant,

$$X_{\rho_L}^L = \{\boldsymbol{\eta} \in X_L \mid S_L(\boldsymbol{\eta}) = \rho_L\} \ . \tag{3.16}$$

The microscopic dynamics are ergodic on this reduced state space since the jump process is assumed to be irreducible. The unique stationary measures are given by the reference measures conditioned on S_L and are normally referred to as the *canonical measures*. The canonical measures have correlations that are not present in the grand canonical measures due to the conditioning. This makes them more difficult to study, which is one motivation for seeking rigorous results on equivalence of ensembles.

We may condition ν^L on S_L being in a measurable set C for which $\nu^L[S_L^{-1}(C)] > 0$,

$$\pi_C^L[\boldsymbol{\eta}] = \nu^L[\boldsymbol{\eta} \mid S_L^{-1}(C)] \ . \tag{3.17}$$

In general we consider a sequence of such sets (C_L) for each lattice size L, this sequence must satisfy certain properties in order that we may apply the large deviations approach discussed in this section (following [91, 92, 93] we call such sequences LD-regular, see Appendix C). In the mathematical literature $C = \bigcap_L \bar{C}_L$ is typically taken to be a non-empty open interval in $\mathbb{R}$ (for example see [90]). However, for us it is most natural to condition on the density being a given value, since the canonical measure then corresponds to the typical long time limiting behaviour that is observed when starting from a fixed number of particles on a fixed system size (in the sense of the ergodic theorem [106]). This is also the case that is most straightforward to simulate and corresponds most closely to the physical situation that one would like to describe. We therefore restrict the following analysis to this situation. It turns out that this case is more diffi-

cult to approach rigorously since the most direct way of showing the sequence of sets is LD-regular, based on convexity arguments, relies on C having non-empty interior.

$\nu_L \circ S_L^{-1}$ is a lattice distribution for which the lattice spacing tends to zero as $L \to \infty$, that is,

$$\nu^L[S_L = a] > 0 \quad \iff \quad a \in \frac{1}{b_L}\mathbb{N} = \{0, 1/b_L, 2/b_L, \ldots\} \ .$$

For the canonical measures to be well defined we must condition on events with positive probability under the reference measure. Therefore we can only condition on sequences of densities (ρ_L) such that for each system size $\rho_L b_L \in \mathbb{N}$, that is the total number of particles must be an natural number. Clearly for each $\rho \in \mathbb{R}$ there exists a sequence that satisfies this condition and converges to ρ as $L \to \infty$; for example we may choose $\rho_L = \lfloor \rho L \rfloor / L$.

Definition 3.8 (Canonical measures)**.** For a sequence (ρ_L) satisfying,

$$\rho_L \in \frac{1}{b_L}\mathbb{N} \quad \text{and} \quad \lim_{L\to\infty} \rho_L = \rho \ , \tag{3.18}$$

we define the *canonical measures*,

$$\pi_\rho^L[\boldsymbol{\eta}] = \nu^L[\boldsymbol{\eta} \mid S_L(\boldsymbol{\eta}) = \rho_L] \ . \tag{3.19}$$

It turns out that under fairly weak assumptions (see Section 3.4.1) the limiting behaviour of the canonical measures is independent of the details of the sequence (ρ_L), and depends only on the limit ρ. We therefore tend to drop the subscript L on the density when writing the canonical measures.

The canonical measures are absolutely continuous with respect to reference measure and their density is given by,

$$\frac{\mathrm{d}\pi_\rho^L}{\mathrm{d}\nu^L}(\boldsymbol{\eta}) = \frac{\mathbb{1}_{S_L^{-1}(\rho_L)}(\boldsymbol{\eta})}{\nu^L[S_L^{-1}(\rho_L)]} \ . \tag{3.20}$$

Since the measures are defined on a countable state space we can re-write (3.20) as,

$$\pi_\rho^L[\boldsymbol{\eta}] = \frac{\nu^L[\boldsymbol{\eta}]\, \mathbb{1}_{S_L^{-1}(\rho_L)}(\boldsymbol{\eta})}{\nu^L[S_L^{-1}(\rho_L)]} \ . \tag{3.21}$$

The normalisation constant in (3.20) is called the *canonical partition function*.

Definition 3.9 (Canonical partition function)**.** For ρ_L as in definition 3.8,

$$Z(L, \rho_L) = \nu^L[S_L^{-1}(\rho_L)] = \sum_{\boldsymbol{\eta} \in X_L} \nu^L[\boldsymbol{\eta}]\, \mathbb{1}_{S_L^{-1}(\rho_L)}(\boldsymbol{\eta}) \tag{3.22}$$

We can also define restricted versions of the canonical ensemble in the same way as we defined the restricted grand canonical ensemble.

Definition 3.10 (Restricted canonical measures)**.** For $m_L \to m \in \mathbb{R}_+$ we define the *restricted canonical measures*,

$$\bar{\pi}^L_{\rho,m}[\boldsymbol{\eta}] = \pi^L_\rho[\boldsymbol{\eta} \mid M_L \leq m_L] \ . \tag{3.23}$$

3.3 Entropies and equivalence of ensembles

In this section we define what we mean by equivalence of ensembles and briefly discuss how this relates to other forms of equivalence of ensembles in the literature. We outline how the relative entropy can be related to the difference of entropy densities, this is made formal in Section 3.4.

3.3.1 Equivalence of ensembles

We define equivalence of ensembles in terms of weak convergence of measures. The scale a_L fixes the rate of convergence of the expected value of bounded cylinder test functions. This gives rise to an equivalence relation on sequences of measures which we denote by $\overset{a_L}{\longleftrightarrow}$. We observe in the Subsection (3.3.2) that the relative entropy (Definition A.1) provides a useful way of testing for equivalence on this level. However, convergence in terms of the specific relative entropy does not define an equivalence relation, and since it requires the measures to be absolutely continuous it is often too restrictive (see Corollary 3.13). We observe in Section 3.4 that convergence on the level of entropy densities gives rise to equivalence on the level of measures as defined below. Equivalence on the level of measures is defined in terms of convergence in total variation, see Appendix A (A.4), of finite dimensional marginals (the measures restricted to finite sub lattices).

Definition 3.11 (Equivalence of Ensembles)**.** We say that the family of measures (ensemble) P^L_ρ is equivalent to the family of measures (ensemble) Q^L_μ on thermodynamic scale (a_L) if for each ρ there exists a $\mu(\rho)$ such that all finite dimensional marginals converge in total variation faster than $\sqrt{a_L/L}$. For each fixed finite sub-lattice $\Lambda \subset \mathbb{Z}^d$

$$\sqrt{\frac{L}{a_L}} \left\| P^{L,\Lambda}_\rho - Q^{L,\Lambda}_{\mu(\rho)} \right\|_{\text{T.V.}} \to 0 \quad \text{as} \quad L \to \infty \ , \tag{3.24}$$

where $P^{L,\Lambda}_\rho$ and $Q^{L,\Lambda}_{\mu(\rho)}$ are, respectively, the finite dimensional marginals of P^L_ρ and $Q^L_{\mu(\rho)}$ restricted to $\mathbb{N}^\Lambda$. We introduce the following notation for equivalence of two measures on this level;

$$P^L_\rho \overset{a_L}{\longleftrightarrow} Q^L_{\mu(\rho)} \quad \text{if and only if (3.24) holds.}$$

In particular if $a_L = L$ Definition 3.11 reduces to convergence in total variation of all finite dimensional marginals. However if $a_L \ll L$ then the total variation distance tends to zero faster than $\sqrt{a_L/L}$.

Remark 3.1. Since the local state space is countable convergence in total variation of finite dimensional marginals is equivalent to convergence of bounded cylinder test functions. A cylinder test function depends on the configuration only on a finite number of sites, the set of bounded cylinder test functions is denoted by C_0^b. It is straightforward to check that

$$P_\rho^L \overset{a_L}{\longleftrightarrow} Q_{\mu(\rho)}^L \quad \text{if and only if} \quad \sqrt{\frac{L}{a_L}} \left| P_\rho^L(f) - Q_{\mu(\rho)}^L(f) \right| \to 0 \quad \text{as} \quad L \to \infty \,, \tag{3.25}$$

for every bounded cylinder test function $f \in C_0^b$.

Remark 3.2. The speed of convergence in Definition 3.11 also implies that the expected value of test functions that are not uniformly bounded in L, still converge, so long as their supreme grows no faster than $\sqrt{L/a_L}$. This is particularly important for proving convergence of certain observables, such as the average current, in the finite-size scaling limit discussed in Chapter 4. We may express the total variation distance of $P_\rho^{L,\Lambda}$ to $Q_{\mu(\rho)}^{L,\Lambda}$ as

$$\left\| P_\rho^{L,\Lambda} - Q_{\mu(\rho)}^{L,\Lambda} \right\|_{\text{T.V.}} = \frac{1}{2} \sum_{\boldsymbol{\eta} \in \mathbb{N}^\Lambda} \left| P^{L,\Lambda}[\boldsymbol{\eta}] - Q^{L,\Lambda}[\boldsymbol{\eta}] \right|$$

(see Appendix A). So for a sequence of cylinder functions $f_L : \mathbb{N}^\Lambda \to \mathbb{R}$ such that $\|f_L\|_\infty < C\sqrt{L/a_L}$ we have,

$$\left| P_\rho^L(f_L) - Q_{\mu(\rho)}^L(f_L) \right| \leq 2C \sqrt{\frac{L}{a_L}} \left\| P^{L,\Lambda} - Q^{L,\Lambda} \right\|_{\text{T.V.}} .$$

So,

$$P_\rho^L \overset{a_L}{\longleftrightarrow} Q_{\mu(\rho)}^L \quad \Longrightarrow \quad \left| P_\rho^L(f_L) - Q_{\mu(\rho)}^L(f_L) \right| \to 0 \quad \text{as} \quad L \to \infty \,. \tag{3.26}$$

3.3.2 Relative entropy and entropy densities

We test for equivalence of ensembles in terms of the specific relative entropy between the canonical and grand canonical measures. Recall that the specific relative entropy of measure π with respect to ν is given by

$$H(\pi \mid \nu) = \begin{cases} \int_\Omega \log \frac{\mathrm{d}\pi}{\mathrm{d}\nu}(w) \pi[\,\mathrm{d}w] & \pi \ll \nu, \\ +\infty & \text{otherwise} \,, \end{cases} \tag{3.27}$$

where $\pi \ll \nu$ means π is absolutely continuous with respect to ν. For countable state space Ω we may write,

$$H(\pi \mid \nu) = \sum_{w \in \Omega} \pi[w] \log \frac{\pi[w]}{\nu[w]} \,.$$

Lemma 3.3. *If the specific relative entropy, on the scale* (a_L)*, of two sequences of probability measures* P_ρ^L *and* $Q_{\mu(\rho)}^L$ *on* X_L *(such that* $P_\rho^L \ll Q_{\mu(\rho)}^L$*) satisfies*

$$\lim_{L\to\infty} \frac{1}{a_L} H(P_\rho^L \mid Q_{\mu(\rho)}^L) = 0 \ , \tag{3.28}$$

then the two measures are equivalent in the sense that they satisfy (3.24)*.*

Proof. This result follows from sub-additivity and positivity of the relative entropy, and the Kemperman-Pinsker inequality (see Appendix A).

Fix some finite sub-lattice Λ, of exactly n sites, so that for $L > n$ we have $\Lambda \subset \Lambda_L$. We denote the marginals, restricted to $\mathbb{N}^\Lambda$, by $P^{L,\Lambda}$ and $Q^{L,\Lambda}$. Let Λ_1 and Λ_2 be disjoint copies of Λ such that $\Lambda_1 \cup \Lambda_2 \subset \Lambda_L$ for $L > 2n$. Then, by sub-additivity (A.2)

$$H(P^{L,\Lambda_1\cup\Lambda_2} \mid Q^{L,\Lambda_1\cup\Lambda_2}) \geq H(P^{L,\Lambda_1} \mid Q^{L,\Lambda_1}) + H(P^{L,\Lambda_2} \mid Q^{L,\Lambda_2}) \ . \tag{3.29}$$

By translation invariance $H(P^{L,\Lambda_1} \mid Q^{L,\Lambda_1}) = H(P^{L,\Lambda_2} \mid Q^{L,\Lambda_2})$ so that

$$H(P^L \mid Q^L) \geq \left\lfloor \frac{L}{n} \right\rfloor H(P^{L,\Lambda} \mid Q^{L,\Lambda}) \geq 0 \ . \tag{3.30}$$

So, $\lim_{L\to\infty} \frac{1}{a_L} H(P^L \mid Q^L) = 0$ implies that

$$\lim_{L\to\infty} \frac{L}{a_L} H(P^{L,\Lambda} \mid Q^{L,\Lambda}) = 0 \ .$$

Then by the Kemperman-Pinsker inequality (A.3) it follows that,

$$\lim_{L\to\infty} \sqrt{\frac{L}{a_L}} \left\| P^{L,\Lambda} - Q^{L,\Lambda} \right\|_{\text{T.V.}} = 0 \ , \tag{3.31}$$

where the total variation norm can be expressed as $\frac{1}{2}\sum_{\boldsymbol{\eta}\in\mathbb{N}^\Lambda} |P^{L,\Lambda}[\boldsymbol{\eta}] - Q^{L,\Lambda}[\boldsymbol{\eta}]|$.

□

Remark 3.4. Convergence in relative entropy also implies converge of the expected value of test functions that are not necessarily bounded, as long as they have finite exponential moments,

$$f \in C_0, \quad \text{and} \quad Q^L\left(e^{tf}\right) < \infty, \quad \text{if } |t| \text{ is sufficiently small.}$$

The proof can be found in [31] Lemma 3.1.

Both the canonical measure and the grand canonical measures are absolutely continuous with respect to the reference measure and both their densities are functions of S_L only. We may exploit this by making a change of variables to calculate the specific relative entropy of the canonical measures with respect to the grand canonical measures by an integral over $\mathbb{R}_+$ rather than the original state space X_L. This is the fundamental step in showing that equivalence of ensembles in terms of specific relative entropy (in

terms of measures) is the same as equivalence in terms of thermodynamic functions. This approach is quite general and summarised in [93] and [91]. Inserting the two densities (3.20) and (3.6) into the definition of the relative entropy,

$$\begin{aligned}\frac{1}{a_L}H(\pi_\rho^L \mid \nu_\mu^L) &= \frac{1}{a_L}\sum_{\boldsymbol{\eta}\in X_L}\pi_\rho^L[\boldsymbol{\eta}]\log\frac{\mathbb{1}_{S_L^{-1}(\rho_L)}(\boldsymbol{\eta})}{\nu^L[S_L^{-1}(\rho_L)]}\frac{z_L^L(\mu)}{e^{a_L\mu S_L(\boldsymbol{\eta})}}\\ &= \frac{1}{a_L}\log\frac{1}{\nu^L[S_L^{-1}(\rho_L)]}\frac{z_L^L(\mu)}{e^{a_L\mu\rho_L}}\\ &= -\frac{1}{a_L}\log\nu^L[S_L=\rho_L] - (\mu\rho_L - p_L(\mu))\ , \end{aligned} \tag{3.32}$$

where from the first to the second line we made the change of variables and integrated over the singleton ρ_L. Since $H(\pi_\rho^L \mid \nu_\mu^L) \geq 0$ the 'best case' in (3.32) is given by the infimum over μ,

$$\begin{aligned}\inf_{\mu\in\mathcal{D}_p}\frac{1}{a_L}H(\pi_\rho^L \mid \nu_\mu^L) &= -\frac{1}{a_L}\log\nu^L[S_L=\rho_L] - \sup_{\mu\in\mathcal{D}_p}\{\mu\rho_L - p_L(\mu)\}\\ &= -\frac{1}{a_L}\log\nu^L[S_L=\rho_L] - p_L^*(\rho)\ . \end{aligned} \tag{3.33}$$

The first term on the right hand side, $\frac{1}{a_L}\log\nu^L[S_L=\rho_L]$, is given by a large deviation principle for the random variable S_L under the reference measure, given that we can show the sequence ρ_L is LD-regular. The second term $p_L^*(\rho)$ is the Legendre-Fenchel transform of the (finite system) pressure.

Definition 3.12 (Canonical entropy density)**.** For (ρ_L) converging to ρ as in (3.18)

$$\bar{s}_{\text{can}}(\rho) = -\limsup_{L\to\infty}\frac{1}{a_L}H(\pi_{\rho_L}^L \mid \nu^L)\ . \tag{3.34}$$

If the limit exists and is independent of the sequence (ρ_L) we define the specific canonical entropy density $s_{\text{can}} : \mathbb{R} \to [-\infty, 0]$ by,

$$s_{\text{can}}(\rho) = -\lim_{L\to\infty}\frac{1}{a_L}H(\pi_{\rho_L}^L \mid \nu^L)\ . \tag{3.35}$$

It turns out by a similar calculation as in (3.32) that the canonical entropy density can be written in terms of the canonical partition function (Definition 3.8),

$$s_{\text{can}}(\rho) = \lim_{L\to\infty}\frac{1}{a_L}\log\nu^L[S_L=\rho_L] = \lim_{L\to\infty}\frac{1}{a_L}\log Z(L,\rho_L)\ .$$

This describes the asymptotic probability of observing a large deviation of the empirical density under the reference measure $\nu^L[S_L \asymp \rho] \sim e^{-a_L s_{\text{can}}(\rho)}$. If s_{can} exists and is upper semi-continuous then the density S_L under the reference measure satisfies a large deviation principle with speed a_L and rate function $-s_{\text{can}}$ (see Appendix C).

The motivation for calling this quantity the *canonical entropy density* is given by the following observation: The Shannon entropy of π_ρ^L is given by $-H(\pi_\rho^L \mid \lambda)$ where

λ is the counting measure. However we have defined a reference measure ν^L on which the ensembles are defined and so we call $-H(\pi^L_{\rho_L} \mid \nu^L)$ the canonical entropy which turns out to be extensive in the sense that it diverges at the scale of (a_L). The relevant quantity in the thermodynamic limit is therefore given by the canonical entropy density.

The grand canonical entropy density is defined in the usual way as the Legendre-Fenchel transform of the pressure [91].

Definition 3.13 (Grand canonical entropy density)**.** $s_{\text{gcan}} : \mathbb{R} \to [-\infty, 0]$ is given by,

$$s_{\text{gcan}}(\rho) = -p^*(\rho) \ . \tag{3.36}$$

For $\rho \in \mathbb{R}$ if there exists a chemical potential $\mu(\rho) \in \mathcal{D}_p$ such that the mean of S_L under the grand canonical measure is ρ then

$$s_{\text{gcan}}(\rho) = -\lim_{L\to\infty} \frac{1}{a_L} H(\nu^L_{\mu(\rho)} \mid \nu^L) \ .$$

This is a straightforward consequence of p being the scaled cumulant generating function for the grand canonical measures. Again this motivates the name *grand canonical entropy density.*

Substituting these two definitions into the limit of the specific relative entropy between the canonical and grand canonical measures we find for an appropriate choice of the chemical potential that

$$\lim_{L\to\infty} \frac{1}{a_L} H(\pi^L_\rho \mid \nu^L_\mu) = s_{\text{gcan}}(\rho) - s_{\text{can}}(\rho) \ . \tag{3.37}$$

In words this relation states that *Equivalence of ensembles holds at the level of measures whenever it holds at the level of thermodynamic functions* [92]. This result is contained explicitly in Theorem 3.6 below.

If the Legendre-Fenchel transform of the thermodynamic pressure is strictly convex at some ρ we have equivalence of ensembles by applying a form of the Gärtner-Ellis theorem [34],[35] (this result is given in Theorem 3.7). In case that the Legendre-Fenchel transform is not strictly convex we calculate the large deviations of the maximum site occupation and apply a contraction principle to recover the canonical entropy density. It may be that the canonical measures do not converge to any grand canonical measure but they do converge to a restricted grand canonical measure. This is the content of Theorem 3.12. We prove this in the case of a scaling limit for the zero-range process and for a size-dependent zero-range process in Chapters 4 and 5.

Definition 3.14 (Restricted entropy densities)**.** The restricted entropy densities are defined in the same way as the previous entropy densities, for $m_L \to m$,

$$s_{\text{can},m}(\rho) = -\lim_{L\to\infty} H(\bar{\pi}^L_{\rho_L,m} \mid \nu^L) \tag{3.38}$$

$$= \lim_{L\to\infty} \frac{1}{a_L} \log \nu^L[S_L = \rho_L, M_L \le m_L] \ . \tag{3.39}$$

The restricted grand canonical entropy density is again given by the Legendre-Fenchel transform,

$$s_{\mathrm{gcan},m}(\rho) = -p_m^*(\rho) \ . \tag{3.40}$$

Again we observe that if there exists a sequence of $\mu_L \in \mathcal{D}_{p_m}$ that fixes the mean of S_L under the restricted grand canonical measures to be ρ_L, then the grand canonical entropy density can be expressed in terms of specific relative entropy,

$$s_{\mathrm{gcan},m}(\rho) = -\lim_{L\to\infty} \frac{1}{a_L} H(\bar{\nu}^L_{\mu_L,m_L} \mid \nu^L) \ .$$

A single site typically containing macroscopically many (of order b_L) particles may contribute to the total entropy on the scale (a_L).

Definition 3.15 (Condensate entropy contribution)**.** For a sequence m_L such that,

$$m_L \in \frac{1}{b_L}\mathbb{N} = \{1/b_L, 2/b_L, \ldots\} \quad \text{and} \quad \lim_{L\to\infty} m_L = m \ , \tag{3.41}$$

we define the *condensate entropy density*,

$$s_{\mathrm{cond}}(m) = \lim_{L\to\infty} \frac{1}{a_L} \log \nu[m_L b_L] \ . \tag{3.42}$$

Here we assume the limit is independent of the details of the sequence (m_L).

Similarly to the density ρ, there certainly exists such sequences for each $m \in \mathbb{R}_+$ since we may choose $m_L = \lfloor mL \rfloor / L$.

Remark 3.5. The condensate entropy contribution is the negative of the information gain (on the scale a_L) that results from conditioning on the maximum site occupation. In terms of specific relative entropy it turns out that

$$s_{\mathrm{cond}}(m) = \lim_{L\to\infty} \frac{1}{a_L} H(\nu^L[\ \cdot\ \mid M_L = m_L] \mid \nu^L) \ ,$$

This essentially follows from Lemma 3.8.

3.3.3 Relationship between forms of equivalence

We briefly discuss how different forms of equivalence of ensembles are interrelated. Equivalence of ensembles in terms of specific relative entropy (3.28) holds, if and only if, there is equivalence of ensembles in terms of the thermodynamic functions (the specific entropy densities). This is the content of Theorem 3.6 below. Equivalence of ensembles in terms of specific relative entropy (3.28) implies convergence in measures in the sense of fast weak convergence 3.11. However, fast weak convergence does not imply convergence in specific relative entropy since the measures need not be absolutely continuous.

It is also possible to define equilibrium macro-states of the canonical and grand canonical measures as concentration points of certain observables under the measures.

The connection between equivalence of ensembles in terms of the entropy densities and macro-state equivalence has been discussed in detail in [120] and [41]. We observe that, quite generally, equivalence on the level of thermodynamic functions (entropy densities) implies both convergence on the level of macro-states, and convergence on the level of measures.

3.4 Results

In this section we state the technical results based on classical results from the theory of large deviations. In particular, Theorem 3.7 is a refinement of the standard Gärtner-Ellis theorem, based on the local limit theorem for triangular arrays.

For the results of this section to hold rigorously we make some technical assumptions on the reference measure. These are satisfied in many situations of interest, such as in the thermodynamic limit for condensing zero-range process, and on the critical scale (see Chapter 4), as well as for size-dependent zero-range processes (see Chapter 5). The general approach and many of the results still apply even if some technical assumptions fail, although rigorous treatment becomes more difficult (see Chapter 6).

3.4.1 Assumptions

We make the following assumptions on the reference measures:

(1) The thermodynamic pressure

$$p(\mu) := \lim_{L\to\infty} \frac{1}{a_L} \log \nu^L \left(e^{\mu a_L S_L}\right)$$

exists as an extended real valued function $p : \mathbb{R} \to \mathbb{R} \cup \{-\infty, \infty\}$.

(2) For all L, p_L and p are differentiable on $\mathcal{D}_p$, and for each $\mu \in \mathcal{D}_p$ the second derivatives of p_L are uniformly bounded in L; that is there exists a $C_p(\mu) < \infty$ such that $\partial_\mu^2 p_L(\mu) := \sigma_L^2 < C_p(\mu)$ for all L.

(3) The reference measures have finite mean, and second moments that do not grow too quickly,

$$\nu_L(\eta_1) := \bar{\rho}_L \to \bar{\rho} < \infty \quad \text{and} \quad \frac{1}{(m_L b_L)^2} \nu_L\left(\eta_1^2\right) \to 0 \ . \tag{3.43}$$

The following assumption is made on the regularity of the reference measure so that we may apply a local limit theorem [33, 99].

(4) We define

$$Q_L = \sum_{k=0}^{\infty} \left(\nu_L[k] \wedge \nu_L[k+1]\right)$$

which is related to the Bernoulli part of the random variable corresponding to the single site occupation under the reference measure. We suppose always that

$\limsup 1/Q_L < \infty$. Typically this property is straightforward to show. For example if the single site marginals ν_L converge to a monotonically decreasing probability distribution then $Q_L \to 1$.

We make the following assumptions on the large deviation scale (a_L) and the density scale (b_L):

(5) The sequences (a_L) and (b_L) diverge to $+\infty$ and

$$\frac{1}{a_L} \log L \to 0 \quad \text{and} \quad \frac{1}{a_L} \log b_L \to 0 \quad \text{as} \quad L \to \infty.$$

This assumption is not satisfied in Chapter 6 for the inclusion process, however the general framework still applies, requiring more (formal) calculations.

(6) The following limit exists and is the contribution to the entropy density due to a macroscopic occupied single site, for $m_L \to m$ as in (3.41),

$$s_{\text{cond}}(m) = \lim_{L\to\infty} \frac{1}{a_L} \log \nu_L[m_L b_L] \ .$$

Also s_{cond} is upper semi-continuous (see Definition C.1).

(7) The large deviations scale (a_L), density scale (b_L) and the sequence (m_L) in (3.41) together satisfy

$$\frac{L}{a_L (b_L m_L)^2} \to 0 \ .$$

If $m_L \to m \in (0, \infty)$ then this condition states $\frac{L}{a_L b_L^2} \to 0$ otherwise for $m_L \to 0$ it states a requirement on the sequence (m_L) also. In particular it is required to consider cut-offs that are not too small.

3.4.2 From specific relative entropy to thermodynamic functions

Theorem 3.6. *If the specific canonical entropy density exists and $\rho \in \mathcal{D}^\circ_{p^*}$, then for $\rho_L \to \rho$ in the sense of* (3.18) *there exists a sequence of chemical potentials $\mu_L(\rho_L) \in \mathcal{D}_{p_L}$ such that,*

$$\lim_{L\to\infty} \frac{1}{a_L} H(\pi^L_\rho \mid \nu^L_{\mu_L(\rho_L)}) = s_{gcan}(\rho) - s_{can}(\rho) \ . \tag{3.44}$$

If ρ is on the boundary of $\mathcal{D}_{p^*}$ then the limit may depend on the details of the sequence (ρ_L).

Proof. The specific relative entropy can be decompose as is (3.32)

$$\frac{1}{a_L} H(\pi^L_\rho \mid \nu^L_\mu) = -\frac{1}{a_L} \log \nu^L[S_L = \rho_L] - (\mu\rho_L - p_L(\mu)) \ .$$

We observe the following properties of the thermodynamic pressure and its Legendre-Fenchel transform. p is convex, by Hölder's inequality, and p^* is convex and lower

semi-continuous, because it is the supremum of linear functions. By Fatous Lemma p_L is lower semi-continuous. So for each L the supremum defining the Legendre-Fenchel transform is attained on the essential domain of p_L, $\mathcal{D}_{p_L}$.

$$p_L^*(\rho_L) = \sup_{\mu \in \mathcal{D}_{p_L}} [\mu\rho_L - p_L(\mu)] \tag{3.45}$$

$$= \mu_L(\rho_L)\rho_L - p_L(\mu(\rho_L)) \quad \text{for some } \mu_L(\rho_L) \in \mathcal{D}_{p_L} \ . \tag{3.46}$$

Since p_L is convex and analytic on the interior of its essential domain, $\mu_L(\rho_L)$ is strictly increasing in ρ_L up to some possibly finite critical value after which it is constant.

We must show that it is permissible to exchange the order of the limit and the Legendre-Fenchel transform,

$$\lim_{L\to\infty} p_L^*(\rho_L) = p^*(\rho) \ .$$

Note that point-wise convergence of p_L^* to p^* is in general not guaranteed. For example consider $\nu^L[S_L = 1/L] = 1$ then $p_L(\mu) = \mu/L \to 0$, while

$$p_L^*(\rho) = \begin{cases} 0 & \text{if } \rho = 1/L \\ \infty & \text{otherwise} \end{cases}$$

and $p^*(0) = 0$. However, the Legendre-Fenchel transform is sequentially continuous with respect to a form of convergence known as Mosco-convergence (see for example [34, 131]). The extended real functions f_n are said to be Mosco-convergent to f if the following two conditions are satisfied,

$$\text{for every } x \in \mathbb{R}, \limsup_{n\to\infty} f_n(x_n) \leq f(x) \text{ for } \textit{some } x_n \to x \ , \tag{3.47}$$

$$\text{for every } x \in \mathbb{R}, \liminf_{n\to\infty} f_n(x_n) \geq f(x) \text{ for } \textit{every } x_n \to x \ . \tag{3.48}$$

In 1971 Mosco showed that if f_n are a sequence of scaled cumulant generating functions converging in this sense to f then f_n^* is Mosco-convergent to f^* (this is a special case of the original result). The scaled pressures p_L are Mosco-convergent to p by assumptions (1) and (2). It remains to show that p_L^* being Mosco-convergent to p^*, and p^* being continuous, together imply $p_L^*(\rho_L) \to p(\rho)$ for all $\rho_L \to \rho$ (in the sense of (3.18)).

Fix ρ such that p^* is Lipschitz continuous on $B_\delta(\rho)$ for some $\delta > 0$. Let ρ_L be a sequence converging to ρ. Fix $\epsilon > 0$, since p^* is continuous and convex there exists a non-empty open subset A of $B_\delta(\rho)$ containing ρ on which p^* is monotonic (without loss of generality assume it is increasing) and $\sup_{x\in A} |p^*(x) - p^*(\rho)| < \epsilon$. So there exists a $y_1, y_2 \in A$ such that $y_1 < \rho < y_2$ and $p^*(y_1) \leq p^*(\rho) \leq p^*(y_2)$. By Mosco-convergence there exist sequences $y_{1,L} \to y_1$ such that $\limsup p_L^*(y_{1,L}) \leq p^*(y_1)$, and $y_{2,L} \to y_2$ such that $\limsup p_L^*(y_{2,L}) \leq p^*(y_2)$. For L sufficiently large $y_{1,L} \leq \rho_L \leq y_{2,L}$ and since p_L^* is

convex and locally monotone,

$$p_L^*(\rho_L) \leq p_L^*(y_{1,L}) \vee p_L(y_{2,L}^*)$$

and so by continuity,

$$\limsup_{L\to\infty} p_L^*(\rho_L) \leq p^*(\rho) + \epsilon \ . \tag{3.49}$$

The result follows by letting $\epsilon \searrow 0$. Together with (3.48) we have that for all $\rho_L \to \rho$ the Legendre transforms of the scaled pressures converge $p_L^*(\rho_L) \to p^*(\rho)$ as required. □

3.4.3 Gärtner-Ellis theorem

The following standard notation is used throughout: For any set A, $\bar{A}$ denotes the closure of A, A° denotes the interior and A^c the complement.

The following theorem states that the grand canonical entropy density bounds the canonical entropy from above, and if the grand canonical entropy density is strictly concave then they are equal. Since the restricted measures are simply a special case of size-dependent measures, the theorem also holds for the restricted ensembles (truncated measures). The following theorem is a particular version of the Gärtner-Ellis Theorem which we are able to prove by means of local limit theorems for triangular arrays of random variables.

Theorem 3.7 (Gärtner-Ellis Theorem)**.** *The grand canonical entropy density bounds the canonical entropy density from above*

$$\bar{s}_{can}(\rho) = \limsup_{L\to\infty} \frac{1}{a_L} \log \nu^L[S_L = \rho_L] \leq -p^*(\rho) = s_{gcan}(\rho) \tag{3.50}$$

If $b_L^2/(a_L L) \to c \in [0,\infty)$ *or* $\nu_L\left(e^{t\sqrt{La_L}b_L^{-1}\eta_x}\right) < \infty$ *for some positive* t *then the limit defining the canonical entropy density exists and*

$$s_{can}(\rho) = s_{gcan}(\rho) \quad \textit{for all } \rho \in E_p^\circ \ , \tag{3.51}$$

where $E_p = E_p(p, s_{gcan})$ *is the set of points for which* s_{gcan} *is strictly concave and the exposing hyperplane of* $-s_{gcan}$ *belongs to* $\mathcal{D}_p^\circ$*. In this case we have equivalence of ensembles in the sense of Definition 3.11.*

Proof. The first part (3.50) follows from the Gärtner-Ellis Theorem (see Theorem C.4) and is a simple application of the exponential Chebychev's inequality that we do not repeat here. Let $\bar{B}_\epsilon(\rho) = \{x \in \mathbb{R}_+ : |\rho - x| \leq \epsilon\}$, then for L sufficiently large we have

$$\frac{1}{a_L} \log \nu^L[S_L = \rho_L] \leq \frac{1}{a_L} \log \nu^L[S_L \in \bar{B}_\epsilon(\rho)] \ . \tag{3.52}$$

By the Gärtner-Ellis theorem (see e.g. [34, 35] for proof),

$$\limsup_{L\to\infty} \frac{1}{a_L} \log \nu^L[S_L \in \bar{B}_\epsilon(\rho)] \leq - \inf_{x\in\bar{B}_\epsilon(\rho)} p^*(x) \ ,$$

and it follows that

$$\limsup_{L\to\infty} \frac{1}{a_L} \log \nu^L[S_L = \rho_L] = \bar{s}_{\rm can}(\rho) \leq - \inf_{x\in\bar{B}_\epsilon(\rho)} p^*(x) \ .$$

Let $\epsilon \searrow 0$, since p^* is lower semi-continuous we obtain

$$\bar{s}_{\rm can}(\rho) \leq -p^*(\rho) = s_{\rm gcan}(\rho) \ .$$

Essentially the result (3.51) is contained in Theorem 6.1 in [93]. However, we must show that the sequence $\{\rho_L\}$ is LD-regular (see Appendix C and [93]), which amounts to showing that the limit defining the canonical entropy density exists. This follows by applying the local limit theorem for triangular arrays [33]. Fix $\rho \in E_p^\circ$ and let $\mu \in \mathcal{D}_p^\circ$ be (normal to) the exposing hyperplane of $-s_{\rm gcan}$ at ρ. By the usual reciprocal relationship for the Legendre transform we have, since p is strictly convex at μ and p is differentiable, $\partial_\mu p(\mu) = \rho$ (see Appendix C). For L sufficiently large $\rho_L \in E_p^\circ$ since $\rho_L \to \rho$. It follows from the local uniform convergence of $\partial_\mu p_L$ to $\partial_\mu p$ (see [73]) that for L sufficiently large there exists a $\mu_L \in \mathcal{D}_p^\circ$ such that $\partial_\mu p_L(\mu_L) = \rho_L$. Since p_L is the scaled cumulant generating function of S_L we have $\nu^L_{\mu_L}(S_L) = \partial_\mu p_L(\mu_L)$ and by definition of the Legendre transform $p_L^*(\rho_L) = \mu_L\rho_L - p_L(\mu_L)$. We may therefore make an exponential change of measure such that,

$$\begin{aligned}\frac{1}{a_L} \log \nu^L[S_L = \rho_L] &= -\mu_L\rho_L + p_L(\mu_L) + \frac{1}{a_L} \log \nu^L_{\mu_L}[S_L = \rho_L] \\ &= -p_L^*(\rho_L) + \frac{1}{a_L} \log \nu^L_{\mu_L}[S_L = \rho_L] \ . \end{aligned} \tag{3.53}$$

It remains to show that the final term tends to zero as $L \to \infty$. This is a result of the local limit theorem for triangular arrays (see Theorem B.2). By definition $S_L = b_L^{-1} \sum_{i=1}^L \xi_{i,L}$ where for each L we have that $\xi_{i,L}$, $1 \leq i \leq L$ are independent random variables. Also we have the following expressions for the mean and variance of $\xi_{i,L}$

$$\begin{aligned}\rho_L = \partial_\mu p_L(\mu_L) &= \nu^L_{\mu_L}(S_L) \\ &= L b_L^{-1} \nu_{\mu_L}(\xi_{1,L}) \ , \end{aligned} \tag{3.54}$$

$$\begin{aligned}\sigma_L^2 := \partial_\mu^2 p_L(\mu_L) &= a_L \nu^L_{\mu_L}\left((S_L - \rho_L)^2\right) \\ &= \frac{a_L L}{b_L^2} {\rm Var}_{\nu_{\mu_L}}[\xi_{i,L}] \ , \end{aligned} \tag{3.55}$$

where $\rho_L \to \rho$ and σ_L^2 is eventually bounded since $a_L S_L$ has finite exponential moments

under $\nu^L_{\mu_L}$. Define,

$$\bar{\xi}_{i,L} := \frac{\xi_{i,L} - \rho_L b_L L^{-1}}{\sigma_L \sqrt{L}} \ . \tag{3.56}$$

Then for every $\epsilon > 0$ if $b_L^2/(a_L L) \to c \in (0, \infty)$,

$$\sum_{i=1}^{L} \mathbb{E}\left[\left|\bar{\xi}_{i,L}\right|^2 \ \mathbb{1}_{|\bar{\xi}_{1,L}| > \epsilon L^{1/2}} \right] = L\mathbb{E}\left[\left|\bar{\xi}_{1,L}\right|^2 \ \mathbb{1}_{|\bar{\xi}_{1,L}| > \epsilon L^{1/2}} \right] \to 0 \ ,$$

as $L \to \infty$ by the dominated convergence theorem since $\mathrm{Var}_{\nu_{\mu_L}}[\xi_{i,L}] < \infty$. It follows that the triangular array $\bar{\xi}_{i,L}$ satisfies the conditions of the Lindeberg-Feller theorem (central limit theorem for triangular arrays) [39] and so $\sum_{i=1}^{L} \bar{\xi}_{i,L}$ converges in distribution to the standard normal. Under assumption (4) $\sum_i \xi_{i,L}$ has normal local limits, by Theorem 1.2 in [33], so for ϕ the standard normal density

$$\sup_k \left| \sigma_L \sqrt{L} \nu^L_{\mu_L}[S_L = k b_L^{-1}] - \phi\left(\frac{k - \rho_L b_L}{\sigma_L \sqrt{L}} \right) \right| \to 0 \quad \text{as} \quad L \to \infty \ .$$

It follows that (with slight abuse of notation),

$$\frac{1}{a_L} \log \nu^L_{\mu_L}[S_L = \rho_L] = -\frac{1}{a_L} \log O\left(\sqrt{L}\right) \to 0 \quad \text{as} \quad L \to \infty \ ,$$

and so we have equivalence of ensembles in the sense of Definition 3.11 since the specific relative entropy tends to zero,

$$\frac{1}{a_L} H(\pi^L_\rho \mid \nu^L_{\mu_L}) = -\frac{1}{a_L} \log \nu^L_{\mu_L}[S_L = \rho_L] \to 0 \tag{3.57}$$

as $L \to \infty$.

In the case that $b_L^2/(a_L L)$ does not converge the proof follows the same method only we let,

$$\bar{\xi}_{i,L} = \frac{\sqrt{a_L L}}{b_L} \xi_{i,L} \ .$$

In this case assumption (2) of Theorem B.3 is satisfied by construction and we may apply this alternative form of the local limit theorem provided $\nu_L\left(e^{a\sqrt{L a_L} b_L^{-1} \eta_x}\right) < \infty$. □

We observe that stronger equivalence also holds in the case that s_{gcan} is strictly concave at ρ since,

$$\begin{aligned} \frac{1}{\hat{a}_L} H(\pi^L_\rho \mid \nu^L_{\mu_L}) &= -\frac{1}{\hat{a}_L} \log \nu^L_{\mu_L}[S_L = \rho_L] \\ &= \frac{1}{\hat{a}_L} \log O(L) \to 0 \quad \text{if } \hat{a}_L \gg \log L \ . \end{aligned} \tag{3.58}$$

3.4.4 Contraction on the maximum

For densities at which the grand canonical entropy density is not strictly concave equivalence of ensembles does not follow from Theorem 3.7. In this case the canonical entropy density may be non-concave. There has been recent research activity in the area of calculating non-concave entropies [28, 29, 119]. Techniques include microcanonical contractions and the use of generalised ensembles [30]. We adopt here an approach that is particularly suited to condensing systems. Broadly, our approach is to contract on a large deviation principle for the joint event of the density and the maximum site occupation under the reference measure. The large deviation principle for the joint event turns out to be simple to compute by use of the restricted ensembles. This is also useful for understanding the behaviour of the maximum on finite systems (canonical large deviations of the maximum). The following result (Theorem 3.10) is in direct analogy with the standard contraction principle (see Appendix C for details). The proof, however, essentially follows an argument that is similar to the proof of Varadhan's Lemma (a Laplace approximation of the integral over all maximum site occupations).

Lemma 3.8. *Given finite mean and variance of ν_L,*

$$\lim_{L\to\infty} \frac{1}{a_L} \log \nu^L[M_L < m_L] \to 0 \quad as \quad m_L \to m \in (0,\infty) \ .$$

Proof. If $M_L(\boldsymbol{\eta}) < m_L$, then for each $x \in \Lambda_L$ we have $\eta_x \leq m_L b_L$, so

$$\frac{1}{a_L} \log \nu^L[M_L < m_L] = \frac{L}{a_L} \log(1 - \nu_L[\eta_1 \geq m_L b_L]) \leq 0 \ . \tag{3.59}$$

Since ν_L has finite second moment we have for all L sufficiently large

$$\nu_L[\eta_1 \geq m_L b_L] < \frac{\nu_L\left(\eta_1^2\right)}{(m_L b_L)^2}$$

by Chebyshev's inequality. Also the right hand side tends to zero by assumption (3). So we may expand the logarithm to first order to obtain the following bound,

$$\frac{1}{a_L} \log \nu^L[M_L < m_L] \geq -\frac{L}{a_L} \frac{\nu_L\left(\eta_1^2\right)}{(m_L b_L)^2} + o\left(\frac{L}{a_L} \frac{\nu_L\left(\eta_1^2\right)}{(m_L b_L)^2}\right) \ .$$

The right hand side tends to zero by assumption (7). □

For a given sequence $m_L \to m \in (0,\infty)$ recall Definition 3.6

$$p_m(\mu) = \lim_{L\to\infty} a_L^{-1} \log \nu^L \left(e^{a_L \mu S_L} \mathbb{1}_{M_L \leq m_L}\right) \ .$$

Corollary 3.9. *The restricted pressures extend the grand canonical pressure. If $m_1 \geq m_2$ then $\mathcal{D}_{p_{m_1}} \subseteq \mathcal{D}_{p_{m_2}}$ and*

$$p_{m_1}(\mu) = p_{m_2}(\mu) \quad for \quad \mu \in \mathcal{D}^\circ_{p_{m_1}} \ .$$

This implies weak convergence of the restricted measures, in the sense of (3.24)*,*

$$\frac{1}{a_L} H(\bar{\nu}^L_{\mu,m_2} \mid \bar{\nu}^L_{\mu,m_1}) \to 0 \quad \textit{as } L \to \infty \quad \textit{for} \quad \mu \in \mathcal{D}^\circ_{p_{m_1}} \ .$$

Proof. The grand canonical measures truncated according to m_1 at chemical potential $\mu \in \mathcal{D}^\circ_{p_{m_1}}$ have finite exponential moments so the proof is a straightforward corollary of Lemma 3.8. By making an exponential change of measure we find,

$$\begin{aligned} p_m(\mu) &= \lim_{L\to\infty} \frac{1}{a_L} \log \nu^L \left(\mathbb{1}_{\{M_L < m_L\}} e^{\mu a_L S_L} \right) \\ &= \lim_{L\to\infty} \frac{1}{a_L} \log \nu^L_\mu [M_L < m_L] + p(\mu) = p(\mu) \ . \end{aligned} \tag{3.60}$$

The same proof holds when comparing two restricted pressures.

Since the densities of the two measures differ only by their normalisation and their support, it follows that,

$$H(\bar{\nu}^L_{\mu,m_2} \mid \bar{\nu}^L_{\mu,m_1}) = \log z^L_{m_1}(\mu) - \log z^L_{m_2}(\mu) \ .$$

It is now clear from the equality of the pressures on $\mathcal{D}^\circ_{p_{m_1}}$ that,

$$\lim_{L\to\infty} \frac{1}{a_L} H(\bar{\nu}^L_{\mu,m_2} \mid \bar{\nu}^L_{\mu,m_1}) = p_{m_1}(\mu) - p_{m_2}(\mu) = 0 \ ,$$

and so the measures converge weakly. □

In the next theorem, for certain values of the density and macroscopic maximum, we are able to derive a rate function for the joint event such that $\nu^L[S_L \asymp \rho,\ M_L \asymp m] \sim e^{-a_L I(\rho,m)}$. The theorem gives rise to an iterative procedure that can be used in applications to extend the range for which we can calculate $I(\rho, m)$. If the point-wise limit defining $I(\rho, m)$ exists then the joint maximum and density under the reference measure satisfy a weak large deviation principle with speed a_L and rate function I (see Appendix C).

Theorem 3.10 (Large deviations for the joint events and contraction on the maximum)**.** *Throughout the theorem $m_L \to m$ as in* (3.41) *and $\rho_L \to \rho$ as in* (3.18)*.*

a) For fixed ρ, if the restricted canonical entropy densities exist,

$$s_{can,m}(\rho - m) = \lim_{L\to\infty} \frac{1}{a_L} \log \nu^L_{m_L} [S_L = (\rho_L - m_L)] \tag{3.61}$$

as an extended real function (not identically $\equiv \infty$) for all $m \in [0, \rho]$, and $s_{can,m}$ is upper semi-continuous, then the joint event satisfies a large deviation principle with rate function,

$$\begin{aligned} I(\rho, m) &:= - \lim_{L\to\infty} \frac{1}{a_L} \log \nu^L [S_L = \rho_L,\ M_L = m_L] \\ &= - \left(s_{cond}(m) + s_{can,m}(\rho - m) \right) \ . \end{aligned} \tag{3.62}$$

Further, a contraction principle holds,

$$s_{can,m}(\rho - m) = - \inf_{m' \in [0,m]} I(\rho - m, m') \ . \tag{3.63}$$

b) There are two cases for which we can prove that the limit in (3.61) exists, and it can be calculated exactly:
i) If $\rho \in E^{\circ}_{p_m}$ is in the set of points for which p^*_m is strictly convex then,

$$s_{can,m}(\rho) = s_{gcan,m}(\rho) \ . \tag{3.64}$$

ii) Otherwise we can contract on further macroscopically occupied sites. The supremum,

$$\sup_{m_2 \in [0,m]} \{ s_{cond}(m_2) + s_{gcan,m_2}(\rho - m_2) \} \tag{3.65}$$

is attained at some $m_2 = m^* \in [0, m]$ and if $(\rho - m^*) \in E^{\circ}_{p_{m^*}}$ then,

$$s_{can,m}(\rho) = s_{cond}(m^*) + s_{can,m^*}(\rho - m^*) \ . \tag{3.66}$$

Proof of Theorem. a) The first part of the theorem follows from permutation invariance of the reference measures (product measures). The following upper and lower bound are obvious by considering the number of ways of arranging the maximum on the lattice that give rise to identical configurations outside of the maximum occupied site,

$$\begin{aligned} \nu^L[S_L = \rho_L, \ M_L = m_L] &\leq L \ \nu[m_L b_L] \ \nu^{L-1}[S_L = (\rho_L - m_L), \ M_{L-1} \leq m_L] \\ &\leq L \ \nu[m_L b_L] \ \bar{\nu}^{L-1}_{m_L}[S_L = (\rho_L - m_L)] \ \nu^{L-1}[M_{L-1} \leq m_L] \end{aligned} \tag{3.67}$$

and

$$\nu^L[S_L = \rho_L, \ M_L = m_L] \geq \nu[m_L b_L] \ \bar{\nu}^{L-1}_{m_L}[S_L = (\rho_L - m_L)] \ \nu^{L-1}[M_{L-1} < m_L] \ . \tag{3.68}$$

Equation (3.62) follows by taking the logarithm and applying Lemma 3.8.

To prove the contraction, Equation (3.63), we first prove the lower bound.

$$\frac{1}{a_L} \log \bar{\nu}^L_{m'}[S_L = \rho_L] \geq \frac{1}{a_L} \log \bar{\nu}^L_{m'}[S_L = \rho_L, M_L = m_L] \quad \text{for each } m_L \in [0, m'] \ . \tag{3.69}$$

Since I is lower semi-continuous it attains its infimum on every non-empty compact set, so there exists $m^* \in [0, m']$ such that $I(\rho, m^*) = \inf_{m \in [0,m']} I(\rho, m)$. By choosing a sequence m^*_L that tends to m^* we have

$$\liminf_{L \to \infty} \frac{1}{a_L} \log \bar{\nu}^L_{m'}[S_L = \rho_L] \geq -I(\rho, m^*) = - \inf_{m \in [0,m']} I(\rho, m) \ .$$

The upper bound follows similarly,

$$\begin{aligned}\frac{1}{a_L}\log\bar{\nu}_m^L[S_L=\rho_L] &= \frac{1}{a_L}\log\sum_{k=1}^{\rho_L b_L}\bar{\nu}_m^L[S_L=\rho_L, M_L=kb_L^{-1}]\\ &\le \frac{1}{a_L}\log\left(\rho_L b_L \bar{\nu}_m^L[S_L=\rho_L, M_L=m_L^*]\right)\\ &= \frac{1}{a_L}\log\rho_L b_L + \frac{1}{a_L}\log\bar{\nu}_m^L[S_L=\rho_L, M_L=m_L^*]\ ,\end{aligned}$$

where $m_L^* = \arg\max_{m'}\nu_m^L[S_L=\rho_L, M_L=m']$. The first term $a_L^{-1}\log\rho_L b_L$ tends to zero by assumption (5). Since $I(\rho,\cdot)\not\equiv\infty$, there exists a sequence $m_L\to m$ such that

$$a_L^{-1}\log\bar{\nu}_m^L[S_L=\rho_L, M_L=m_L]\to -I(\rho,m) > -\infty\ ,$$

so

$$-\infty < \frac{1}{a_L}\log\bar{\nu}_m^L[S_L=\rho_L, M_L=m_L] \le \frac{1}{a_L}\log\bar{\nu}_m^L[S_L=\rho_L, M_L=m_L^*] \le 0\ .$$

This implies that $a_L^{-1}\log\nu_m^L[S_L=\rho_L, M_L=m_L^*]$ must eventually be contained in a sequentially compact set. Also m_L^* belongs to a sequentially compact set $[0,m]$, therefore we may choose a subsequence L_k that attains the lim sup as its limit and for which $m_{L_k}^*$ converges, so

$$\begin{aligned}\limsup_{L\to\infty}\frac{1}{a_L}\log\bar{\nu}_m^L[S_L=\rho_L] &\le \limsup_{L\to\infty}\frac{1}{a_L}\log\bar{\nu}_m^L[S_L=\rho_L, M_L=m_L^*]\\ &= \lim_{k\to\infty}\frac{1}{a_{L_k}}\log\bar{\nu}_m^{L_k}[S_{L_k}=\rho_{L_k}, M_{L_k}=m_{L_k}^*] \le -\inf_{m'\in[0,m]} I(\rho,m')\ .\end{aligned}$$

b) The proof of the first part, Equation (3.64), is given by the second part of theorem 3.7. A lower bound for the second part, (3.66), can be found exactly following the proof of part a). For the upper bound we do not know that $I(\rho,m_2)$ exists for $m_2\neq m^*$, however, an upper bound for the lim sup is given by the first part of theorem 3.7.

□

For fixed ρ, shifting the rate function for the joint $I(\rho,\cdot)$ so that its minimum is 0 gives rise to a rate function describing the canonical large deviations of the maximum, denoted by $I_\rho(\cdot)$. Formally this can be expressed as $\pi_\rho^L[M_L\asymp m]\sim e^{-a_L I_\rho(m)}$, where $I_\rho(m)$ can be interpreted as a free energy function for the maximum under the canonical measures.

Corollary 3.11 (Canonical large deviations of the maximum)**.** *For fixed ρ and m if $s_{can}(\rho)$ and $I(\rho,m)$ exist, then the canonical large deviations of the maximum are given*

by,

$$I_\rho(m) := -\lim_{L\to\infty} \frac{1}{a_L} \log \pi^L_{\rho_L}[M_L = m_L]$$
$$= I(\rho, m) + s_{can}(\rho) \ . \tag{3.70}$$

Proof. This follows immediately from writing out the conditioning in terms of the joint event,

$$\frac{1}{a_L} \log \pi^L_{\rho_L}[M_L = m_L] = \frac{1}{a_L} \log \nu^L[M_L = m_L \mid S_L = \rho_L]$$
$$= \frac{1}{a_L} \log \nu^L[M_L = m_L,\ S_L = \rho_L] - \frac{1}{a_L} \log \nu^L[S_L = \rho_L] \ .$$

□

Corollary 3.12 (Canonical equivalence with the restricted measures)**.** *If $s_{can}(\rho) = s_{can,m}(\rho)$, and $s_{can,m}(\rho) = s_{gcan,m}(\rho)$, then $\pi^L_{\rho_L}$ converges to $\bar{\nu}^L_{\mu(\rho),m_L}$ in the sense of* (3.24)*.*

Proof. The proof is in two steps; first we show weak convergence of the canonical measures with the restricted canonical measures and then the restricted canonical measures with the cut-off grand-canonical. Recall the definition of the restricted canonical measures $\bar{\pi}^L_{\rho,m}[\cdot] = \pi^L_\rho[\,. \mid M_L \leq m_L]$.

i) Firstly since the restricted canonical measures are absolutely continuous with respect to the canonical measure we observe that,

$$\frac{1}{a_L} H(\bar{\pi}^L_{\rho,m} \mid \pi^L_\rho) = \frac{1}{a_L} \log \nu^L[S_L = \rho_L] - \frac{1}{a_L} \log \nu^L[S_L = \rho_L, M_L = m_L]$$
$$\to s_{\mathrm{can}}(\rho) - s_{\mathrm{can},m}(\rho) = 0 \quad \text{as} \quad L \to \infty \ .$$

The second line follows from Definitions 3.12 and 3.14. This implies that $\bar{\pi}^L_{\rho,m}$ converges in the sense of (3.24) to π^L_ρ.

ii) The second step is to show that the restricted canonical measures converge to the restricted grand-canonical measures. This is an immediate consequence of the second part of Theorem 3.7.

The result now follows from the triangle inequality. □

Define the canonical background measure on $X_{\Lambda_{L-1}}$ which describes the distribution of configurations outside of the maximum occupied site. This gives the canonical probability of observing a background configuration of $\boldsymbol{\eta} \in X_{\Lambda_{L-1}}$ after sampling a full configuration from $\pi^L_{\rho_L}$ and discarding the maximum occupied site. In order to give a succinct definition of the canonical background measure we define the cut operator (after [4, 52]) $C : X_L \to X_{\Lambda_{L-1}}$ as in Equation (2.37). Then the background measure is

given by,

$$\hat{\pi}^L_{\rho_L}[\boldsymbol{\eta}] = \pi^L_{\rho_L}\left[C^{-1}(\boldsymbol{\eta})\right] \quad \text{for} \quad \boldsymbol{\eta} \in X_{\Lambda_{L-1}} \ . \tag{3.71}$$

Corollary 3.13 (Equivalence for the background)**.** *If*

$$s_{can}(\rho) = -\inf_{m\in[0,\rho]} I(\rho, m) = s_{cond}(m^*) + s_{gcan,m^*}(\rho - m^*)$$

then $\hat{\pi}^L_{\rho_L}$ *and* $\nu^{L-1}_{\mu(\rho-m^*),m^*_L}$ *converge in the sense of* (3.24)*.*

Proof. Again the proof is split into two steps because $\hat{\pi}^L_{\rho_L}$ is not absolutely continuous with respect to $\nu^{L-1}_{\mu(\rho-m*),m^*_L}$. We introduce some notation for the proof. Let

$$\hat{X}^L_{\rho_L} = C(X^L_{\rho_L}) \subset X_{\Lambda_{L-1}}$$

and the number of canonical configurations in $X^L_{\rho_L}$ (see (3.16)) that have background $\boldsymbol{\eta} \in \hat{X}^L_{\rho_L}$ is given by

$$K_{L,\rho_L}(\boldsymbol{\eta}) = \left|\{\boldsymbol{\zeta} \in X^L_{\rho_L} \mid C(\boldsymbol{\zeta}) = \boldsymbol{\eta}\}\right| \ .$$

Denote the macroscopic size of the second most occupied site,

$$M^{(2)}_L(\boldsymbol{\eta}) = \frac{1}{b_{L-1}} \max_{x\in\Lambda_{L-1}} (C(\boldsymbol{\eta}))_x \ .$$

Through the proof we fix $\mu = \mu(\rho - m^*)$.

i) The first step is to show that the canonical background measures $\hat{\pi}^L_{\rho_L}$ converge in the sense of (3.24) to the restricted canonical background measures,

$$\hat{\pi}^L_{\rho,m^*}[\boldsymbol{\eta}] = \hat{\pi}^L_{\rho}[\boldsymbol{\eta} \mid M_{L-1} \le m^*_L] \ . \tag{3.72}$$

This follows by examining the specific relative entropy. Both measures have densities with respect to the reference measure or $X_{\Lambda_{L-1}}$,

$$\frac{\mathrm{d}\hat{\pi}^L_{\rho}}{\mathrm{d}\nu^{L-1}}(\boldsymbol{\eta}) = \frac{K_{L,\rho_L}(\boldsymbol{\eta})\nu[b_L\rho_L - \Sigma_{L-1}(\boldsymbol{\eta})]}{\nu^L[S_L^{-1}(\rho_L)]}\mathbb{1}_{\hat{X}^L_{\rho_L}}(\boldsymbol{\eta}) \tag{3.73}$$

$$\frac{\mathrm{d}\hat{\pi}^L_{\rho,m^*}}{\mathrm{d}\nu^{L-1}}(\boldsymbol{\eta}) = \frac{K_{L,\rho_L}(\boldsymbol{\eta})\nu[b_L\rho_L - \Sigma_{L-1}\boldsymbol{\eta}]}{\nu^L[S_L^{-1}(\rho_L), M^{(2)}_L \le m^*_L]}\mathbb{1}_{\hat{X}^L_{\rho_L}}(\boldsymbol{\eta})\mathbb{1}_{\{M_{L-1}\le m^*_L\}}(\boldsymbol{\eta}) \ . \tag{3.74}$$

Since the canonical measures concentrate on configurations for which the second highest occupied site is less than $m^*_L b_L$ it follows that in the limit we have,

$$\lim_{L\to\infty} \frac{1}{a_L} \log \nu^L[S_L^{-1}(\rho_L), M^{(2)}_L \le m^*_L] = s_{\mathrm{can}}(\rho) \ .$$

So the relative entropy tends to zero,

$$\frac{1}{a_L} H(\hat{\pi}^L_{\rho,m^*} \mid \hat{\pi}^L_{\rho}) = \frac{1}{a_L} \log \nu^L[S_L^{-1}(\rho_L)] - \frac{1}{a_L} \log \nu^L[S_L^{-1}(\rho_L), M_L^{(2)} \leq m_L^*] \to 0$$

as $L \to \infty$, and both terms converge to the canonical entropy density since the canonical measures concentrate on configurations with macroscopic maximum m^*.

ii) We now show that,

$$\lim_{L\to\infty} \frac{1}{a_L} H(\hat{\pi}^L_{\rho_L,m_L^*} \mid \nu^{L-1}_{\mu(\rho-m^*),m_L^*}) = 0 \ .$$

It follows from the densities (3.73) that,

$$\begin{aligned} \frac{1}{a_L} H(\hat{\pi}^L_{\rho_L,m_L^*} \mid \nu^{L-1}_{\mu,m_L^*}) = \frac{1}{a_L} \hat{\pi}^L_{\rho_L,m_L^*} \Big(\log K_{L,\rho_L}(\boldsymbol{\eta}) \, \nu[b_L\rho_L - \Sigma_{L-1}(\boldsymbol{\eta})] \Big) \\ - \frac{1}{a_L} \log \nu^L \big[S_L^{-1}(\rho_L), M_L^{(2)} \leq m_L^* \big] + s_{\mathrm{gcan},m^*}(\rho - m^*) \ . \end{aligned} \tag{3.75}$$

Since the canonical measures concentrate on configurations for which the second highest occupied site is less than $m_L^* b_L$ it follows that in the limit we have,

$$\lim_{L\to\infty} \frac{1}{a_L} \log \nu^L[S_L^{-1}(\rho_L), M_L^{(2)} \leq m_L^*] = s_{\mathrm{can}}(\rho) \ .$$

Since $1 \leq K_{L,\rho_L}(\boldsymbol{\eta}) \leq L$ the mean of the log tends to zero on the scale of a_L. The remaining part of the first term can be written as an expected value of the maximum under the truncated canonical measures,

$$\hat{\pi}^L_{\rho_L,m_L^*} \left(\frac{1}{a_L} \log \nu \left[b_L(\rho_L - S_{L-1}(\boldsymbol{\eta})) \right] \right) = \pi^L_{\rho_L} \left(\frac{1}{a_L} \log \nu[b_L M_L(\boldsymbol{\eta})] \mid M_L^{(2)} \leq m_L^* \right) \ . \tag{3.76}$$

Since the canonical measures concentrate on configurations with macroscopic maximum m^*, and the condensed entropy contribution is bounded on $[0, \rho]$, in the limit we arrive at,

$$\lim_{L\to\infty} \frac{1}{a_L} \hat{\pi}^L_{\rho_L,m_L^*} \left(\log \nu[b_L(\rho_L - S_{L-1}(\boldsymbol{\eta}))] \right) = s_{\mathrm{cond}}(m^*) \ . \tag{3.77}$$

Taking the limit in (3.75) it follows that,

$$\lim_{L\to\infty} \frac{1}{a_L} H(\hat{\pi}^L_{\rho_L,m_L^*} \mid \nu^{L-1}_{\mu,m_L^*}) = s_{\mathrm{cond}}(m^*) + s_{\mathrm{gcan},m^*}(\rho - m^*) - s_{\mathrm{can}}(\rho) = 0 \ ,$$

this implies the truncated background measure converges in the sense of (3.24) to the truncated grand canonical measures.

The result follows by applying the triangle inequality. □

3.5 Connection to the large deviation principle

Throughout this chapter we have derived point-wise estimates of the exponential speed at which the probability of certain rare events tends to zero. In this section we show how these point-wise limits are typically stronger, and hence give rise to, the large deviation principle as stated in C.3. The large deviation principle is stated in terms of upper and lower bounds on closed and open sets, respectively. It is defined in this way so that it may be weak enough to hold in many situations whilst still being useful in deriving general results. Many useful and far reaching results follow from the large deviation principle, such as Varadhan's Lemma and concentration of measure inequalities (see Appendix C, also more details can be found for example [34, 35]). In order that we may apply these general results we show here that the large deviation principle often follows from the limits we derive. It is possible for us to derive these more refined large deviation estimates, in the case described in this chapter, because of the lattice nature of the distributions and the availability of relevant local limit theorems.

Proposition 3.14. *If the canonical entropy density exists,*

$$s_{can}(\rho) = \lim_{L\to\infty} \frac{1}{a_L} \log \nu^L \left[S_L = \rho_L\right] \quad \textit{for all} \;\; \rho_L \to \rho, \quad \textit{in the sense of} \; (3.18),$$

and $-s_{can}$ is a rate function in the sense of Definition C.2, then $\nu^L \circ S_L^{-1}$ obeys a weak large deviation principle with rate function $-s_{can}$ and speed a_L.

Proof. Let $O \subset \mathbb{R}_+$ be an non-empty open set. Since s_{can} is upper semi-continuous it attains its maximum on the closer, $\overline{O}$. We fix $\rho \in \overline{O}$ such that $s_{\text{can}}(\rho) = \sup_{x\in\overline{O}} s(x)$. Now fix a sequence $(\rho_L) \in O$, such that $\rho_L \to \rho$ as in (3.18). Then,

$$\liminf_{L\to\infty} \frac{1}{L} \log \nu^L[S_L \in O] \geq \liminf_{L\to\infty} \frac{1}{L} \log \nu^L[S_L = \rho_L] = s_{\text{can}}(\rho) \geq \sup_{x\in O} s(x) \;,$$

this provides the large deviation lower bound.

It is sufficient to show the upper bound for closed balls by the standard approximation argument for compact sets. Fix $\rho > r > 0$,

$$\begin{aligned}\frac{1}{a_L} \log \nu^L \left[S_L \in \overline{B}_r(\rho)\right] &\leq \frac{1}{a_L} \log \sum_{k=\lfloor b_L(\rho-r)\rfloor}^{\lceil b_L(\rho+r)\rceil} \nu^L \left[S_L = k/b_L\right] \\ &\leq \frac{1}{a_L} \log \left((2\lfloor b_L r\rfloor + 1)\, \nu^L[S_L = k_L^*/b_L] \right)\end{aligned}$$

where $k_L^* = \arg\max_{k\in A} \nu^L \left[S_L = k/b_L\right]$, and A is the set the sum runs over. It follows that,

$$\limsup_{L\to\infty} \frac{1}{a_L} \log \nu^L \left[S_L \in \overline{B}_r(\rho)\right] \leq \limsup_{L\to\infty} \frac{1}{a_L} \log \nu^L[S_L = k_L^*/b_L] = a \in [-\infty, 0] \;.$$

We may choose a subsequence converging to this limit, and since sequence k_L^*/b_L is bounded we may choose a further subsequence such that this limit exists and is given

by $\rho^\dagger \in \overline{B}_r(\rho)$. We therefore have the required upper bound for compact sets,

$$\limsup_{L\to\infty} \frac{1}{a_L} \log \nu^L \left[S_L \in \overline{B}_r(\rho) \right] \leq s_{\rm can}(\rho^\dagger) \leq \sup_{x\in\overline{B}_r(\rho)} s_{\rm can}(x) \ .$$

□

Proposition 3.15. *Assume that the following limit exists, for each sequence $m_L \to m \in [0,\rho]$ according to* (3.41) *and satisfying assumption (7),*

$$\begin{aligned} I_\rho(m) &= -\lim_{L\to\infty} \frac{1}{a_L} \log \pi^L_{\rho_L}[M_L = m_L] \\ &= I(\rho, m) + s_{can}(\rho) \ , \end{aligned} \tag{3.78}$$

and that I_ρ is a good rate function. Then $\pi^L_{\rho_L} \circ M_L^{-1}$ satisfies a large deviation principle with speed a_L and rate function I_ρ.

Proof. For any subset of $(0,\rho]$ the proof follows that of Proposition 3.14. Notice that for $m_L \to 0$ we are restricted in which sequences we consider by assumption (7), and so it is not immediately clear that,

$$\limsup_{L\to\infty} \frac{1}{a_L} \log \pi^L_{\rho_L} \left[\ M_L \in [0,\epsilon] \ \right] \leq -\inf_{x\in[0,\epsilon]} I_\rho(x) \ .$$

However, for any sequence $m_L \to 0$ there is some m'_L satisfying assumption (7) such that,

$$\begin{aligned} \limsup_{L\to\infty} \frac{1}{a_L} \log \nu^L[S_L = \rho_L, M_L = m_L] &\leq \limsup_{L\to\infty} \frac{1}{a_L} \log \nu^L[S_L = \rho_L, M_L \leq m'_L] \\ &\leq \limsup_{L\to\infty} \frac{1}{a_L} \log \nu^L_{m'_L}[S_L = \rho_L - m'_L] = I(\rho, 0) \ , \end{aligned}$$

where the second line follows from Lemma 3.8. The result follows from Theorem 3.10.

□

3.6 Discussion

The main results of this section are contained in Theorems 3.7 and 3.10. Theorem 3.7 states that if the Legendre-Fenchel transform of the pressure is convex then we have equivalence of ensembles. This not only holds for the canonical and grand canonical ensembles but also for the restricted versions. If we also know that the canonical ensembles concentrate on configurations with a particular bound on the maximum then this can lead to equivalence between the unrestricted canonical ensemble and the restricted grand canonical ensemble. This is the content of Corollary 3.12. Under the canonical measures, the macroscopic maximum site occupation concentrates on the global minimum of $I_\rho(\cdot)$.

The rate function for the joint density and maximum under the grand canonical

measures, $I(\rho, m)$, can be calculated following Theorem 3.10. Notice that conditioning the canonical measures at density ρ to have macroscopic maximum less than or equal to ρ does not impose any restriction. This implies that $s_{\mathrm{can},\rho}(\rho) = s_{\mathrm{can}}(\rho)$ so Theorem 3.10 allows us to calculate the canonical entropy by contracting on the maximum occupied site. The second part of Theorem 3.10 states that we need not know the entire rate function, only its value at the minimum, in order to perform the contraction. We may be required to iterate the contraction for fixed ρ to find the full rate function $I(\rho, m)$ and finally $s_{\mathrm{can}}(\rho)$. If there exists an $\bar{m}$ such that $\mathcal{D}_{p_{\bar{m}}} \supset \mathcal{D}_p$ (that is there is a value of the cut-off that provides a non-trivial extension of the pressure) then for any $\rho > 0$ we have to perform this iterative procedure only finitely many times to calculate $I(\rho, \cdot)$. This implies that $s_{\mathrm{can}}(\rho)$ exists and we can calculate it by applying the contraction on finitely many macroscopically occupied sites.

The results of this chapter do not rely on the random variable S_L being positive. They therefore also hold for the re-centred density,

$$T_L(\boldsymbol{\eta}) = \frac{1}{b_L} \sum_{x \in \Lambda_L} \left(\eta_x - \nu\left(\eta_1\right)\right) \tag{3.79}$$

which counts the 'excess' density in the system, above or below the expected number under ν on the scale b_L. The moderate deviations of this random variable give rise to the leading order finite-size effects in Chapter 4, and can be found using the results of this chapter.

The methods of this chapter are essentially equivalent to applying Laplace/steepest-descent methods to asymptomatically estimate the finite sums defining the canonical partition function $Z(L, \rho)$ and the truncated version $Q(L, \rho, m)$ (see Appendix D.1), which gives rise to the cumulative probability distribution for the largest mass, for details on this approach see [47].

In the following chapters the results are applied to three examples; finite size effects in a standard condensing zero-range process, a size-dependent zero-range process, and the recently introduced inclusion process. The methods apply in general to any system that conserves mass and exhibits stationary product measures. For instance they can be applied to study other size-dependent zero-range processes such as those analysed in [114]. There it was shown that, depending on the size-dependence of the jump rates, multiple condensates can be stabilised in the thermodynamic limit. This included the case of finitely many macroscopic condensates as well as infinitely many mesoscopic condensates. The former case can be analysed in the context of the results in this chapter, however, to derive useful rigorous results on the latter case would require contracting over a number of mesoscopically occupied sites growing with L. This would require a slight adjustment of Theorem 3.10 to allow for contractions on the events that include the excess mass being distributed over a growing number of lattice sites.

It is also possible to apply similar methods to continuous mass versions of the systems discussed here, in which the local state space is replaced with $\mathbb{R}_+$. If the single site marginals are equivalent to the Lebesgue measure (absolutely continuous with respect to

one another) then, with some technical effort, one can extend the analysis in this chapter to these continuous mass systems. It is then possible to define canonical measures by conditioning the reference measures on a single real value of the mass (despite the set having measure zero). Care must be taken, since the canonical measures of a system of size L are defined on an $L-1$ dimensional simplex, and so the relative entropy must be taken with respect to ν^{L-1}. Interesting metastability phenomena have been observed for size-dependent continuous mass transport systems in [133]. Another family of continuous mass models that these results could apply to is given by the Brownian energy and Brownian momentum processes [56, 57], which are closely related to the inclusion process discussed in Chapter 6.

Necessary and sufficient conditions for the existence of product stationary measures for a large class of discrete and continuous mass transport systems have been found [49, 63, 132]. Also the accuracy of mean-field predictions derived from approximations of the stationary measures by product measures have been investigated for continuous mass systems [134]. It follows from these studies that the results of this chapter apply to a wide range of mass transport systems that may exhibit a condensation transition. It would be interesting to extend the results here to systems with weak correlations between sites. For such systems extended condensates could be formed, over more than a single lattice site. In this case the surface tension associated with the formation of a condensate may also contribute to the canonical entropy densities. There has been recent work in this area, considering mass transport models with pair-factorised steady states [126, 127, 128]. The models in this work represent a good starting point for generalising the methods in this chapter.

Another possible extension are processes with multiple particle species [65]. In this case the relevant thermodynamic quantities such as the pressure and entropy densities are defined on higher dimensional spaces, and an extension of the analysis requires some technical work.

Chapter 4

Finite-size effects in zero-range condensation

4.1 Introduction

In this Chapter we study zero-range processes which are known to exhibit a condensation transition, where above a critical density a non-zero fraction of all particles accumulates on a single lattice site. This phenomenon has been a subject of recent research interest and is well understood in the thermodynamic limit (as explained in Section 2.3). However, the system shows large finite-size effects, and we observe a switching between metastable fluid and condensed phases close to the critical point, in contrast to the continuous limiting behaviour of relevant observables. We describe the leading order finite-size effects and establish a discontinuity near criticality in a rigorous scaling limit, using the methods of Chapter 3. We also characterise the metastable phases using a current matching argument and an extension of the fluid phase to supercritical densities. This constitutes an interesting example where the thermodynamic limit fails to capture essential parts of the dynamics, which are particularly relevant in applications with moderate system sizes such as traffic flow or granular clustering [68, 83, 89, 124]. The phenomenon we observe in the scaling limit is very similar to that observed in the thermodynamic limit of the size-dependent system (Chapter 5). Using a heuristic approach we are able to accurately predict the metastable switching between the fluid and condensed states as well as the dynamics of the condensate.

We consider a zero-range process as defined in Section 2.2.1, with generator (2.12), the main results focus on jump rates $g : \mathbb{N}_0 \to \mathbb{R}_+$ of the form

$$g(n) = \begin{cases} 1 + \frac{b}{n^\gamma} & \text{if } n > 0 \\ 0 & \text{if } n = 0 \end{cases} \tag{4.1}$$

with $\gamma \in (0, 1)$ and $b > 0$. These jump rates were first introduced by Evans [42] and represent a fairly general class of models exhibiting a condensation transition. For presentation in this chapter we focus on lattices $\Lambda_L = \{1, 2, \ldots, L\}$ with periodic boundary conditions. This is not essential for the stationary results and a discussion on other

geometries and on extending these results to the case $\gamma = 1$ and $b \geq 3$ can be found in Section 4.6.

While most of the results so far consider the thermodynamic limit, finite-size effects in the model with jump rates $g(n)$ and $\gamma = 1$ have been investigated in [44, 98] using saddle point methods, and in [3] for a variant of the model with a single defect site. In the condensed phase region of the phase diagram in the thermodynamic limit, finite systems are found to exhibit a large overshoot of the stationary current above its critical value. For $\gamma < 1$, the main focus of this chapter, finite systems exhibit a metastable switching behaviour between the two phases, which is prevalent in Monte Carlo simulations for a wide range of parameters. We describe this phenomenon in a scaling limit by deriving the large deviation rate function I_ρ, or free energy landscape, for the maximum site occupation (see Section 4.4.1). We find that above the critical density this exhibits a double well structure, signalling metastability as discussed in Section 2.4. One local minimum corresponds to maximum site occupations that are sub-extensive, corresponding to a fluid state, and the other minimum is at large maximum site occupations corresponding to a condensed (phase separated) state. As the total density in the system increases, the relative depth of the minima changes. This way we rigorously establish the discontinuous behaviour on the critical scale, even though the bulk density and average current are continuous functions in the thermodynamic limit. These results are shown to be in agreement with recent findings on the condensation transition at the critical density [5]. Based on the exact scaling limit, we can also predict the lifetime of the metastable phases for large finite systems by a heuristic random walk argument.

We recall, from Section 2.2.1, that the zero-range process has stationary single site weights which are given by $w(k) = \prod_{i=1}^{k} g^{-1}(i)$ for $k \geq 1$ and $w(0) = 1$. For the jump rates (4.1), the stationary weights are normalisable (see Chapter 2.2.1). We define the reference measure (see Chapter 3.2.1) as the product of these single site marginals, which have stretched exponential tails,

$$\nu_L[n] = \nu[n] = \frac{w[n]}{\sum_{k=0}^{\infty} w[k]} \sim e^{-\frac{b}{1-\gamma} n^{1-\gamma}} \quad \text{for} \quad \gamma \in (0,1) \ . \tag{4.2}$$

Since the single site marginals of the reference measures are independent of L we drop the subscript. So the reference measure on a system of size L is given by $\nu^L[\boldsymbol{\eta}] = \prod_{x\in\Lambda} \nu[\eta_x]$, and since the measures have stretched exponential tails, all finite moments exist, in particular the mean and variance,

$$\rho_c := \nu\left(\eta_x\right) < \infty \ , \quad \sigma_c^2 := \nu\left(\eta_x^2\right) - \rho_c^2 < \infty \ . \tag{4.3}$$

The reference measures therefore correspond to the critical product measures with average density ρ_c, this choice simplifies the presentation of the analysis in Section 4.4.

The chapter is organized as follows: In Section 4.2 we extend previous results on the thermodynamic limit. In Section 4.3 we make a numerical and heuristic study of the behaviour on a finite system and derive the rigorous scaling limit in Section 4.4.

In Section 4.5 we connect these results to the lifetimes of the metastable phases, and dynamics of the condensate. We end with a discussion of the results and outlook in Section 4.6.

4.2 Thermodynamic limit

4.2.1 Equivalence of ensembles

We quickly recall previous results on the equivalence of ensembles and condensation transition for model (4.1) in the thermodynamic limit (summarized in Section 2.3), here in the context of the general results of Chapter 3. As the particle number N and lattice size L tend to infinity such that $\rho_L := N/L \to \rho$, all finite dimensional marginals of the canonical measure $\pi^L_{\rho_L}$ converge to the grand canonical measure with density ρ if $\rho \leq \rho_c$. If $\rho > \rho_c$ then there is no grand canonical measure with density ρ and all finite dimensional marginals of $\pi^L_{\rho_L}$ converge to the grand canonical measure with density ρ_c. In this case the excess mass condenses on a single lattice site.

In the thermodynamic limit, following Section 3.2.1, the order parameter is the total number of particles in the system divided by the system size L. We therefore introduce the random variable S_L that gives the empirical density of a configuration (see Definition 3.1),

$$S_L(\boldsymbol{\eta}) = \frac{1}{L} \sum_{x \in \Lambda_L} \eta_x \ .$$

This corresponds to fixing the scale $b_L = L$ and it turns out that the large deviations of the density under the reference measure decay on the scale $a_L = L$.

The canonical stationary measures, corresponding to the unique ergodic measure on a finite system at density ρ_L are given by

$$\pi^L_\rho[\boldsymbol{\eta}] = \nu^L[\boldsymbol{\eta} \mid S_L = \rho_L] \quad \text{for } \rho_L \to \rho \ .$$

For the canonical measures to be well defined we consider sequences (ρ_L) as defined by (3.18). The canonical partition function is defined in the usual way,

$$Z(L, \rho_L) = \nu^L[S_L = \rho_L] \ . \tag{4.4}$$

As discussed in Section 2.2.1 the stationary current under the canonical measures is given by a ratio of partition functions,

$$j^{\text{can}}_L(\rho_L) := \pi^L_\rho \left(g(\eta_x) \right) = \frac{Z(L, \rho_L - 1/L)}{Z(L, \rho_L)} \ . \tag{4.5}$$

For this model the grand canonical pressure, from Definition 3.2, is independent of

system size and given by

$$p(\mu) = \begin{cases} \log \nu \left(e^{\mu \eta_1}\right) & \text{for } \mu \in \mathcal{D}_p = (-\infty, 0] \\ \infty & \text{otherwise.} \end{cases} \tag{4.6}$$

With the sub-exponential decay (4.2), the grand canonical measures exist for all $\mu \in (-\infty, 0]$ and are given by the product of the single site marginals (c.f. Section 2.2.1),

$$\nu_\mu[n] = \frac{\nu[n] e^{\mu n}}{z(\mu)} \quad \text{where } z(\mu) = \nu\left(e^{\mu \eta_1}\right) \ . \tag{4.7}$$

The pressure $p(\mu)$ is strictly increasing and convex on its domain $\mathcal{D}_p$. Since the pressure is the scaled cumulant generating function for S_L under the grand canonical measures, we observe that the average density, at chemical potential μ, is given by

$$\begin{aligned} R(\mu) &:= \nu_\mu^L \left(S_L\right) = \nu_\mu^L \left(\eta_1\right) \\ &= \frac{1}{z(\mu)} \sum_{k=0}^{\infty} k \nu[k] e^{k\mu} = \partial_\mu p(\mu) \ . \end{aligned} \tag{4.8}$$

The grand canonical current is given by

$$j_L^{\mathrm{gc}}(\mu) = \nu_\mu \left(g_L(\eta_x)\right) = \frac{1}{z_L(\mu)} \sum_{n=0}^{\infty} g(n) e^{\mu n} \nu[n] = e^\mu \ .$$

For details see Section 2.2.1. We denote the inverse of R by $\mathcal{M} : (0, \rho_c] \to (-\infty, 0]$. So the grand canonical measures can be parametrized by the average density ρ for all $\rho < \rho_c$. We may extend the function $\mathcal{M}$ to all densities following Theorem 3.6,

$$\bar{\mu}(\rho) = \begin{cases} \mathcal{M}(\rho) & \text{for } \rho < \rho_c \\ \mu_c = 0 & \text{for } \rho \geq \rho_c \ . \end{cases} \tag{4.9}$$

The entropy densities in the thermodynamic limits are identified by a superscript 'TD', following Definitions 3.12 and 3.13, we have

$$s_{\mathrm{can}}^{\mathrm{TD}}(\rho) = \lim_{L \to \infty} \frac{1}{L} \log Z(L, \rho_L) \quad \text{as } \rho_L \to \rho \tag{4.10}$$

$$s_{\mathrm{gcan}}^{\mathrm{TD}}(\rho) = -p^*(\rho) = \log z(\bar{\mu}(\rho)) - \bar{\mu}(\rho)\rho \ , \tag{4.11}$$

where p^* is the Legendre-Fenchel transform of the pressure (4.6). We observe that $s_{\mathrm{gcan}}^{\mathrm{TD}}(\rho)$ is strictly concave up to ρ_c, and then constant and equal to zero for all $\rho \geq \rho_c$. We now restate Theorem 2.7 from Section 2.3 in terms of the general results of Chapter 3.

Theorem 4.1 (Thermodynamic limit equivalence of ensembles)**.** *For all $\rho > 0$,*

$$\lim_{L\to\infty} \frac{1}{L} H(\pi^L_{\rho_L} \mid \nu^L_{\bar{\mu}(\rho)}) = s^{TD}_{gcan}(\rho) - s^{TD}_{can}(\rho) = 0 \ . \tag{4.12}$$

So $\pi^L_{\rho_L} \overset{L}{\longleftrightarrow} \nu^L_{\bar{\mu}(\rho)}$, in the senses of Definition 3.11, as $L \to \infty$ and $\rho_L \to \rho$.

For $\rho < \rho_c$ this is a direct result of Theorem 3.7. Above the critical density $s^{\mathrm{TD}}_{\mathrm{gcan}}$ is constant, in order to calculate $s^{\mathrm{TD}}_{\mathrm{can}}$ above the critical point we contract on the maximum site occupation. We find that the canonical entropy density is still equal to the grand canonical entropy density, and so the canonical measures converge to the grand canonical measure at ρ_c, and the excess mass condenses in a vanishing volume fraction, as discussed in Section 2.3. To show that the condensate typically resides on a single site, using the methods of Chapter 3, it is necessary to consider corrections to the thermodynamic limit (given in the next Section 4.2.2).

Following the methods of Chapter 3 we calculate the large deviations of the maximum component (on the macroscopic scale L) in the thermodynamic limit. These also give rise to the equivalence of ensembles above ρ_c, by the contraction described in Section 3.4.4. The macroscopic maximum site occupation, following Definition 3.5, is given by the random variable $M_L(\boldsymbol{\eta}) = \frac{1}{L}\max_x \eta_x$. We calculate a rate function $I_\rho(m)$ that describes the asymptotic probability of observing a maximum site occupation equal to $(mL + o(L)) \in [0, \rho]$. Precisely, we will consider the limit as defined by (3.18) and (3.41), and find that

$$\pi^L_\rho \left[M_L = m_L\right] \sim e^{-LI^{\mathrm{TD}}_\rho(m)} \ . \tag{4.13}$$

To this end we define the following function for finite systems,

$$F^L_{\rho_L}(m_L) = -\frac{1}{L}\log \pi^L_{\rho_L}\left[M_L = m_L\right] \ , \tag{4.14}$$

where m_L is a sequence with positive measure defined by (3.41). If the maximum occupied site has a *macroscopic* size m, then the density of particles outside of the maximum must be $\rho - m$. We call the density outside of the maximum occupied site the *background density* and denote it by $\rho_{\mathrm{bg}} = (\rho - m)$.

Theorem 4.2. *In the thermodynamic limit as $\rho_L \to \rho$ as in* (3.18)*,*

$$I^{TD}_\rho(m) := \lim_{L\to\infty} F^L_{\rho_L}(m_L) = s^{TD}_{gcan}(\rho) - s^{TD}_{gcan}(\rho_{bg}) \quad \textit{with } \rho_{bg} = (\rho - m), \tag{4.15}$$

for all $m_L \to m \in [0, \rho]$, where s^{TD}_{gcan} is given by (4.11)*. So for $\rho > \rho_c$ (supercritical case), $I^{TD}_\rho(m) = 0$ for each $m \le (\rho - \rho_c)$ (see Fig. 4.1). Note that by Theorem 4.1 $s^{TD}_{can} \equiv s^{TD}_{gcan}$.*

For $m = 0$ or ρ, the limit actually depends on the precise scaling of m_L, which we do not discuss here (see [4] for more details).

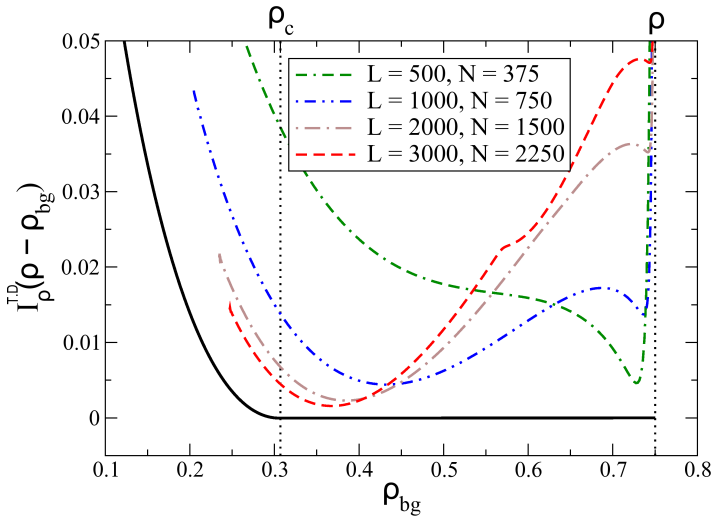

Figure 4.1: Thermodynamic limit rate function for a fixed system density $\rho = 0.75$ with $\gamma = 0.5$ and $b = 4$. $I^{\mathrm{TD}}_{\rho}(\rho - \rho_{\mathrm{bg}})$ is shown by a solid black line. The dashed lines show $F^{L}_{\rho_L}(\rho - \rho_{\mathrm{bg}})$ against ρ_{bg}, with $\rho_L = 0.75$, for several values of L calculated by exact numerics using Eq. (2.24). Note that convergence to $I^{\mathrm{TD}}_{\rho}(\rho_{\mathrm{bg}})$ (solid black) is slow and initially non-monotonic above ρ_c.

Proof. The proof follows the results in Chapter 3. It is straightforward to check that all the assumptions in Section 3.4.1 are satisfied. The condensate contribution tends to zero, since the reference measure has stretched exponential tails,

$$s^{\mathrm{TD}}_{\mathrm{cond}}(m) = \lim_{L\to\infty} \frac{1}{L} \log \nu_L[m_L L] = 0 \quad \text{for all } (m_L) \in [0, \rho] \ .$$

The restricted pressure p_m has the same essential domain as p and is therefore equal to the grand canonical pressure, since the following partial sums diverge for $\mu \notin \mathcal{D}_P$,

$$\sum_{k=0}^{m_L L} \nu_L[k] e^{\mu k} \to \infty \quad \text{for } \mu > 0 \ .$$

Therefore the grand canonical entropy density of the restricted ensembles is equal to the grand canonical entropy density for all m, $s^{\mathrm{TD}}_{\mathrm{gcan},m}(\rho) = s_{\mathrm{gcan}}(\rho)$. So by Theorem 3.10 we have,

$$\begin{aligned} I^{\mathrm{TD}}(\rho, m) &= -s^{\mathrm{TD}}_{\mathrm{gcan}}(\rho - m) \quad \text{for } \rho > m > (\rho - \rho_c) \quad \text{and} \\ I^{\mathrm{TD}}(\rho, m) &\geq -s^{\mathrm{TD}}_{\mathrm{gcan}}(\rho - m) \quad \text{for } m \leq (\rho - \rho_c) \ . \end{aligned}$$

By iterating the contraction once, it is clear that the lower bound is also an upper bound, and $I^{\mathrm{TD}}(\rho, m) = -s^{\mathrm{TD}}_{\mathrm{gcan}}(\rho - m)$ for all $\rho > 0$ and $m \in (0, \rho)$. Alternatively, for $m \leq (\rho - \rho_c)$ the upper bound follows by arranging the excess mass in the background among a finite number of sites so that each site contains at most m particles. This provides a sub-exponential lower bound for $\bar{\nu}^{L-1}_{m}[S_{L-1} = \rho_L - m_L]$. The result now

follows from Corollary 3.11. □

4.2.2 Leading order corrections to the thermodynamic limit

In this subsection we study the rate of convergence to the thermodynamic limit. This gives rise to a large deviation rate function for the maximum above ρ_c on a finer scale, which indicates that the maximum typically contains $(\rho - \rho_c)L$ particles and occupies a single lattice site. Since the grand canonical measures have finite exponential moments below ρ_c, convergence to the thermodynamic limit is quick, following (3.58),

$$\frac{1}{\hat{a}_L} H(\pi_\rho^L \mid \nu_{\mu(\rho)}^L) \to 0 \quad \text{for all } \rho < \rho_c \text{ and } \hat{a}_L \gg \log L \ . \tag{4.16}$$

However, convergence to the thermodynamic limit above ρ_c is dominated by the entropy cost of putting a macroscopic mass into a vanishing volume fraction, which is much slower as can be seen in Figure 4.1. Informally speaking, the goal of this subsection is to zoom in on the flat part of this rate function for supercritical densities, and to understand the correction

$$\text{“ } s_{\text{can}}(\rho) \simeq s_{\text{can}}^{\text{TD}}(\rho) + \frac{a_L}{L} s_{\text{can}}^{\text{LO}}(\rho) \text{” } .$$

We denote the leading order contribution to the entropy densities and the rate function for the maximum site occupation, above the critical point, by a superscript ‘LO’.

The critical measures have stretched exponential tails (4.2), so if the excess mass occupies only a finite number of sites, it will contribute to the entropy density at a scale $a_L = L^{1-\gamma}$. The contribution due to order L particles occupying a single site is given by

$$s_{\text{cond}}^{\text{LO}}(m) = \lim_{L\to\infty} \frac{1}{a_L} \log \nu_L[m_L L] = \frac{-b}{1-\gamma} m^{1-\gamma} \ , \tag{4.17}$$

and the grand canonical pressure on this scale is given by

$$\begin{aligned} p^{\text{LO}}(t) &= \lim_{L\to\infty} \frac{1}{a_L} \log \nu^L \left(e^{t a_L S_L}\right) = \lim_{L\to\infty} L^\gamma \log z((tL^{-\gamma})\eta_1) \\ &= \begin{cases} \rho_c t & \text{for } t \le 0 \\ \infty & \text{otherwise.} \end{cases} \end{aligned} \tag{4.18}$$

So the grand canonical entropy density is infinite below ρ_c, which is clear since it was non-zero in the the thermodynamic limit, and it is still zero above ρ_c,

$$s_{\text{gcan}}^{\text{LO}}(\rho) = -(p^{\text{LO}})^*(\rho) = \begin{cases} -\infty & \text{for } \rho < \rho_c \\ 0 & \text{for } \rho \ge \rho_c \ . \end{cases} \tag{4.19}$$

The following theorem states that this is the correct scale for observing the convergence to the thermodynamic limit above criticality and gives the leading order correction to the canonical entropy density, and the rate function for the maximum site occupation

(these are summarised in Figure 4.2).

Theorem 4.3. *The leading order behaviour above criticality is on the scale* $a_L = L^{1-\gamma}$. *The canonical entropy density is given by*

$$s^{LO}_{can}(\rho) = \lim_{L\to\infty} L^{\gamma-1} \log Z(L, \rho_L) \quad \text{as } \rho_L \to \rho \ \text{ following (3.18)} \tag{4.20}$$

$$= \begin{cases} -\infty & \text{for } \rho < \rho_c \\ s^{LO}_{cond}(\rho - \rho_c) & \text{for } \rho \geq \rho_c \ , \end{cases} \tag{4.21}$$

and the rate function of the maximum site occupation is given by

$$I^{LO}_{\rho}(m) = \begin{cases} s^{LO}_{can}(\rho) - \left\lfloor \frac{(\rho-\rho_c)}{m} \right\rfloor s^{LO}_{cond}(m) - s^{LO}_{cond}(r) & \text{for } m \leq (\rho - \rho_c) \\ \infty & \text{for } (\rho - \rho_c) < m \leq \rho \end{cases} , \tag{4.22}$$

where $(\rho - \rho_c) = \lfloor \frac{(\rho-\rho_c)}{m} \rfloor m + r$. *Upwards deviations of the maximum require the bulk to lose a macroscopic number of particles and are described on the scale of* L *by Theorem 4.2.*

We recall that $\lfloor x \rfloor$ denotes the integer floor of the real number x. For clarity we give the explicit form of I^{LO}_{ρ} (for an illustration see Fig. 4.2),

$$I^{\mathrm{LO}}_{\rho}(m) = \begin{cases} \infty & \text{for } (\rho - \rho_c) < m \leq \rho \\ s^{\mathrm{LO}}_{\mathrm{can}}(\rho) - s^{\mathrm{LO}}_{\mathrm{cond}}(m) - s^{\mathrm{LO}}_{\mathrm{cond}}(\rho - \rho_c - m) & \text{for } \frac{(\rho-\rho_c)}{2} \leq m \leq (\rho - \rho_c) \\ s^{\mathrm{LO}}_{\mathrm{can}}(\rho) - 2s^{\mathrm{LO}}_{\mathrm{cond}}(m) - s^{\mathrm{LO}}_{\mathrm{cond}}(\rho - \rho_c - 2m) & \text{for } \frac{(\rho-\rho_c)}{3} \leq m \leq \frac{(\rho-\rho_c)}{2} \\ \dots & \dots \\ s^{\mathrm{LO}}_{\mathrm{can}}(\rho) - ns^{\mathrm{LO}}_{\mathrm{cond}}(m) - s^{\mathrm{LO}}_{\mathrm{cond}}(\rho - \rho_c - nm) & \text{for } \frac{(\rho-\rho_c)}{(n+1)} \leq m \leq \frac{(\rho-\rho_c)}{n} \\ \dots & \dots \end{cases}$$

It follows that above ρ_c the canonical measures concentrate on configurations in which all the excess mass resides on a single lattice site. The rate function for the maximum below $(\rho - \rho_c)$ states that the large deviations decay as a stretched exponential of the system size, $\pi^L_\rho[M_L = m_L] \sim e^{-L^{1-\gamma} I^{\mathrm{LO}}_{\rho}(m)}$. These large deviations are attained by arranging the excess mass on the smallest possible number of sites. The proof of this theorem and the results in the scaling limit rely on the following lemmas that give rise to the truncated pressures.

Lemma 4.4. *Consider two sequences $x_n \in \mathbb{N}$, $t_n \in (0,\infty)$, such that $x_n \to \infty$, $t_n \to 0$ and $x_n^\gamma t_n \to C$ as $n \to \infty$ with $C \in [0, \frac{b}{1-\gamma})$. Then for each $i \in \mathbb{N}_0$*

$$\limsup_{n\to\infty} \sum_{k\le x_n} k^i w(k) e^{t_n k} < \infty \ ,$$

and if $x_n^\gamma t_n > \frac{b}{1-\gamma}$ for n sufficiently large,

$$\lim_{n\to\infty} \sum_{k\le x_n} k^i w(k) e^{t_n k} = \infty.$$

Proof. From the asymptotic behaviour of $w(k)$ Eq. (4.2) we know there exists a $C_0 \in (0,\infty)$ such that $w(k) \le C_0 e^{\frac{-b}{1-\gamma}k^{1-\gamma}}$ for all k. So,

$$\sum_{k\le x_n} k^i w(k) e^{t_n k} \le C_0 \sum_{k\le x_n} k^i e^{\frac{-b}{1-\gamma}k^{1-\gamma}+t_n k}. \tag{4.23}$$

Fix $0 \le \epsilon < (\frac{b}{1-\gamma} - C)$. Then there exists $\bar{n} \in \mathbb{N}$ such that $t_n \le (C+\epsilon)x_n^{-\gamma}$ for $n \ge \bar{n}$. It follows that $t_n \le (C+\epsilon)k^{-\gamma}$ for all $k \le x_n$ and $n \ge \bar{n}$. By applying this upper bound on t_n we can bound the sum above uniformly in $n > \bar{n}$ as follows,

$$\begin{aligned}\sum_{k\le x_n} k^i w(k) e^{t_n k} &\le C_0 \sum_{k\le x_n} k^i e^{\frac{-b}{1-\gamma}k^{1-\gamma}+(C+\epsilon)k^{1-\gamma}} \\ &\le C_1 \int_0^\infty u^i e^{\frac{-b}{1-\gamma}u^{1-\gamma}+(C+\epsilon)u^{1-\gamma}}\,\mathrm{d}u < \infty. \end{aligned}\tag{4.24}$$

The inverse is clear, since from Eq. (4.2) we know there exists a $C_2 \in (0,\infty)$ such that,

$$\sum_{k\le x_n} k^i w(k) e^{t_n k} \ge C_2 \sum_{k\le x_n} k^i e^{\frac{-b}{1-\gamma}k^{1-\gamma}+t_n k}, \tag{4.25}$$

and the final term in the sum diverges if $x_n^\gamma t_n > \frac{b}{1-\gamma}$. □

Lemma 4.5. *Under the assumptions of Lemma 4.4 we may bound the remainder in the Taylor expansion of each moment under the restricted ensembles introduced in Section 3.2.3. We have*

$$\begin{aligned}\nu\left(e^{t_n\eta_1}\mathbb{1}_{\{\eta_x\le x_n\}}(\eta_1)\right) &= 1 + t_n\partial_\mu z(0) + \frac{t_n^2}{2}\partial_\mu^2 z(0) + o(t_n^2), \\ \nu\left(\eta_1^i e^{t_n\eta_1}\mathbb{1}_{\{\eta_x\le x_n\}}(\eta_1)\right) &= \nu\left(\eta_1^i\right) + t_n\partial_\mu\nu_0\left(\eta_1^i\right) + \frac{t_n^2}{2}\partial_\mu^2\nu_0\left(\eta_1^i\right) + o(t_n^2).\end{aligned}$$

Proof. This Lemma follows from Lemma 4.4 by dominated convergence. For a proof by direct computation see [25] Lemma 2. □

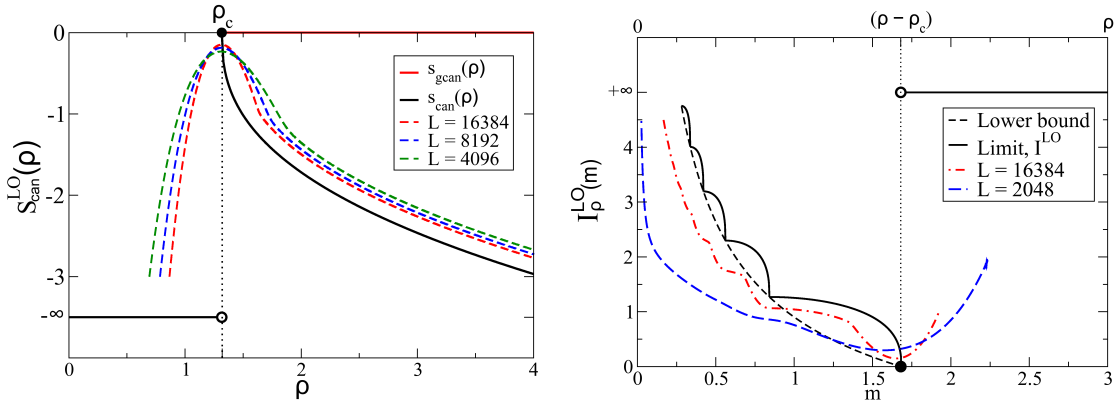

Figure 4.2: Convergence to the thermodynamic limit above the critical density ρ_c, as described by Theorem 4.3. System with $\gamma = 0.6$, $b = 0.8$. Left: The leading order canonical entropy density, the black line shows the limit $s^{\mathrm{LO}}_{\mathrm{can}}(\rho)$. The dashed coloured lines show exact numerics on finite systems. For $\rho < \rho_c$ the large deviations are on the scale L and so diverge on these plots. Right: The leading order canonical rate function for the maximum. The black line shows the limit $I^{\mathrm{LO}}_{\rho}(m)$. The dashed coloured lines show exact numerics on finite systems. For $m > (\rho - \rho_c)$ the large deviations are on the scale L and so diverge on these plots. The convergence to the limits in Theorem 4.3 appears to be very slow.

Proof of Theorem 4.3. We can calculate the truncated pressures from the previous Lemmas.

$$\begin{aligned} p^{\mathrm{LO}}_m(\mu) &= \lim_{L\to\infty} \frac{1}{a_L} \log \nu^L \left(e^{a_L \mu S_L} \mathbb{1}_{M_L \le m_L} \right) \\ &= \lim_{L\to\infty} L^\gamma \log \nu \left(e^{(\mu L^{-\gamma})\eta_1} \mathbb{1}_{\eta_1 \le m_L L} \right) \\ &= \begin{cases} \rho_c \mu & \text{if } \mu < \frac{b}{m^\gamma(1-\gamma)} \\ +\infty & \text{otherwise.} \end{cases} \end{aligned}$$

So the restricted grand canonical entropy density is given by

$$s^{\mathrm{LO}}_{\mathrm{gcan},m}(\rho) = \begin{cases} \frac{(\rho-\rho_c)b}{m^\gamma(1-\gamma)} & \text{if } \rho \ge \rho_c \\ -\infty & \text{otherwise.} \end{cases} \tag{4.26}$$

The result now follows by iterating the contraction in Theorem 3.10. □

4.3 Overshoot of the canonical current

In this section we present results obtained from exact numerics and Monte Carlo simulations in the canonical ensemble. We can calculate the canonical current, given by Eq. (4.5), by making use of the the recursion relations given in Appendix D.1. Similarly, we can calculate the canonical distribution of the maximum site occupation using the recursion relation for the truncated canonical partition function. See Appendix D.1 for

more details on the computations.

Firstly we recall the behaviour of the system in the thermodynamic limit (these results follow from Theorems 4.1 and 4.3), and have been found previously as summarised in Section 2.3). The macroscopic maximum site occupation $M_L(\boldsymbol{\eta}) = \frac{1}{L}\max_x \eta_x$ obeys a weak law of large numbers,

$$M_L \xrightarrow{\pi_\rho^L} \begin{cases} 0 & \text{if } \rho \leq \rho_c \\ \rho - \rho_c & \text{if } \rho > \rho_c \end{cases} . \tag{4.27}$$

This result can also be stated in terms of the behaviour of the bulk of the system. We denote the density of particles outside of the maximally occupied site by

$$S_L^{\mathrm{bg}}(\boldsymbol{\eta}) = \rho_L - M_L(\boldsymbol{\eta}) .$$

The background density converges in probability, under the canonical measures, as

$$S_L^{\mathrm{bg}}(\boldsymbol{\eta}) \xrightarrow{\pi_\rho^L} \begin{cases} \rho & \text{if } \rho \leq \rho_c \\ \rho_c & \text{if } \rho > \rho_c \end{cases} . \tag{4.28}$$

A similar result holds for the behaviour of the canonical current in the thermodynamic limit. With Eq. (2.17) the equivalence of ensembles (see Definition 3.11) implies that

$$j_L^{\mathrm{can}}(\rho_L) \to e^{\bar{\mu}(\rho)} \quad \text{as } L \to \infty \quad \text{and} \quad \rho_L \to \rho . \tag{4.29}$$

So the current and the background density are both continuous with respect to the total system density in the thermodynamic limit. Also both are strictly increasing up to ρ_c and constant for $\rho > \rho_c$. We recall from Section 2.3 that if $\rho_L \to \rho \leq \rho_c$ the system is said to be in the **fluid** phase region and if $\rho_L \to \rho > \rho_c$ the system is in the **condensed** phase region, in the thermodynamic limit.

4.3.1 Observations on finite systems

Using again the background density $\rho_{\mathrm{bg}} = (\rho_L - m_L)$, we have

$$\pi_{\rho_L}^L [M_L = m_L] = \pi_{\rho_L}^L \left[S_L^{\mathrm{bg}} = \rho_{\mathrm{bg}}\right] .$$

This variable is more useful for illustrations and is more intuitive, since the background density characterises all but a single lattice site, while the formulation involving M_L is more convenient for computations. Therefore keeping both formulations in parallel is the best option for a concise presentation of our results. It turns out that typically the background is distributed asymptotically independently with density ρ_{bg}. However, to realise large deviations in the maximum site occupation, which are important for the dynamics, sometimes the background can contain sub-condensates on the same scale as the condensate itself (see Section 4.5).

On large finite systems we observe significant finite-size effects above the critical

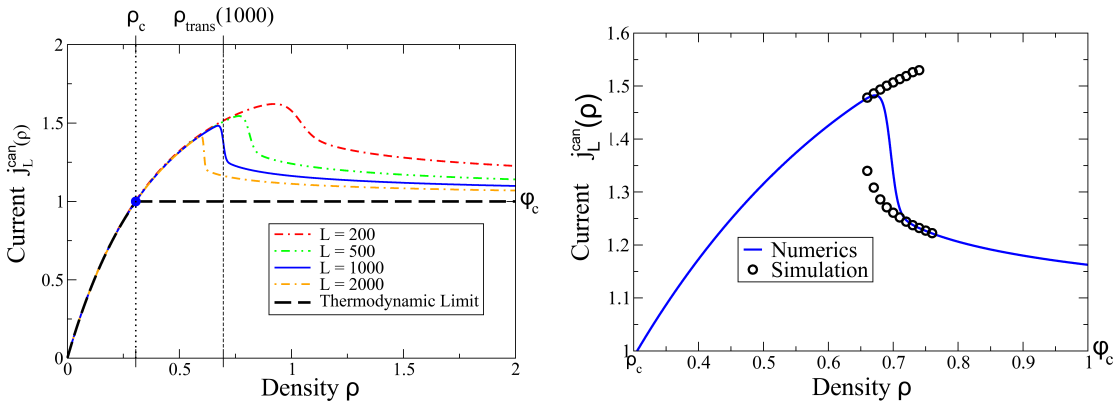

Figure 4.3: Finite-size effects and current overshoot for $\gamma = 0.5$ and $b = 4$. Left: The canonical current for various system sizes as a function of the density $\rho = \rho_L$ are plotted. The dashed black line shows the thermodynamic current as a function of the system density ρ. Right: The overshoot region for $L = 1000$ showing the two distinct currents measured from Monte Carlo simulations for various densities near the maximum current. All simulations of the zero-range process were performed using the update algorithm described in Appendix D.2.

density ρ_c, Fig. 4.3 shows the typical behaviour of the canonical current. Below ρ_c the current is very close to the thermodynamic limit result even on relatively small systems ($L \sim 100$) and the leading order finite-size effects can be understood immediately from the proof of the thermodynamic limit result [69]. However, the canonical current and background density significantly overshoot their critical values (see Fig. 4.3 and Fig. 4.4). The current increases monotonically with density ρ_L, in a way that appears to vary only very slightly with system size, up to some size-dependent maximum current at $\rho_{\text{trans}}(L)$. For $\rho_L < \rho_{\text{trans}}(L)$ the background density in the system is typically very close to ρ_L (Fig. 4.4). For a fixed system size L we associate $\rho_L < \rho_{\text{trans}}(L)$ with a **putative fluid phase region**. Close to $\rho_L = \rho_{\text{trans}}(L)$ there is an abrupt decrease in the current and background density. For $\rho_L > \rho_{\text{trans}}(L)$ the current and background density are both decreasing in ρ_L and tend to their respective critical value as $\rho_L \to \infty$. We associate $\rho_L > \rho_{\text{trans}}(L)$ with a **putative condensed phase region** where the increasing density is entirely taken up by a large number of particles condensing on a single lattice site. The size of the effective fluid overshoot increases with increasing b and with decreasing γ, and is already very pronounced at $\gamma = 0.5$, $b = 4$.

For ρ_L close to $\rho_{\text{trans}}(L)$ we observe that the canonical distribution over background densities (or maximum site occupation) has two maxima of similar magnitude (Fig. 4.4) and Monte Carlo simulations show that the system switches between the two metastable states associated with the putative phase regions. Fig. 4.5 shows the typical behaviour of the current close to $\rho_{\text{trans}}(L)$ as a function of time, the fluid and condensed states can be clearly distinguished by the current. For $\rho_L \approx \rho_{\text{trans}}(L)$ in the condensed state the location of the condensate does not change (over a large time frame), while its position fluctuates heavily in the fluid state, supporting the fact that the particles are distributed homogeneously.

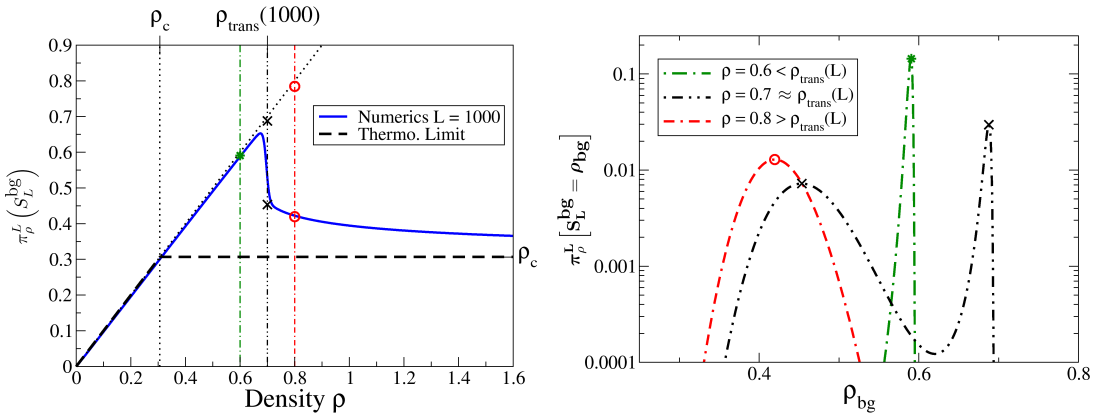

Figure 4.4: Finite-size effects for the background density S_L^{bg} (4.28) for $\gamma = 0.5$, $b = 4$ and $L = 1000$. Left: The expected value of the background density. The dashed black line shows the thermodynamic limit result. Right: Distribution of the background density at three system densities shown by corresponding dash-dotted lines on the left, calculated exactly using Eq. (2.24). The position of local maxima of the distributions are marked on both plots ($*$ for $\rho = 0.6$, $\times$ for $\rho = 0.7$, $\circ$ for $\rho = 0.8$). The high background density maximum at $\rho = 0.8$ occurs with extremely low probability and is off the scale.

The empirical distribution of lifetimes of the two states is very close to an exponential (Fig. 4.5 right). This suggests that the switching process is approximately Markovian over the range of parameters and jump distributions observed, and constitutes a genuine metastability phenomenon. The rate of the switching depends on the parameters b and γ as well as the jump distribution $p(x)$, which will be discussed in Section 4.5 in more detail.

Naturally, the thermodynamic limit result gives no indication of the sharp transition from fluid to condensed phase region or the metastable switching observed on large finite systems. For $\rho_L \to \rho > \rho_c$ the system will appear to be condensed for sufficiently large L, since $\rho_{trans}(L) \searrow \rho_c$ as $L \to \infty$ (see Fig. 4.3). Therefore the leading order finite-size effects of Theorem 4.3 neither describe the sharp transition nor the metastability, as can be seen in Fig. 4.1. The apparent double well structure of $\frac{1}{L} \log \pi^L_{\rho_L}[M_L = m_L]$ is less pronounced for higher L, and the location of the global minimum shifts towards ρ_c. To capture the sharp transition and the metastability we will replace the thermodynamic limit by an appropriate scaling limit in section 4.4.

4.3.2 Heuristics

Current Matching

As suggested by the form of the current overshoot in Figure 4.3, our approach is to approximate the fluid states above ρ_c by extending the grand canonical current above the critical value $e^{\mu_c} = 1$. This is achieved by means of a cut-off grand canonical measure, a restricted ensemble as defined in Chapter 3. Since the total number of particles is fixed canonically to $\rho_L L$ the system cannot explore states where any single

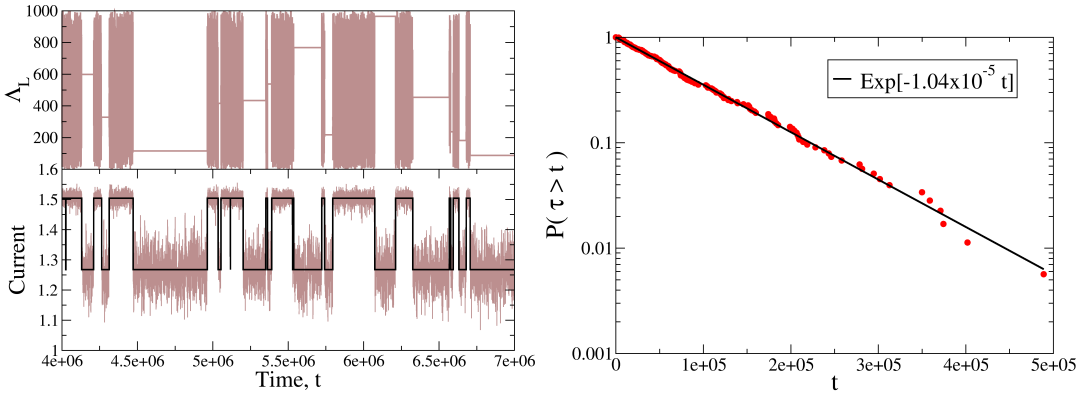

Figure 4.5: Switching dynamics for $\gamma = 0.5$, $b = 4$ and $L = 1000$ taken at $N/L = \rho_{\text{trans}}(1000) = 0.695$. Left: (Bottom) Current against time from Monte Carlo simulations, calculated by taking the average number of jumps in the system over small time windows. The black line indicates the transition between the fluid and condensed states. (Top) The location of the maximum does not change until the system is fluid. Right: Cumulative tail of the distribution of the lifetime of the fluid state on a log linear scale. The solid line shows an exponential fit.

site contains more than $\rho_L L$ particles. We therefore expect the distribution of particles in the background under the canonical measure will always be closer (in any reasonable sense) to a grand canonical measure, with some suitably chosen cut-off, and chemical potential chosen to fix the correct density of particles, than it is to the unconditioned distribution. Following Definition 3.7 in Section 3.2.3, for cut-off $m_L L \in \mathbb{N}$ the restricted grand canonical measures, on the scale of the thermodynamic limit, are defined by single site marginals with support on $\{0, 1, \ldots, m_L L\}$,

$$\begin{aligned} \bar{\nu}_{\mu,m}\left[\eta_x = n\right] &:= \nu_\mu\left[\eta_x = n | \eta_x \leq m_L b_L\right] \\ &= \frac{1}{\bar{z}_m(\mu)} \nu[n] e^{n\mu} \quad \text{for} \quad n \leq m_L L \end{aligned} \tag{4.30}$$

where the normalisation is given by the finite sum

$$\bar{z}_m(\mu) = \sum_{k=0}^{m_L L} \nu[k] e^{k\mu}. \tag{4.31}$$

These measures are well defined for all $\mu \in \mathbb{R}$ and the current is given by

$$\bar{\nu}_{\mu,m}\left(g(\eta_x)\right) = e^{\mu}\left(1 - \frac{\nu[m_L L] e^{m_L L \mu}}{\bar{z}_m(\mu)}\right). \tag{4.32}$$

Also the average density in the cut-off ensemble

$$R_m(\mu) := \bar{\nu}_{\mu,m}\left(\eta_x\right) = \frac{1}{z_m(\mu)} \sum_{k=0}^{m} k \nu_{\mu,m}(k) \tag{4.33}$$

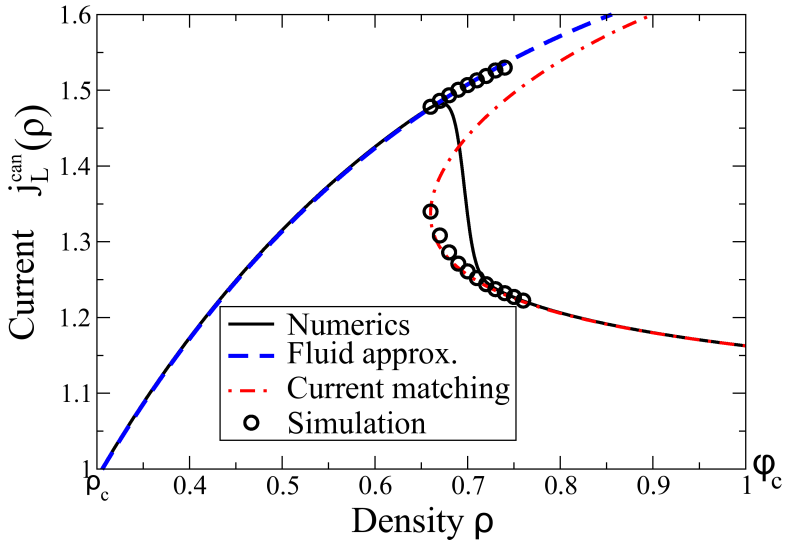

Figure 4.6: Current estimates above the critical point $\rho > \rho_c$ and $j_L^{\text{can}}(\rho) > e^{\mu_c} = 1$, for $L = 1000$, $\gamma = 0.5$ and $b = 4$. The fluid approximation (4.36) and the current matching (4.37) agree well with canonical numerics and the metastable branches from Monte Carlo simulations (cf. Figs. 4.3 and 4.5).

is a strictly increasing function from $[0, \infty)$ onto $[0, \infty)$ and so we denote its inverse

$$\mathcal{M}_m(\rho_{\text{bg}}) := R_m^{-1}(\rho_{\text{bg}}). \tag{4.34}$$

To simplify the notation we introduce the truncated fugacity (in general the fugacity is given by the exponential of the chemical potential)

$$\Phi_m(\rho) := e^{\mathcal{M}_m(\rho)} \ . \tag{4.35}$$

To a first approximation we estimate the current in the fluid state using Eq. (4.32),

$$j_L^{\text{can}}(\rho) \approx \Phi_\rho(\rho) \tag{4.36}$$

under the assumption that $\left(1 - \nu[\rho_L L] e^{\rho_L L \mu} / \bar{z}_\rho(\mu)\right) \approx 1$ for values of $\rho_L L$ under consideration. This approximation is shown in Fig. 4.6 by the blue dashed line for $\gamma = 0.5$, $b = 4$ and a system size of $L = 1000$. The approximation is extremely close to the canonical current for $\rho_L < \rho_{\text{trans}}(L)$ and for $\rho_L \approx \rho_{\text{trans}}(L)$ is in good agreement with the empirically measured fluid currents from Monte Carlo simulations. We demonstrate in Section 4.4 that this estimate can be improved by choosing the cut-off more carefully following the methods set out in Chapter 3.

We approximate the current in the condensed (phase separated) states by a current matching argument, between the fluid and the condensed phase, a similar heuristic argument has been given before in [83]. The existence of a stable condensate implies that the average rate of particles exiting the condensate must be equal to the average rate of particles entering it. Conditioned on the occupation of the condensate $m_L L$, the

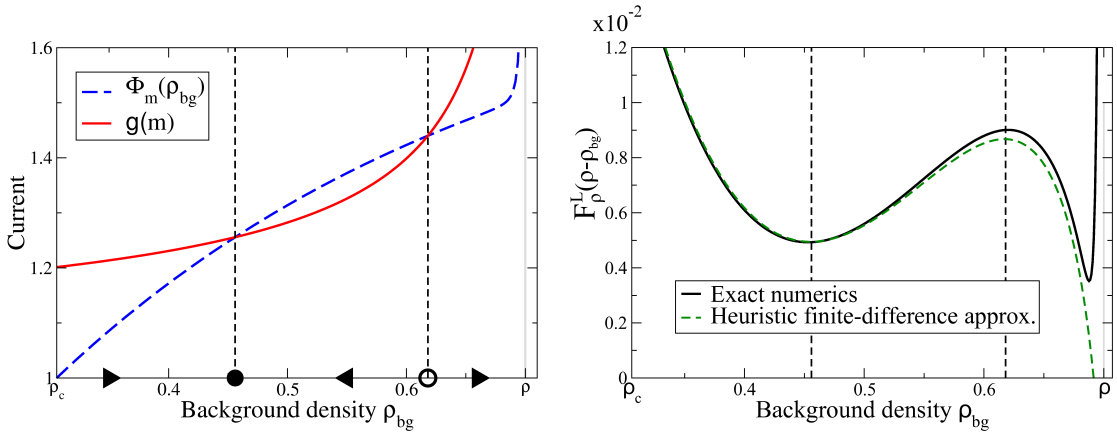

Figure 4.7: Current matching on a finite system with $L = 1000$ and $\rho = 0.7$ close to $\rho_{\text{trans}}(1000)$ for $\gamma = 0.5$, $b = 4$. Left: The current in the background $\Phi_m(\rho_{\text{bg}})$ and current out of the maximum $g(m)$ plotted against ρ_{bg}. Right: Exact numerics of $F^L_{\rho_L}$ using (2.24) shown in solid black and approximation (4.39) in dashed green. Vertical lines show the correspondence between current matching and critical points of $F^L_{\rho_L}$. The first local minimum corresponds to the lower stable branch of the current matching curve in Fig. 4.6 and the local maximum corresponds to the upper unstable branch.

exit rate is simply $g(m_L L)$ while the entry rate is well approximated by the stationary current in the background. This is assumed to be in a fluid state described by $\bar{\nu}_{\mu(\rho_{\text{bg}}),m_L}$, which leads to the current matching condition;

$$\Phi_m(\rho_{\text{bg}}) = g(m_L L) \quad \text{where} \quad \rho_{\text{bg}} = \rho_L - m_L \ . \tag{4.37}$$

The lower branch of solutions to this equation define the condensed current approximation (Fig. 4.6 red dashed line). This is extremely close to the canonical current for $\rho_L > \rho_{\text{trans}}(L)$ and for $\rho_L \approx \rho_{\text{trans}}(L)$ the results are in good agreement with the empirically measured condensed currents from Monte Carlo simulations.

Metastability

We can understand the metastability on a heuristic level in terms of a simple current matching argument. $F^L_{\rho_L}(m_L)$ (as defined in (4.14)) can be calculated efficiently for system sizes $L < 4000$ using exact numerics and even for much larger systems (see Eq. (2.24)). In Fig. 4.7 we see a clearly defined double well structure close to $\rho_{\text{trans}}(L)$ which accounts for the observed switching behaviour. We may extract the contribution due to the maximum site occupation from $F^L_{\rho_L}(m_L)$ and apply an exponential change of measure so that the average density on the remaining $L-1$ sites is $\rho_{\text{bg}} = \rho_L - m_L$,

$$\begin{aligned} F^L_{\rho_L}(m_L) \approx{}& (\log \bar{z}_m(\mu) - \rho_{\text{bg}}\mu) - \frac{1}{L}\log \nu[m_L L] \\ & - \frac{1}{L}\log \bar{\nu}^{L-1}_{\mu,m}\left[S_{L-1} \asymp \rho_{\text{bg}}\right] + \frac{1}{L}\log Z(L,\rho_L) \ . \end{aligned} \tag{4.38}$$

We may choose $\mu = \mathcal{M}_{m_L}(\rho_{\text{bg}})$ so that the mean under the cut-off grand-canonical distribution is ρ_{bg}. The gradient of $F^L_{\rho_L}(m_L)$ is given by a one step finite difference. If we assume for large L that $\bar{\nu}^{L-1}_{\mathcal{M}_{m_L}(\rho_{\text{bg}}),m_L}[S_{L-1} \asymp \rho_{\text{bg}}] \sim \frac{1}{\sqrt{2\pi L\sigma_c^2}}$, which is valid in the scaling limit under certain conditions according to a local limit for triangular arrays (see Theorem 4.6 for details), then a straightforward calculation shows

$$F^L_{\rho_L}(m_L - 1/L) - F^L_{\rho_L}(m_L) \approx \frac{1}{L}\left(\mathcal{M}_{m_L}(\rho_{\text{bg}}) - \log g(m_L)\right) \ . \tag{4.39}$$

The first term on the right-hand side follows in direct analogy with the thermodynamic limit for which $\partial_\rho s_{\text{gcan}}(\rho) = -\mu(\rho)$ (cf. [65]), and the second term is the finite difference of the maximum site contribution using Eq. (2.15).

This result holds rigorously in scaling limit and even for relatively small systems ($L \approx 1000$) $F^L_{\rho_L}$ is well approximated by Eq. (4.39) as is shown in Fig. 4.7. The approximation breaks down for background densities close to ρ since it relies on $m_L \gg 1/L$. By the above argument we expect that solutions to the current matching equation (4.37) correspond to local maxima or minima of the rate function. Whilst the current out of the maximum occupied site is greater than the current in the background we expect the background density to increase and vice versa. Therefore the first point that the two currents cross is locally stable and so a local minimum of the rate function. The next point they cross is a local maximum by the same argument, and there is another local minimum at a point close to ρ associated with fluid configurations, which the current matching argument predicts to be at the boundary. This is shown in Fig. 4.7.

4.4 Rigorous scaling limit

In this section we explore the finite-size effects by examining the leading order behaviour at the critical scale on which metastability persists. This scale is essentially found by balancing the moderate deviations of the sum of independent site occupations (in the background) with the contribution due to a macroscopic mass accumulating on a single lattice site. See [34] for details on moderate deviations. This allows us to describe the behaviour of the canonical measures close to the transition point and the metastable behaviour exhibited by the system.

We consider the system at a size L and density $\rho_L \to \rho_c$ such that,

$$\frac{L}{b_L}(\rho_L - \rho_c) \to \delta\rho \in (-\infty, \infty) \ . \tag{4.40}$$

Alternatively, in terms of the total number of particles in the system $\rho_L L$ this corresponds to,

$$\rho_L L = \rho_c L + \delta\rho b_L + o(b_L) \ .$$

Equivalence and non-equivalence of ensembles in the scaling limit is given by the large

deviation behaviour of the random variable,

$$T_L(\boldsymbol{\eta}) = \frac{1}{b_L} \sum_{x \in \Lambda_L} (\eta_x - \rho_c) \ , \tag{4.41}$$

under the critical measure (c.f. Def. 3.1). Following the method set out in Chapter 3 we define the canonical and grand canonical measures on the large deviation scale (a_L), and density scale (b_L).

$$\begin{aligned} \pi^{L,\delta}_{\delta\rho}[\boldsymbol{\eta}] &= \nu^L[\boldsymbol{\eta} \mid T_L = \delta\rho_L] \\ &= \frac{\nu^L[\boldsymbol{\eta}]}{Z(L, \delta\rho_L)} \mathbb{1}_{T_L^{-1}(\delta\rho_L)}(\boldsymbol{\eta}) \end{aligned} \tag{4.42}$$

where $Z(L, \delta\rho_L) = \nu^L[T_L^{-1}(\delta\rho_L)]$ and $\delta\rho_L \to \delta\rho$ as in (3.18). The grand canonical measures in the scaling limit are given by

$$\begin{aligned} \nu^{L,\delta}_{\mu}[\boldsymbol{\eta}] &= \frac{e^{a_L \mu T_L(\boldsymbol{\eta})}}{\nu^L\left(e^{a_L \mu T_L}\right)} \nu^L[\boldsymbol{\eta}] \\ &= \prod_{x \in \Lambda_L} \frac{e^{(a_L b_L^{-1})\mu\eta_x} \nu[\eta_x]}{z((a_L b_L^{-1})\mu)} \ . \end{aligned} \tag{4.43}$$

We distinguish these from the thermodynamic canonical and grand canonical ensembles by the superscripts δ. The measures in the scaling limit are related to the canonical and grand canonical measures introduced in Section 4.2 on any finite system, by

$$\begin{aligned} &\pi^{L,\delta}_{\delta\rho}[\boldsymbol{\eta}] = \pi^L_{\rho_L}[\boldsymbol{\eta}] \quad \text{where} \ \ \rho_L = \rho_c + \delta\rho_L(b_L L^{-1}) \\ &\nu^{L,\delta}_{\mu}[\boldsymbol{\eta}] = \nu^L_{(a_L b_L^{-1})\mu}[\boldsymbol{\eta}] \ . \end{aligned} \tag{4.44}$$

The restricted ensembles as defined in Def. 3.7 are given by

$$\bar{\nu}^{L,\delta}_{\mu,m}[\boldsymbol{\eta}] = \nu^{L,\delta}_{\mu}[\boldsymbol{\eta} \mid \overline{M}_L \leq m] \tag{4.45}$$

where the macroscopic maximum of a configuration $\overline{M}_L(\boldsymbol{\eta})$ is defined on the same scale as the excess mass T_L,

$$\overline{M}_L(\boldsymbol{\eta}) = \frac{1}{b_L} \max_{x \in \Lambda_L} \eta_x \ . \tag{4.46}$$

The canonical entropy density (see Definition 3.12) is given by

$$s_{\text{can}}(\delta\rho) = \lim_{L \to \infty} \log \nu^L[T_L = \delta\rho_L] \quad \text{as } \delta\rho_L \to \delta\rho \text{ as in (3.18)} \ . \tag{4.47}$$

The grand canonical pressure in the scaling limit is given by

$$\begin{aligned} p(\mu) &= \lim_{L\to\infty} \frac{1}{a_L} \log \nu^L \left(e^{a_L \mu T_L}\right) \\ &= \lim_{L\to\infty} \frac{L}{a_L} \log \nu \left(e^{\eta_1 (a_L b_L^{-1})\mu}\right) \ , \end{aligned} \tag{4.48}$$

and the grand canonical entropy density is given in the usual way by the Legendre transform $s_{\text{gcan}}(\delta\rho) = -p^*(\delta\rho)$. The contribution to the canonical entropy density due to a macroscopic number of particles residing on a single site (on the same scale as the excess mass b_L), is given by

$$s_{\text{cond}}(m) = \lim_{L\to\infty} \frac{1}{a_L} \log \nu[m_L b_L] \quad \text{as } m_L \to m \text{ as in (3.41)} \ . \tag{4.49}$$

The correct scales (a_L) and (b_L) to capture the canonical overshoot and metastability can be determined heuristically by our previous current matching argument (4.37). If we assume that close to ρ_c the fluid current (4.36) can be approximated by the first term in the Taylor expansion around ρ_c then

$$\Phi_m \left(\rho_c + \delta\rho_{\text{bg}} \left(b_L L^{-1}\right)\right) - 1 \simeq \frac{\delta\rho_{\text{bg}}}{\sigma_c^2} \left(b_L L^{-1}\right) \ .$$

The current matching equation (4.37) then implies

$$\frac{\delta\rho_{\text{bg}}}{\sigma_c^2} \, b_L L^{-1} \simeq g\left((\delta\rho - \delta\rho_{\text{bg}}) b_L\right) - 1 = b(\delta\rho - \delta\rho_{\text{bg}})^{-\gamma} b_L^{-\gamma} \ ,$$

which leads to $b_L = L^{\frac{1}{1+\gamma}}$. The scale a_L then follows by insisting we have a non-degenerate limit for the condensed entropy contribution, so $a_L = L^{\frac{1-\gamma}{1+\gamma}}$. Equivalently these scales can be found by insisting that the pressure in the scaling limit is non-degenerate, which fixes a relationship between a_L and b_L, and then again insisting we have a non-degenerate limit for the condensed entropy contribution specifies a_L and b_L completely. To summarise, in the rest of this section we fix,

$$a_L = L^{\frac{1-\gamma}{1+\gamma}}, \qquad b_L = L^{\frac{1}{1+\gamma}} \ . \tag{4.50}$$

The exponents are written as,

$$\alpha = \frac{1-\gamma}{1+\gamma} \ , \quad \beta = \frac{1}{1+\gamma}, \quad \text{and} \ \ 2\beta = 1 + \alpha \ . \tag{4.51}$$

By applying Lemmas 4.4 and 4.5 we can calculate the grand canonical pressure,

$$p(\mu) = \begin{cases} \frac{\sigma_c^2 \mu^2}{2} & \text{for } \mu \le 0 \\ +\infty & \text{otherwise,} \end{cases} \tag{4.52}$$

and hence the grand canonical entropy density,

$$s_{\text{gcan}}(\delta\rho) = \begin{cases} -\frac{\delta\rho^2}{2\sigma_c^2} & \text{for } \delta\rho \leq 0 \\ 0 & \text{for } \delta\rho > 0 \ . \end{cases} \tag{4.53}$$

The grand canonical entropy density is strictly concave only for $\delta\rho < 0$ (see Figure 4.8). This implies that downside moderate deviations of the density under the critical measure are realised by the grand canonical measures at the appropriate chemical potential. Therefore for all negative $\delta\rho$ we immediately have equivalence of ensembles. However, the grand canonical entropy density fails to fully describe the situation for moderate deviations above the critical density, $\delta\rho \geq 0$, since it is constant. Following the methods set out in Chapter 3, we explore this region by contracting on the maximum occupied site. This also leads to a detailed, rigorous description of the overshoot and metastability on the critical scale.

4.4.1 The rate functions

In this section we contract on the maximum occupied site to find the full equivalence of ensembles as well as the canonical rate function for the maximum in the scaling limit. We examine the asymptotic behaviour of $F^L_{\rho_L}$ introduced in (4.14). We will see in Corollary 4.6 that under the appropriate scaling $F^L_{\rho_L}(m_L)$ is finite and non-zero. Firstly, we find the rate function for the joint scaled density and maximum under the critical measure,

$$I(\delta\rho, m) = \lim_{L\to\infty} \frac{1}{L^\alpha} \log \nu^L[T_L = \delta\rho_L, \overline{M}_L = m_L] \tag{4.54}$$

as $\delta\rho_L \to \delta\rho$ and $m_L \to m$ as in (3.18), and (3.41). From here we are able to calculate the canonical entropy density (Definition 3.12 in Section 3.3),

$$\begin{aligned} s_{\text{can}}(\delta\rho) :&= \lim_{L\to\infty} \frac{1}{L^\alpha} \log Z(L, \delta\rho_L) \\ &= -\inf_{m\in[0,\delta\rho]} I(\delta\rho, m) \ , \end{aligned} \tag{4.55}$$

and the canonical large deviations of the maximum in the scaling limit (Corollary 3.11),

$$I_{\delta\rho}(m) :\!= \lim_{L\to\infty} \frac{1}{L^\alpha} \log \pi^{L,\delta}_{\delta\rho}[\overline{M}_L = m_L] \tag{4.56}$$

$$= I(\delta\rho, m) + s_{\text{can}}(\delta\rho) \ . \tag{4.57}$$

Since $I^{\text{TD}}_\rho(m) = 0$ for $(\rho - m) \geq \rho_c$ (see Section 4.2), this definition implies,

$$\pi^L_{\rho_c+\delta\rho_L L^{\beta-1}} \left[L^{-\beta} \max_{x\in\Lambda_L} \eta_x \asymp m \right] \sim e^{-L^\alpha I_{\delta\rho}(m)} \ . \tag{4.58}$$

The large deviation results are summarised in the following theorem.

Theorem 4.6. *In the scaling limit* (4.50) *the large deviation rate function for the joint density and maximum under the critical measure is given by*

$$\begin{aligned} I(\delta\rho, m) &= \lim_{L\to\infty} \frac{1}{L^\alpha} \log \nu^L[T_L = \delta\rho_L, \overline{M}_L = m_L] \qquad (4.59)\\ &= \begin{cases} -\Big(s_{cond}(m) + s_{fluid}(\delta\rho - m)\Big) & \text{provided } (\delta\rho - m) < \frac{b\sigma_c^2}{(1-\gamma)m^\gamma} \\ -s_{cond}(m) + \inf_{x\in[0,m]} I(\delta\rho - m, x) & \text{otherwise.} \end{cases} \end{aligned}$$

Here the fluid entropy density and condensed contribution are given by

$$s_{fluid}(\delta\rho_{bg}) = -\frac{\delta\rho_{bg}^2}{2\sigma_c^2} \qquad \text{and} \qquad s_{cond}(m) = -\frac{b}{1-\gamma} m^{1-\gamma} \ . \qquad (4.60)$$

The canonical rate function for the maximum in the scaling limit is given by renormalising,

$$I_{\delta\rho}(m) = I(\delta\rho, m) - \inf_{x\in[0,\rho]} I(\delta\rho, x) \ . \qquad (4.61)$$

The result requires iteration for $(\delta\rho - m) \geq \frac{b\sigma_c^2}{(1-\gamma)m^\gamma}$ due to the large probability of a second sub-condensate forming on the same scale as the condensate. It turns out that for all $\delta\rho \in (-\infty, \infty)$ and $m \in [0, \delta\rho]$ we have to perform the iteration in (4.59) only finitely many times. More details of the iteration are given in Chapter 5. The region described by $(\delta\rho - m) < \frac{b\sigma_c^2}{(1-\gamma)m^\gamma}$ already covers all the critical points for fixed $\delta\rho$. That is the fluid minimum, condensed minimum and local maximum that constitutes a potential barrier. The proof of the theorem follows from the general results in Chapter 3 once we have found the restricted grand canonical entropy densities that describe the background phase.

Proof of Theorem 4.6. Following the methods in Chapter 3 we can split the joint event as follows,

$$\begin{aligned} \frac{1}{a_L} \log \nu^L[T_L = \delta\rho_L, \overline{M}_L = m_L] = \frac{1}{a_L} \log \nu[m_L b_L] \ + \\ + \ \frac{1}{a_L} \log \bar{\nu}_m^{L-1}[T_{L-1} = (\delta\rho - m)] + o(1) \ . \qquad (4.62) \end{aligned}$$

The first term converges to $s_{\text{cond}}(m)$. To calculate the second term (the large deviations of T_L under the truncated reference measure) we apply an exponential change of measure. If there exists a chemical potential such that the expected value of T_L under the truncated measure is $(\delta\rho - m)$ then the final term converges to $s_{\text{gcan},m}(\delta\rho - m)$. This is true as long as the truncated grand canonical entropy density is strictly concave at $(\delta\rho - m)$. Otherwise we iterate the contraction. The restricted grand canonical entropy density $s_{\text{gcan},m}(\delta\rho - m)$ is strictly concave provided $(\delta\rho - m) < \frac{b\sigma_c^2}{(1-\gamma)m^\gamma}$ and the result follows from Theorems 3.7 and 3.10, by applying Lemma 4.7 below. □

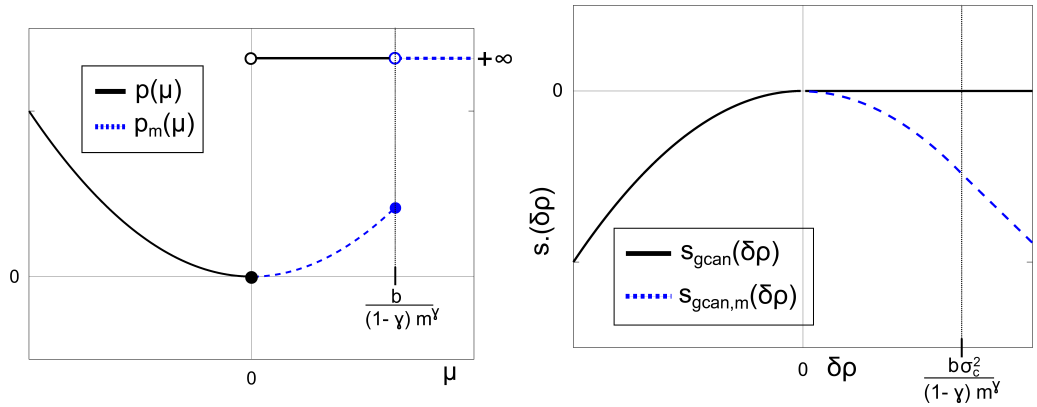

Figure 4.8: Left: The grand canonical pressure in the scaling limit is shown in solid black. The restricted pressure at restriction m extends the grand canonical pressure up to $\frac{b}{(1-\gamma)m^\gamma}$ (see Lemma 4.7), shown by the blue dashed line. Right: The grand canonical entropy densities are given by the Legendre-Fenchel transform of the pressures (left). The grand canonical entropy density is shown in solid black and the restricted grand canonical entropy density, with restriction m, is shown in dashed blue.

Lemma 4.7 (Restricted pressure)**.** *The pressures associated with the restricted ensembles in the scaling limit (4.50) are,*

$$\begin{aligned} p_m(\mu) &= \lim_{L\to\infty} \frac{1}{a_L} \log \nu^L \left(e^{a_L \mu T_L} \mathbb{1}_{\overline{M}_L \leq m_L} \right) \\ &= \begin{cases} \frac{\sigma_c^2 \mu^2}{2} & \text{for } \mu \leq \frac{b}{(1-\gamma)m^\gamma} \ , \\ +\infty & \text{otherwise.} \end{cases} \end{aligned} \tag{4.63}$$

So the restricted grand canonical entropy densities, given by the Legendre transform, are

$$\begin{aligned} s_{gcan,m}(\delta\rho_{bg}) &= p_m^*(\delta\rho_{bg}) \\ &= \begin{cases} -\frac{\delta\rho_{bg}^2}{2\sigma_c^2} & \text{for } \delta\rho_{bg} \leq \frac{b\sigma_c^2}{(1-\gamma)m^\gamma} \ , \\ -\frac{b\delta\rho_{bg}}{(1-\gamma)m^\gamma} + \frac{\sigma_c^2 b^2}{2(1-\gamma)^2 m^{2\gamma}} & \text{for } \delta\rho_{bg} > \frac{b\sigma_c^2}{(1-\gamma)m^\gamma} \ . \end{cases} \end{aligned} \tag{4.64}$$

See Figure 4.8.

Proof. The proof is a simple application of Lemmas 4.4 and 4.5. □

Provided $s_{\mathrm{gcan},m}$ is strictly concave at $\delta\rho_{\mathrm{bg}}$ there exists a chemical potential μ such that $\bar{\nu}_{\mu,m}^{L,\delta}(T_L) = \delta\rho_{\mathrm{bg}}$. We may therefore parametrize the restricted measures by $\delta\rho_{\mathrm{bg}}$ provided $\delta\rho_{\mathrm{bg}} < \frac{b\sigma_c^2}{(1-\gamma)m^\gamma}$.

Lemma 4.8 (Current scaling limits)**.** *In the scaling limit* (4.50) *the current out of a macroscopically occupied site is asymptotically given by*

$$g(m_L b_L) = 1 + \frac{b}{m^\gamma} L^{\beta-1} + o(L^{\beta-1}) \quad \text{as} \quad m_L \to m \ , \tag{4.65}$$

and provided $\delta\rho_{bg} < \frac{b\sigma_c^2}{(1-\gamma)m^\gamma}$ *the average current under the restricted grand canonical*

measures, with restriction m, at density $\delta\rho_{bg}$ is asymptotically given by

$$\bar{\nu}^{L,\delta}_{\delta\rho_{bg},m}\left(g(\eta_1)\right) = 1 + \frac{\delta\rho_{bg}}{\sigma_c^2}L^{\beta-1} + o(L^{\beta-1}) \ , \tag{4.66}$$

which may be interpreted as the average current in the fluid background phase. From (4.50) *we have* $\beta - 1 = -\frac{\gamma}{1+\gamma}$.

Proof. The result for the current out of the condensate is immediate from the definition of the jump rates (4.1) and the scaling limit (4.50). By definition of the restricted measures we observe that,

$$\begin{aligned}\bar{\nu}^{L,\delta}_{\mu,m}\left(g(\eta_1)\right) &= e^{(a_L b_L^{-1})\mu}\left(1 - \nu[m_L b_L]e^{a_L m_L \mu}\right) \\ &= 1 + \mu L^{-\frac{\gamma}{1+\gamma}} + o(L^{-\frac{\gamma}{1+\gamma}}) \ ,\end{aligned} \tag{4.67}$$

provided $\mu \in [0, \frac{b}{(1-\gamma)m^\gamma})$. The proof of the asymptotic form of the average current in the background follows from a Taylor expansion of the truncated density function $R_m(\mu)$, introduced in (4.33), details on the expansion are contained in Lemmas 4.4 and 4.5.

$$R_m(\mu L^{-\frac{\gamma}{1+\gamma}}) = \rho_c + \sigma_c^2 \mu L^{-\frac{\gamma}{1+\gamma}} + o(L^{-\frac{\gamma}{1+\gamma}})$$

for all $\mu \in [0, \frac{b}{(1-\gamma)m^\gamma})$. Since we may choose the chemical potential μ such that the expected value of T_L under the restricted measures in the scaling limit is $\delta\rho_{\mathrm{bg}}$ the result follows. □

Theorem 4.6 together with Lemma 4.8 imply that in the scaling limit given by (4.50) the derivative of the scaling rate function for canonical large deviations of the maximum, $I_{\delta\rho}$, is given by the difference in the current out of the condensate and the average current in the background. This is made precise in the Corollary 4.9 below, which is a rigorous version of the current matching argument of Section 4.3.2.

Corollary 4.9 (Current matching)**.**

$$\partial_m I_{\delta\rho}(m) = \frac{b}{m^\gamma} - \frac{\delta\rho_{bg}}{\sigma_c^2} \quad \textit{where} \quad \delta\rho_{bg} = (\delta\rho - m) \ , \tag{4.68}$$

and the two terms on the right-hand side are exactly the limiting current curves from Lemma 4.8 above the critical point.

This implies that

$$\partial_m I_{\delta\rho}(m) \to -\infty \quad \text{as } m \to 0 \ , \tag{4.69}$$

so that I_m always exhibits a boundary minimum at $m = 0$.

4.4.2 Equivalence of ensembles and overshoot

Depending on the value of $\delta\rho$, the rescaled rate function has one of three qualitative forms characterised by the number of its extreme points, or equivalently the number of roots of (4.68), and the position of the global minimum. With the threshold

$$c_0(\gamma, b) = \frac{1+\gamma}{\gamma}\big(\sigma_c^2 \gamma b\big)^{1/(1+\gamma)} \ , \tag{4.70}$$

Eq. (4.68) has no real roots for $\delta\rho < c_0$, exactly one for $\delta\rho = c_0$, and two for $\delta\rho > c_0$. The latter correspond to a local minimum at $m = m^* \in (0, \delta\rho)$ and a local maximum at $m = m_*$, with $m_* < m^*$ (cf. Fig. 4.10 on the right). As usual, minima of $I_{\delta\rho}$ correspond to metastable states, and the depth of the local minimum at m^* as compared to the one at the boundary determines which of the states is stable (i.e. corresponds to the global minimum). So c_0 marks the threshold above which (for $\delta\rho > c_0$) there exists a metastable condensed state. Stability of the states changes when both minima have the same depth; the density at which this is the case is given by $\rho_{trans}(L)$ introduced in Section 4.3.1. In the scaling limit (4.50) this behaves as

$$\rho_{trans}(L) = \rho_c + \delta\rho_{trans} L^{\frac{-\gamma}{1+\gamma}} + o(L^{\frac{-\gamma}{1+\gamma}}) \ ,$$

and from Theorem 4.6 and Corollary 4.9 we get the explicit expression

$$\delta\rho_{\text{trans}} = \sigma_c^{\frac{2}{1+\gamma}}(1+\gamma)(2\gamma)^{-\frac{\gamma}{1+\gamma}}\left(\frac{b}{1-\gamma}\right)^{\frac{1}{1+\gamma}} \ . \tag{4.71}$$

Note that both c_0 and $\delta\rho_{trans}$ are increasing with γ and b. Their ratio simplifies to

$$\delta\rho_{\text{trans}}/c_0 = \frac{1}{2}\Big(\frac{2}{1-\gamma}\Big)^{1/(1+\gamma)} \ , \tag{4.72}$$

which also increases monotonically with γ. In particular, $\delta\rho_{trans} > c_0$ for all $\gamma > 0$ which implies existence of an extended metastability region.

We can now summarise the critical behaviour of the system at scale (4.50) in three cases, which are also illustrated in Fig. 4.10 (right).

Case 1 ($\delta\rho < c_0$). There exists a unique minimum of the scaling rate function at $m = 0$,

$$I_{\delta\rho}(0) = 0 \ ,$$

corresponding to a stable fluid state. The most likely background density under the canonical measure is $S_L^{\text{bg}} = \rho_c + \delta\rho L^{\beta-1} + o(L^{\beta-1})$, and according to the results in Appendix C the canonical measures concentrate on configurations with maximum site occupation smaller than $O(L^\beta)$. It turns out that the background is asymptotically independent and distributed according to the restricted grand canonical measures at the correct chemical potential.

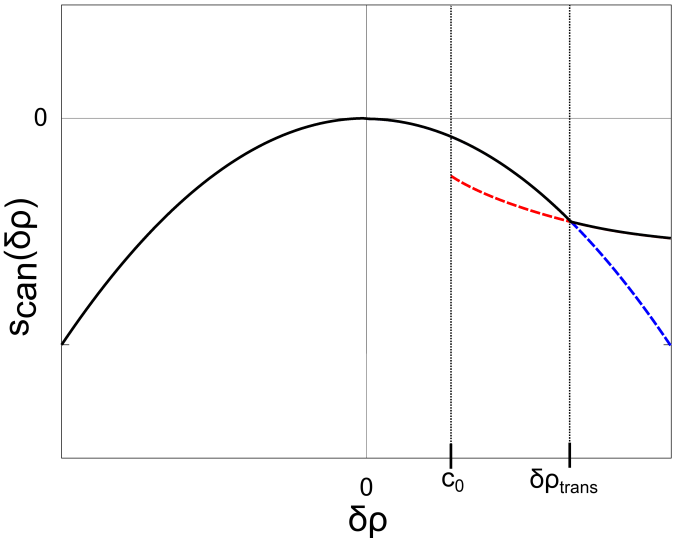

Figure 4.9: The scaling limit canonical entropy density gives rise to the equivalence and non equivalence of ensembles. Solid black: The canonical entropy density in the scaling limit. Dashed red: The condensed entropy branch. Dashed blue: the fluid entropy branch.

Case 2 ($c_0 < \delta\rho < \delta\rho_{\text{trans}}$). There are two local minima of the scaling rate function

$$I_{\delta\rho}(m^*) > I_{\delta\rho}(0) = 0 \ ,$$

corresponding to a stable fluid state with $m = 0$ and a metastable condensed state with $m = m^*$. The most likely background density under the canonical measure is still $S_L^{\text{bg}} = \rho_c + \delta\rho L^{\beta-1} + o(L^{\beta-1})$.

Case 3 ($\delta\rho > \delta\rho_{\text{trans}}$). There are two local minima of the scaling rate function

$$I_{\delta\rho}(0) > I_{\delta\rho}(m^*) = 0 \ ,$$

corresponding to a metastable fluid state with $m = 0$ and a stable condensed state with $m = m^*$. The most likely background density under the canonical measure is now $S_L^{\text{bg}} = \rho_c + (\delta\rho - m^*)L^{\beta-1} + o(L^{\beta-1})$ and a finite fraction of the excess mass condenses on a single lattice site with total occupation typically $m^*L^\beta + o(L^\beta)$ (in the sense of concentration of the canonical measures, see Appendix C).

The value of $\delta\rho_{\text{trans}}$, and for $\delta\rho > \delta\rho_{\text{trans}}$ the position of the global minimum, agree with recent results on the distribution of the maximum at the critical scale [5]. The expected value of the maximum site occupation under the canonical measure is given by the stable solution of the current matching argument as described above.

We can make the discussion above more precise by contracting on the maximum occupied site to find the canonical entropy density in the scaling limit using (4.55).

Corollary 4.10 (Equivalence of ensembles)**.** *The canonical entropy density in the scal-*

ing limit (4.50) *is given by ,*

$$s_{can}(\delta\rho) = \begin{cases} s_{gcan}(\delta\rho) & \text{if } \delta\rho < 0 \\ s_{fluid}(\delta\rho) & \text{if } 0 \le \rho \le \delta\rho_{trans} \\ s_{cond}(m^*) + s_{fluid}(\delta\rho - m^*) & \text{if } \rho > \rho_{trans} \end{cases} . \tag{4.73}$$

Following Definition 3.11 and Lemma 3.3, this gives rise to the following results describing the equivalence of ensembles. In terms of fast weak convergence, as $L \to \infty$*,*

$$\pi^{L,\delta}_{\delta\rho} \overset{L^\alpha}{\longleftrightarrow} \begin{cases} \nu^{L,\delta}_{\mu(\delta\rho)} & \text{if } \delta\rho < 0 \\ \bar{\nu}^{L,\delta}_{\mu(\delta\rho),m_*} & \text{if } 0 \le \rho < \delta\rho_{trans} \end{cases}$$

$$\hat{\pi}^{L,\delta}_{\delta\rho} \overset{L^\alpha}{\longleftrightarrow} \bar{\nu}^{L-1,\delta}_{\mu(\delta\rho - m^*),m^*} \quad \text{if } \rho > \rho_{trans} \tag{4.74}$$

where $\hat{\pi}^{L,\delta}_{\delta\rho}$ *is the canonical distribution of the background over* $L-1$ *sites after removing the maximum, defined in* (3.71) *(see Cor. 3.13 for details). These results are illustrated in Fig. 4.9.*

Proof. The canonical entropy density follows from Theorem 4.6 by applying the contraction, Theorem 3.10. Equivalence of ensembles for $\delta\rho < 0$ follows from Theorem 3.7. For $0 \le \delta\rho \le \delta\rho_{\text{trans}}$ equivalence follows from Corollary 3.12. Above the condensation transition point, $\delta\rho > \delta\rho_{\text{trans}}$ the equivalence of the background follows from Corollary 3.13. □

Below c_0 there is a single stable phase, since the canonical entropy density is equal to the truncated grand canonical entropy density (with small enough truncation). This implies equivalence between the canonical measures and the restricted product measures.

Since the jump rate off a single site is a bounded cylinder function the results on the equivalence of ensembles give rise to the canonical current overshoot in the scaling limit. Recall $j^{\text{can}}_L(\rho_L) = \pi^L_{\rho_L}(g(\eta_1))$ and

$$\pi^{L,\delta}_{\delta\rho}[\boldsymbol{\eta}] = \pi^L_{\rho_L}[\boldsymbol{\eta}] \quad \text{where } \rho_L = \rho_c + \delta\rho_L L^{\beta-1} . \tag{4.75}$$

Corollary 4.11 (Canonical current overshoot)**.** *Under the conditions of Theorem 4.6, with*

$$\rho_L = \rho_c + \delta\rho L^{\beta-1} + o(L^{\beta-1}) \quad as \quad L \to \infty,$$

we have, for $\delta\rho < \delta\rho_{trans}$

$$j^{can}_L(\rho_L) - 1 = \frac{\delta\rho}{\sigma_c^2} L^{\beta-1} + o(L^{\beta-1}), \tag{4.76}$$

and for $\delta\rho > \delta\rho_{trans}$

$$j^{can}_L(\rho_L) - 1 = \frac{b}{(m^*)^\gamma} L^{\beta-1} + o(L^{\beta-1}). \tag{4.77}$$

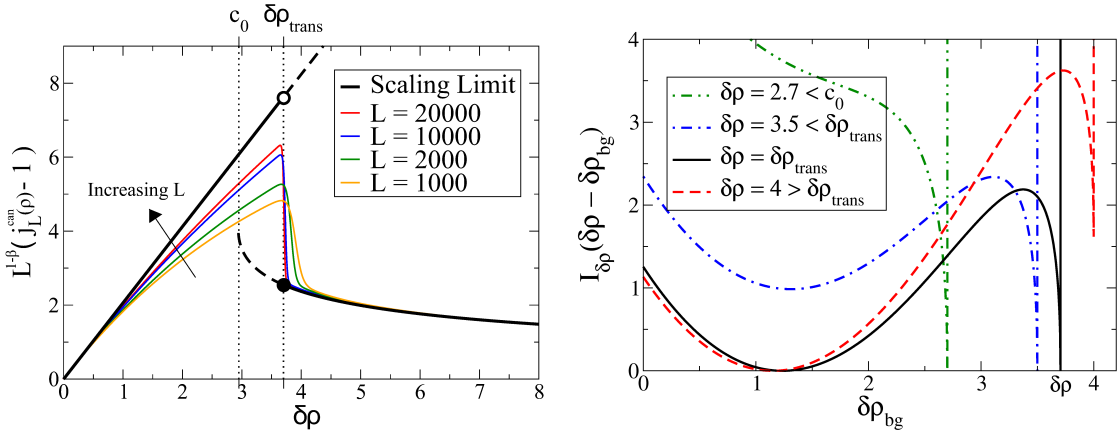

Figure 4.10: Scaling limit for $\gamma = 0.5$ and $b = 4$. Left: The thick black line shows the scaling limit result for the current, including metastable branches (dashed). Thin coloured lines show the rescaled canonical currents from exact numerics, slowly approaching the scaling limit as L increases. The transition point is given by $\delta\rho_{\text{trans}}$. Right: $I_{\delta\rho}(\delta\rho - \delta\rho_{\text{bg}})$ (defined in (4.61)) for various values of $\delta\rho$. Solid black corresponds to $\delta\rho = \delta\rho_{\text{trans}}$ where the depth of the two local minima are equal. The green dashed-dot-dot curve shows $I_{\delta\rho}$ for $\delta\rho < c_0$, blue dot-dashed curve corresponds to $c_0 < \delta\rho < \delta\rho_{\text{trans}}$ and red dashed line to $\delta\rho > \delta\rho_{\text{trans}}$.

Proof. The equivalence of ensembles (4.74) gives rise to fast convergence of bounded cylinder test functions (see Def. 3.11), so

$$L^{(1-\alpha)/2}\left|j_L^{\text{can}}(\rho_L) - \bar{\nu}^{L,\delta}_{\mu(\delta\rho),m_*}\left(g(\eta_1)\right)\right| \to 0 \quad \text{if } 0 \le \rho < \delta\rho_{\text{trans}}$$
$$L^{(1-\alpha)/2}\left|j_L^{\text{can}}(\rho_L) - \bar{\nu}^{L-1,\delta}_{\mu(\delta\rho-m^*),m^*}\left(g(\eta_1)\right)\right| \to 0 \quad \text{if } \rho > \rho_{\text{trans}}\ .$$

Also the current under the truncated grand canonical measures is asymptotically given by (4.66). The corollary follows by combining these two results, Since $(1-\alpha)/2 = 1-\beta$ (see (4.50)). □

This result is illustrated in Fig. 4.10 (left). At the transition point $\delta\rho = \delta\rho_{\text{trans}}$ we must examine higher order terms to demonstrate that the system will asymptotically be in a condensed phase, see [5] and Section 4.5.

4.5 Dynamics and metastability

Having established the existence of metastable states on the level of large deviations, we can use heuristic arguments to get an estimate of their lifetime. The corresponding switching dynamics are illustrated in Fig. 4.5. Previous studies include results on the dynamics of fluctuations in a finite system [71] and the dynamics of the condensate [59, 61, 69] in the thermodynamic limit. Our approach here follows mostly the one in [66] where metastability in a different zero-range process has been studied, and [61] where a random walk argument was used to find the characteristic time of the motion of the condensate.

In this section we consider the dynamics in the scaling limit defined by Eq. (4.50), that is the total number of particles grows as,

$$\rho_L L = \rho_c L + \delta\rho L^{\frac{1}{1+\gamma}} + o(L^{\frac{1}{1+\gamma}}) \ .$$

In the previous section we have seen that for $\delta\rho > c_0$ the system exhibits two metastable states, we assume in the following that we are in this region. So for sufficiently large L we know $F^L_{\rho_L}(m)$ exhibits a local maximum between the fluid and condensed minima, and in the scaling limit the position converges to m_*, the local maximum of $I_{\delta\rho}$. For computations on finite systems it is more accurate to approximate the position of the local maximum of $F^L_{\rho_L}$ by the closest integer to the largest root of Eq. (4.37) (see Section 4.3.2), however for the sake of minimal notation we always write m_*. We define the metastable fluid (condensed) state as all configurations for which the maximum site occupation is below (above) m_*, i.e.

$$\begin{aligned} \pi^{L,\text{fluid}}_{\delta\rho} &:= \pi^{L,\delta}_{\delta\rho_L}[\cdot|\overline{M}_L(\boldsymbol{\eta}) \le m_*] \\ \pi^{L,\text{cond}}_{\delta\rho} &:= \pi^{L,\delta}_{\delta\rho_L}[\cdot|\overline{M}_L(\boldsymbol{\eta}) > m_*] \ . \end{aligned} \tag{4.78}$$

Since the process spends very little time close to the maximum of $F^L_{\rho_L}$, the precise choice of m^* is not relevant for results in the scaling limit (cf. also [8] for a slightly different approach). The lifetimes of the two metastable states can be expressed in terms of the following hitting time,

$$\tau_L := \inf\left\{t \ge 0 : \overline{M}_L(\boldsymbol{\eta}(t)) = m_*\right\} \ .$$

We take

$$T_{\text{fluid}} := 2\mathbb{E}^{\pi^{L,\text{fluid}}_{\delta\rho}}[\tau_L] \quad \text{and} \quad T_{\text{cond}} := 2\mathbb{E}^{\pi^{L,\text{cond}}_{\delta\rho}}[\tau_L] \ , \tag{4.79}$$

where the expectation is with respect to the dynamics (2.12) with initial distribution given by $\pi^{L,\text{fluid}}_{\delta\rho}$ or $\pi^{L,\text{cond}}_{\delta\rho}$ (see Chapter 2 for details). The factor of 2 comes from the fact that once m_* is reached the process can still return to the same metastable state with probability 1/2.

By ergodicity of the process $\big(\boldsymbol{\eta}(t) : t \ge 0\big)$ on $X_{L,N}$ the ratio of lifetimes is directly related to the stationary distribution,

$$\frac{T_{\text{fluid}}}{T_{\text{cond}}} = \frac{\pi^{L,\delta}_{\delta\rho}[\overline{M}_L(\boldsymbol{\eta}) \le m_*]}{\pi^{L,\delta}_{\delta\rho}[\overline{M}_L(\boldsymbol{\eta}) > m_*]} = \frac{\sum_{k=0}^{m_*} e^{-LF^L_\rho(k)}}{\sum_{k=m_*}^{N} e^{-LF^L_\rho(k)}} \ . \tag{4.80}$$

	Approx. (4.82)	MF	1D $p = 1$	1D $p = 3/4$
T_{fluid}	1.61×10^5	1.65×10^5	1.21×10^5	2.05×10^5
T_{cond}	1.51×10^5	1.52×10^5	1.07×10^5	1.94×10^5

Table 4.1: Lifetime of metastable states for $L = 1000$ and $N = 695$, with $\gamma = 0.5$ and $b = 4$. Using approximation (4.82) compared to measurements from Monte Carlo simulations on a fully connected lattice (MF), a one dimensional lattice with probability of jumping to the left $q(1) = 1$ and to the right with $q(-1) = 3/4$.

Applying the scaling limit result of Theorem 4.6, we get for large L

$$\begin{aligned}\frac{T_{\text{fluid}}}{T_{\text{cond}}} &\simeq \int_0^{m_*} e^{-a_L I_{\delta\rho}(x)}\,\mathrm{d}x \left(\int_{m_*}^{\delta\rho} e^{-a_L I_{\delta\rho}(x)}\,\mathrm{d}x\right)^{-1} \\ &\simeq \frac{\Gamma(1+\frac{1}{1-\gamma})\left(\frac{1-\gamma}{b}\right)^{\frac{1}{1-\gamma}}\sqrt{\partial_x^2 I_{\delta\rho}(m^*)}}{\sqrt{2\pi L}}\, e^{-L^\beta(I_{\delta\rho}(0)-I_{\delta\rho}(m^*))}\,. \end{aligned} \tag{4.81}$$

The second line follows by a saddle point approximation of the denominator at the local minimum m^* (corresponding to condensed configurations), and by expanding $I_{\delta\rho}(0)$ in the numerator at the boundary minimum (corresponding to fluid configurations), keeping the leading order singular term. To leading order in the exponent, this result implies that the ratio of the lifetimes is given by the relative depth of the minima, as expected. The lower order term $\sqrt{L}$ in the denominator implies that at the transition density $\delta\rho_{\text{trans}}$ in the scaling limit the condensed state is stable and the fluid state is metastable, in accordance with results in [5]. However the scaling with L is difficult to verify in Monte Carlo simulations, since system sizes have to be relatively small (at most of the order of $L = 1000$) to get good statistics on switching times. In this regime higher order finite-size effects still play a role and can affect the location of $\rho_{\text{trans}}(L)$ and therefore the relative depth of the minima of $F^L_{\rho_L}$.

We estimate the two lifetimes by approximating the number of particles in the condensate by a continuous time random walk. Since it is difficult to validate the scaling with L, as discussed above, we will demonstrate the validity of our approach by estimating the lifetimes directly for finite systems. The actual lifetimes are not only related to the potential barrier given by the maximum of $F^L_{\rho_L}$ ($I_{\delta\rho}$ in the scaling limit), but also depend on the underlying dynamics. The occupation of the maximum $\big(b_L\overline{M}_L(\boldsymbol{\eta}(t)) : t \geq 0\big)$ is a non-Markovian, stationary, ergodic process with state space $\Omega^* = \{\lceil\rho_L\rceil, \lceil\rho_L\rceil + 1, \ldots, b_L m^*, b_L m^* + 1, \ldots, \rho_L L\}$ and stationary distribution $P(n) = e^{-L\,F^L_{\rho_L}(n/L)}$. Since the process exhibits only single steps, it can be approximated by a continuous time random walk on Ω^* (the validity of this Markovian assumption is discussed later) where a particle leaves the maximum ($n \to n-1$) with rate $g(n)$. The rates corresponding to $n \to n+1$ are then fixed by the stationary distribution P. In the scaling limit this implies that particles enter the condensate with rate given by the current in the background, see Corollary 4.9. The lifetime of the metastable fluid state is approximated by the mean first passage time of the random walk starting in

position $\lceil \rho_L \rceil$ to reach $b_L m_*$. For the metastable condensed state it is given by the mean first passage time starting at $\rho_L L$, and both have a factor of 2 in front due to the possibility of reaching $b_L m_*$ and not actually switching state. These can be calculated using standard techniques (see e.g. [102] for the discrete time analogue),

$$\begin{aligned} T_{\text{fluid}} &\approx 2 \sum_{i=\lceil \rho_L \rceil + 1}^{b_L m_*} \frac{P(i-1)}{g(i)P(i)} + 2 \sum_{i=\lceil \rho_L \rceil + 2}^{b_L m_*} \frac{1}{g(i)P(i)} \sum_{j=\lceil \rho_L \rceil}^{i-2} P(j) \\ T_{\text{cond}} &\approx 2 \sum_{i=b_L m_* + 1}^{\rho_L L} \frac{1}{g(i)} + 2 \sum_{i=b_L m_* + 1}^{\rho_L L} \frac{1}{g(i)P(i)} \sum_{j=i-1}^{\rho_L} P(j). \end{aligned} \tag{4.82}$$

These two approximations can be calculated numerically for reasonably large systems (up to $L \approx 4000$) since we can calculate $P(n) = e^{-L F^L_{\rho_L}(m)}$ exactly using Eq. (2.24). Applying the scaling limit result and using saddle point approximations we recover an Arrhenius estimate with a pre-factor for the lifetime of the two metastable states,

$$\begin{aligned} T_{\text{fluid}} &\approx 2 \int_0^{m_*} e^{a_L I_{\delta\rho}(x)} \int_0^x e^{-a_L I_{\delta\rho}(y)} \,\mathrm{d}y \,\mathrm{d}x \\ &\approx \Gamma\left(1 + \frac{1}{1-\gamma}\right) \left(\frac{b}{1-\gamma}\right)^{\frac{-1}{1-\gamma}} \sqrt{\frac{2\pi L}{\partial_r^2 I_{\delta\rho}(m_*)}} \, e^{L^\alpha (I_{\delta\rho}(m_*) - I_{\delta\rho}(0))} \\ T_{\text{cond}} &\approx 2 \int_{m_*}^{\delta\rho} e^{a_L I_{\delta\rho}(x)} \int_x^{\delta\rho} e^{-a_L I_{\delta\rho}(y)} \,\mathrm{d}y \,\mathrm{d}x \\ &\approx \frac{2\pi L}{\sqrt{\partial_m^2 I_{\delta\rho}(m_*) \partial_m^2 I_{\delta\rho}(m^*)}} \, e^{L^\alpha (I_{\delta\rho}(m_*) - I_{\delta\rho}(m^*))}. \end{aligned} \tag{4.83}$$

Here m_* is the location of the local maximum of the rate function, m^* is the local minimum corresponding to condensed configurations and there is a boundary minimum at 0 corresponding to fluid configurations. To leading order we recover the Arrhenius law as discussed in Section 2.4. This result agrees with the ratio of the lifetimes already discussed. However as with the previous results the asymptotic form is difficult to validate due to higher order finite-size effects, the exact expression Eq. (4.82) is therefore more appropriate for relevant system sizes.

We expect the above random walk approximation to be accurate if particles exiting the maximum equilibrate in the bulk before returning to the condensate. This condition is best fulfilled for a fully connected lattice (mean-field geometry) and we expect it to be a reasonably good approximation for one dimensional totally asymmetric systems since particles have to pass through the whole fluid bulk before returning. For partial asymmetry and in higher dimensions a return without penetrating the fluid bulk is possible. To a first approximation the lifetimes have to be multiplied by the inverse probability of the event that particles escape into the bulk, since only such particles have a chance to equilibrate and contribute on the right scale. This pre-factor can be estimated using another random walk argument. If a particle jumps to the right with probability $q(1)$ and to the left with probability $q(-1)$ where $q(1)+q(-1) = 1$ (see (2.12)) and $q(1) \neq 1/2$ then the probability of a particle reaching some macroscopic distance

before returning to the condensate is asymptotically $|q(1) - q(-1)|$. We therefore expect the lifetime to increase by a factor of $1/|q(1) - q(-1)|$ for partial asymmetry. As a special case, for symmetric systems in one dimension this leads to an increase of lifetimes by a factor of L by the same argument (c.f. the 'gamblers ruin' problem). For a detailed investigation and validation of this Markovian ansatz see [61]. We find that this argument gives a good approximation for fully connected lattices, and totally asymmetric jumps in one dimension, see Table 4.1. We observe that the one dimensional totally asymmetric case is a factor of approximately 1.4 faster than the mean-field case, which is due to internal structure in the fluid background, and has also been observed and discussed in [61]. For partial asymmetry in one dimension with $q(1) = 3/4$ the process is slower than the totally asymmetric case by a factor of approximately 1.8 supporting the arguments above which predict an increase by a factor of 2.

The characteristic time for the motion of the condensate in the thermodynamic limit, $\rho_L \to \rho > \rho_c$, can be approximated by considering Eq. (4.50) with a sequence of $\delta\rho$ increasing like $L^{1-\beta}$. The corresponding rescaled location of the condensed minimum $m^* \to (\rho - \rho_c)$, since the condensed state has limiting background density ρ_c. Our rigorous results do not technically hold in this limit, however our estimates of the lifetimes of the metastable states agree with the characteristic times found by Godreche and Luck [59, 61]. Our results demonstrate that close to the transition point in finite systems (i.e. $\delta\rho \approx \delta\rho_{\text{trans}}$) the condensate typically moves via the system entering the fluid state (cf. Fig. 4.5), and therefore its new position is expected to be chosen uniformly at random on Λ_L. For $\delta\rho$ large, however, the lifetime of the fluid state becomes small and the condensate can re-locate whilst the system remains in the condensed state, via the mechanism described in [61]. A sub-condensate starts to grow in the fluid background phase, and the potential barrier the process has to cross for condensate motion is associated with the probability of the excess mass shared equally between two sites. This is the relevant mechanism in the thermodynamic limit. For finite systems one can estimate which of these re-location processes dominates, by considering the distribution of the second largest site using the same techniques as in the previous section. It has recently been shown that the second mechanism via a sub-condensate can lead to a non-uniform relocation of the condensate [8]. The two different mechanisms of condensate motion are discussed in more details in Section 5.4, where both mechanisms persist in the thermodynamic limit.

4.6 Discussion

In general, finite system size can lead to effective long-range interactions and non-convexity of thermodynamic potentials, as has been observed for various models (see for example [6, 78] and references therein). We find in Chapter 5 that for the zero-range process with size-dependent jump rates metastability can be manifested even in the thermodynamic limit [66], and large crossover effects in these systems have already been observed in [42]. The finite-size behaviour of the zero-range process considered here

also exhibits the above non-convexity, with the additional feature of a sharp crossover between fluid and condensed states in the non-convex part. This leads to a metastable switching behaviour which disappears in the thermodynamic limit, intriguingly contradicting the usual expectation of finite systems to behave in a smoother fashion than the limiting prediction. The onset of phase coexistence at criticality is a classical question of general interest in phase separating systems, see for example [11, 12] for the formation of equilibrium droplets in the Ising model which also form suddenly on a critical scale. Rigorous results on metastability regarding the dynamics of the condensate in zero-range processes have also been a subject of recent research interest [7, 8], and our work provides a contribution in that direction and new insight in the mechanisms of condensate dynamics on finite systems (this is explained in detail in Section 4.5).

We have shown that a prototypical class of zero-range processes, that are known to undergo a condensation transition, exhibit large finite-size effects including a metastable switching phenomenon for a large range of system parameters. We have characterized this behaviour using the macroscopic maximum as an order parameter, by rigorously deriving a large deviation rate function for its distribution in an appropriate scaling limit, which shows a double well structure. These results agree with recent work on the zero-range process at the critical scale [5], which we extend by establishing metastable fluid and condensed states. Our methods give rise to a simple interpretation of these results in terms of a stationary current balance between the fluid background and the condensate. All results presented here, except those in Section 4.5, concern properties of the canonical stationary distribution and are therefore independent of the geometry or dimension of the lattice, so long as it permits homogeneous stationary distributions.

A proper understanding of the metastability phenomenon exhibited by zero-range processes on finite systems is of particular importance for recent applications with moderate system sizes. Clustering phenomena in granular media can be described by zero-range processes (see [117, 123] and references therein), and metastable switching between homogeneous and condensed states has been observed experimentally [122, 124]. In the spirit of the mapping introduced in [81] the zero-range process with jump rates $g(n)$ has also been applied as a simplified traffic model [83, 89], where condensation corresponds to the occurrence of a traffic jam. A key feature of traffic models is the existence of a broad range of densities over which metastability between free flowing and jammed states is observed (see for example [130] and references therein). Although the study is motivated by such applications, in this Chapter we have aimed to give general understanding of finite-size effects and their implications for a generic class of zero-range processes, rather than a detailed analysis of particular cases. Both of these applications (granular clustering and traffic) exhibit metastability phenomena, and typical system sizes are of order $10^2 - 10^3$, the region where metastability effects in our analysis are most relevant. Since our results hold for a large generic class of zero-range models, they suggest that the apparent metastability in many applications is not necessarily the result of a particular choice of the jump rates, but rather a generic finite-size phenomenon. While the results in the scaling limit hold for all zero-range processes with the same tail

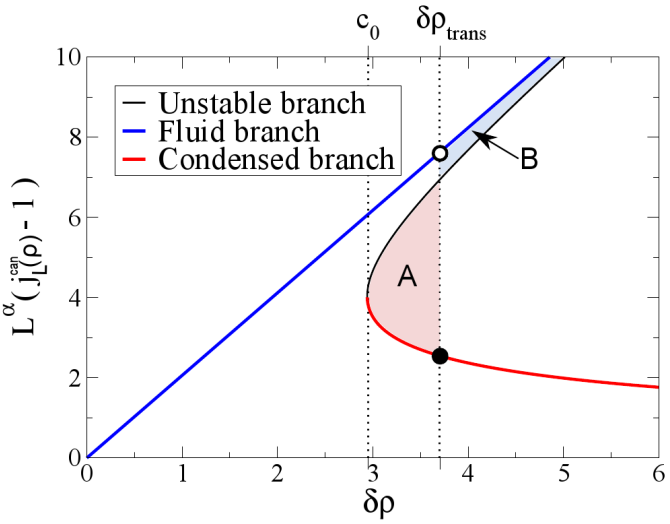

Figure 4.11: Maxwell's equal area rule for the current overshoot in the scaling limit for $\gamma = 0.5$ and $b = 4$. The blue line shows the limiting fluid current. The red line shows the limiting condensed current. The black line is the unstable branch given by current matching. The transition $\delta\rho_{\text{trans}}$ occurs when area A is equal to area B. The scaling exponent is $\alpha = \frac{\gamma}{1+\gamma}$, as given in (4.50)

behaviour as the rates (4.1), the strength of the effect for relevant system sizes will of course depend on the details of the particular application. Traffic modelling is an example where metastability is particularly pronounced [130], and it is an interesting question to investigate in detail the applicability of the zero-range process and our results in that area.

We may interpret the canonical rate function for the maximum as a free energy function. Due to the relationship between the scaling limit currents and the rate function for the maximum as given in Corollary 4.9, the transition $\delta\rho_{\text{trans}}$ occurs when the area enclosed by the fluid current, the unstable condensed branch and the transition line is equal to the area between the condensed current curve and the transition line. This is in direct analogy with Maxwell's equal area rule in thermodynamics, see for example [107], illustrated in Figure 4.11.

Our results allow us to estimate the lifetime of the two metastable states using a heuristic random walk argument. The estimates agree with previous studies of the dynamics of the condensate in the thermodynamic limit [61]. We show that in the critical scaling limit the lifetime of the two states is growing with system size, as a stretched exponential, and derive the appropriate Arrhenius law including prefactor. We have also demonstrated that on finite systems the re-location dynamics of the condensate is dominated by switching to the metastable fluid state for a large parameter range, rather than growing a second condensate whilst the background remains fluid. We find that at very high densities, in the scaling limit, the condensate typically moves via the second sub-condensate, which is consistent with the relevant mechanism in the thermodynamic limit, assumed in previous results. We give more details in Chapter 5 as to how the large deviation rate function allows us to distinguish between which mechanism dominates.

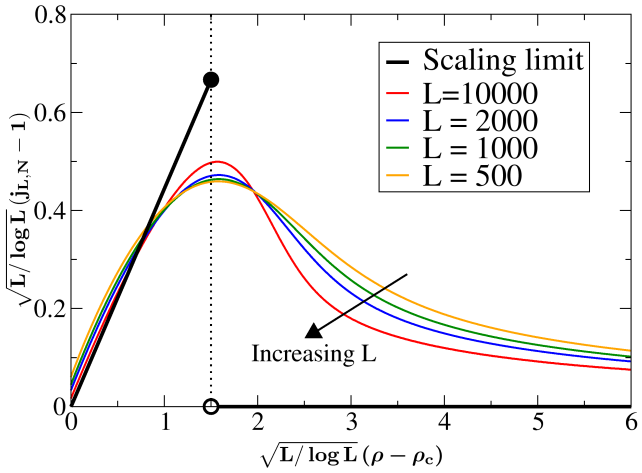

Figure 4.12: The current overshoot in the scaling limit for $\gamma = 1$ and $b = 4$. The thick black line shows the scaling limit result and the rescaled canonical currents are shown for various system sizes by thin coloured lines, slowly approaching the scaling limit as L increases. The transition point is given by $c_0(1, 4)$ which is given in [5].

The scaling limit rate function in Theorem 4.6 could also be derived using a slightly modified version of the saddle point methods applied in [44, 47, 98]. However, the direct approximation of the fluid and condensed metastable states used in this chapter seems more intuitive for our purpose, and is consistent with the general methods described in Chapter 3.

Using the same methods, a direct application of the findings in [5] allows us to extend our results on the current overshoot to zero-range processes with rates (4.1) where $\gamma = 1$ and $b > 3$, see Fig. 4.12. The critical scale in this case turns out to be of order $\sqrt{L/\log L}$, and the system also shows a discontinuous current overshoot in the scaling limit. However, as can be seen in Fig. 4.12, convergence is very slow and there are no metastable states on the critical scale. Although metastability might occur on higher order scales, it will hardly be relevant in any finite-size simulation or application.

The results in this chapter give rise to the typical size of the macroscopic maximum under the canonical distributions on the critical scale, in terms of concentration of probability. Using more refined large deviation approximations, due to Nagaev [103], Armendáriz et al. [5] have been able to describe the fluctuations of the maximum. They found that for $\delta\rho < \delta\rho_{\text{trans}}$ the maximum is typically of order $O((\log L)^{1/(1-\gamma)})$ and fluctuations of the maximum are the same as under the critical measure. For $\delta\rho > \delta\rho_{\text{trans}}$ they found the maximum to exhibit Gaussian fluctuations of order $\sqrt{L}$. Evans and Majumdar [47] discuss the fluctuations of the maximum in the power law case $\gamma = 1$, and $b > 2$. Using saddle point calculations they show that below criticality the maximum is $O(\log L)$ with Gumbel fluctuations, at the critical point the maximum is $O(L^{1/(b-1)})$ with limiting Fréchet distribution and above criticality the maximum is order L with Gaussian or stable law fluctuations. These results are also extended in Armendáriz et al. [5] to include the exact scale of the transition and to describing the fluctuations at the transition between critical and super-critical case.

Chapter 5

A size-dependent zero-range process

5.1 Introduction

In this chapter we apply the general framework outlined in Chapter 3 to study a condensation transition in a size-dependent zero-range process. The equivalence of ensembles result presented has previously been shown by [66] (by direct calculation), however we show how the results here significantly simplify the analysis and place the results in a wider context. The entropy methods also give rise to the full large deviations of the condensate and to the joint large deviations of finitely many macroscopically occupied sites in the thermodynamic limit, extending the previous results in [66]. Based on this we present a detailed heuristic analysis of the dynamic metastability that is observed in the system. This includes two distinct mechanisms for condensate motion in the system dependent on the total particle density. The results in this chapter will be summarised in the forthcoming publication [24].

The original motivation for studying a size-dependent model comes from experiments on granular media reported in [122, 124]. Several attempts have been made to study the behaviour of the condensate in this experiment, using a flux model based on kinetic theory for dilute granular gases [122, 123, 124] and also based on an urn model [27, 97]. Both of these models have been shown to be equivalent to zero-range processes [117], in the former case the jump rate depends on the size of the lattice and in the latter on the total number of particles in the system. A heuristic analysis of the behaviour of the average number of particles in a fixed compartment (site) agrees with experimental observations and shows that the transition is discontinuous and the system exhibits hysteresis and metastability. The analysis discussed above suggested that the origin of the discontinuous transition and metastability is the system size-dependent jump rates.

The condensation transition observed in previous studies of the single species zero-range process without size dependence have been shown to be continuous, with respect to the expectation of bounded observable such as the current as a function of the control parameter, density, ρ. A discontinuous transition has previously been observed on two

species systems [60] and can be observed in the scaling limit on a single species system (Chapter 4 and [25]). However in this chapter we observe that the condensation transition can be discontinuous in the thermodynamic limit for a single species size-dependent model. It was shown by Ruelle and Lanford, using a sub-additivity argument, that for homogeneous systems with short range interactions, the entropy densities are concave in the thermodynamic limit, under general conditions [88, 111]. In essence, the system size dependence of the jump rates (5.1) induces a long-range interaction in the thermodynamic limit, leading to a first order phase transition and non-concave canonical entropies (cf. work on Kac potentials summarized in [107] Section 4.1.2). The study of systems with long range interaction, such as gravitating particles, and calculation of their respective entropy densities is the subject of current research, see for example [119] and references there in.

In this chapter we study a particular prototype model that displays the same qualitative phenomena described above. We consider a zero-range process on a translation invariant lattice Λ_L, defined by the generator 2.12 where the rates are given by a step function,

$$g_L(0) = 0 \quad \text{and } g_L(k) = \begin{cases} c_0, & \text{if } 1 \leq k \leq J_L \\ c_1, & \text{if } k > J_L \end{cases} , \tag{5.1}$$

with $c_0 > c_1$, which have been studied in [66] and also [42] for J_L independent of L. The size dependence of the jump rates enters through the location of the jump J_L, which is dependent on the total number of lattice sites. J_L is chosen to depend on the system size asymptotically linearly, such that

$$J_L \to \infty \ \text{ and } \ J_L/L \to a \ \text{ as } \ L \to \infty, \tag{5.2}$$

where $a > 0$.

The choice of the model makes the application of the results in Chapter 3 particularly straight-forward and elegant. This is due to the simple choice of the jump rates and because the discontinuous transition and metastability are stabilised in the usual thermodynamic limit via the size dependence.

We study the dynamics of the condensate, in particular two types of condensate motion are observed, depending on the system density. The condensate moves either via a metastable fluid phase or by the growth of a second condensate, whilst the bulk remains at a constant density. The first type of motion suggests little or no correlation in the location of the next condensate, whereas the second type of motion could be more complicated, similarly to the relocation process discussed in [8]. Relevance of the thermodynamic limit to finite systems is supported by a detailed numerical study. Also dynamical predictions and heuristic arguments on condensate motion are supported by extensive simulations.

The chapter is organized as follows. In Section 5.2 we present the stationary measures and the relevant ensembles along with their corresponding entropy densities. By

applying the results of Chapter 3 we described the stationary behaviour of the system in the thermodynamic limit in Section 5.3, including equivalence and non equivalence of ensembles. In Section 5.4 we analyse the metastability based on the stationary large deviations for the most occupied sites. Finally, in Section 5.5 we summarize our results and discuss areas of future work.

5.2 Stationary measures

We recall that process exhibits single site stationary weights, derived in [66], and following (2.15),

$$w_L(k) = \prod_{i=0}^{k} g_L^{-1}(i) = \begin{cases} c_0^{-k}, & \text{if } 0 \leq k \leq J_L \\ c_0^{-J_L} c_1^{J_L - k}, & \text{if } k > J_L \ . \end{cases} \tag{5.3}$$

If the single site weights are normalisable than the normalised product of these weights and their tilted versions are stationary measures (see Section 2.2.1 for details).

5.2.1 Reference measure

We would like to choose the product of the normalised weights to be the reference measure, however for $c_1 \leq 1$ the single site weights are not normalisable. This can easily be dealt with by an a priori tilting of the single site weights so that they become normalisable. Therefore, we assume without loss of generality that $c_1 > 1$ so the single site weights are normalisable, which corresponds to a simple change of time scale (i.e. multiplying all the rates by a factor). The reference measure for a system of size L is a product of the single site marginals given by

$$\nu_L[k] = \frac{w_L(k)}{\sum_{n=0}^{\infty} w_L(n)} \ . \tag{5.4}$$

The probability of a configuration $\boldsymbol{\eta} \in X_L$ under the reference measure is then given by,

$$\nu^L[\boldsymbol{\eta}] = \prod_{x \in \Lambda_L} \nu_L[\eta_x] \ . \tag{5.5}$$

5.2.2 Grand canonical (tilted) measures

We wish to examine the usual thermodynamic limit, for which the total number of particles divided by the system size is the order parameter. We therefore consider tilted and conditioned versions of the reference measures with respect to the empirical density,

$$S_L(\boldsymbol{\eta}) = \frac{1}{L} \sum_{x \in \Lambda_L} \eta_x \ .$$

In the context of Chapter 3, this corresponds to taking $b_L = L$, and it turns out that large deviations of the density under the reference measure also occur on scale $a_L = L$.

This turns out to be the correct scale for observing metastability in the system in the thermodynamic limit, because J_L scales linearly with the system size (since the parameter $a > 0$ introduced in (5.2)).

The scaled pressure (cumulant generating function of S_L) on a finite system Λ_L is given by

$$\begin{aligned} p_L(\mu) &= \frac{1}{a_L} \log \nu^L \left(e^{\mu a_L S_L} \right) = \frac{1}{L} \log \nu^L \left(e^{\mu L S_L} \right) = \log \nu_L \left(e^{\mu \eta_1} \right) \\ &= \log \left(\frac{c_0 - 1}{c_0 - e^\mu} \right) + \log \left(1 + \left(\frac{e^\mu}{c_0} \right)^{J_L+1} \left(\frac{c_0 - c_1}{c_1 - e^\mu} \right) \right) \\ &\qquad - \log \left(1 + \left(\frac{1}{c_0} \right)^{J_L+1} \left(\frac{c_0 - c_1}{c_1 - 1} \right) \right) , \end{aligned} \tag{5.6}$$

which follows from

$$\sum_{n=0}^{\infty} w_L(n) e^{\mu n} = \frac{c_0}{c_0 - e^\mu} \left(1 + \left(\frac{e^\mu}{c_0} \right)^{(J_L+1)} \left(\frac{c_0 - c_1}{c_1 - e^\mu} \right) \right) . \tag{5.7}$$

By taking the limit, as L tends to infinity, we find the grand canonical pressure,

$$\begin{aligned} p(\mu) &= \lim_{L \to \infty} p_L = \lim_{L \to \infty} \frac{1}{a_L} \log \nu^L \left(e^{\mu a_L S_L} \right) \\ &= \begin{cases} \log \left(\frac{c_0 - 1}{c_0 - e^\mu} \right) & \text{if } \mu < \log c_1 \\ \infty & \text{otherwise.} \end{cases} \end{aligned} \tag{5.8}$$

We observe that $\mathcal{D}_p = \{\mu \in \mathbb{R} : p(\mu) < \infty\} = (-\infty, \log c_1)$. Notice that the convergence in the final line *is not* uniform on $(-\infty, \log c_1)$. However it is locally uniform in the sense that for all $\mu \in \mathcal{D}_p^\circ$ there exists a $\delta = (\log c_1 - \mu)/2$ such that the convergence is uniform on $B_\delta(\mu)$. This is sufficient to fulfil the required assumptions of the pressure made in Section 3.4.1. Following Definition 3.3, the grand canonical measures ν_μ^L exist for chemical potentials strictly less than $\mu_c = \log c_1$ with single site marginals,

$$\nu_{L,\mu}[k] = \frac{\nu_L[k] e^{\mu k}}{z_L(\mu)} . \tag{5.9}$$

The single site grand canonical partition function is $z_L(\mu) = \nu_L \left(e^{\mu \eta_1} \right)$.

The average particle density on a finite system under the grand canonical measure with chemical potential μ is given by,

$$\begin{aligned} R_L(\mu) &= \nu_\mu^L \left(S_L \right) = \nu_{L,\mu} \left(\eta_x \right) = \partial_\mu p_L(\mu) \\ &= \frac{e^\mu}{c_0 - e^\mu} + \left(\frac{e^\mu}{c_0} \right)^{J_L+1} \left(\frac{J_L + 1 + e^\mu/(c_1 - e^\mu)}{\frac{c_1 - e^\mu}{c_0 - c_1} + (e^\mu/c_0)^{J_L+1}} \right) . \end{aligned} \tag{5.10}$$

Note that $R_L(\mu)$ is strictly increasing in μ and that for each fixed system size $R_L(\mu) \to \infty$ as $\mu \to \log c_1$. This means that on a fixed finite system there exist grand canonical

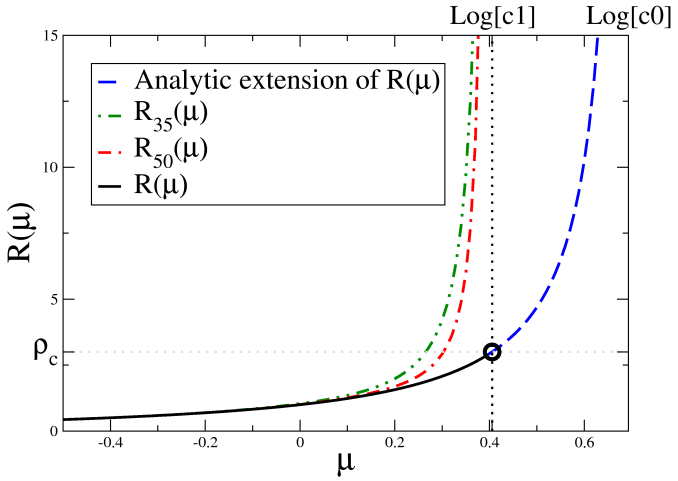

Figure 5.1: Grand canonical densities as a function of the chemical potential for $c_0 = 2$, $c_1 = 1.5$, $a = 0.2$. The dashed-dotted curves show the average density under the grand canonical measures on finite systems $R_L(\mu)$ as a function of the chemical potential (from (5.10)). The solid black curve shows the limit $R(\mu)$ (see (5.11)). The blue dashed line shows the analytic extension of $R(\mu)$ which exists upto $\log c_0$. Note the non uniform convergence of R_L as $L \to \infty$.

stationary measures for all densities. However, for fixed μ the average density under the grand canonical measures converges pointwise,

$$R_L(\mu) \to R(\mu) = \frac{e^\mu}{c_0 - e^\mu} \quad \text{for each } \mu < \log c_1 \ . \tag{5.11}$$

The limit does not diverge as $\mu \to \log c_1$ and the convergence is not uniform, see figure 5.1.

The expected jump rate off a site is proportional to the average stationary current or, in case the first moment $\sum_z z\, p(z)$ vanishes, to the diffusivity. For simplicity we therefore refer to **current** as the average jump rate off a site as in the previous chapter, which is clearly site independent under the homogeneous stationary distribution. In the grand canonical ensemble the current is simply given by,

$$j_L^{\mathrm{gc}}(\mu) = \nu_{L,\mu}\left(g_L(\eta_x)\right) = \frac{1}{z_L(\mu)} \sum_{n=0}^{\infty} g_L(n) e^{\mu n} \nu_L[n] = e^\mu \ , \tag{5.12}$$

(analogous to Chapter 4).

5.2.3 Restricted grand canonical measures

We define the restricted grand canonical measures as in Section 3.2.3 by truncating the grand canonical measures at the scale $b_L = L$. We recall, from Definition 3.5, the random variable corresponding to the macroscopic size of the maximum site occupation,

$$M_L(\boldsymbol{\eta}) = \frac{1}{L} \max_{x \in \Lambda_L} \eta_x \ .$$

The restricted grand canonical measures are given by,

$$\begin{aligned}\bar{\nu}^L_{\mu,m}[\boldsymbol{\eta}] &= \nu^L_\mu[\boldsymbol{\eta} \mid M_L \leq m_L] \\ &= \frac{e^{\mu \sum_{x\in\Lambda_L} \eta_x} \mathbb{1}_{\{M_L \leq m_L\}}(\boldsymbol{\eta})}{z^L_m(\mu)} \nu^L[\boldsymbol{\eta}] \\ &= \prod_{x\in\Lambda} \frac{e^{\mu\eta_x}}{\bar{z}_{L,m}(\mu)} \nu_L[\eta_x] \mathbb{1}_{\{\eta_x \leq m_L L\}}(\boldsymbol{\eta}) \ , \end{aligned} \tag{5.13}$$

where $\bar{z}_{L,m}(\mu) = \nu_L\left(e^{\mu\eta_x}\mathbb{1}_{\{\eta_x\leq m_L L\}}\right)$. Assumption (7) of Section 3.4.1 is fulfilled for $m_L \to m \in (0,\infty)$, and if $m = 0$ we need $m_L \to 0$ no slower than $1/L$, so we do not truncate too quickly.

We are now in a position to calculate the essential domains of the truncated pressures. Following (3.15), and inserting the form of the single site weights (5.3) into the definition of the reference measure (5.4), the restricted single site partition function is given by,

$$\bar{z}_{L,m}(\mu) = \begin{cases} \dfrac{1}{W_L} \displaystyle\sum_{k=0}^{m_L L} c_0^{-k} e^{k\mu} & \text{if } m_L L \leq J_L \\ \dfrac{1}{W_L} \left(\displaystyle\sum_{k=0}^{J_L} c_0^{-k} e^{k\mu} + c_0^{-J_L} \sum_{k=J_L+1}^{m_L L} c_1^{J_L-k} e^{k\mu} \right) & \text{if } m_L L > J_L \end{cases} \tag{5.14}$$

where W_L is the normalisation of the reference measure, from (5.7),

$$W_L = \frac{c_0}{c_0 - 1} \left(1 + c_0^{-(J_L+1)} \left(\frac{c_0 - c_1}{c_1 - 1} \right) \right) \ .$$

We observe that if $m > a$, then $m_L L > J_L$ for L sufficiently large, so the final term in $\bar{z}_{L,m}(\mu)$ is divergent for $\mu > \log c_1$ and converging to a constant for $\mu = \log c_1$. Therefore $\log \bar{z}_{L,m}(\mu) \to \infty$ as $L \to \infty$ if and only if $\mu \geq \log c_1$. It follows from Corollary 3.9 (or alternatively by dominated convergence) that $\mathcal{D}_{p_m} = \mathcal{D}_p$ and

$$p_m(\mu) = \lim_{L\to\infty} \log \bar{z}_{L,m}(\mu) = p(\mu) \quad \text{for } \mu \in \mathcal{D}_p \tag{5.15}$$

for all $m > a$. It also follows from 3.9 that the truncated grand canonical measures converge weakly, in the sense of (3.24), to the grand canonical measures at the same chemical potential for $\mu \in \mathcal{D}_p$ as $L \to \infty$.

If $m < a$ then the truncation occurs before the jump rates decrease (for sufficiently large L). In this case we have

$$\begin{aligned}\bar{z}_{L,m}(\mu) = \frac{1}{W_L} \sum_{k=0}^{m_L L} c_0^{-k} e^{k\mu} &= \frac{\frac{c_0 - c_0^{m_L L}}{c_0 - e^\mu}}{\frac{c_0}{c_0-1}\left(1 + c_0^{-(J_L+1)}\left(\frac{c_0-c_1}{c_1-1}\right)\right)} \\ &\to \frac{c_0 - 1}{c_0 - e^\mu} \quad \text{for } \mu \in (-\infty, \log c_0) \quad \text{as} \quad L \to \infty \ . \end{aligned} \tag{5.16}$$

So, for $m < a$,

$$p_m(\mu) = \log\left(\frac{c_0 - 1}{c_0 - e^{\mu}}\right) \quad \text{and} \quad \mathcal{D}_{p_m} = (-\infty, \log c_0) \supset \mathcal{D}_p \ . \tag{5.17}$$

The truncated pressure is clearly the analytic extension of the grand canonical pressure, c.f. (5.8).

Note that there are only two cases. The first is if cut-off is larger than J_L then the restricted ensemble is equivalent (in the sense Definition 3.11) to the unrestricted grand canonical ensemble. In this case the system still 'feels' the slow jump rate c_1. The second case is if the cut-off is smaller than J_L then the restricted ensembles are equivalent to the 'fluid' grand canonical measure corresponding to a system that has constant jump rates c_0. In this case the restricted measures are independent of c_1. These preliminary results are summarised in figure Fig. 5.2.

Since these are the only distinct cases, up to equivalence of ensembles, for the restricted measures we introduce *fluid measures* to simplify notation. These are the stationary measures of the process with constant jump rate $g(k) = c_0$ for all k. The single site marginals are simple geometric distributions,

$$\nu_{\mu,\infty} = \left(\frac{c_0}{c_0 - e^{\mu}}\right) e^{\mu\eta_x} c_0^{-\eta_x} \ , \tag{5.18}$$

with corresponding pressure,

$$p_\infty(\mu) = \log\left(\frac{c_0 - 1}{c_0 - e^{\mu}}\right) \quad \text{for } \mu \in \mathcal{D}_\infty := (-\infty, \log c_0) \ . \tag{5.19}$$

We may now summarise the preliminary results discussed in this section as follows (recall convergence in relative entropy implies equivalence in the sense of Definition 3.11),

$$\frac{1}{L} H(\nu^L_{\mu,m} \mid \nu^L_{\mu,\infty}) \to 0 \quad \text{for } \mu \in \mathcal{D}_p \ , \quad \text{if } m \in (a, \infty] \ , \tag{5.20}$$

and the limiting measures do not exist for $\mu \geq \log c_1$. For small m we have convergence to the fluid measures over an extended range of chemical potentials,

$$\frac{1}{L} H(\nu^L_{\mu,m} \mid \nu^L_{\mu,\infty}) \to 0 \quad \text{for } \mu \in \mathcal{D}_\infty \ , \quad \text{if } m < a \ . \tag{5.21}$$

Since p_∞ is steep at its boundary $\log c_0$ the fluid measures exist for all densities. Weak convergence (from (3.24)) only implies convergence of the expected value of *bounded* cylinder test functions, however, in general the system densities S_L also converge since it is given by the first derivative of the pressures.

Definition 5.1 (Fluid entropy density)**.** We define the grand canonical fluid entropy density as the Legendre-Fenchel transform of the fluid pressure (5.19), that is the pres-

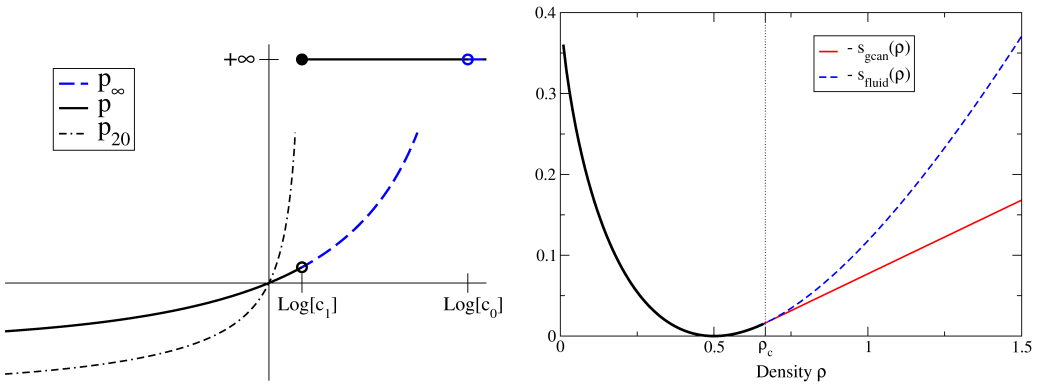

Figure 5.2: Left: The grand canonical pressure $p(\mu)$ in solid and the analytic extension $p_\infty(\mu)$ dashed as functions of the chemical potential μ. $p_\infty(\mu)$ is steep at $\log c_0$. Right: The Legendre transform of the grand canonical pressure (solid) and the Legendre transform of its analytic extension (dashed). They agree up to ρ_c and are both given by the thick black curve.

sure of the restricted measures with truncation less than a,

$$s_{\text{fluid}}(\rho) = - \sup_{\mu \in \mathcal{D}_{p_\infty}} \{\rho\mu - p_\infty(\mu)\} \ . \tag{5.22}$$

Since p_∞ is strictly convex and steep at $\log c_0$ the supremum in (5.22) is attained by some $\mu \in \mathcal{D}_{p_\infty}$ dependent on ρ,

$$\mathcal{M}_\infty(\rho) = (\partial_\mu p_\infty)^{-1}(\rho) = \log \frac{c_0\rho}{1+\rho} \ . \tag{5.23}$$

This states that the fluid measures (with cut-off less than aL) exist for all densities, and the chemical potential that realises density ρ is $\mathcal{M}_\infty(\rho)$. It follows that the fluid entropy is given by,

$$\begin{aligned} s_{\text{fluid}}(\rho) &= p_\infty\left(\mathcal{M}_\infty(\rho)\right) - \rho\mathcal{M}_\infty(\rho) \\ &= (1+\rho)\log(1+\rho) - \rho\log c_0\rho + \log(1-c_0^{-1}) \ . \end{aligned} \tag{5.24}$$

This is entropy density (with respect to the reference measure) associated with the fluid measures defined in (5.18) at average density ρ. More details on the Legendre-Fenchel transform for differentiable convex functions can be found in Appendix C.

5.2.4 Canonical (conditioned) measures

For a fixed lattice Λ_L, and initial conditions with fixed number of particles, the process is a finite state irreducible Markov process, and the unique stationary measures belong to the canonical ensemble (see Section 2.2.1 for details). Following Definition 3.8 the

canonical measures are given by,

$$\begin{aligned}\pi_\rho^L[\boldsymbol{\eta}] &= \nu^L[\boldsymbol{\eta} \mid S_L(\boldsymbol{\eta}) = \rho_L] \\ &= \frac{\mathbb{1}_{S_L^{-1}(\rho_L)}}{Z(L,\rho_L)}\nu^L[\boldsymbol{\eta}] \ . \end{aligned} \tag{5.25}$$

where ρ_L is a sequence converging to ρ as $L \to \infty$ in the sense of (3.18). The limiting behaviour is independent of the details of the sequence so long as $\rho > 0$.

The canonical partition function is given by the finite sum,

$$Z(L,\rho_L) = \nu^L[S_L = \rho_L] \ . \tag{5.26}$$

As discussed in Section 2.2.1 the stationary current under the canonical measures is given by a ratio of partition functions,

$$j_L^{\text{can}}(\rho_L) := \pi_\rho^L\left(g(\eta_x)\right) = \frac{Z(L,\rho_L - 1/L)}{Z(L,\rho_L)} \ . \tag{5.27}$$

5.3 Results

5.3.1 Equivalence of ensembles below ρ_c

For densities smaller than some critical value, ρ_c, equivalence of ensembles follows immediately from Theorem 3.7. The grand canonical entropy density is defined by the negative Legendre-Fenchel transform of the grand canonical pressures (see Definition 3.13),

$$s_{\text{gcan}}(\rho) = -p^*(\rho) \ . \tag{5.28}$$

We can calculate this exactly from the grand canonical pressure (5.8),

$$\begin{aligned} s_{\text{gcan}}(\rho) &= -\sup_{\mu \in \mathcal{D}_p}\left[\rho\mu - p(\mu)\right] \\ &= \begin{cases} (1+\rho)\log(1+\rho) - \rho\log(c_0\rho) + \log(1-c_0^{-1}) & \text{if } \rho < \frac{c_1}{c_0 - c_1}, \\ -\rho\log c_1 + \log\left(\frac{c_0-1}{c_0-c_1}\right) & \text{otherwise} \ . \end{cases} \end{aligned} \tag{5.29}$$

We observe that for densities strictly less than $\frac{c_1}{c_0-c_1}$ the grand canonical entropy density is strictly concave, and above this value it decreases linearly (therefore not strictly concave). This defines the critical density for this model,

$$\rho_c = \frac{c_1}{c_0 - c_1} \ .$$

Theorem 5.1 (Equivalence below ρ_c)**.** *For $\rho < \rho_c$ and $\rho_L \to \rho$ in the sense of* (3.18)*,*

$$\lim_{L\to\infty} \frac{1}{L} \log Z(L, \rho_L) := s_{can}(\rho) = s_{gcan}(\rho) \tag{5.30}$$

and we have equivalence of ensembles in the sense of Definition 3.11; there exists a sequence of chemical potentials $\mu_L(\rho_L)$ such that,

$$\pi_\rho^L \overset{L}{\longleftrightarrow} \nu^L_{\mu_L(\rho_L)} \quad \text{if } \rho_L \to \rho < \rho_c \ . \tag{5.31}$$

Proof. This is a direct result of the general theorems of Chapter 3. We show that the size-dependent system satisfies the assumptions of Section 3.4.1. Assumptions (1) and (2) on the thermodynamic pressure were shown in the previous section. The reference measure has finite exponential moments and the mean and variance converge to $\partial_\mu p(0)$ and $\partial_\mu^2 p(0)$ respectively, which is sufficient for assumption (3). The regularity assumption on the reference measures (4) is clearly satisfied because the single marginals of the reference measures are monotonic decreasing in the occupation number. Assumption (5) is clear from the choice of scale $a_L = L$. Assumption (6) on the condensate contribution to the entropy is also clear, s_{cond} is given explicitly below in (5.41). Assumption (7) is satisfied so long as $m_L \to m \in (0, \infty)$ or $m_L \gg 1/L$.

From (5.29) $s_{\text{gcan}}(\rho)$ is strictly convex and differentiable, so $-\partial_\rho s_{\text{gcan}}(\rho) \in \mathcal{D}_p^\circ$ for all $\rho < \rho_c$. By Theorem 3.7 $s_{\text{can}}(\rho) = s_{\text{gcan}}(\rho)$ for $\rho < \rho_c$. The equivalence of ensembles result then follows by applying Theorem 3.6. □

Corollary 5.2 (Convergence of the canonical current below ρ_c)**.** *For $\rho < \rho_c$ we have,*

$$\mu_L(\rho_L) \to (\partial_\mu p)^{-1}(\rho) =: \mu(\rho) \tag{5.32}$$

$$= \log \frac{c_0 \rho}{1+\rho} \tag{5.33}$$

and the canonical current converges to the grand canonical current,

$$j_L^{can}(\rho_L) \to e^{\mu(\rho)} = \frac{c_0\rho}{1+\rho} \quad \text{as } L \to \infty \ \text{ and, } \rho_L \to \rho < \rho_c \ . \tag{5.34}$$

Proof. Let,

$$R_L(\mu) := \nu_\mu^L(S_L) \tag{5.35}$$

$$= \partial_\mu p_L(\mu) \tag{5.36}$$

which is strictly increasing so invertible on $(-\infty, c_1)$. By definition we have

$$\mu_L(\rho_L) = (R_L)^{-1}(\rho_L) \ . \tag{5.37}$$

Since R_L converges locally uniformly to $\partial_\mu p(\mu)$ and since its inverse is also continuous

it follows that,

$$\mu_L(\rho_L) \to \partial_\mu p(\mu) \ . \tag{5.38}$$

as required.

The equivalence of ensembles, from Theorem 5.2, implies week convergence for bounded continuous cylinder test functions, see Section 3.3, so for $f \in C_0^b$,

$$\left| \pi_\rho^L(f) - \nu_{\mu_L(\rho_L)}^L(f) \right| \to 0 \quad \text{as} \quad \rho_L \to \rho < \rho_c \ .$$

The jump rate off a single site is clearly a bounded cylinder function. We observe that the grand canonical currents (5.12) converge as,

$$j_L^{\text{gc}}(\mu_L(\rho_L)) = \nu_{\mu_L(\rho_L)}^L(g(\eta_1)) = e^{\mu_L(\rho_L)} \to e^{\mu(\rho)} \ .$$

The result (5.34) then follows from the triangle inequality. □

5.3.2 Contracting on the most occupied site(s)

In this section we will see how contracting on the maximum occupied site allows us to calculate the full large deviation principle for the density under the reference measure. These give rise to the canonical entropy density. By applying this contraction we are able to separate the entropy density into a contribution due to a 'fluid' background of asymptotically independent sites and the contribution due to a macroscopically large number of particles (of order of the lattice size) occupying finitely many sites.

If the truncation in the restricted ensembles are at small enough or the remaining density in the background is low enough, then the large deviations of the restricted measures can be calculated by the Gärtner Ellis theorem (Theorem 3.7). However, at high densities it may be possible to condition on a maximum site occupation for which the background density is still significantly above ρ_c, and the truncation is not smaller than J_L, in this case we may have to contract on further macroscopically occupied sites. We show that for any density the canonical entropy can be derived by making only finitely many contractions. It is possible to find the (point-wise) large deviations of the joint event that the density is ρ_L and the maximum contains $m_L L$ particles, by the general results in Chapter 3. The canonical entropy density can then be derived by a contraction. This leads to results that go significantly beyond the first study of this model in [66].

We define the macroscopic size, on the scale L, of the maximum occupied site following Definition 3.5,

$$M_L(\boldsymbol{\eta}) = \frac{1}{L} \max_{x \in X} \eta_x.$$

We show that the following limit, which gives rise to a large deviation principle for the

joint density and maximum under the reference measure (see Appendix C), exists

$$I(\rho, m) = -\lim_{L\to\infty} \frac{1}{L} \log \nu^L[S_L = \rho_L, M_L = m_L] \quad \text{as} \quad \rho_L \to \rho \text{ and } m_L \to m \tag{5.39}$$

where the sequence (ρ_L) and (m_L) satisfy (3.41) and (3.18). By Theorem 3.10 this gives rise to the canonical entropy density,

$$s_{\text{can}}(\rho) = -\inf_{m\in[0,\rho]} I(\rho, m) \ .$$

By Corollary 3.11, it also gives rise to the canonical large deviations of the maximum,

$$\begin{aligned} I_\rho(m) &:= \lim_{L\to\infty} \frac{1}{L} \log \pi^L_{\rho_L}[M_L = m_L] \\ &= I(\rho, m) + s_{\text{can}}(\rho) \ . \end{aligned}$$

The basis of finding the large deviations of the joint distribution for the density and maximum site occupation lies in the following observation, based on the permutation invariance of the reference measure. There are L sites on which the maximum could be located, each of which is equally likely, so

$$\nu^L[S_L{=}\rho_L, M_L{=}m_L] = L\nu[m_L L]\nu^{L-1}[S_{L-1}{=}(\rho_L{-}m_L),\ \eta_i{<}m_L L\ \forall i \in \{1, \dots, L{-}1\}] \ .$$

It follows that we may decompose the logarithm as

$$\begin{aligned} \frac{1}{L} \log \nu^L[S_L{=}\rho_L, M_L{=}m_L] =& \frac{1}{L} \log \nu_L[m_L L] + \frac{1}{L} \log \bar\nu^{L-1}_{m_L}[S_{L-1}{=}(\rho_L - m_L)] + \\ &+ \frac{1}{L} \log L + \log \nu_L[\eta_1 < m_L L] \end{aligned} \tag{5.40}$$

where $\bar\nu^L_{m_L}[\boldsymbol{\eta}] = \nu^L[\boldsymbol{\eta} \mid \eta_1, \dots, \eta_L < m_L L]$.

Inserting the form of the single site marginals of the reference measure (5.3) and (5.4) into Definition 3.15 of the condensed entropy contribution we find

$$\begin{aligned} s_{\text{cond}}(m) &= \lim_{L\to\infty} \frac{1}{L} \log \nu_L[m_L L] \quad \text{as} \quad m_L \to m \\ &= \begin{cases} -m \log c_0, & \text{if } m \le a \\ -a \log(c_0/c_1) - m \log c_1, & \text{if } m > a. \end{cases} \end{aligned} \tag{5.41}$$

So the condensate entropy contribution is a piecewise linear, continuous convex function.

The entropy contribution outside of the maximum,

$$s_{\text{can,m}}(\rho - m) = \lim_{L\to\infty} \frac{1}{L} \log \bar\nu^{L-1}_{m_L}[S_{L-1}{=}(\rho_L - m_L)]$$

can be calculated immediately from Theorem 3.7 so long as $m < a$ or $(\rho - m) < \rho_c$. If $m < a$ then the truncated system asymptotically does not 'feel' the slower jump rate, and by (5.17) the truncated pressure is steep at its boundary and so the Legendre-Fenchel

transform is strictly convex for all densities. In the second case, if $(\rho - m) < \rho_c$, then the Legendre-Fenchel transform of the truncated pressure is strictly convex at $(\rho - m)$ since the grand canonical entropy density is strictly concave here.

Contracting on the maximum

We are now in a position to calculate the canonical entropy density up to $(\rho_c + a)$.

Lemma 5.3 (Contraction on the maximum)**.** *For $\rho < \rho_c + a$,*

$$I(\rho, m) = -\left(s_{cond}(m) + s_{fluid}(\rho - m)\right) \ , \tag{5.42}$$

which has a unique boundary minimum at $m = 0$ so,

$$s_{can}(\rho) = s_{fluid}(\rho) \ . \tag{5.43}$$

Proof. By Definition 3.14 and Equation (3.62),

$$I(\rho, m) = -\left(s_{\mathrm{cond}}(m) + s_{\mathrm{can,m}}(\rho - m)\right) \ ,$$

(assuming the limits exist). If $m < a$, then $p_m(\mu) = p_\infty(\mu)$, and since the Legendre-Fenchel transform of p_∞ is strictly concave (see Fig. 5.2) Theorem 3.10 Part (b) implies $s_{\mathrm{can,m}}(\rho) = s_{\mathrm{fluid}}(\rho)$ for all $\rho > 0$. If $m \geq a$, then since $\rho < \rho_c + a$, we have $\rho - m < \rho_c$ and the same result holds. $I(\rho, m)$ has a unique minimum at $m = 0$ since $\partial_m I(\rho, m) > 0$ for all m and so (5.43) follows from the contraction principle in Theorem 3.10. □

Contracting on finitely many sites

If $\rho > \rho_c + a$ we cannot calculate the large deviations of the maximum for $m \in [a, \rho - \rho_c]$ by contracting only on the maximum, since for $m > a$, $s_{\mathrm{gcan},m}(x)$ is not strictly concave for $x \geq \rho_c$. This is because if $m > a$ we have $s_{\mathrm{gcan},m}(x) = s_{\mathrm{gcan}}(x)$ (which follows from (5.15)) and this is only strictly concave up to ρ_c. So a single contraction is only sufficient whilst $m < a$ or $(\rho - m) < \rho_c$. The problem arises because the truncation is large enough that the single site occupation, outside of the maximum, can still be greater than J_L and so experience the slow jump rate, and also the total density in the background is greater than ρ_c. In this case we must iterate the contraction on the next most occupied site.

If we assume a priori that the limits exist the process of iterating the contraction can be described as follows (see Section 3.4.4 for details),

$$s_{\mathrm{can}}(\rho) = -\inf_{m \in [0,\rho]} I(\rho, m) = \sup_{m \in [0,\rho]} \left(s_{\mathrm{cond}}(m) + s_{\mathrm{can,m}}(\rho - m)\right) \ ,$$

where,

$$s_{\text{can,m}}(\rho - m) := \lim_{L\to\infty} \frac{1}{L} \log \nu^L_{m_L}[S_L = (\rho - m)]$$
$$= \sup_{m' \in [0,m]} \left(s_{\text{cond}}(m') + s_{\text{can,m'}}(\rho - m') \right) \ .$$

Lemma 5.4. *Each iteration of the contraction extends the accessible range of densities, for which we can calculate $s_{can}(\rho)$, by at least a,*

$$I(\rho, m) = -\begin{cases} s_{cond}(m) + s_{fluid}(\rho - m) & \text{if } m < a \text{ or } m > (\rho - \rho_c), \\ s_{cond}(m) - \inf_{m^{(2)} \in [0,m]} I(\rho - m, m^{(2)}) & \text{otherwise.} \end{cases} \tag{5.44}$$

Proof. For all $\rho > 0$ if $m < a$ or $(\rho - m) < \rho_c$ then by Lemma 5.3,

$$I(\rho, m) = -\left(s_{\text{cond}}(m) + s_{\text{fluid}}(\rho - m) \right) \ .$$

Assume we know $I(x, y)$ for all $x \leq \rho$ and $y \leq x$ (for $y > x$, $I(x, y) = \infty$ by definition) then

$$I(\rho + a, m) = -s_{\text{cond}}(m) + \inf_{m^{(2)} \in [0,m]} I(\rho - m, m^{(2)}) \ , \tag{5.45}$$

by Theorem 3.10 Part (a). □

So we can calculate $I(\rho, m)$ and hence $s_{\text{can}}(\rho)$ by only finitely many contractions for each $\rho > 0$. We interpret $s_{\text{cond}}(m)$ (the first term in (5.45)) as the cost of putting a macroscopic mass m on a single lattice site, and the second term as the cost associated with the most likely way of arranging the rest of the mass in the systems subject to no site containing more than m particles. This is a specific case of the principle "a large deviation is typically realised in the least unlikely of all the unlikely ways" ([35] page 10).

Since Lemma 5.4 gives the joint large deviations for all densities $\rho > 0$, and $m \leq \rho$ by only finitely many contractions, it also gives rise to the canonical large deviations of the maximum, by Corollary 3.11,

$$I_\rho(m) = I(\rho, m) - \inf_{x \in [0,\rho]} I(\rho, x) \ , \tag{5.46}$$

where the final term ensures the minimum is at 0 for each ρ. Way may write this explicitly for $m < a$ or $m > \rho - \rho_c$, by inserting Equations (5.24) and (5.41) into (5.44). Otherwise we may calculate it by means of the contraction in Lemma 5.4. We do not write the formula out in full here, since it would be lengthy and uninformative and refer to Figures 5.3 and 5.4.

It is clear that for fixed ρ, $I_\rho(m)$ always has a local minimum on the boundary at $m = 0$. Notice that for $\rho > \rho_c + a$ there is also a local minimum at $(\rho - \rho_c)$. This

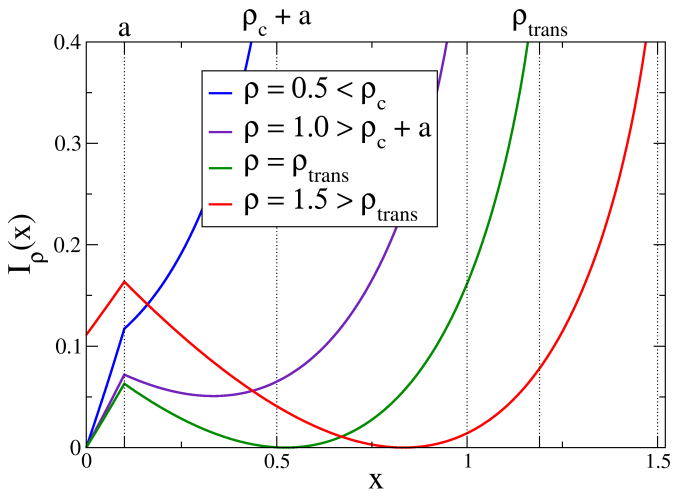

Figure 5.3: $I_\rho(x)$ at various values of ρ showing the single well for $\rho < \rho_c + a$ and double well with global minimum at 0 for $\rho_c + a < \rho < \rho_{\text{trans}}$ and double well with global minimum at $(\rho - \rho_c)$ for $\rho > \rho_{\text{trans}}$. At higher densities (not shown here) there is even more structure (see Fig. 5.4).

follows directly by differentiating s_{fluid}, given explicitly in (5.24), and s_{cond}, given by (5.41). These are the only possible local minima of I_ρ, since the entropy contribution of the background $s_{\text{can,m}}(\rho)$ is decreasing in ρ for $\rho > \rho_c$. We define the transition density ρ_{trans} as the density at which both minima of $I_{\rho_{\text{trans}}}$ are of equal depth, given by the unique solution of

$$\begin{aligned} I_\rho(0) &= I_\rho(\rho - \rho_c), \quad \text{or equivalently,} \\ s_{\text{fluid}}(\rho) &= s_{\text{cond}}(\rho - \rho_c) + s_{\text{fluid}}(\rho_c) \ . \end{aligned} \tag{5.47}$$

From the explicit expression (5.24) and (5.41) it is easy to show that this equation has a unique solution $\rho = \rho_{\text{trans}}$, which is illustrated in Fig. 5.6. For $\rho < \rho_{\text{trans}}$ there is a unique minimum of $I_\rho(m)$ at the bonder $m = 0$ and for $\rho > \rho_{\text{trans}}$ there is a unique minimum at $m = (\rho - \rho_c)$.

Depending on the total density ρ the large deviation rate function for the maximum under the canonical measures $I_\rho(m)$ has one of four qualitative forms, illustrated in Fig. 5.3. If $\rho < (\rho_c + a)$ then $I_\rho(m)$ has a unique minimum at $m = 0$ and is strictly increasing on $[0, \rho]$. If $(\rho_c + a) < \rho < \rho_{\text{trans}}$ then $I_\rho(m)$ has a global minimum at $m = 0$ and a local minimum at $m = (\rho - \rho_c)$, corresponding to metastable condensed states. For $\rho > \rho_{\text{trans}}$ the minimum at $m = (\rho - \rho_c)$ becomes the global minimum and so the condensed state becomes stable, and the fluid state (corresponding to $m = 0$) becomes metastable. For ρ much larger than the transition density $I_\rho(m)$ can display more structure in the region $m \in [a, \rho - \rho_c]$ due to large deviations being realised by multiple condensates (see Fig. 5.4). At the transition point $\rho = \rho_{\text{trans}}$ we must examine higher order terms and it can be shown by explicit computations that the condensed state is stable [66].

Notice that at high densities (if $\rho > \rho_{\text{trans}} + a$) a large deviation in the maximum in the region $m \in (a, \rho - \rho_{\text{trans}})$ may typically be achieved by multiple macroscopically

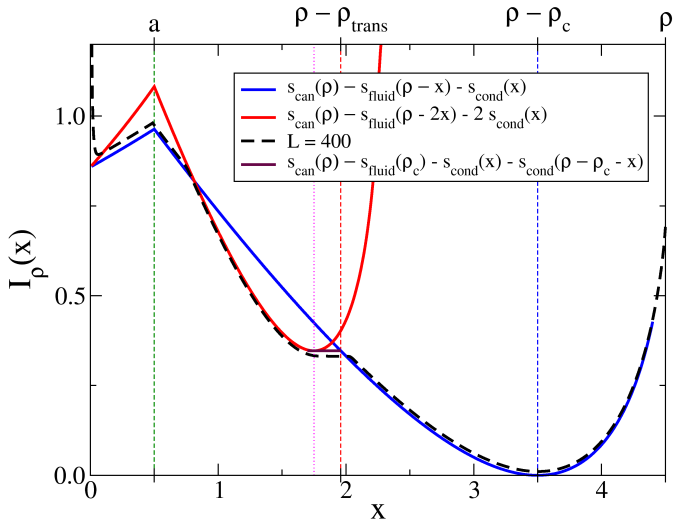

Figure 5.4: I_ρ for $c_1 = 1$, $c_0 = 2$, $a = 0.5$, and $\rho = 4.5$. We see that for $\rho > \rho_{\text{trans}} + a$ (significantly larger) a large deviation of the maximum M_L in the region $a < x < \rho - \rho_{\text{trans}}$ can be achieved in the most likely way by multiple condensates (macroscopically occupied sites). Such events are always exponentially unlikely in the system sizes and so do not affect the stationary behaviour, but they may still be relevant for the dynamics.

occupied sites rather than a very high background density, see Fig. 5.4. This is because the excess mass in the background (outside of the maximum occupied site) is still greater than the transition density and the truncation m is also greater than a so the system still 'feels' the slower jump rate. Although these are always exponentially unlikely events they are still relevant for the dynamics, see Section 5.4.

5.3.3 Current matching

The large deviations of the maximum under the canonical measures can be understood (in the region $m < a$ and $m > \rho - \rho_{\text{trans}}$) in terms of a current matching argument. If the current into the maximum from the background is lower than the jump rate out of the condensate then the condensate is expected to decrease in size and vice versa, this is illustrated in Fig. 5.5. It turns out the this argument also holds rigorously in the following sense.

Corollary 5.5 (Current matching)**.** *Provided $m < a$ or $m > (\rho - \rho_{trans})$,*

$$\begin{aligned} \partial_m I_\rho(m) &= \lim_{L\to\infty} (\log g_L(m_L L)) - \log j^{fluid}(\rho - m) \\ &= \begin{cases} \log c_0 - \log\left(\frac{c_0(\rho-m)}{1+(\rho-m)}\right) & \text{if } m < a \\ \log c_1 - \log\left(\frac{c_0(\rho-m)}{1+(\rho-m)}\right) & \text{if } m > a\ , \end{cases} \end{aligned} \tag{5.48}$$

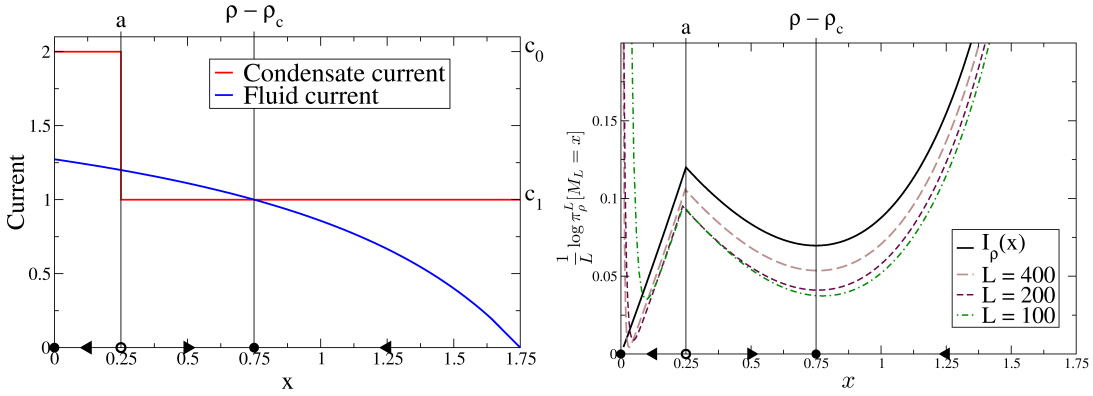

Figure 5.5: Current matching, with $c_0 = 2$, $c_1 = 1$ and $a = 0.25$. Left: The jump rate out of the maximum as given by $g_L(x)$ plotted in red and the average jump rate in the background given by $\nu^L_{\mu(\rho-m),\infty}(g_L)$ (see (5.49)). Right: Large deviation for the maximum under the canonical measure. Vertical lines show the correspondence between turning points of the rate function and current matching. If the current out of the maximum is greater than the average current in the background then the maximum is on average decreasing and vice versa. This gives rise to the stability of each turning point and the boundaries points.

where the average current in the fluid background, j^{fluid}, can be characterised by,

$$\begin{aligned} \log j^{fluid}(\rho) = \mathcal{M}_\infty(\rho) &= -\partial_\rho s_{fluid}(\rho) \\ &= \log\left(\frac{c_0\rho}{1+\rho}\right) \end{aligned} \tag{5.49}$$

This result is directly analogous to Corollary 4.9 in Chapter 4.

Proof. From Lemma 5.4, and the definition of ρ_{trans}, we have

$$I_\rho(m) = s_{\text{can}}(\rho) - s_{\text{cond}}(m) - s_{\text{fluid}}(\rho - m) \quad \text{provided} \quad m < a \text{ or } m > (\rho - \rho_{\text{trans}})$$

Taking the derivative with respect to m, using the explicit forms of s_{cond} and s_{fluid} in Equations (5.41) and (5.23), respectively, we find

$$\partial_m I_\rho(m) = \begin{cases} \log c_0 - \mathcal{M}_\infty(\rho - m) & \text{if } m < a \\ \log c_1 - \mathcal{M}_\infty(\rho - m) & \text{if } m > a\ . \end{cases}$$

We may identify the chemical potential of the fluid measures $\mathcal{M}_\infty(\rho)$ with the logarithm of the average jump rate in the usual way for stationary product measures of a zero-range process (see (2.17)),

$$\log j^{\text{fluid}}(\rho) := \log \nu^L_{\mathcal{M}_\infty(\rho),\infty}(g_L) = \mathcal{M}_\infty(\rho)\ .$$

□

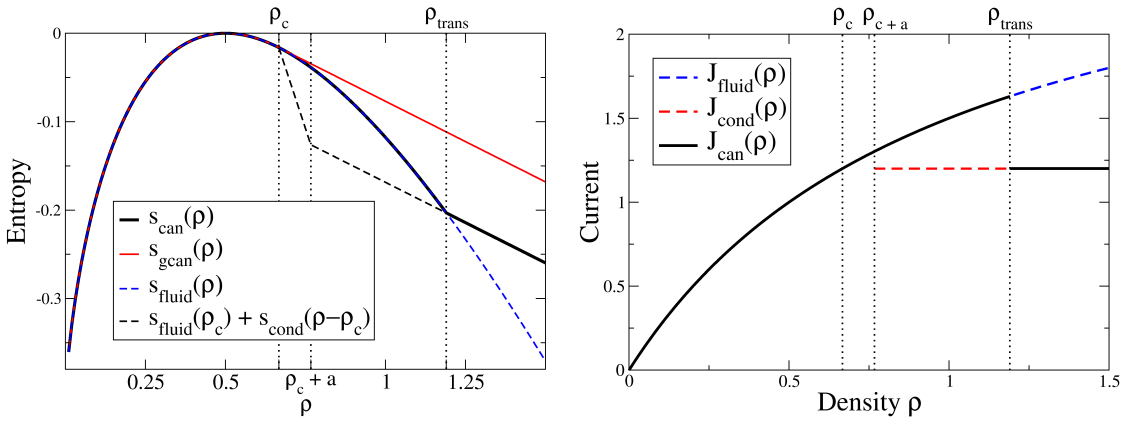

Figure 5.6: Left: The grand-canonical and canonical entropy agree up to ρ_c and so we have equivalence of ensembles. Between ρ_c and ρ_{trans} the canonical entropy is equal to the fluid entropy so the canonical measures converge to the fluid measures at the appropriate density $\rho > \rho_c$. Above ρ_{trans} the canonical entropy is equal to $s_{\text{fluid}}(\rho_c) + s_{\text{cond}}(\rho - \rho_c)$ and the background converges to the fluid measures at ρ_c (see Theorem 5.6). Right: The average current is given by the derivative of the entropies.

5.3.4 Summary and equivalence of ensembles

The large deviations for the density and the maximum give rise to the full canonical entropy density, and thus by the results in Chapter 3 to equivalence and non equivalence of ensembles. Below ρ_c we have $s_{\text{can}}(\rho) = s_{\text{gcan}}(\rho)$ and so we have equivalence of ensembles between the canonical and grand canonical measures (at the appropriate density). For $\rho_c < \rho < \rho_{\text{trans}}$ we have $s_{\text{can}}(\rho) = s_{\text{fluid}}(\rho)$ and we have equivalence of ensembles between the canonical and fluid measures (at the appropriate density). For $\rho > \rho_c + a$ there exists a metastable condensed state with exponential lifetime corresponding to the local minimum of $I_\rho(m)$ at $m = (\rho - \rho_c)$. For $\rho > \rho_{\text{trans}}$ we have $s_{\text{can}}(\rho) = s_{\text{cond}}(\rho - \rho_c) + s_{\text{fluid}}(\rho_c)$ and a breakdown of the usual equivalence of ensembles. At such high densities the canonical measures after removing the maximally occupied site converge to the fluid measures with density ρ_c. The results are summarised in the following theorem and in Figures 5.6 and 5.7.

Theorem 5.6 (Equivalence of ensembles)**.** *The canonical entropy density,*

$$s_{can}(\rho) = \begin{cases} s_{gcan}(\rho) & \text{if } 0 < \rho < \rho_c \\ s_{fluid}(\rho) & \text{if } \rho_c \le \rho \le \rho_{trans} \\ s_{gcan}(\rho_c) + s_{cond}(\rho - \rho_c) & \text{if } \rho > \rho_{trans} \ , \end{cases} \tag{5.50}$$

which gives rise to the following results describing the equivalence of ensembles,

$$\pi_\rho^L \overset{L}{\longleftrightarrow} \begin{cases} \nu^L_{\mu(\rho)} & \text{if } 0 < \rho < \rho_c \\ \nu^L_{\mu(\rho),\infty} & \text{if } \rho_c \le \rho < \rho_{trans} \end{cases} \tag{5.51}$$

$$\hat{\pi}_\rho^L \overset{L}{\longleftrightarrow} \nu^{L-1}_{\mu(\rho_c),\infty} \quad \text{if} \quad \rho \ge \rho_{trans} \ . \tag{5.52}$$

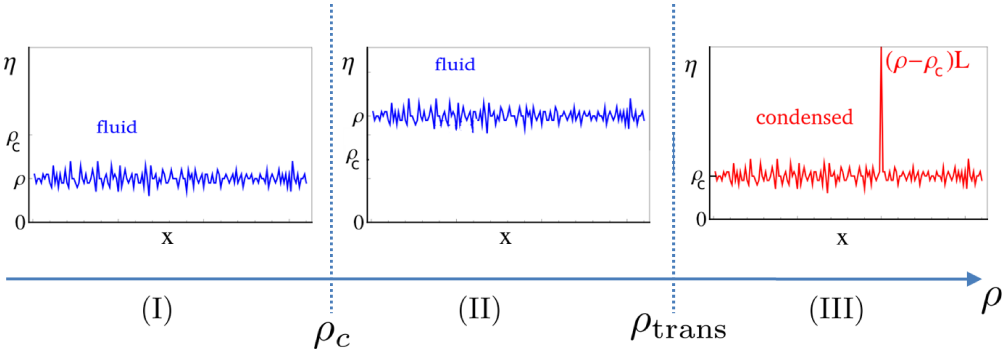

Figure 5.7: Equivalence of ensembles. (I) For $\rho < \rho_c$ the sites are asymptotically independent and distributed according to the grand canonical measures at the appropriate chemical potential. (II) For $\rho > \rho_c$ there no longer exist grand canonical measures with density ρ. However for $\rho < \rho_{\text{trans}}$ the sites remain asymptotically independent and there is equivalence with the fluid grand canonical measures at the appropriate chemical potential. (III) For $\rho > \rho_{\text{trans}}$, a large deviation in the density under the reference measure is typically realised by a single highly occupied site whilst the remaining sites contain on average ρ_c particles. This signals the onset of condensation whereby $(\rho - \rho_c)L + o(L)$ particles typically accumulate on a single lattice site.

where $\overset{L}{\longleftrightarrow}$ *denotes equivalence in the sense of bounded cylinder test functions (Def. 3.11).* $\hat{\pi}^L_\rho$ *is the canonical distribution of the background, defined in* (3.71) *(See Corollary 3.13 for details).*

Proof. The canonical entropy density follows immediately by taking the infinimum over m of $I(\rho, m)$ in Lemma 5.4. Equivalence of ensembles for $\rho < \rho_c$ follows from Theorem 3.7.

For $\rho_c \leq \rho < \rho_{\text{trans}}$, $I_\rho(m)$ has a unique minimum at $m = 0$ and so restricting the canonical measures to have maximum less than a does not effect the entropy density. That is, for all $0 < m < a$ we observe $s_{\text{can}}(\rho) = s_{\text{can,m}}(\rho) = s_{\text{fluid}}(\rho)$. The equivalence with the fluid measure for $\rho < \rho_{\text{trans}}$ therefore follows by Corollary 3.12.

For $\rho > \rho_{\text{trans}}$ stationary configurations typically contain a macroscopic maximum containing $(\rho - \rho_c)L + o(L)$ particles and the canonical entropy is given by the sum of the contribution due to the maximum and a contribution due to a fluid background at density ρ_c. The result, $\hat{\pi}^L_\rho \overset{L}{\longleftrightarrow} \nu^{L-1}_{\mu(\rho_c),\infty}$, is a consequence of Corollary 3.13. □

Since the jump rates are bounded test functions this implies that the canonical current converges as (see Figure 5.6),

$$j^{\text{can}}_L(\rho_L) \to \begin{cases} j^{\text{fluid}}(\rho) & \text{if } \rho < \rho_{\text{trans}} \\ c_1 & \text{if } \rho > \rho_{\text{trans}} \ . \end{cases} \tag{5.53}$$

Corollary 5.7 (Law of Large numbers for the maximum)**.** *The macroscopic size of the*

maximum site occupation, $M_L(\boldsymbol{\eta}) = \frac{1}{L}\max_{x\in\Lambda_L}\eta_x$*, obeys a weak law of large numbers,*

$$M_L \xrightarrow{\pi_\rho^L} \begin{cases} 0 & \text{if } \rho < \rho_{trans} \\ \rho - \rho_c & \text{if } \rho > \rho_{trans} \end{cases} , \tag{5.54}$$

where $\xrightarrow{\pi_\rho^L}$ *denotes convergence in probability as defined in Section 2.3.2.*

Proof. Follows from the global minimum of I_ρ by concentration of measure in Appendix C, Theorem C.6. □

These results can be refined, for instance to cover the fluctuations, with more precise large deviation estimates. For example see the methods in [5] and [4] (these use refined large deviation estimates due to Nagaev [103, 104, 105]). Since the large deviation rate function for the maximum is locally parabolic at $m = (\rho - \rho_c)$ under the extra condition that the fluid pressure is complex analytic (at the origin) we may deduce that fluctuations of the scaled maximum are locally Gaussian [21]. At the boundary $m = 0$ fluctuations of the maximum are expected to be given by extreme value statistics under the fluid measure, which can be calculated following [47].

5.4 Metastability and dynamics of the condensate

In this section we discuss the physical interpretation of the local minimum of the canonical rate function for the maximum site occupation $I_\rho(m)$ (see Fig. 5.3 and 5.4). The equivalence of ensembles results in Theorem 5.6 only gives information about the globally stable state, which below ρ_{trans} is fluid in the sense that the sites are asymptotically independent and distributed according to the weak limit of the restricted ensembles (with restriction lower than a). Above ρ_{trans} the stable state is condensed in the sense that the system phase separates into a condensate containing $(\rho-\rho_c)L$ particles and the remaining mass is distributed according to the fluid measure in the background phase. The local minima of $I_\rho(m)$ for $\rho > \rho_c + a$ correspond to metastable fluid and condensed states in sense discussed in Section 2.4. It can be observed in Monte Carlo simulations, that the dynamics exhibit metastable switching between the two states, exactly analogous to the switching in the finite size effects (see Section 4.5). For the purpose of measuring the lifetimes of the two phases in simulations, we say the configurations are fluid if the maximum site occupation is less than $J_L = aL$, and condensed if the maximum site occupation is above aL. As in Section 4.5 the lifetimes of the two phase are found to be exponentially distributed. Close to the transition density the picture looks the same as in Fig. 4.5 (for more details see [66]).

According to the above decomposition of the state space, we define the two metastable distributions as follows,

$$\pi_\rho^{L,\text{fluid}}[\cdot] = \pi_\rho^L[\cdot \mid M_L \le a] \tag{5.55}$$

$$\pi_\rho^{L,\text{cond}}[\cdot] = \pi_\rho^L[\cdot \mid M_L > a] \ . \tag{5.56}$$

Proposition 5.8. *For all $\rho > 0$,*

$$\pi_\rho^{L,fluid} \overset{L}{\longleftrightarrow} \nu^L_{\mu(\rho),\infty} \quad \textit{and} \quad M_L \xrightarrow{\pi_\rho^{L,fluid}} 0 \ ,$$

and for $\rho > \rho_c + a$,

$$\hat{\pi}_\rho^{L,cond} \overset{L}{\longleftrightarrow} \nu^{L-1}_{\mu(\rho_c),\infty} \quad \textit{and} \quad M_L \xrightarrow{\pi_\rho^{L,cond}} (\rho - \rho_c) \ ,$$

where $\hat{\pi}_\rho^{L,cond}$ is the distribution of the background, defined in (3.71).

Proof. The equivalence of the metastable fluid distribution with the fluid measure follows from Corollary 3.12, since $s_{\mathrm{can,a}}(\rho) = s_{\mathrm{fluid}}(\rho)$. The law of large numbers for M_L follows from concentration of measure, see Appendix C for details. The equivalence of the condensed background measure follows from Corollary 3.13, with only a slight adaptation of the proof. □

Typical configurations in the condensed state are not translation invariant, since there is a macroscopic maximum at a particular site. Therefore, this state exhibits an obvious multiplicity and can be further decomposed with respect to the location of the condensate into a further L states $\pi_\rho^{L,x} := \pi_\rho^{L,\mathrm{cond}}[\cdot \mid \eta_x/L = M_L]$. In this sense the condensed minimum of I_ρ at $(\rho - \rho_c)$ has an L fold degeneracy, corresponding to each of the positions that the maximum could reside. Considering only the rate function for the most occupied site, I_ρ, is therefore not sufficient for a full understanding of the condensate dynamics.

We show heuristically that the lifetimes of these metastable phases grow exponentially quickly in L, and the typical paths between these states are given by a minimum action principle as described in Section 2.4. Since the occupation number of each site can change by at most one in each transition of the underlying Markov process, in order for the system to change between metastable states, or for the maximum to relocate, the system must visit a configuration in which the maximum and second most occupied site (second maximum) differ by at most a single particle. We denote the macroscopic size of the second most occupied site,

$$M_L^{(2)}(\boldsymbol{\eta}(t)) = \frac{1}{L} \max_{x \in \Lambda_{L-1}} C(\boldsymbol{\eta}) \ ,$$

the cut operator C is defined in (2.37). It follows that the scaled maximum and second maximum $(M_L(\boldsymbol{\eta}(t)), M_L^{(2)}(\boldsymbol{\eta}(t)))$ perform a two dimensional random walk on the restricted simplex;

$$S = \{(x,y) \in [0,\rho]_L \times [0,\rho]_L \mid x+y \le \rho, y \le x\} \quad \text{where } [0,\rho]_L = \{0, 1/L, \dots, \lfloor \rho L \rfloor / L\} \subset \frac{1}{L}\mathbb{Z} \, .$$

The metastable lifetimes can be expressed in terms of the following hitting times,

$$\begin{aligned}\tau_L^{\text{fluid}} &= \inf\{t \geq 0 \mid M_L(\boldsymbol{\eta}(t)) \geq a\} \\ \tau_L^{\text{cond}} &= \inf\{t \geq 0 \mid M_L(\boldsymbol{\eta}(t)) \leq a\} \\ \tau_L^{\text{move}} &= \inf\{t \geq 0 \mid M_L(\boldsymbol{\eta}(t)) \leq M_L^{(2)}(\boldsymbol{\eta}(t)) + 1/L\} \ . \end{aligned} \tag{5.57}$$

The expected lifetime of the fluid state, condensed state, and time to observe condensate motion are given respectively by,

$$\begin{aligned} T_{\text{fluid}} &= \mathbb{E}^{\pi_\rho^{L,\text{fluid}}}\left[\tau_L^{\text{fluid}}\right] \\ T_{\text{cond}} &= \mathbb{E}^{\pi_\rho^{L,\text{cond}}}\left[\tau_L^{\text{cond}}\right] \\ T_{\text{move}} &= 2\mathbb{E}^{\pi_\rho^{L,\text{cond}}}\left[\tau_L^{\text{move}}\right] \ , \end{aligned} \tag{5.58}$$

where the expectations are with respect to measure on path space defined by the generator $\mathcal{L}_L$ (2.12) and initial condition given by the metastable distributions.

By ergodicity of the underlying process $(\boldsymbol{\eta}(t) : t \geq 0)$ the ratio of the fluid and condensed lifetimes is directly related to the stationary distribution,

$$\begin{aligned} \frac{T_{\text{fluid}}}{T_{\text{cond}}} &= \frac{\pi_\rho^L[M_L \leq a]}{\pi_\rho^L[M_L \geq a]} \\ &\approx \frac{\sqrt{\partial_m^2 I_\rho(\rho - \rho_c)}}{\sqrt{2\pi L}\partial_m I_\rho(0)} e^{-L(I_\rho(\rho) - I_\rho(\rho - \rho_c))} \end{aligned} \tag{5.59}$$

where the second line follows by a saddle point (Laplace) approximation of the integrals, and the derivative in the denominator is understood as the derivative from the right.

By construction the two dimensional random walk $(M_L(\boldsymbol{\eta}(t)), M_L^{(2)}(\boldsymbol{\eta}(t)))$ is a non Markovian ergodic process on state space, S, and has stationary distribution $\pi_\rho^L[M_L = m_L^{(1)}, M_L^{(2)} = m_L^{(2)}]$. So its stationary large deviations are given by the joint canonical rate function for the maximum and second maximum. This can be calculated exactly as a straightforward extension of Lemma 5.4, using also equations 5.41 and 5.24,

$$\begin{aligned} I_\rho^{(2)}(m^{(1)}, m^{(2)}) &= \lim_{L\to\infty} \pi_\rho^L[M_L = m_L^{(1)}, M_L^{(2)} = m_L^{(2)}] \\ &= s_{\text{can}}(\rho) - s_{\text{cond}}(m^{(1)}) + I(\rho - m^{(1)}, m^{(2)}) \ . \end{aligned} \tag{5.60}$$

It corresponds to the free energy landscape for the highest, and second highest occupied sites. The first term $s_{\text{can}}(\rho)$ is the canonical normalisation and ensures that the minimum resides at zero, the second term is the contribution due to macroscopic maximum $m^{(1)}$ and the final term is the contribution to to the remaining system containing a density

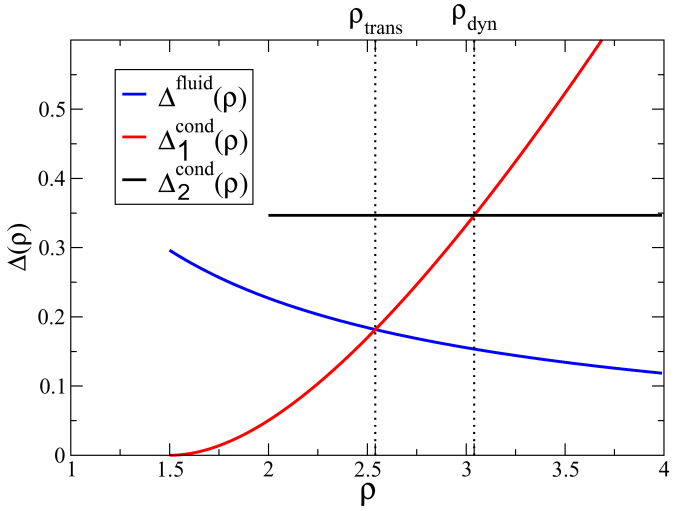

Figure 5.8: The exponential rates of the lifetimes and condensate motion time, given by (5.65), for $c_0 = 2$, $c_1 = 1$, $a = 0.5$. For $\rho < \rho_c + a = 1.5$ the rate function for the maximum has a unique minimum at $m = 0$ and there are no exponential barriers or metastability. $\Delta^{\text{fluid}}(\rho)$ is strictly decreasing, $\Delta_1^{\text{cond}}(\rho)$ is strictly increasing, and $\Delta_2^{\text{cond}}(\rho)$ is constant. $\Delta^{\text{fluid}}(\rho)$ intersects $\Delta_1^{\text{cond}}(\rho)$ at ρ_{trans}, and $\Delta_1^{\text{cond}}(\rho)$ intersects $\Delta_2^{\text{cond}}(\rho)$ at ρ_{dyn} as defined in (5.66). The exponential rate of the relocation time of a condensate is given by the minimum of $\Delta_1^{\text{cond}}(\rho)$ and $\Delta_2^{\text{cond}}(\rho)$.

of $(\rho - m^{(1)})$ and the maximum in this part of the system being $m^{(2)}$. Note that,

$$s_{\text{cond}}(m^{(1)}) + s_{\text{cond}}(m^{(2)}) = \begin{cases} -(m^{(1)}+m^{(2)}) \log c_0 & \text{if } m^{(2)} \le m^{(1)} \le a \ , \\ -a \log(\frac{c_0}{c_1}) - m^{(1)} \log c_1 - m^{(2)} \log c_0 & \text{if } m^{(2)} \le a \le m^{(1)} \ , \\ -2a \log(\frac{c_0}{c_1}) - (m^{(1)}+m^{(2)}) \log c_1 & \text{if } a \le m^{(2)} \le m^{(1)} \ . \end{cases} \tag{5.61}$$

So if the background is fluid ($m^{(2)} < a$ or $\rho - m^{(1)} - m^{(2)} < \rho_{\text{trans}}$) then $I_\rho^{(2)}(m^{(1)}, m^{(2)})$ is constant on $m^{(1)} + m^{(2)} = \text{const}$ if $m^{(1)} < a$ or $m^{(2)} > a$. Also $I_\rho^{(2)}(m^{(1)}, m^{(2)})$ is linear on $m^{(1)} + m^{(2)} = \text{const}$ if $m^{(1)} > a$ or $m^{(2)} < a$.

In analogy to Section 4.5 we approximate the two dimensional process $(M_L(\boldsymbol{\eta}(t)), M_L^{(2)}(\boldsymbol{\eta}(t)))$ by a continuous time Markov process $(X_L(t), Y_L(t))$ on S where the transition from state (x, y) to $(x - 1/L, y)$ and $(x, y - 1/L)$ occurs at rate $g(xL)$ and $g(yL)$ respectively. The maximum and second maximum gain particles corresponding to a transition from (x, y) to $(x + 1/L, y)$ and $(x, y + 1/L)$ at a rate fixed by the stationary distribution $\nu_\rho^L[M_L = x, M_L^{(2)} = y]$. This is a two dimensional birth-death process and it is straightforward to show that it is ergodic with unique stationary measure $\pi_\rho^L[M_L = x, M_L^{(2)} = y]$. It follows that the rate at which particles enter the maximum and second maximum is proportional to the stationary current in the background $j_{L-1}^{\text{can}}(\rho - x - y)$. Configurations with $x \le a$ belong to the fluid state, and those for which $x > a$ to the condensed state. In order for the condensate to relocate the two dimensional process must reach the line $x = y$ on the simplex.

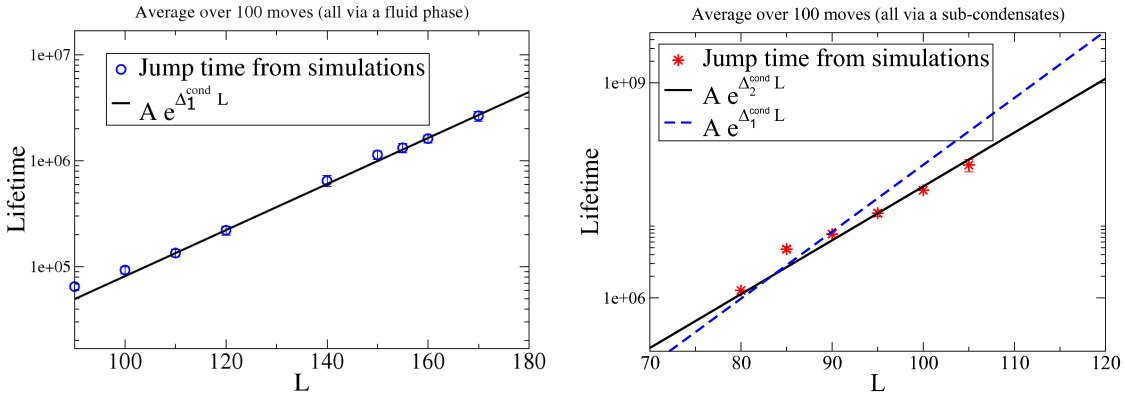

Figure 5.9: Average time for condensate motion as measured in simulations, for a system with $c_0 = 2$, $c_1 = 1$ and $a = 0.25$, symbols show the average relocation time from simulations, sample standard deviation is the size of the symbols. Left: $\rho = 1.75 < \rho_{\text{dyn}}$, the second largest site was always smaller than aL when the condensate moved. Relocation time grows with exponential factor given by Δ_1^{cond} (see (5.65)). Right: $\rho = 2.4 > \rho_{\text{dyn}}$, the second largest site was always larger than aL and the bulk density (outside the maximum and second largest) was on average ρ_c when the condensate moved. Re-location time grows with exponential factor given by Δ_2^{cond} (see (5.65)).

Under these assumptions we can compute any expected hitting times exactly by solving the inhomogeneous Dirichlet problem (see e.g. [15]). Let the generator of the random walk $(X_L(t), Y_L(t))$ be $\mathcal{G}_L$ and denote the hitting times by $\tau_A = \inf\{t \geq 0 \mid (X_L(t), Y_L(t)) \in A\}$. Then we can calculate the hitting times by solving the linear problem,

$$-\mathcal{G}_L w_A(x,y) = \begin{cases} 1 & \text{if } (x,y) \in A^c \ , \\ 0 & \text{if } (x,y) \in A \ , \end{cases} \tag{5.62}$$

where,

$$w_A(x,y) = \begin{cases} \mathbb{E}_{(x,y)}[\tau_A] & \text{if } (x,y) \in A^c \ , \\ 0 & \text{if } (x,y) \in A \ . \end{cases} \tag{5.63}$$

This allows us to calculate an approximation to the metastable exit times T_{fluid}, T_{cond} and T_{move}. By making a saddle point approximation to the resulting sums from (5.62) it is clear that these grow exponentially with L according to,

$$\begin{aligned} \lim_{L\to\infty} \frac{1}{L} \log T_{\text{fluid}} &= \Delta^{\text{fluid}}(\rho) \\ \lim_{L\to\infty} \frac{1}{L} \log T_{\text{cond}} &= \Delta_1^{\text{cond}}(\rho) \\ \lim_{L\to\infty} \frac{1}{L} \log T_{\text{move}} &= \Delta_1^{\text{cond}}(\rho) \wedge \Delta_2^{\text{cond}}(\rho) \end{aligned} \tag{5.64}$$

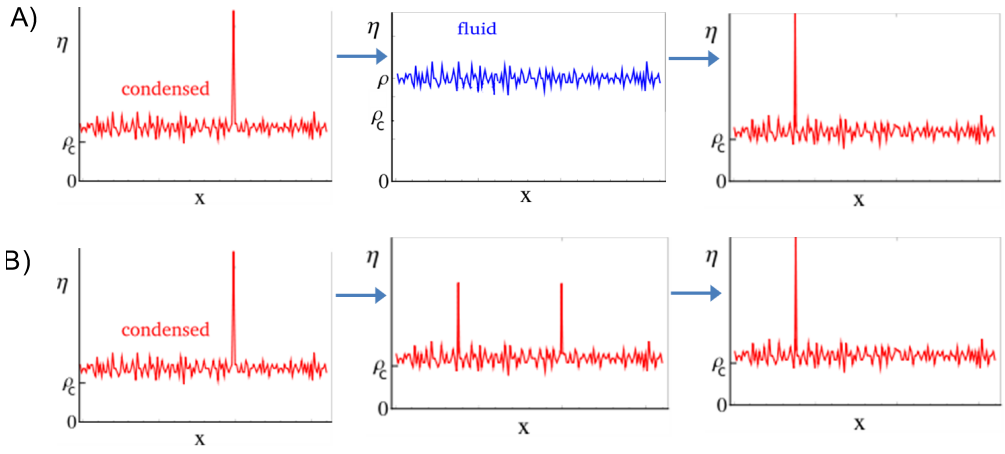

Figure 5.10: Mechanisms of condensate motion. A) For $\rho < \rho_{\text{dyn}}$, the condensate moves by losing particles to the bulk. The average occupation of the remaining sites increases homogeneously until the systems reaches a fluid state. A condensate then reforms on a lattice site chosen uniformly at random independently of the previous location. B) For $\rho > \rho_{\text{dyn}}$ the fluid sate is exponentially less likely than sharing the excess mass between two sub condensates. This becomes the dominating mechanism for condensate re-location. The position of the condensate after it moves is dependent on its initial position.

where,

$$\begin{aligned}
\Delta^{\text{fluid}}(\rho) &= I_\rho(a) - I_\rho(0) \\
&= s_{\text{fluid}}(\rho) - s_{\text{cond}}(a) - s_{\text{fluid}}(\rho - a) \\
\Delta_1^{\text{cond}}(\rho) &= I_\rho(a) - I_\rho(\rho - \rho_c) \\
&= s_{\text{fluid}}(\rho_c) + s_{\text{cond}}(\rho - \rho_c) - s_{\text{cond}}(a) - s_{\text{fluid}}(\rho - a) \\
\Delta_2^{\text{cond}}(\rho) &= I_\rho^{(2)}(\rho - \rho_c - a, a) - I_\rho(\rho - \rho_c) \\
&= s_{\text{cond}}(\rho - \rho_c) - 2s_{\text{cond}}((\rho - \rho_c)/2) \\
&= a \log \frac{c_0}{c_1} \ .
\end{aligned} \tag{5.65}$$

Note that the saddle point at $m^{(1)} = (\rho - \rho_c - a)$, $m^{(2)} = a$ corresponding to Δ_2^{cond} only exists if $\rho > \rho_c + 2a$ and the system can sustain two macroscopically occupied sites. In general, metastable exit times are dominated (exponentially) by the lowest maximum that a continuous path connecting the metastable states has to cross. In the case of condensate motion there are two scenarios for such paths, leading to the minimum in (5.64), which corresponds to choosing the fastest path. For details of the computation restricted to one dimension see Section 4.5.

Since $\Delta_1^{\text{cond}}(\rho)$ is increasing with ρ and $\Delta_2^{\text{cond}}(\rho)$ is constant (see Fig. 5.8), these results imply that there is a dynamic transition at some density ρ_{dyn} defined by,

$$\Delta_1^{\text{cond}}(\rho) \wedge \Delta_2^{\text{cond}}(\rho) = \begin{cases} \Delta_1^{\text{cond}}(\rho) & \text{for } \rho < \rho_{\text{dyn}} \\ \Delta_2^{\text{cond}}(\rho) & \text{for } \rho > \rho_{\text{dyn}} \ . \end{cases} \tag{5.66}$$

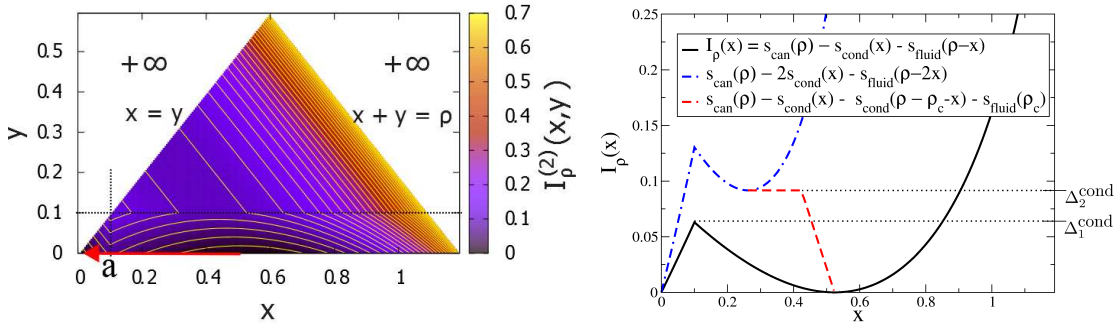

Figure 5.11: Mechanism A for condensate motion for $\rho = \rho_{trans} < \rho_{dyn}$ with parameters $c_0 = 3, c_1 = 1.2$, and $a = 0.1$. Left: Surface plot of the joint rate function $I_\rho^{(2)}$ (5.60), where the red arrow indicates the minimal action path. Right: The projection along the x-axis $I_\rho(x) = I_\rho^{(2)}(x, 0)$ is shown as a full black line, and the dashed blue line denotes the projection along the diagonal $I_\rho^{(2)}(x, x)$. To reach the diagonal, the minimal action path follows the black line in mechanism A. The dashed red line denotes the projection along the most likely path into the local minimum on the diagonal, which is not followed here. $\Delta_1^{cond} < \Delta_2^{cond}$ denote the corresponding exponential costs as given in (5.65).

If $\rho < \rho_{\text{dyn}}$ condensate motion typically occurs by the maximum losing particles to the rest of the system which remains fluid. The second maximum never becomes macroscopically large and the condensate motion occurs via the fluid state (which may be globally stable $\rho < \rho_{\text{trans}}$ or only metastable $\rho > \rho_{\text{trans}}$). We refer to this as motion via *mechanism A*, see Figure 5.10 for a diagrammatic representation. However, if $\rho > \rho_{\text{dyn}}$ then it is exponentially more costly to reach the fluid state than growing a second macroscopically occupied site. In this case the condensate typically moves by giving up particles to another macroscopically occupied site (the second maximum) which are transported by the fluid bulk at ρ_c. This is referred to as *mechanism B*. This dynamic transition is observed in simulations, see Figure 5.9. These are the only two types of condensate motion typically observed on a large system since any other configuration is exponentially more unlikely.

It is also possible to predict the typical trajectories leading to transitions between the states. This scenario is in accordance with the minimal action paths of the Freidlin Wentzell theory explained in Section 2.4. The action for a certain path $\psi : [0, T] \to S$ on the restricted simplex is given by,

$$\frac{1}{2} \int_0^T \left| \dot{\psi}(s) - \nabla I_\rho^{(2)}(\psi(s)) \right| \, \mathrm{d}s \; . \tag{5.67}$$

For $\rho < \rho_{\text{dyn}}$ the minimal action path is along the axis with $M_L^{(2)} = 0$, as shown Fig. 5.11, corresponding to mechanism A. At higher densities, $\rho > \rho_{\text{dyn}}$ the saddle point at $I_\rho^{(2)}(a, 0)$ becomes higher than the one at $I_\rho^{(2)}(\rho - \rho_c - a, a)$, and the minimal action path from the condensed minimum at $((\rho - \rho_c), 0)$ to $x = y$, is shown in Fig. 5.12.

It is possible to calculate the canonical probability distribution over the maximum and second most occupied sites using the methods described in Appendix D.1. This

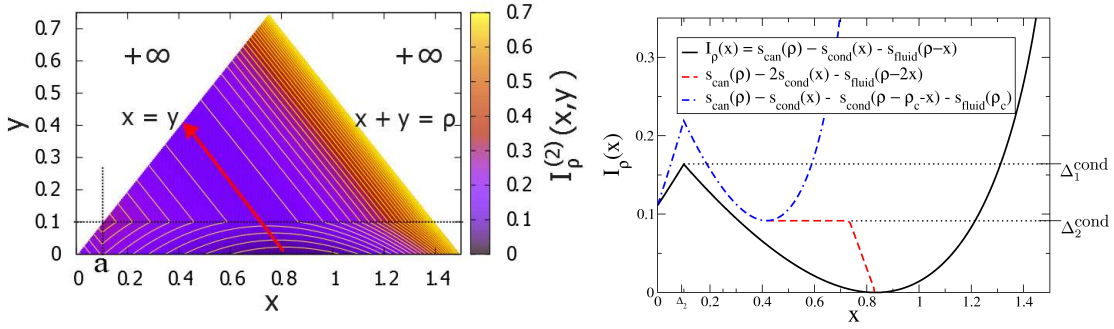

Figure 5.12: Mechanism B for condensate motion for $\rho = 1.5 > \rho_{dyn}$ with parameters $c_0 = 3, c_1 = 1.2$, and $a = 0.1$. Left: Surface plot of the joint rate function $I_\rho^{(2)}$ (5.60), where the red arrow indicates the minimal action path. Right: The projection along the x-axis $I_\rho(x) = I_\rho^{(2)}(x, 0)$ is shown as a full black line, and the dashed blue line denotes the projection along the diagonal $I_\rho^{(2)}(x, x)$. As opposed to Fig. 5.11, the diagonal is now typically reached along the dashed red line since the corresponding costs $\Delta_1^{cond} > \Delta_2^{cond}$ (5.65) have changed order.

allows us to calculate the finite size equivalence of $I_\rho^{(2)}$ exactly for each system size. For a moderate system size of $L = 100$ this is shown in Fig. 5.13. The corresponding minimal paths are also shown.

5.5 Discussion

In this section we have have provided rigorous results on the equivalence of ensembles for a size-dependent zero-range process using the entropy methods of Chapter 3. In particular we observe equivalence between the canonical and grand canonical measure below ρ_c. Grand canonical measures do not exist above the critical density, however we observe that canonical measures are equivalent to restricted grand canonical measures (which converge weakly to 'fluid' measures) in the thermodynamic limit for densities up to ρ_{trans}. The associated pressure and entropy of this fluid measure are given by the analytic extension of the grand canonical versions. Above the transition density we observe a breakdown of the equivalence of ensembles and phase separation. The system separates into a homogeneous background equivalent to the fluid measures at ρ_c and the excess mass accumulates on a single lattice site.

We identify local minima of the large deviation rate function for the maximum site occupation under the canonical measures as metastable states. At densities above the transition density if the system is prepared in a homogeneous state it will remain 'close' to the metastable fluid measures for a length of time growing exponentially with L at rate $\Delta^{\text{fluid}}(\rho)$. At densities below the transition density but above $\rho_c + a$, if the system is prepared in a condensed state with more than aL particles on a single lattice site it will remain in such a state for a length of time also growing exponentially with L at rate $\Delta_1^{\text{cond}}(\rho)$. This is observed in Monte Carlo simulations and a detailed analysis of the metastable behaviour has been given under a Markovian assumption. We associate

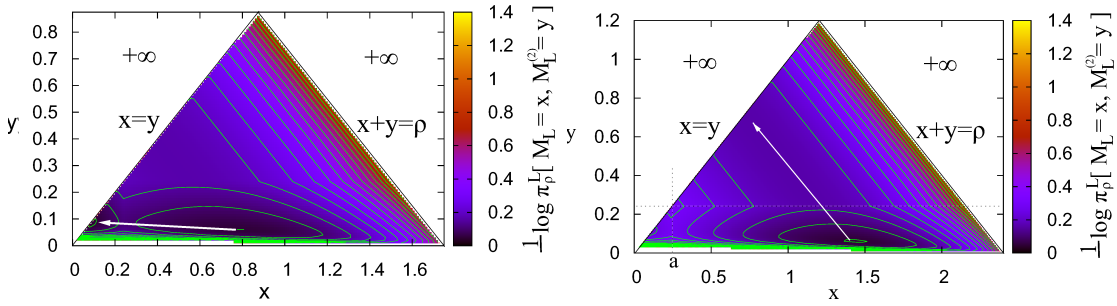

Figure 5.13: Exact numerics on a finite system $L = 100$ with $c_0 = 2$, $c_1 = 1$ and $a = 0.25$. The typical path to realise condensate motion is marked by the white arrow. For the condensate to move the second largest site must contain the same number of particles as the largest site (given by the line $x = y$). Left: $\rho_L = 1.75$. At this density the system is most likely to reach this point by increasing the bulk density, decreasing the maximum whilst the second maximum remains small. Right: $\rho_L = 2.40$. At such a high density it is more likely to reach $x = y$ from the global minimum by following a line for which the density outside of the two largest sites remains at ρ_c (cf. Figures (5.11) and (5.12)) .

appropriately restricted measures with metastable distributions for which we can derive the average current and entropies exactly. These are shown to correspond with the observed metastable branches from Monte Carlo simulations.

It has also been shown that the typical mechanism of condensate motion depends on the total system density ρ. If the total density is low (below ρ_{dyn}) then the condensate typically moves by the system first reaching the fluid state. However, at high total densities (above ρ_{dyn}) the condensate typically moves by growing a second macroscopically occupied site whilst the background remains at ρ_c.

Since the two dimensional random walk describing the maximum and second maximum site occupation is not Markovian, the results on the metastable dynamics are heuristic. Recently, it has been shown rigorously for a reversible condensing zero-range process on a finite lattice as the particle density tends to infinity that the location process of the condensate is asymptotically Markovian and the metastable dynamics have been identified using a potential theoretic approach [8]. An addition challenge here is the increasing number of metastable states in the thermodynamic limit, as well as the different mechanisms of condensate motion. In the cases of reversible dynamics (with nearest neighbour jumps $q(1) = q(-1) = 1/2$) it should also be possible to derive rigorous results on metastability for the model consider in this chapter (for example using the techniques in [16]). This present an interesting avenue for future work. It would also be interesting to extend these results to the non-reversible case, however, there are currently no comparable techniques available for this.

Chapter 6

Condensation in the inclusion process

6.1 Introduction

In this chapter we study an inclusion processes as introduced in Chapter 2.2.3. Recall that particles are subject to nearest neighbour attraction (inclusion), as well as performing independent random walks on the lattice (diffusion). We study a class of inclusion processes with system size-dependent diffusion strength. Depending on the rate of diffusion relative to the rate of attraction, the canonical measures are either equivalent to the grand canonical measures at all densities, or there is non-equivalence of ensembles at all positive densities, signalling a condensation transition. In Sections 6.3 and 6.4 we show that if the rate of diffusion is not too small then there is equivalence of ensembles at all densities. This implies that we can estimate the canonical expected value of bounded observables by the grand canonical expectations. It is also shown from simulations that this holds for the average current, which is actually an unbounded observable. We are also able to show that the canonical measures concentrate on configurations in which no site contains of order L particles. In Sections 6.5 we show that if the rate of diffusion is very small relative to the rate particles attract each other, then there is condensation at all densities. We show that typically, under the canonical measures, all the mass resides on a single lattice site and we have non-equivalence of ensembles. This type of 'complete' condensation has also been studied for zero-range processes with jump rates that vanish as the occupation number tends to infinity [79].

In Chapter 3 we described a general approach to studying equivalence of ensembles, and the large deviations of the maximum, in condensing particle systems, under various assumptions. We showed in Chapters 4 and 5 that these assumptions are satisfied for a wide class of interesting problems. In this chapter we show how the general approach outlined in Chapter 3 can still be applied even when some of the technical assumptions breakdown. If the diffusion rate tends to zero with the system size we find that there is no well defined, suitable reference measure. In particular, in Section 6.4, the regularity assumption on the reference measures (assumption (4) in Section 3.4.1) breaks down.

In Section 6.5 we find that the relevant scale for the large deviations does not satisfy the scale assumption (assumption (5) in Section 3.4.1) required to apply general results from the theory of large deviations.

Recall from Chapter 2.2.3, the dynamics on a finite lattice Λ_L are defined by the generator,

$$\mathcal{L}_L f(\boldsymbol{\eta}) = \sum_{x,y\in\Lambda_L} \eta_x(d_L + \eta_y)p(x,y)\left(f(\boldsymbol{\eta}^{x\to y}) - f(\boldsymbol{\eta})\right) \ , \tag{6.1}$$

where we include explicitly the L dependence on the diffusion rate d_L.

We observe that a condensation transition can occur in the limit of weak diffusion $d_L \to 0$ when the convergence to zero is fast enough. We consider the case of constant diffusion rate in Section 6.3, weak diffusion in Section 6.4 ($1/L \ll d_L \ll 1$), and very weak diffusion (strong attraction) in 6.5 ($d_L \ll 1/L$). We discuss the dynamics of the condensate in Chapter 6.6, with a focus on the totally asymmetric process on a one dimensional lattice with periodic boundary conditions. We are able to describe heuristically the motion of the condensate and how two condensates interact when they get in contact.

6.2 Stationary measures

The focus of this chapter will be on the usual thermodynamic limit, as in Chapter 5, in which the total number of particles in the system N grows linearly with system size L. The relevant order parameter is therefore,

$$S_L(\boldsymbol{\eta}) = \frac{1}{L}\sum_{x\in\Lambda_L} \eta_x \tag{6.2}$$

corresponding to the choice $b_L = L$ in Chapter 3. We will see that if $d_L \to 0$ as $L \to \infty$ then the relevant scale for the large deviations a_L is smaller than L.

6.2.1 Reference measures

For the symmetric case (SIP) stationary product measures were found in [58]. These results were generalised to include homogeneous systems on translation invariant lattices in [70] as discussed in Section 2.2.3. In this Chapter we focus on finite translation invariant lattices Λ_L which are subsets of $\mathbb{Z}^d$ with periodic boundary conditions. We also restrict the dynamics to having homogeneous jump distribution, as in previous Chapters. Then the condition in (2.26) implies that there exist homogeneous product stationary measures. Recall from Section 2.2.3 that in this case the single site weights are given by

$$w_L(n) = \frac{\Gamma(d_L + n)}{n!\Gamma(d_L)} \ . \tag{6.3}$$

and obey the following recursion relation,

$$w_L(n+1) = \frac{d_L + n}{n+1} w(n) \ . \tag{6.4}$$

By applying Stirling's approximation these behave asymptotically, for large n as,

$$w_L(n) \sim d_L n^{d_L - 1} \ , \tag{6.5}$$

which is not normalizable. Thus, we define the stationary reference measures ν^L by products of tilted single site marginals,

$$\nu_L[\eta_x] = \frac{w_L(\eta_x) e^{d_L \mu_0 \eta_x}}{(1 - e^{d_L \mu_0})^{-d_L}} \ , \tag{6.6}$$

for some $\mu_0 < 0$. The normalisation is given by the identity,

$$\sum_{n=0}^{\infty} w_L(n) e^{d_L \mu_0 n} = \left(1 - e^{d_L \mu_0}\right)^{-d_L} \ ,$$

which follows by computing the Taylor expansion of the right hand side. The a-priori tilting of the stationary weight by $d_L \mu_0 < 0$ ensures that they are normalisable and the mean and standard deviation of the density converge. The mean density under the reference measure is give by,

$$\bar{\rho}_L = \nu^L (S_L) = \nu_L (\eta_1) = \frac{d_L e^{d_L \mu_0}}{1 - e^{d_L \mu_0}} \tag{6.7}$$

$$\to \bar{\rho} = -\frac{1}{\mu_0} \quad \text{if } d_L \to 0 \text{ as } L \to \infty \ . \tag{6.8}$$

The variance of the density is given by,

$$\bar{\sigma}_L^2 = \nu_L \left(\eta_1^2\right) - \bar{\rho}_L^2 = \bar{\rho} \left(1 + \frac{\bar{\rho}}{d_L}\right) \tag{6.9}$$

$$\to \infty \quad \text{if } d_L \to 0 \text{ as } L \to \infty \ . \tag{6.10}$$

If the jump distribution is asymmetric, $q(x) \neq q(-x)$, then the reference measures are not reversible and the system can support a non zero stationary current.

6.2.2 Canonical measures

The inclusion process (2.25) clearly conserves the total number of particles and is irreducible on the finite canonical state space,

$$X_\rho^L = \{\boldsymbol{\eta} \in X_L | S_L(\boldsymbol{\eta}) = \rho_L\}$$

and therefore ergodic. The sequence ρ_L is assumed to be of the form (3.18), and the *canonical measures* are given by the conditioned reference measures (see Section 2.2.3

for details),

$$\pi_\rho^L[\boldsymbol{\eta}] = \nu^L[\boldsymbol{\eta}|S_L = \rho_L] = \frac{\nu^L[\boldsymbol{\eta}]\mathbb{1}_{S_L^{-1}(\rho_L)}}{Z(L,\rho_L)} \tag{6.11}$$

The canonical current is defined as the average jump rate off a site (as in previous chapters this is proportional to the true current in the system for non symmetric dynamics and otherwise is proportional to the diffusivity),

$$j_L^{\text{can}}(\rho) = \pi_\rho^L\left(\eta_x \sum_{y\in\Lambda_L}(d_L + \eta_y)q(y-x)\right) \ . \tag{6.12}$$

Since stationary measures conditioned on fixed particle number are no longer product measures this quantity is difficult to calculate.

6.2.3 Grand canonical measures

The grand canonical measures are tilted versions of the reference measure (see Section 3.2.2) which are defined with respect to the scale a_L,

$$\nu_\mu^L[\boldsymbol{\eta}] = \frac{e^{a_L\mu S_L(\boldsymbol{\eta})}\nu^L[\boldsymbol{\eta}]}{\nu^L\left(e^{a_L\mu S_L}\right)} = \prod_{x\in\Lambda_L}\frac{e^{(a_L L^{-1})\mu\eta_x}\nu_L[\eta_x]}{z(\mu)} \tag{6.13}$$

where the single site grand canonical partition function is given by,

$$z_L(\mu) = \nu_L\left(e^{(a_L L^{-1})\mu\eta}\right) = \left(\frac{1-e^{d_L\mu_0}}{1-e^{d_L\mu_0+(a_L L^{-1})\mu}}\right)^{d_L} \tag{6.14}$$

which is finite, and so the grand canonical measures exist, for all $\mu < -\frac{d_L L}{a_L}\mu_0$.

The grand canonical pressure on a finite system is given by,

$$\begin{aligned} p_L(\mu) &= \frac{1}{a_L}\log\nu^L\left(e^{a_L\mu S_L}\right) \\ &= \frac{d_L L}{a_L}\log\nu_L\left(e^{(a_L L^{-1})\mu\eta}\right) \\ &= \frac{d_L L}{a_L}\log\left(\frac{1-e^{d_L\mu_0}}{1-e^{d_L\mu_0+a_L L^{-1}\mu}}\right) \ , \end{aligned} \tag{6.15}$$

The derivative of the pressure (scaled cumulant generating function) at μ is the average density under the grand canonical measure with chemical potential μ,

$$\begin{aligned} R_L(\mu) = \partial_\mu p_L(\mu) &= \nu_\mu^L\left(S_L\right) \\ &= \frac{d_L e^{d_L\mu_0+(a_L L^{-1})\mu}}{1-e^{d_L\mu_0+(a_L L^{-1})\mu}} \ . \end{aligned} \tag{6.16}$$

For each L this is a strictly increasing function of the chemical potential with range $(0,\infty)$. Therefore the grand canonical measures exist for all densities independently of

the choice of scale a_L. With a slight abuse of notation we denote the inverse of R_L by μ_L and so the grand canonical measure on a system of size L and with density ρ is given by $\nu^L_{\mu_L(\rho)}$.

The grand canonical current is simple to calculate due to the sites being independent,

$$j^{\mathrm{gc}}_L(\rho) = \nu^L_{\mu(\rho)} \left(\eta_x \sum_{y \in \Lambda_L} (d_L + \eta_y) q(y-x) \right) = \rho(\rho + d_L) \ . \tag{6.17}$$

So if $d_L \to 0$ the grand canonical current converges to ρ^2.

The asymptotic behaviour of the grand canonical measures as $d_L \to 0$ was studied in [70], where it was shown that the single site marginals obey,

$$\nu_{L,\mu_L(\rho)}[0] = \left(\frac{d_L}{\rho}\right)^{d_L} (1 + o(1)) \to 1 \quad \text{and} \tag{6.18}$$

$$\nu_{L,\mu_L(\rho)}[n] = d_L \left(\frac{d_L}{\rho}\right)^{d_L} \left(1 - \frac{d_L}{\rho}\right)^n n^{d_L - 1}(1 + o(1)) \to 0 \text{ for } n \geq 1 \ . \tag{6.19}$$

This implies,

$$\frac{1}{d_L} \nu_{L,\mu_L(\rho)}[n] \to \frac{1}{n} \quad \text{for } n \geq 1 \ , \tag{6.20}$$

as $L \to \infty$ and $d_L \to 0$. We observe that for small diffusivity, d_L, sites are empty with very high probability and the average density ρ is attained by few sites containing a very large number of particles. It follows from this asymptotic behaviour that for small d_L the single site marginals show an approximate power law decay (n^{-1}) for small n with an exponential cut-off at large n,

$$\nu_{L,\mu_L(\rho)}[n] \simeq d_L \begin{cases} n^{-1} & \text{if } 1 \ll n \ll \rho/d_L \\ \left(1 - \frac{d_L}{\rho}\right)^n n^{d_L - 1} & \text{if } n \gg \rho/d_L \ . \end{cases} \tag{6.21}$$

This behaviour can result in a type of condensation being observed purely in the grand canonical ensemble, for details see [70]. In this chapter we are concerned with a stronger form of condensation that occurs in the canonical ensemble and leads to a breakdown of the equivalence of ensembles.

The equivalence or non-equivalence of ensembles (in the sense of Definition 3.11) can be determined from the relative entropy at the scale a_L,

$$\begin{aligned} \lim_{L \to \infty} \frac{1}{a_L} H(\pi^L_\rho | \nu^L_{\mu_L(\rho_L)}) &= p_L(\mu_L(\rho_L)) - \mu_L(\rho_L)\rho_L - \frac{1}{a_L} \log Z(L, \rho_L) \\ &= (-p^*)(\rho) - s_{\mathrm{can}}(\rho) \quad \text{as } \rho_L \to \rho \text{ according to (3.18)} \ , \end{aligned} \tag{6.22}$$

where the final line follows from Theorem 3.6 (see Section 3.3 for more details). The thermodynamic pressure is $p(\mu) := \lim_{L \to \infty} p_L(\mu)$ and is dependent on the choice of scale a_L.

6.3 Fixed diffusion rate

Firstly we consider the case of fixed diffusion rate $d_L = d$ independent of the system size. In this case there is no condensation transition and we find that there is equivalence of ensemble at all densities.

6.3.1 Determining the relevant scale (a_L)

First we find the relevant scale a_L that describes the large deviations of the density under the reference measure. This is the scale on which the canonical and grand canonical entropy densities are defined. The thermodynamic pressure on scale a_L is given by,

$$\begin{aligned} p(\mu) &= \lim_{L\to\infty} \frac{1}{a_L} \log \nu^L \left(e^{a_L \mu S_L} \right) \\ &= \lim_{L\to\infty} \frac{dL}{a_L} \log \left(\frac{1 - e^{d\mu_0}}{1 - e^{d\mu_0 + a_L L^{-1} \mu}} \right) \end{aligned} \tag{6.23}$$

following (6.15). By applying L'Hôpital's rule we find the relevant scale a_L at which large deviations of the density under the reference measure decay;

Case 1: $a_L \gg L$,

$$p(\mu) = \begin{cases} 0 & \text{if } \mu \leq 0 \\ \infty & \text{if } \mu > 0 \end{cases} \tag{6.24}$$

Case 2: $a_L = L$,

$$p(\mu) = \begin{cases} d \log \left(\frac{1 - e^{d\mu_0}}{1 - e^{d\mu_0 + \mu}} \right) & \text{if } \mu < -d\mu_0 \\ \infty & \text{if } \mu \geq -d\mu_0 \end{cases} \tag{6.25}$$

Case 3: $a_L \ll L$,

$$p(\mu) = \bar{\rho} \mu \tag{6.26}$$

It follows from the Gärtner-Ellis Theorem [34, 35], that large deviations of the density under the reference measure decay on the scale L, this is therefore the correct scale to derive non-trivial results on the equivalence of ensembles from the relative entropy method (c.f. Theorem 3.7). We therefore fix $a_L = L$ for the non size-dependent case.

Now the grand canonical measures as defined in Section 6.2.3 for chemical potentials in $\mu \in \mathcal{D}_p = (-\infty, -d\mu_0)$ are given by,

$$\nu_\mu^L[\boldsymbol{\eta}] = \frac{e^{L\mu S_L(\boldsymbol{\eta})} \nu[\boldsymbol{\eta}]}{\nu^L \left(e^{L\mu S_L} \right)} = \prod_{x \in \Lambda_L} \frac{e^{\mu \eta_x} \nu_L[\eta_x]}{z(\mu)} \tag{6.27}$$

where the single site grand canonical partition function is independent of L and given

by,

$$z(\mu) = \nu_L\left(e^{\mu\eta}\right) = \left(\frac{1 - e^{d\mu_0}}{1 - e^{d\mu_0+\mu}}\right)^d \ . \tag{6.28}$$

The average density under the grand canonical measures is also independent of L for fixed μ and is given by,

$$R(\mu) = \nu_\mu^L\left(S_L\right) = \partial_\mu p(\mu) = \frac{de^{d\mu_0+\mu}}{1 - e^{d\mu_0+\mu}} \tag{6.29}$$

and we denote its inverse by $\mu(\rho)$ (the L index is not required in this case),

$$\mu(\rho) = \log\frac{\rho}{d+\rho} - d\mu_0 \ . \tag{6.30}$$

So the Legendre-Fenchel transform of the grand canonical pressures is,

$$\begin{aligned} p^*(\rho) &= -s_{\text{gcan}}(\rho) = \rho\mu(\rho) - p(\mu(\rho)) \\ &= \rho\left(\log\rho - d\mu_0\right) - (d+\rho)\log\left(d+\rho\right) + d\log\left(\frac{d}{1 - e^{d\mu_0}}\right) \ , \end{aligned} \tag{6.31}$$

which is strictly convex on $(0, \infty)$.

The restricted pressures, see Definition 3.6, are equal to the thermodynamic pressure p on $\mathcal{D}_p$ by Corollary 3.9, so we have $\mathcal{D}_{p_m} = \mathcal{D}_p$ and

$$p_m(\mu) = p(\mu) \quad \text{for all } \mu \in (-\infty, -d\mu_0) \ . \tag{6.32}$$

Therefore the restricted grand canonical measures, see Definition 3.7,

$$\bar{\nu}_{\mu,m}^L[\boldsymbol{\eta}] = \nu_\mu^L[\boldsymbol{\eta}|M_L < m_L] \ , \tag{6.33}$$

exist for all $m \in (0, \infty)$ and $\mu \in \mathcal{D}_p$. Also, by Corollary 3.9, for each restriction m the restricted measures at chemical potential μ converge weakly to the grand canonical measure at μ. This result is intuitively very clear, since the grand canonical single site marginals have exponential tails the maximum of L independent samples from this distribution is of order $\log L$, the grand canonical measures therefore concentrate (exponentially) on configurations with maximum less than $m_L L$.

6.3.2 Equivalence of ensembles

Since the thermodynamic pressure (6.25) is steep at its boundary, $-d\mu_0$, the Legendre-Fenchel transform is strictly convex on the entire domain $(0, \infty)$. Equivalence of ensembles follows immediately from Theorem 3.7.

Proposition 6.1. *The canonical measures conditioned on density ρ_L converge in specific relative entropy, on the scale a_L, to the grand canonical measure with chemical potential chosen to fix the average density,*

$$\lim_{L\to\infty} \frac{1}{L} H(\pi_\rho^L | \nu_{\mu(\rho)}^L) = s_{gcan}(\rho) - s_{can}(\rho) = 0 \quad \textit{for all } \rho > 0 \ . \tag{6.34}$$

So $\pi_\rho^L \overset{L}{\longleftrightarrow} \nu_{\mu(\rho)}^L$, and we have convergence of expected values of bounded cylinder test functions (see Definition 3.11).

Also the canonical current converges to the grand canonical current, given by (6.17),

$$j_L^{\rm can}(\rho_L) \to j^{\rm gc}(\rho) = \rho(\rho + d) \quad \text{as } L \to \infty \text{ and } \rho_L \to \rho \ . \tag{6.35}$$

Note that this does not simply follow from the equivalence, since the current in the inclusion process is an unbounded test function (this is not the case in the zero-range process). The on site occupation numbers are asymptotically independent and distributed according to $\nu_{\mu(\rho)}^L$. Also, by following the comment made after Theorem 3.7, the equivalence result can be strengthened to,

$$\lim_{L\to\infty} \frac{1}{\hat{a}_L} H(\pi_\rho^L | \nu_{\mu(\rho)}^L) = 0 \quad \text{for all } \hat{a}_L \gg \log L \ . \tag{6.36}$$

Although it is not required for finding the large deviations of the density, that give rise to equivalence of ensembles, we may still calculate the large deviations of the maximum. Following Section 3.4.4 the large deviations of the maximum can be expressed in terms of the restricted canonical entropy density and the condensate contribution. The condensed entropy contribution is given by,

$$s_{\rm cond}(m) = \lim_{L\to\infty} \frac{1}{L} \log \nu_L[m_L L] \quad \text{for } m_L \to m \text{ as in (3.41)} \tag{6.37}$$

$$= (d\mu_0) m \ . \tag{6.38}$$

Since the reference measures have exponential tails we observe that the exponential 'cost' of a macroscopic maximum of size m is linear in m. The entropy density of the restricted canonical measures is given by the Legendre-Fenchel transform of the grand canonical pressure, since the restricted pressures are equal to the thermodynamic pressure (6.25), and the Legendre-Fenchel transform of the pressure is strictly convex on its essential domain. That is, by Theorem 3.10, we have

$$s_{\rm can,m}(\rho) = \lim_{L\to\infty} \nu^L[S_L = \rho_L | M_L \le m_L]$$

$$= -p^*(\rho) \ , \tag{6.39}$$

where $p^*(\rho)$ is given explicitly in (6.31). By Applying Theorems 3.7 and 3.10 the large deviations of the joint maximum and density under the reference measure are described

by the rate function,

$$\begin{aligned} I(\rho, m) &= -\left(s_{\text{cond}}(m) + s_{\text{gcan}}(\rho - m)\right) \\ &= p^*(\rho - m) - (d\mu_0)m \ . \end{aligned}$$

Proposition 6.2. *As $\rho_L \to \rho$ and $m_L \to m$, following* (3.18)*and* (3.41)*, the canonical large deviations of the maximum are give by,*

$$\begin{aligned} I_\rho(m) :&= \lim_{L\to\infty} \frac{1}{L}\pi_\rho^L[M_L = m_L] = -s_{gcan}(\rho - m) - s_{cond}(m) + s_{gcan}(\rho) \\ &= p^*(\rho - m) - \mu_0 md - p^*(\rho) \qquad (6.40) \\ &= (\rho - m)\log\left(\frac{\rho - m}{d + \rho - m}\right) - \rho\log\left(\frac{\rho}{d+\rho}\right) + d\log\left(\frac{d+\rho}{d+\rho-m}\right) \ . \qquad (6.41) \end{aligned}$$

We observe that for all densities ρ, this has a unique boundary minimum at $m = 0$ and is strictly increasing on $[0, \rho]$.

6.4 Size-dependent diffusion rate: Fluid regime

In case of $d_L \to 0$ slowly we observe that the situation is qualitatively the same as for d_L constant. However, assumption (4) of Chapter 3 is not satisfied. We present a further calculation that allows us in principle to apply the same results. In this section we consider

$$d_L \to 0 \quad \text{such that} \quad d_L L/\log L \to \infty \ .$$

The mean and variance under the reference measure, Equation (6.6), are given by,

$$\bar{\rho} = \nu^L(\eta_1) \to -\frac{1}{\mu_0} \qquad (6.42)$$

$$\bar{\sigma}_L^2 = \nu^L\left(\eta_1^2\right) - \bar{\rho}^2 \simeq -\frac{1}{\mu_0}\left(1 - \frac{1}{d_L\mu_0}\right) \ . \qquad (6.43)$$

So the second moments grows like $1/d_L$,

$$d_L\nu^L\left(\eta_1^2\right) \to \frac{1}{\mu_0^2} \quad \text{as } L \to \infty \ . \qquad (6.44)$$

6.4.1 Determining the relevant scale (a_L)

Recall the thermodynamic pressure on scale a_L is given by (6.23). By applying L'Hôpital's rule we find the relevant scale a_L at which large deviations of the density under the reference measure decay;
Case 1: $a_L \gg d_L L$,

$$p(\mu) = \begin{cases} 0 & \text{if } \mu \le 0 \\ \infty & \text{if } \mu > 0 \end{cases}$$

Case 2: $a_L = d_L L$,

$$p(\mu) = \begin{cases} -\log(1-\bar{\rho}\mu) & \text{if } \mu < 1/\bar{\rho} \\ \infty & \text{if } \mu \geq 1/\bar{\rho} \end{cases} \tag{6.45}$$

Case 3: $a_L \ll d_L L$,

$$p(\mu) = \bar{\rho}\mu$$

We therefore fix $a_L = d_L L$.

We again define the grand canonical measures at scale a_L for chemical potentials in $\mathcal{D}_p = (-\infty, 1/\bar{\rho})$. Unlike the fixed d_L case the single site marginals are now size-dependent,

$$\nu_\mu^L[\boldsymbol{\eta}] = \frac{e^{d_L L \mu S_L(\boldsymbol{\eta})} \nu^L[\boldsymbol{\eta}]}{\nu^L\left(e^{d_L L \mu S_L}\right)} = \prod_{x \in \Lambda_L} \frac{e^{d_L \mu \eta_x} \nu_L[\eta_x]}{z_L(\mu)} \tag{6.46}$$

where the single site grand canonical partition function is given by,

$$z_L(\mu) = \nu_L\left(e^{d_L \mu \eta}\right) = \left(\frac{1 - e^{d_L \mu_0}}{1 - e^{d_L(\mu_0+\mu)}}\right)^{d_L} . \tag{6.47}$$

The average density under the grand canonical measures is dependent on L for fixed μ, but converges as $L \to \infty$,

$$\begin{aligned} R_L(\mu) = \nu_\mu^L(S_L) = \partial_\mu p_L(\mu) &= \frac{d_L e^{d_L(\mu_0+\mu)}}{1 - e^{d_L(\mu_0+\mu)}} \\ \to R(\mu) = \frac{\bar{\rho}}{1-\bar{\rho}\mu} &= \partial_\mu p(\mu) . \end{aligned} \tag{6.48}$$

This is a strictly increasing function of the chemical potential with range $(0, \infty)$. Therefore the grand canonical measures exist for all densities. Just as in the previous section we will denote the inverse $R^{-1}(\rho)$ by $\mu(\rho)$,

$$\mu(\rho) = \frac{1}{\bar{\rho}} - \frac{1}{\rho} . \tag{6.49}$$

So the Legendre-Fenchel transform of the grand canonical pressures is given by,

$$\begin{aligned} p^*(\rho) = -s_{\text{gcan}}(\rho) &= \rho\mu(\rho) - p(\mu(\rho)) \\ &= \left(\frac{\rho}{\bar{\rho}} - 1\right) + \log\frac{\bar{\rho}}{\rho} , \end{aligned} \tag{6.50}$$

which is strictly convex on $(0, \infty)$.

The restricted pressures, see Definition 3.6, are equal to the thermodynamic pressure p on $\mathcal{D}_p$ by straightforward extension of Corollary 3.9. Since the variance of the reference measure diverges we must consider the restriction $m_L L$ to grow faster than $1/d_L$. So

we have $\mathcal{D}_{p_m} = \mathcal{D}_p$ and

$$p_m(\mu) = p(\mu) \quad \text{for all } \mu \in (-\infty, 1/\bar{\rho}) \ . \tag{6.51}$$

Therefore the restricted grand canonical measures, see Definition 3.7,

$$\bar{\nu}^L_{\mu,m}[\boldsymbol{\eta}] = \nu^L_\mu[\boldsymbol{\eta}|M_L < m_L] \ , \tag{6.52}$$

exist for all $m \in (0, \infty)$ and $\mu \in (-\infty, 1/\bar{\rho})$. Also by Theorem 3.10 for each restriction m the restricted measures at chemical potential μ converge weakly to the grand canonical measure at μ. So for all $m_L \gg 1/(d_L L)$ we have equivalence between the restricted and the unrestricted grand canonical measures.

6.4.2 Equivalence of ensembles

All assumptions of Section 3.4.1 are satisfied except the required regularity of the reference measure (4). We propose two methods so that we may apply the same general results. It is clear that assumptions (1) to (3) are satisfied. Assumption (5) is clear from the choice of scale $a_L = d_L L$,

$$\frac{1}{L d_L} \log L \to 0 \quad \text{since} \quad d_L \gg \log L / L \ .$$

We can compute the condensate entropy contribution from the asymptotic behaviour of the single site reference measure (6.5),

$$\begin{aligned} s_{\text{cond}}(m) &= \lim_{L\to\infty} \frac{1}{d_L L} \log \nu_L[m_L L] \quad \text{for } m_L \to m \text{ as in (3.41)} \\ &= m\mu_0 \ , \end{aligned} \tag{6.53}$$

so assumption (6) is also satisfied. Assumption (7) holds so long as the macroscopic maximum satisfies,

$$m_L \gg \frac{1}{\sqrt{L \log L}} \ , \tag{6.54}$$

since,

$$\frac{L}{a_L (m_L b_L)^2} = \frac{1}{L^2 d_L m_L^2} \ll \frac{1}{L \log L m_L^2} \ .$$

This implies that we can only give an upper bound on the large deviation probability for sequences for which the maximum is smaller than $\sqrt{1/L \log L}$.

The breakdown of assumption (4) is due to the high probability of each site containing *exactly* 0 particles,

$$\nu_L[0] = \left(\frac{d_L}{\bar{\rho}}\right)^{d_L} (1 + o(1)) \to 1 \quad \text{as } d_L \to 0, \text{ and} \tag{6.55}$$

$$(1 - \nu_L[0]) \simeq -d_L \log d_L \ , \tag{6.56}$$

which leads to $Q_L \to 0$ in assumption (4). In fact, it is this behaviour of the single site marginals that actually drives the condensation transition in this model, as we will see in Section 6.5. We outline two methods for dealing with this issue.

The simplest way of avoiding the regularity assumption (4) altogether is to avoid the use of the local limit theorem. This can be done by conditioning the canonical measures on a set of densities with non-empty interior in the thermodynamic limit, known as a *density shell*. This is the approach typically adopted by Lewis et al. [90]. For instance we may define the ϵ shell canonical measures,

$$\pi^L_{\rho,\epsilon}[\boldsymbol{\eta}] = \nu^L[\boldsymbol{\eta} | S_L \in (\rho - \epsilon, \rho + \epsilon)] \ . \tag{6.57}$$

Then the canonical entropy density is given by,

$$s^\epsilon_{\text{can}}(\rho) = \lim_{L\to\infty} \frac{1}{a_L} \log \nu^L[S_L \in (\rho - \epsilon, \rho + \epsilon)] = \sup_{x\in(\rho-\epsilon,\rho+\epsilon)} s_{\text{gcan}}(x) \ , \tag{6.58}$$

which follows directly from the Gärtner-Ellis theorem and continuity of the rate function $-s_{\text{gcan}}(x)$. We may prove this result directly by applying Chebyshev's inequality for the upper bound, and using the Lindberg-Feller central limit theorem for the lower bound (which applies since the variance of the single site density does not grow too fast). Equivalence of ensembles follows immediately from (6.58) and Theorem 6 in [93]. The limit $\epsilon \to 0$ may be taken formerly after the thermodynamic limit. However this is not very natural for applications, for example our canonical simulations are always run from initial conditions with a fixed number of particles.

The second approach is to condition the reference measures on each site containing at least one particle. The conditional measures clearly satisfy assumption (4) since the single site marginals are decreasing for $n > 0$ and $\nu_L[1] \to 0$. For this method we follow a similar contraction as in Section 3.4.4. However, here we contract on the number of empty sites instead of the occupation of the maximum. The number of empty sites in a configuration is given by

$$\mathcal{E}_L(\boldsymbol{\eta}) = \sum_{x\in\Lambda_L} \mathbb{1}_0(\eta_x) \ . \tag{6.59}$$

Then by applying the grand canonical change of measure the canonical normalisation can be written as,

$$\begin{aligned} Z(L,\rho)e^{a_L p^*_L(\rho)} &= \nu^L[S_L = \rho_L]e^{a_L p^*_L(\rho)} = \nu^L_{\mu(\rho)}[S_L = \rho_L] \\ &= \sum_{e_L=0}^{L} \nu^L_{\mu(\rho)}[S_L = \rho_L \mid \mathcal{E}_L = e_L]\nu^L_{\mu(\rho)}[\mathcal{E}_L = e_L] \\ &= \sum_{e_L=0}^{L} \nu^{L-e_L}_{\mu(\rho)}\left[S_{L-e_L} = \frac{\rho_L}{1-e_L/L} \;\middle|\; \mathcal{E}_{L-e_L} = 0\right] \nu^L_{\mu(\rho)}[\mathcal{E}_L = e_L] \ . \end{aligned} \tag{6.60}$$

We may estimate the sum in the same way as in the contraction on the maximum. Then,

$$\nu_{\mu(\rho)}^{L-e_L^*}\left[S_{L-e_L^*}=\frac{\rho_L}{1-e_L^*/L}\;\middle|\;\mathcal{E}_{L-e_L^*}=0\right]\nu_{\mu(\rho)}^{L}[\mathcal{E}_L=e_L^*]\leq Z(L,\rho)e^{a_L p_L^*(\rho)}$$
$$\leq L\nu_{\mu(\rho)}^{L-e_L^*}\left[S_{L-e_L^*}=\frac{\rho_L}{1-e_L^*/L}\;\middle|\;\mathcal{E}_{L-e_L^*}=0\right]\nu_{\mu(\rho)}^{L}[\mathcal{E}_L=e_L^*]\;, \tag{6.61}$$

for some $e_L^*\in\{0,\dots,L\}$ that gives rise to the maximum under the sum. We only need the lower bound in the following, and for that we choose e_L^* to be the integer part of the mean of $\mathcal{E}_L$ which is $\nu_{L,\mu(\rho)}[0]L$. Taking the logarithm in (6.61) and dividing through by the scale a_L the final term tends to zero,

$$0\geq\frac{1}{a_L}\log\nu_{\mu(\rho)}^{L}[\mathcal{E}_L=e_L^*]=\frac{1}{a_L}\log\nu_{\mu(\rho)}^{L}[\mathcal{E}_L=\lfloor\nu_{L,\mu(\rho)}[0]L\rfloor\,]\to 0\;, \tag{6.62}$$

since the variance of each term in the sum $\mathcal{E}_L$ tends to zero,

$$\nu_{L,\mu(\rho)}\left(\left(\mathbb{1}_0-\nu_{L,\mu(\rho)}[0]\right)^2\right)=\nu_{L,\mu(\rho)}[0](1-\nu_{L,\mu(\rho)}[0])\to 0\;.$$

It follows that,

$$\frac{1}{a_L}\log Z(L,\rho_L)+p^*(\rho)\geq\frac{1}{a_L}\log\nu_{\mu(\rho)}^{L-e_L^*}\left[S_{L-e_L^*}=\frac{\rho_L}{1-e_L^*/L}\;\middle|\;\mathcal{E}_{L-e_L^*}=0\right]+o(1)\;. \tag{6.63}$$

The mean of the single site marginals $\nu_{L,\mu(\rho)}[\cdot|\eta_1>0]$ can be approximated by,

$$\nu_{L,\mu(\rho)}\left(\eta_1|\eta_1\geq 1\right)=\frac{\nu_{L,\mu(\rho)}\left(\eta_1\right)}{1-\nu_{L,\mu(\rho)}[0]}\simeq\frac{\rho_L}{1-e_L^*/L}\to\infty\;, \tag{6.64}$$

since $\left(1-\nu_{L,\mu(\rho)}[0]\right)\to 0$. Note that for the distribution conditioned on $\eta_x\geq 1$ assumption (4) of Section 3.4.1 is fulfilled. We therefore conjecture that a local limit theorem similar to that stated in [99] Theorem 1 is still satisfied, and so we obtain the lower bound,

$$\nu_{\mu(\rho)}^{L-e_L^*}\left[S_{L-e_L^*}=\frac{\rho_L}{1-e_L^*/L}\;\middle|\;\mathcal{E}_{L-e_L^*}=0\right]\gtrsim 1/(L-e_L^*)\;.$$

Since we choose $e_L^*=L\nu_{L,\mu(\rho)}[0]$ we have,

$$L-e_L^*=L(1-\nu_{L,\mu(\rho))}[0])\simeq Ld_L\log\frac{1}{d_L}\;,$$

and since $a_L=Ld_L$ we have,

$$0\geq\frac{1}{a_L}\log Z(L,\rho_L)+p^*(\rho)\gtrsim\frac{1}{Ld_L}\log\left(Ld_L\log\frac{1}{d_L}\right)\to 0\;. \tag{6.65}$$

The argument above implies that the results of theorem 3.7 still hold, this is summarised in the following conjecture.

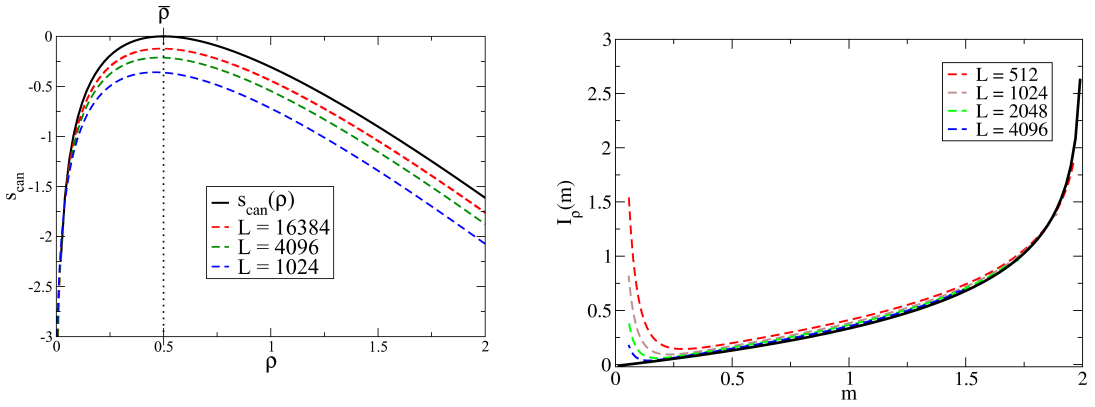

Figure 6.1: Left: The canonical entropy density $s_{\rm can}(\rho) = s_{\rm gcan}(\rho)$ from Conjecture 6.1 shown by the solid black curve. This is strictly concave for all densities. Dashed coloured curves show $\frac{1}{a_L}\log Z(L,\rho)$ on finite systems, converging to $s_{\rm can}$. Right: The large deviations of the maximum are described by $I_\rho(m)$ in (6.68).

Conjecture 6.1. *The grand canonical entropy density is strictly concave on its domain and we have equivalence of ensembles for all densities. We have,*

$$\lim_{L\to\infty}\frac{1}{a_L}H(\pi^L_\rho|\nu^L_{\mu(\rho)}) = s_{gcan}(\rho) - s_{can}(\rho) = 0 \quad \textit{for all } \rho > 0\ , \tag{6.66}$$

which implies $\pi^L_\rho \overset{a_L}{\longleftrightarrow} \nu^L_{\mu(\rho)}$ *in the sense of Definition 3.11, by Lemma 3.3.*

We also observe from simulations that the canonical current converges to the grand canonical current (as given in (6.17)), see Fig 6.2,

$$j^{\rm can}_L(\rho_L) \to j^{\rm gc}(\rho) = \rho^2 \quad \text{as } L\to\infty \text{ and } \rho_L \to \rho\ . \tag{6.67}$$

This calculation, along with (6.51) allows us to calculate the large deviation function for the maximum under the canonical measures (see Fig. 6.1),

$$\begin{aligned} I_\rho(m) &= -(s_{\rm cond}(m) + s_{\rm gcan}(\rho - m)) + s_{\rm gcan}(\rho) \\ &= -\left(m\mu_0 + \log\frac{\rho}{(\rho-m)} + \frac{m}{\bar\rho}\right)\ . \end{aligned} \tag{6.68}$$

As in the case of fixed d_L we observe that the canonical measures concentrate on configurations for which no site contains a macroscopic (order L) number of particles.

6.5 Size-dependent diffusion rate: Condensed regime

In case of $d_L \to 0$ quickly, we observe a breakdown in the equivalence of ensembles and typically all the particles condense on a single lattice site in the thermodynamic limit. We consider $d_L \ll 1/L$, such that

$$d_L = L^{-\gamma} \quad \text{with } \gamma > 1\ . \tag{6.69}$$

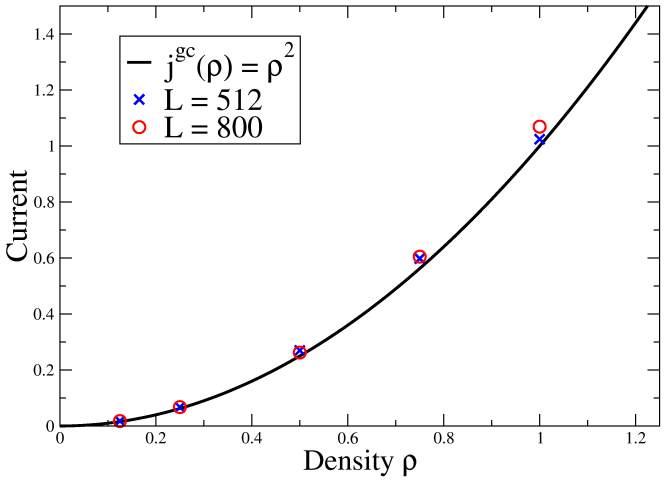

Figure 6.2: The average jump rate of a single site as a function of the system density. The solid curve shows the limiting value of the grand canonical current, $j^{\mathrm{gc}}(\rho)$, given in (6.17). The data points show measurements of the average current from canonical Monte-Carlo simulations, in good agreement with the grand canonical current. The standard error of the measurements are of order of the symbol size.

In this case the relevant scale in the fluid regime, $a_L = d_L L$, does not diverge. It turns out that the relevant scale a_L, that gives rise to non-degenerate entropy densities and the large deviations of the maximum, does not satisfy the scale condition (assumption (5)). This means that combinatorial factors, such as the number distinct configurations that are identical after removing the maximum, also contribute on the scale of the large deviations.

Although the general results of Chapter 3 do not apply we are able to follow the same principles in order to find the canonical and grand canonical entropy densities and described the large deviations of the maximum. The analysis is done by direct computations and the results are supported by exact numerics and canonical simulations.

6.5.1 Determining the relevant scale (a_L)

Firstly we examine the thermodynamic pressure, for scale a_L given by,

$$p(\mu) = \lim_{L\to\infty} \frac{1}{a_L} \log \nu^L \left(e^{a_L \mu S_L}\right) \tag{6.70}$$

$$= \lim_{L\to\infty} \frac{d_L L}{a_L} \log \left(\frac{1 - e^{d_L \mu_0}}{1 - e^{d_L \mu_0 + a_L L^{-1} \mu}} \right) . \tag{6.71}$$

For $d_L \to 0$ faster than $1/L$ there is only one case, we have for all $a_L \to \infty$

$$p(\mu) = \begin{cases} 0 & \text{if } \mu \le 0 \\ \infty & \text{if } \mu > 0 \ , \end{cases} \tag{6.72}$$

since

$$p(\mu) \simeq \frac{d_L L}{a_L} \log \frac{d_L L}{a_L} \frac{\mu_0}{\mu} \quad \text{and} \quad \frac{d_L L}{a_L} \to 0 \text{ as } L \to \infty \ .$$

So the grand canonical entropy density is zero,

$$s_{\text{gcan}}(\rho) = 0 \text{ for } \rho \geq 0 \ . \tag{6.73}$$

Therefore considering the thermodynamic pressure alone is insufficient to find the relevant scale.

We can calculate the scale on which a positive number of particles residing on a single lattice site contributes to the entropy from the asymptotic behaviour of the single site marginals (6.18),

$$s_{\text{cond}}(m) = \lim_{L\to\infty} \frac{1}{a_L} \log \nu_L[m_L L] \quad \text{as } m_L \to m \text{ according to (3.41)} \ . \tag{6.74}$$

Case 1: $a_L \gg \log L$,

$$s_{\text{cond}}(m) = 0 \quad \text{for all } m \geq 0 \tag{6.75}$$

Case 2: $a_L = \log L$,

$$s_{\text{cond}}(m) = \begin{cases} 0 & \text{if } m_L = 0 \ , \quad \text{for all } L \\ -(\gamma + x) & \text{if } m_L = O(L^{x-1}) \ , \ x \in (0,1) \\ -(\gamma + 1) & \text{if } m_L \to m > 0 \end{cases} \tag{6.76}$$

Case 3: $a_L \ll \log L$,

$$s_{\text{cond}}(m) = \begin{cases} 0 & \text{if } m_L = 0 \ , \quad \text{for all } L \\ -\infty & \text{otherwise.} \end{cases} \tag{6.77}$$

We therefore fix $a_L = \log L$, since this is the scale on which any occupied site contributes to the entropy. This clearly does not satisfy the assumptions of chapter 3.

6.5.2 Non-equivalence of ensembles and condensation

To find the canonical entropy density and large deviations of the maximum we follow the same framework as in Chapter 3 doing explicit calculations. Recall from Definition 3.12,

$$\bar{s}_{\text{can}}(\rho) := \limsup_{L\to\infty} \frac{1}{a_L} \log \nu^L[S_L = \rho_L]$$
$$\underline{s}_{\text{can}}(\rho) := \liminf_{L\to\infty} \frac{1}{a_L} \log \nu^L[S_L = \rho_L] \ ,$$

and if the limit exists,

$$s_{\rm can}(\rho) = \lim_{L\to\infty} \frac{1}{a_L} \log \nu^L[S_L = \rho_L] \ .$$

Proposition 6.3. *On the scale $a_L = \log L$ an $b_L = L$ we find, for $\gamma > 1$*

$$-\gamma \leq \underline{s}_{can}(\rho) \leq \bar{s}_{can}(\rho) \leq -\gamma + 1 < 0 = s_{gcan}(\rho) \ , \tag{6.78}$$

for all $\rho > 0$, and so the canonical and grand canonical measures do not converge in specific relative entropy. For $\gamma > 2$ the lower bound is tight,

$$s_{can}(\rho) = \begin{cases} 0 & \text{if } \rho = 0 \\ -\gamma & \text{if } \rho > 0 \ . \end{cases} \tag{6.79}$$

Remark 6.4. The condition $\gamma > 2$ is required for the estimate made in (6.87) and could be improved with finer estimates. We believe, and the numerics suggest, that the same result should hold for all $\gamma > 1$.

Proof. We firstly consider the joint distribution with $a_L = \log L$ and $b_L = L$. There are exactly L states with all the mass is on a single lattice site, $m_L = \rho_L$, so we have directly

$$\begin{aligned} \frac{1}{a_L} \log \nu^L[S_L(\boldsymbol{\eta}) = \rho_L, M_L(\boldsymbol{\eta}) = \rho_L] &= \frac{1}{a_L} \log L + \frac{1}{a_L} \log \nu_L[\rho_L b_L] - \frac{L}{a_L} \log \nu_L[0] \\ &\to 1 - (\gamma + 1) = -\gamma \quad \text{as } L \to \infty \ . \end{aligned} \tag{6.80}$$

Since there is a finite cost, on scale a_L , to place any number of particles greater than zero on another site (see (6.76)) we have for $\rho_L > 0$ and $m_L < \rho_L$,

$$\frac{1}{a_L} \log \nu^{L-1}[S_{L-1} = (\rho_L - m_L), M_{L-1} \leq m_L] \geq \frac{1}{a_L} \log L \nu_L[(\rho_L - m_L)L] \to -\gamma \tag{6.81}$$

$$\frac{1}{a_L} \log \nu^{L-1}[S_{L-1} = (\rho_L - m_L), M_{L-1} \leq m_L] \leq \frac{1}{a_L} \log \nu_L[\eta_1 \geq 1] \to -\gamma \ . \tag{6.82}$$

The lower bound follows by putting all the mass uniformly in the system, and the upper bound follows from putting any mass anywhere in the system, we observe

$$\begin{aligned} \nu_L[\eta_1 \geq 1] = 1 - \nu_L[0] &\simeq -d_L \log d_L \\ &= \gamma L^{-\gamma} \log L \end{aligned}$$

and since $a_L = \log L$ this give rise to (6.82). So the probability of observing a density ρ_L under the reference measures, and a maximum strictly smaller than $\rho_L L$, is small

$$\limsup_{L\to\infty} \frac{1}{a_L} \log \nu^L[S_L(\boldsymbol{\eta}) = \rho_L, M_L(\boldsymbol{\eta}) = m_L] \leq -2\gamma \quad \text{for } m_L < \rho_L \ . \tag{6.83}$$

We are now in a position to derive the asymptotic behaviour of the canonical entropy

density. It follows from these bounds that the upper and lower canonical entropy densities are given by,

$$\begin{aligned}
\bar{s}_{\text{can}}(\rho) &= \limsup_{L\to\infty} \frac{1}{a_L} \log \sum_{m_L} \nu^L[S_L(\boldsymbol{\eta}) = \rho_L, M_L(\boldsymbol{\eta}) = m_L] \\
&\leq \lim_{L\to\infty} \frac{1}{a_L} \log \left(\rho_L L \nu^L[S_L(\boldsymbol{\eta}) = \rho_L, M_L(\boldsymbol{\eta}) = \rho_L]\right) \qquad (6.84) \\
\underline{s}_{\text{can}}(\rho) &= \liminf_{L\to\infty} \frac{1}{a_L} \log \sum_{m_L} \nu^L[S_L(\boldsymbol{\eta}) = \rho_L, M_L(\boldsymbol{\eta}) = m_L] \\
&\geq \lim_{L\to\infty} \frac{1}{a_L} \log \nu^L[S_L(\boldsymbol{\eta}) = \rho_L, M_L(\boldsymbol{\eta}) = \rho_L] \ . \qquad (6.85)
\end{aligned}$$

It follows from the limit in (6.80),

$$-\gamma \leq \underline{s}_{\text{can}}(\rho) \leq \bar{s}_{\text{can}}(\rho) \leq -\gamma + 1 < 0 = s_{\text{gcan}}(\rho) \ , \qquad (6.86)$$

and so we have non-equivalence of ensembles. In this case, also the canonical current *does not* converge to the grand canonical current (see Figure 6.4).

If $\gamma > 2$ we can make more precise estimates of the canonical entropy density and also derive the large deviations of the maximum.

$$\begin{aligned}
&\frac{1}{a_L} \log \nu^L[S_L(\boldsymbol{\eta}) = \rho_L] = \frac{1}{a_L} \log \sum_{m_L} \nu^L[S_L(\boldsymbol{\eta}) = \rho_L, M_L(\boldsymbol{\eta}) = m_L] \\
&\quad = \frac{1}{a_L} \log \nu^L[S_L(\boldsymbol{\eta}) = \rho_L, M_L(\boldsymbol{\eta}) = \rho_L] \\
&\qquad + \frac{1}{a_L} \log \left(1 + \sum_{m_L \neq \rho_L} \frac{\nu^L[S_L(\boldsymbol{\eta}) = \rho_L, M_L(\boldsymbol{\eta}) = m_L]}{\nu^L[S_L(\boldsymbol{\eta}) = \rho_L, M_L(\boldsymbol{\eta}) = \rho_L]}\right) \\
&\quad \lesssim \frac{1}{a_L} \log \nu^L[S_L(\boldsymbol{\eta}) = \rho_L, M_L(\boldsymbol{\eta}) = \rho_L] + \frac{1}{a_L} \log \left(1 + L e^{(-\gamma+1)\log L}\right) \\
&\quad \to -\gamma \quad \text{as } L \to \infty \ , \qquad (6.87)
\end{aligned}$$

since $L^{-\gamma+2} \to 0$. Therefore,

$$s_{\text{can}}(\rho) = \begin{cases} 0 & \text{if } \rho = 0 \\ -\gamma & \text{if } \rho > 0 \end{cases} \ . \qquad (6.88)$$

□

We can use the same method used to derive the canonical entropy density to derive the large deviation behaviour of the maximum. However, since the scale a_L is only logarithmic in the system size we must take care when estimating the probabilities of certain events, since combinatorial effects are also important. The probability that the maximum contains $m_L \geq \rho_L/2$ is dominated by the remaining mass being on a single site, by the same argument that gave rise to the canonical entropy density being dominated by all the mass residing on a single site. However, there are $O\left(L(L-1)\right)$

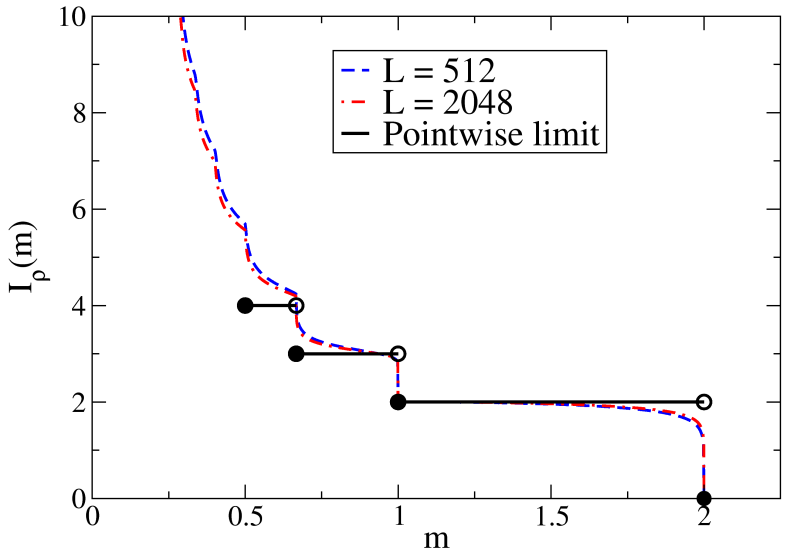

Figure 6.3: The canonical large deviations of the maximum, for $d_L = L^{-2}$ (that is $\gamma = 2$) and $\rho = 2$, as described by $I_\rho(m)$ from Proposition 6.5, shown by the step function in solid black (only shown for $m \geq 0.5$). The dashed lines show $-\frac{1}{a_L} \log \pi_\rho^L[M_L = m]$ on finite systems. We observe point-wise convergence.

such configurations since the maximum can reside on any of the L lattice sites and the remaining mass concentrates on one of the remaining $L-1$ sites. Asymptotically we therefore find,

$$\frac{1}{a_L} \log \nu^L[S_L(\boldsymbol{\eta}) = \rho_L, M_L(\boldsymbol{\eta}) = m_L] \to 2 - 2(\gamma + 1) = -2\gamma \quad \text{for } \rho_L/2 \leq m_L < \rho_L \ . \tag{6.89}$$

The same argument can be applied to $\rho_L/3 \leq m_L \leq \rho_L/2$. Such a large deviation is now dominated by the event that the mass is divided over exactly three sites giving rise to $O(L^3)$ ways of arranging the sites containing particles. There is also an extra combinatorial factor due to the number of ways of arranging the mass outside the maximum between the remaining two sites, again this is of order L. It follows that,

$$\frac{1}{a_L} \log \nu^L[S_L(\boldsymbol{\eta}) = \rho_L, M_L(\boldsymbol{\eta}) = m_L] \to -3\gamma + 1 \quad \text{for } \rho_L/3 \leq m_L < \rho_L/2 \ . \tag{6.90}$$

With care taken over the combinatorial contributions the asymptotic distribution of the maximum on the scale $\log L$ can be found for all $m_L \in (0, \rho_L]$. The calculations are summerised in the following proposition.

Proposition 6.5. *The point-wise large deviations of the maximum under the canonical measure are given by,*

$$I_\rho(m) = -\lim_{L\to\infty} \frac{1}{a_L} \log \pi_\rho^L[M_L = m_L] \tag{6.91}$$

$$= -\lim_{L\to\infty} \frac{1}{a_L} \log \nu^L[S_L(\boldsymbol{\eta}) = \rho_L, M_L(\boldsymbol{\eta}) = m_L] + s_{can}(\rho)$$

$$= \begin{cases} 0 & m = \rho \\ \gamma & \rho/2 \le m < \rho \\ 2\gamma - 1 & \rho/3 \le m < \rho/2 \\ n\gamma - (n-1) & \rho/(n+1) \le m < \rho/n \quad \textit{for } n \in \mathbb{N} \end{cases} \tag{6.92}$$

See Figure 6.3.

Remark 6.6. Since $\gamma > 1$ this result implies that for all $\epsilon > 0$

$$-\lim_{L\to\infty} \frac{1}{a_L} \log \pi_\rho^L[\ M_L \in [0, \rho - \epsilon]\ ] > 0$$

so that the macroscopic maximum site occupation converges in probability to the total density ρ,

$$M_L \xrightarrow{\pi_\rho^L} \rho\ .$$

This is often referred to as complete condensation (for example see [79]).

Although I_ρ is a good rate function (see Definition C.2), this does not give rise to a large deviation principle for the maximum, because the scale a_L is logarithmic in the system size. The discontinuous jumps come from the fact that putting even a single particle on a separate site costs on the scale a_L.

Since the canonical measures concentrate on configurations in which all the mass resides on a single lattice site, and the jump rate out of such a state, $d_L \to 0$ as $L \to \infty$, we expect the canonical current to also tend to zero in the thermodynamic limit. In the grand canonical distribution, on the other hand, the current converges to ρ^2 from (6.17), see Fig. 6.4.

6.6 Dynamics

In this section we apply the previous insights on the stationary measures to give a heuristic analysis of the dynamics of the process. These depend on the geometry, and we focus mostly on one-dimensional nearest neighbour dynamics and finish with some remarks on other geometries.

6.6.1 Totally asymmetric dynamics

We firstly consider the dynamics of the condensate in the totally asymmetric inclusion process on a one dimensional lattice with periodic boundary conditions. If $q(1) = 1$,

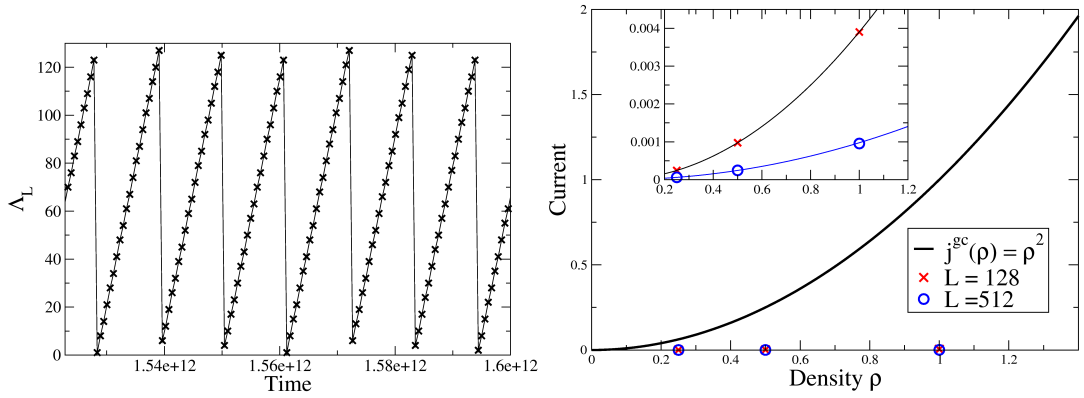

Figure 6.4: Speed of the condensate in the condensed regime $d_L \ll 1/L$ for totally asymmetric dynamics. Left: The position of the condensate on the lattice Λ_L, with $L = 128$ sites and $\rho_L = 1$, as a a function of time. We observe ballistic motion with speed $\rho_L d_L$ L, the vertical jumps are an artefact of the periodic boundary conditions. Right: The average current as a function of the system density. The thick black curve shows the grand canonical current density relation, and the data points show the average canonical current measured in simulations. The inset plot is zoomed in on the canonical currents, and the thin solid lines show the scaling prediction in (6.97). All simulations of the inclusion process were performed using the update algorithm described in Appendix D.2.

and $q(x) = 0$ for x not equal to one, particles can only jump one lattice site to the right at each transition. We recall that the generator (2.25) in this case is given by

$$\mathcal{L}_L f(\boldsymbol{\eta}) = \sum_{x \in \Lambda_L} \eta_x (d_L + \eta_{x+1}) \left(f(\boldsymbol{\eta}^{x \to x+1}) - f(\boldsymbol{\eta}) \right) \ . \tag{6.93}$$

In the following we will show by simple arguments that there is a separation of time scales and the dynamics of condensates are dominated by the time it takes for a single particle to escape the condensate.

Single condensate dynamics

For $\gamma > 2$ we observe that the canonical distribution is dominated by configurations for which the entire mass resides on a single lattice site. Starting from such a configuration, with the condensate residing on site x, the only possible transition is a particle leaving the condensate and moving to site $(x+1) \mod L$, which happens at rate $d_L \rho_L L$ (tending to zero as $L \to \infty$). For simplicity of notation we will omit ' $\mod L$' in the following. After that transition, the single particle could move one space to the right at rate d_L, or the condensate could lose a further particle to site $(x+1)$ at a much faster rate $(\rho_L L - 1)$ (diverging with $L \to \infty$) from the inclusion interaction. In fact, the total time T for all particles to proceed to site $x+1$ is a sum of independent exponential variables

$$T = \sum_{k=1}^{\rho_L L - 1} t_k \ , \quad \text{where} \quad t_k \sim Exp\big((\rho_L L - k)k\big) \tag{6.94}$$

with asymptotic mean given by

$$\mathbb{E}[T] = \sum_{k=1}^{\rho_L L - 1} \frac{1}{(\rho_L L - k)k} \simeq \frac{1}{L} \int_{1/L}^{\rho - 1/L} \frac{1}{x(\rho - x)}\, dx \simeq \frac{2}{\rho L}\, \log(\rho L)\ . \tag{6.95}$$

Due to the quadratic scaling of the inclusion interaction the process speeds up and this vanishes as $L \to \infty$. In contrast, the rate at which any particle escapes form site $x+1$ is bounded above by $d_L \rho_L L \to 0$ with $L \to \infty$. Similar to the above, the standard deviation of T can be shown to scale as $1/L \ll \mathbb{E}[T]$, and therefore the probability that a particle escapes to site $x+1$ during the time the condensate moves is bounded above by

$$\mathbb{P}\big(\tau < T\big) \lesssim d_L \rho_L L \mathbb{E}[T] \sim d_L \log L\ , \quad \text{where} \quad \tau \sim Exp(d_L \rho_L L)\ , \tag{6.96}$$

vanishing for $L \to \infty$ (here τ is a random time that dominates the time a particles takes to exit site $x+1$). So with high probability a single condensate on an otherwise empty lattice moves ballistically with speed $\rho_L d_L\ L$ or, equivalently, on time scale $\tau_L^{move} = 1/(d_L L)$ (see Figure 6.4) with $\rho_L \to \rho > 0$. Combining (6.96) with the rate of motion, we expect that condensates are stable on time scales at least of order $(d_L^2 L \log L)^{-1}$, which are much larger than τ_L^{move}.

We also expect this mechanism to dominate the stationary current, and therefore predict

$$j_L^{\text{can}}(\rho_L) \simeq \rho_L d_L\ L \frac{\rho_L L}{L} \simeq \rho^2 d_L L \to 0 \quad \text{as } L \to \infty \text{ and } \rho_L \to \rho\ , \tag{6.97}$$

which is confirmed by the simulation data in Figure 6.4 Right.

Condensate interaction

We now consider the interaction of two condensates (sites containing of order L particles). We observe that large condensates catch up with smaller ones and then pass them by means of a 'slinky' motion. By the previous argument the speed of the condensate is proportional to the number of particles on the site. Larger condensates therefore tend to 'catch-up' with smaller condensates. We now consider the typical situation of a larger condensate containing N_1 particles behind a smaller condensate containing N_2 particles, such that N_1 and N_2 are both order L. They interact via inclusion when there is a single lattice site between them. The probability of the smaller condensate moving away from the larger one is dominated by the probability that the smaller condensate loses a particle by diffusion before the larger. This occurs with probability $N_2/(N_1 + N_2) < 1/2$. However if the larger condensate loses a particle first (with probability greater than $1/2$) then on a time scale that is much shorter than the diffusion the larger condensate continues to lose particles to the site in-between (following the above arguments). On average the number of particles on the site between the two condensates continues to increase, until the condensate at the back reduces to a similar height as the leading con-

densate. At this point the rate of particles leaving the site between the two condensates and joining the leading condensate becomes greater than the rate of particles exiting the trailing condensate. On average the leading condensate grows until there is again no particles between the two.

The average behaviour described above can be made more precise in terms of a (heuristic) scaling limit. We consider the initial condition $\boldsymbol{\eta}$ where $\eta_1 = x_0 L$, $\eta_3 = y_0 L$ with $x_0 > y_0$ and $\eta_2 = \epsilon L$. Every other site is empty, $\eta_x = 0$ for all $x \in \{4, \dots, L\}$, so the total density is $\rho_L = x_0 + y_0 + \epsilon$. The time evolution of the expected value of the single site occupations can be derived from the generator (6.93) by the forward equation,

$$\begin{aligned}
\frac{\mathrm{d}\mathbb{E}^{\boldsymbol{\eta}}[\eta_1(t)]}{\mathrm{d}t} &= -d_L \mathbb{E}^{\boldsymbol{\eta}}[\eta_1(t)] - \mathbb{E}^{\boldsymbol{\eta}}[\eta_1(t)]\ \mathbb{E}^{\boldsymbol{\eta}}[\eta_2(t)] \\
\frac{\mathrm{d}\mathbb{E}^{\boldsymbol{\eta}}[\eta_2(t)]}{\mathrm{d}t} &= d_L(\mathbb{E}^{\boldsymbol{\eta}}[\eta_1(t)] - \mathbb{E}^{\boldsymbol{\eta}}[\eta_2(t)]) + \mathbb{E}^{\boldsymbol{\eta}}[\eta_1(t)]\ \mathbb{E}^{\boldsymbol{\eta}}[\eta_2(t)] - \mathbb{E}^{\boldsymbol{\eta}}[\eta_2(t)]\ \mathbb{E}^{\boldsymbol{\eta}}[\eta_3(t)] \\
\frac{\mathrm{d}\mathbb{E}^{\boldsymbol{\eta}}[\eta_3(t)]}{\mathrm{d}t} &= d_L(\mathbb{E}^{\boldsymbol{\eta}}[\eta_2(t)] - \mathbb{E}^{\boldsymbol{\eta}}[\eta_3(t)]) + \mathbb{E}^{\boldsymbol{\eta}}[\eta_2(t)]\ \mathbb{E}^{\boldsymbol{\eta}}[\eta_3(t)]\ ,
\end{aligned} \tag{6.98}$$

under the 'mean-field' assumption that the correlation functions factorize (as is the case under the stationary distribution). As before, for any finite time t the probability of observing a diffusive event before time t is equal to $1 - e^{-\alpha \rho_L L t}$ which converges to zero since $d_L \to 0$ faster than $1/L$. We therefore have neglected any terms due to particles escaping site 3. Since the total number of particles is conserved on the three sites under this approximation, we effectively have a two dimensional process that we parametrize by the occupation number of site 1 and site 3 (trailing and leading condensates respectively). We slow down time by $1/L$ and consider the occupation of each site rescaled by $1/L$,

$$x(\hat{t}) = \frac{\mathbb{E}^{\boldsymbol{\eta}}[\eta_1(\hat{t}/L)]}{L}, \quad y(\hat{t}) = \frac{\mathbb{E}^{\boldsymbol{\eta}}[\eta_3(\hat{t}/L)]}{L}, \rho - x(\hat{t}) - y(\hat{t}) = \frac{\mathbb{E}^{\boldsymbol{\eta}}[\eta_3(\hat{t}/L)]}{L}, \quad \text{where } \hat{t} = tL\ . \tag{6.99}$$

In the limit $L \to \infty$ we can derive the following coupled differential equations from (6.98), describing the time dependence of the mean occupation of the two condensates,

$$\frac{\mathrm{d}x}{\mathrm{d}\hat{t}} = -\rho x + x^2 + yx \tag{6.100}$$

$$\frac{\mathrm{d}y}{\mathrm{d}\hat{t}} = \rho y - y^2 - yx \tag{6.101}$$

where $\rho = \lim_{L\to\infty} \rho_L$. For initial conditions x_0 and y_0 such that $(x_0 + y_0) < \rho$ and $2x_0 > \rho$ we can solve these directly (this is done by a change of variables $z_1 = x + y$ and $z_2 = x - y$ followed by a time change $\mathrm{d}s/\,\mathrm{d}t = (z_1 - c)$). We find,

$$x(t) = \frac{1}{2}\left(\rho - D \tanh\left(\frac{Dt}{2} - A\right)\right) \to \frac{\rho - D}{2} \quad \text{as } t \to \infty \tag{6.102}$$

$$y(t) = \frac{2y_0 x_0}{\rho - D\tanh\left(\frac{Dt}{2} - A\right)} \to \frac{2x_0 y_0}{\rho - D} \quad \text{as } t \to \infty \tag{6.103}$$

where $D = \sqrt{\rho^2 - 4x_0y_0}$ and $A = \tanh^{-1}\left(\frac{2x_0-\rho}{D}\right)$. If we take the limit as the initial density on the middle site ϵ tends to zero we find,

$$(x_0 + y_0) \to \rho \quad \text{and} \quad D \to x_0 - y_0 > 0 \; . \tag{6.104}$$

So by taking the limit of small ϵ after $t \to \infty$ we find that the average number of particles on the first site is proportional to y_0 and the average number of particles on the 3rd site is proportional to x_0. This implies that the condensates exchange positions with, on average, no net transfer of mass between them. So instead of the large condensate absorbing the smaller one (as one might have expected a priori), the condensates penetrate each other. This mechanism is very particular for totally asymmetric dynamics and has first been observed for the models studied in [125] in a slightly different scaling limit.

The state in which all particles reside on a single lattice site is effectively absorbing since condensates divide only with very small probability (cf. (6.96)). So, by random fluctuations, a coarsening process takes place until only a single condensate resides on the lattice.

Coarsening dynamics

We now derive the expected time scale for this coarsening process. Consider two macroscopic condensates on the lattice, which move at relative speed of order $d_L L$, since both move at speed of this order. So the average time between two encounters is of order $L/(d_L L) \sim 1/d_L$. In order for one of them to be absorbed by the other it has to gain of order L particles. According to the above argument, particle exchanges during a single encounter of condensates are unbiased and expected to be of order $\sqrt{L}$ in size. Therefore, of order L encounters of the condensates are necessary until only one of them is left or a macroscopic fraction of mass has moved from one to the other. Thus the coarsening dynamics are expected to run on the time-scale $\tau_L^{coars} = L/d_L$, which is much larger than the typical time-scale of motion of a condensate $\tau_L^{move} = 1/(d_L L)$. This is in contrast to the zero-range process defined in (4.1), where the condensate motion is on a slower time scale than the coarsening (see [59] and references therein). In that model the coarsening is driven by particle exchange via the bulk of the system and the condensate sites remain fixed. This is not possible in the inclusion process, since the bulk is essentially empty with vanishing particle current, and the coarsening is driven by condensate motion instead.

Starting from a homogeneous initial distribution ν_0 where the $\eta_x(0)$ are iidrv's with mean ρ_L (e.g. Poisson distributed), we expect that due to the fast inclusion interaction initially condensates form quickly. The equilibration dynamics is then dominated by coarsening on the time scale τ_L^{coars}, and we therefore expect a scaling behaviour of relevant observables. For example, for the variance $\sigma_L^2(t) = \mathbb{E}^{\nu_0}\left[\eta_x^2(t)\right]$ we expect for

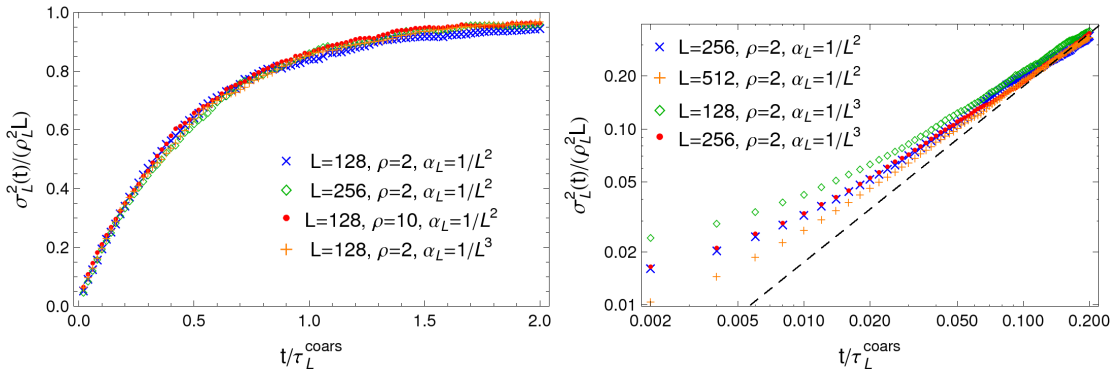

Figure 6.5: Left: Data collapse for the variance $\sigma_L^2(t)$ using the scaling relation given in (6.105). We observe a good data collapse for the range of parameters investigated. Right: Double logarithmic plot of the data collapse in the coarsening regime, $\sigma_L^2/(\rho_L^2 L) < 2/3$. The dashed line shows a power law with exponent -1 for reference.

large L

$$\sigma_L^2(t) \simeq \rho_L^2 L \; f(t/\tau_L^{coars}) \; , \tag{6.105}$$

with a scaling function f such that $f(0) = 0$ and $f(x) \to 1$ as $x \to \infty$. This behaviour is confirmed by the data collapse for different system sizes in Figure 6.5 (left). It remains an interesting question to determine the actual form of the scaling function. Note that in the case of two large condensates that share the total mass in a uniform way, the expected value of the observable is $\sigma_L^2/(\rho_L^2 L) = 2/3$. When only two clusters are left, the system is clearly already in a saturation regime. The system is therefore only in the coarsening regime whilst $\sigma_L^2/(\rho_L^2 L) < 2/3$, so we would only expect the function f to show a power-law scaling behaviour, in this regime. A double logarithmic plot in Figure 6.5 (right) does not give conclusive evidence, and the question whether or not there is a window with asymptotic power law behaviour and what is the underlying mechanism remains open and will be addressed in future studies.

Stability of the condensates on the coarsening time scale is vital for the above arguments to hold. Following (6.96), we have argued that condensates are stable on time scales of order $(d_L^2 L \log L)^{-1}$, which is much larger than τ_L^{coars} as long as $d_L \ll 1/(L^2 \log L)$ which is the case for $\gamma > 2$.

6.6.2 Symmetric and general dynamics

If the process is not totally asymmetric condensates do not necessarily perform the same ballistic motion and the analysis becomes more complicated. However, under more restrictive assumptions on d_L one can still establish a separation of time scales and show that the dynamics is governed by motion of stable condensates. In the following we focus on symmetric nearest neighbour dynamics in one dimension, i.e. $q(1) = q(-1) = 1/2$, and comment on other geometries later.

Symmetric dynamics

Firstly, consider again the stationary situation, i.e. a configuration with all the $\rho_L L$ particles on a single site, x. The first particle moves again with rate $d_L \rho_L L$, now either to $y = x + 1$ or $x - 1$. Now the effective dynamics between the two sites can be described by a symmetric random walk $\eta_y(t)$ with state space $\{0, 1, \ldots, \rho_L L\}$ with state dependent rates $(\rho_L L - k)k$, $k \geq 1$ as before. The walk starts an excursion from state 0 with vanishing rate $d_L \rho_L L$, and if the excursion first reaches the other boundary at $\rho_L L$ then the condensate has moved to y. The time T this takes is given by the first passage time for the right boundary, which can be derived by standard methods similar to the above arguments (c.f. formula given in (4.82)) to have expected value

$$\mathbb{E}[T] \simeq \frac{1}{\rho} \log(\rho L) \sim \log L \ . \tag{6.106}$$

So with $d_L \sim L^\gamma$, $\gamma > 2$, this is still much faster than the typical escape time of any particle to a third site, and we have a separation of time scales as in the asymmetric case. In case the excursion of $\eta_y(t)$ ends at 0 it is even quicker on average, and the condensate has not moved. Since the walk is symmetric, the probability of an excursion leading to an actual motion of the condensate to y is $1/L$. So the number of excursions until condensate motion is a geometric random variable with success rate $1/L$, which is known to scale to an exponential random variable in the limit $L \to \infty$. So for large L we expect the stationary condensate to be stable, and to perform itself a symmetric, continuous-time random walk on the lattice with rate $d_L \rho_L$, i.e. the time scale of motion is now $\tau_L^{move} = 1/d_L$, a factor of L slower than before.

To understand the coarsening dynamics, consider again two condensates. As in the asymmetric case, they start exchanging mass if they are separated by one site, say site 2 as in the previous notation. By the special form of the jump rates the marginal process on site 2 has exactly the same law as $\eta_y(t)$ above. In particular, an excursion (a period of $\eta_2(t) > 0$) takes expected time (6.106) and is much faster than periods of no interaction with $\eta_2 = 0$. Following from the above arguments using symmetry, with probability of order $1/L$ an interaction period or excursion consists of order L^2 transitions (larger than in the asymmetric case), and thus leads to an exchange of a macroscopic number of particles which is unbiased. One possible outcome now is also that both condensates actually merge on site 2. As in the asymmeric case the coarsening dynamics is effectively limited by condensate motion, and we need of order L interactions to see a macroscopic change in configuration numbers. However, the time until two condensates meet on the lattice now scales like $L^2 \tau_L^{move} = L^2/d_L$ since they perform unbiased random walks, and in total we end up with the prediction $\tau_L^{coars} = L^2/d_L$ which is a factor of L^2 slower than the totally asymmetric case. This relation is different to what has been observed for zero-range processes [59], but note that the interaction mechanisms here are very different as explained above.

The time scale for the stability of condensates is the same as before, $(\alpha_L^2 L \log L)^{-1}$, and therefore our predictions should hold as long as $\alpha_L \ll 1/(L^4 \log L)$ which would

require $\gamma > 4$. However, simulation times in such systems are very high and not feasible, and we do not have good numerical data available at the moment to corroborate our results.

Remarks on other geometries

On a complete graph, i.e. $q(x) = 1/(L-1)$ for all $x \neq 0$, the dynamics will be entirely dominated by the inclusion interaction and the picture is very different and, in fact, much simpler. The rescaled occupation numbers $\frac{1}{\rho_L L}\big(\eta_1(t), \dots, \eta_L(t)\big)$ approximate a Wright-Fisher diffusion (see e.g. [77]) on the $(L-1)$-dimensional unit simplex with very small mutation rate α_L. To derive the relaxation time we ignore α_L for the moment. Analogous to above arguments, by the special quadratic form of the jump rates (2.25), the marginal process $\eta_y(t)$ on a given site y is itself a symmetric random walk on $\{0, \dots, \rho_L L\}$ with state dependent rate $k\big(\rho_L L - k\big)$ and absorbing boundaries. By conservation of mass these processes are of course coupled, and by total connectivity the full process $\boldsymbol{\eta}(t)$ has L absorbing states, where all the mass is condensed on a single site. Say the time evolution leads to condensation of mass on site y, then the process $\eta_y(t)$ is a random walk with above rates conditioned on reaching the boundary $\rho_L L$. If initial occupation numbers on all sites are of order 1 (homogeneous initial conditions), from the above calculations for the symmetric case (6.106) we know that the expected time to reach that boundary is of order $\log L$. Since on that time scale typically no diffusion event with rate α_L occurred, this is also the relaxation time of the full system. The stationary dynamics of the condensate is then again limited by diffusion, and given by a random walk with rate α_L on the complete graph.

We have discussed in some detail three extreme cases of geometries, which exhibit quite different features. Intermediate geometries, such as general networks or partially asymmetric dynamics on regular lattices, will have to be treated on a case by case basis with a combination of the above arguments.

6.7 Discussion

The symmetric inclusion process with two sites can in fact be interpreted as a Moran model, which describes the time evolution of two competing genotypes in a fixed population [101]. The inclusion interaction corresponds to competition due to reproduction and the diffusion corresponds to mutation, which naturally happens at a small rate in many applications. With more than two sites, the inclusion process can therefore be interpreted as a multi-type Moran model. For a review of the Moran process and recent applications see [13]. From a theoretical perspective, scaling limits of Moran type models lead to Wright-Fisher diffusions, which have also attracted a lot of recent research interest (see e.g. [77] and references therein). Most results up to now focus on two genotype models (corresponding to only two lattice sites), and the analysis of the symmetric inclusion process could lead to interesting generalizations for many species which are of great interest (see e.g. [121]).

There is much scope for a more detailed understanding of the equilibration dynamics. In particular if the jump process is not totally asymmetric. It would also be interesting to study the case $d_L \sim 1/L$, which is not covered by our analysis. It is expected that in this case one typically observes hierarchically structured configurations and it may be possible to compute scaling solutions for the full time evolution [70]. The use of known self-duality relations for the inclusion process [58] can be useful in a rigorous study of the dynamics.

We have shown that depending on the rate of diffusion d_L the inclusion process is either fluid or condensed at all densities in the thermodynamic limit. If d_L tends to zero fast enough we observe complete condensation, whereby, typically all the mass concentrates on a single lattice site in the thermodynamic limit. In case of an asymmetric jump process the condensate performs ballistic motion on the lattice. If the jump process is symmetric the condensate would diffuse on the lattice although this case has not yet been studied in detail. For $d_L \ll 1/L$ we have shown how two condensates interact, on a finite system, in terms of the time evolution of the average on site occupation (on the macroscopic scale). It would also be interesting to study the fluctuations in this simple interaction. This argument holds for the totally asymmetric jump process only, a natural extension would be to partial asymmetry. For the case of symmetric jump distribution the process is reversible and techniques from potential theory could be applied. Studies of this nature could help to understand the coarsening dynamics from an initially uniform configuration in much more detail than presented here. In the reversible case such results could be applied to a deeper understanding of the Brownian Energy and Brownian momentum processes due to the duality with the inclusion process [57, 58, 70]. This is an interacting diffusion process with continuous local state space, but otherwise behaves very similarly to the inclusion process.

If $d_L \gg 1/L$ there is equivalence of ensembles at all densities, however a large fraction of the sites are empty. The proportion of empty sites in any finite window, in the fluid regime, is asymptotically the same as under the grand canonical measures. However, the proportion of empty sites on the entire lattice can not be represented in terms of a bounded cylinder test function, and its asymptotic behaviour is not covered by the equivalence of ensembles. There is also much scope for studying the distribution of the maximum in the fluid regime.

Chapter 7

Conclusion and outlook

In this Chapter we summarise the main findings of the thesis, and give a brief outlook of future research. We aim to supplement the conclusions and outlook provided at the end of each chapter by giving a more general perspective.

In this thesis we considered several stochastic models that exhibit jamming and condensation transitions. In particular we focused on models that are ergodic on finite systems and exhibit stationary measures that are of a product form. The canonical stationary measures, that describe the long time behaviour of the system starting from arbitrary initial conditions on a finite lattice, are not of product form due to the restriction to a fixed number of particles. We generalised previous rigorous results on the equivalence of ensembles for such systems in the context of large deviation and entropy methods. These results are sufficient to characterise the expected value of a wide and important class of observables in the thermodynamic limit, as the system size tends to infinity, in terms of the much simpler product grand canonical measures. These methods were also shown to give rise to rigorous results on the large deviations of the maximum site occupation. The maximum site occupation is an important observable in condensing systems, since it carries a finite fraction of the total mass in the thermodynamic limit. However, it is not typically covered by the standard equivalence of ensembles results. As well as giving rigorous results on the stationary distribution of the maximum site occupation, we also provided a detailed non-rigorous analysis of the dynamics of the condensate, based on the saddle point structure of the relevant large deviation rate functions.

In Chapter 3 we introduced the main techniques and presented some general rigorous results that are used throughout the thesis. These results rely on tools from the theory of large deviations and local limit theorems for triangular arrays. These entropy methods significantly generalise those used to first give rigorous results on the equivalence of ensembles in zero-range condensation [69]. This work is similar to the large deviations approach and thermodynamic formalism pioneered by Lewis and Pfister [91]. The novelties in Chapter 3, compared to this previous work, were that here the local state space is non-compact, the canonical measures are conditioned on a single value of the density rather than a 'shell', and we may calculate the canonical entropy density in the

non-concave region by contracting on the most occupied sites. This lead to a complete description of the equivalence of ensembles and the breakdown of equivalence between the canonical and grand canonical measures. We observed that, for high densities, if the canonical measures do not converge to any grand canonical measure they may still converge to some truncated version of the grand canonical measure that belongs to the restricted ensemble. All the results in this chapter were presented for a general choice of the large deviation scale and density scale (called (a_L) and (b_L) respectively).

In Chapter 4 we demonstrated how we may exploit the generality of the scales used in Chapter 3 to study the leading order finite-size effects in a condensing zero-range process around the critical point. It was shown that the homogeneous fluid states continue to exist above the critical point, and at the transition point both the bulk density and average current are discontinuous. Close to the transition point the system exhibits metastable switching between the fluid and condensed states. The fluid extension was characterised in terms of truncated grand canonical measures under which it is possible to calculate the leading order correction to bounded observables, that depend on only finitely many lattice sites, such as the average current. The metastable branches of these observables were calculated exactly. We observed two threshold densities, above the first threshold the metastable condensed branch exists, before becoming stable at the second threshold. After the condensed branch becomes stable the fluid branch, which exists for all densities, becomes metastable and can be characterised by the analytic extension of relevant thermodynamic functions such as the the pressure. Before the transition, the excess density of mass in the system above the critical density is typically distributed homogeneously across the lattice. At the transition point the fraction of the excess distributed in the bulk abruptly decreases, and is absorbed by a single lattice site; as the excess mass continuous to increase, a greater fraction of the excess typically resides on this one condensate. The dynamics of the metastable switching between fluid and condensed states were analysed under a random walk approximation. The random walk was constructed in such a way that its stationary distribution is exactly the stationary distribution of the maximum site occupation.

In Chapter 5 we considered a zero-range process for which the jump rates depend on the system size. The jump rates were chosen to stabilise the metastable effects, observed in Chapter 4, in the standard thermodynamic limit, whilst keeping calculations simple. This allowed us to study in more detail the phenomenology of the previous Chapter. In particular, we gave a much more detailed study of the metastable switching, and dynamics of the condensate. It was found that there is a dynamic transition at density ρ_{dyn}, above the transition density, at which the typical mechanism of condensate motion changes. Below ρ_{dyn} the condensate typical moves by the system first reaching the fluid state, and then regrowing a condensate on a uniformly chosen site. Above ρ_{dyn} the condensate typical moves by loosing particles that are transported through the fluid bulk to a second sub-condensate which grows until it dominates the previous condensate. In this case the location of the new condensate depends on the previous position. There is a completely analogous transition in the non size-dependent system, in the finite size

scaling limit of Chapter 4; however, in this case the calculations required to prove that such a transition occurs are more lengthy, and were not presented.

In Chapter 6 we studied a recently introduce stochastic particle system known as the inclusion process. This system also exhibits a condensation transition, but the origin is different from that in the zero-range process. For this process some of the technical assumptions of Chapter 3 do not hold. The same approach can still be applied in the fluid regime. In the condensed regime the general results of Chapter 3 no longer apply directly; however, the same principles may still be applied via direct calculations. It was found that the dynamics of the condensate are very different compared to the zero-range process. Here, the analysis of the condensate motion is, in many ways, simpler due to a strong separation of time scales. A detailed heuristic analysis of the condensate motion was given for the totally asymmetric dynamics. The symmetric case is more complicated, and offers an opportunity for future research.

Several interesting and important open questions follow directly from the work in this thesis. Under natural restrictions on the dynamics it should be possible to extend the methods of Chapter 3 to systems with continuous mass (local state space $\mathbb{R}_+$). However this would offer little new insight whilst requiring significantly more technical details for the proofs. Another natural extension of the content of Chapter 3 would be to non-product measures. A reasonable starting point for research in this direction would be to attempt a similar analysis for systems that exhibit pair factorised stationary measures [126]. The analysis of the metastability and condensate motion has shed new light on dynamical aspects of these processes, and it poses a significant challenge in a currently very active area of applied probability research to give rigorous proofs of such results. It would also be interesting to further explore potential applications of this work, for example the zero-range process as a traffic model (on roads or other networks), or the inclusion process as a simple model for evolutionary dynamics in biological systems.

Appendix A

Relative entropy

In the following we summarize some properties of the relative entropy which are used in the thesis. Proofs and more detailed information can be found in [31, 129], [86] Appendix 1.8 or, [32] Chapter I.3.

Definition A.1. For two arbitrary probability measures π and ν on a state space $\mathcal{X}$ the *relative entropy* is given by,

$$H(\pi \mid \nu) = \begin{cases} \int_{\mathcal{X}} \log \frac{\mathrm{d}\pi}{\mathrm{d}\nu}(w)\pi[\,\mathrm{d}w] & \pi \ll \nu, \\ +\infty & \text{otherwise.} \end{cases} \tag{A.1}$$

For countable state space $\mathcal{X}$, if $\pi \ll \nu$, we may write

$$H(\pi \mid \nu) = \sum_{w \in \Omega} \pi[w] \log \frac{\pi[w]}{\nu[w]} \ .$$

Here $\pi \ll \nu$ means that π is absolutely continuous with respect to ν ($\nu[A] = 0 \Rightarrow \pi[A] = 0$).

The relative entropy is positive,

$$H(\pi \mid \nu) \geq 0, \quad H(\pi \mid \nu) = 0 \Leftrightarrow \pi[x] = \nu[x] \text{ for all } x \in \mathcal{X} \ .$$

The relative entropy is sub-additive, that is if the measures π, ν have marginals π_1,π_2 and ν_1,ν_2 respectively, on subspaces $X_1, X_2 \subset X$ with $X_1 \cap X_2 = \emptyset$, then

$$H(\pi \mid \nu) \geq H(\pi_1 \mid \nu_1) + H(\pi_2 \mid \nu_2) \ . \tag{A.2}$$

The relative entropy can be written in terms of a Legendre-Fenchel transform (c.f. Appendix C),

$$H(\pi \mid \nu) = \sup_{C^b(\mathcal{X},\mathbb{R})} \{\pi\,(f) - \log \nu\left(e^f\right)\}$$

where $C^b(\mathcal{X}, \mathbb{R})$ denotes bounded continuous functions from $\mathcal{X} \to \mathbb{R}$. A direct conse-

quence of this variational form is the entropy inequality,

$$\pi\left(f\right) \leq \frac{1}{\alpha}\left(\log \nu\left(e^{\alpha f}\right) + H(\pi \mid \nu)\right) \ ,$$

for all $\alpha > 0$. This can be used to estimate the expected value of functions under the measure π in terms of the exponential moments of the measure ν.

For relating convergence in specific relative entropy to convergence in expectation of bounded cylinder functions we use the Kemperman-Pinsker inequality,

$$2H(\pi \mid \nu) \geq \|\pi - \nu\|_{T.V.}^2, \tag{A.3}$$

where $\|\cdot\|_{T.V.}$ is the total variation norm,

$$\|\pi - \nu\|_{T.V.} = \sup_{A \in \mathcal{B}} \left|\pi\left[A\right] - \nu\left[A\right]\right| \ . \tag{A.4}$$

If the state space $\mathcal{X}$ is countable then the total variation distance can be expressed as,

$$\|\pi - \nu\|_{T.V.} = \frac{1}{2}\sum_{x \in \mathcal{X}} \left|\pi\left[x\right] - \nu\left[x\right]\right| \ .$$

Appendix B

Local limit theorems

In the following we state relevant limit theorems for triangular arrays that are used to derive the general results in Chapter 3. Details and a proof of the central limit theorem can be found in, for example, [39]. The local limit theorems can be found in [33] and [99]. More precise large deviation estimates for the sum of i.i.d random variables (not triangular arrays) relevant for the non size-dependent condensing zero-range process are given in a series of papers by Nagaev [103, 104, 105].

Throughout we fix the following notation. For each n, let $\xi_{i,n}$, $1 \leq i \leq n$, be independent random variables with law $P_{i,n}$. Note that for application in Chapter 3 for each fixed system sizes the site occupations are identically distributed under the reference measure, analogously $P_{i,n} = P_n$ independent of i.

Theorem B.1 (The Lindeberg-Feller central limit theorem)**.** *Suppose* $\mathbb{E}[\xi_{i,n}] = 0$*, and*

(i) $\sum_{i=1}^{n} \mathbb{E}[\xi_{i,n}^2] \to 1$ *as* $n \to \infty$*.*

(ii) For all $\epsilon > 0$*,* $\sum_{i=1}^{n} \mathbb{E}\left[|\xi_{i,n}|^2 \mathbb{1}_{|X_{i,n}|>\epsilon}\right] \to 0$ *as* $n \to \infty$*.*

Then $\sum_{i=1}^{n} \xi_{i,n}$ *converges in distribution to the standard normal as* $n \to \infty$*.*

We now restrict ourselves to considering lattice distributions. For constant lattice spacing $h > 0$ and shift b, $P_{i,n}[\xi_{i,n} \in b + h\mathbb{Z}] = 1$, where $b + h\mathbb{Z} = \{b + hz : z \in \mathbb{Z}\}$. The largest h for which this holds is called the *span* of the distribution. For any given span h the transformation,

$$\xi'_{i,n} = \frac{\xi_{i,n} - a}{h} \ ,$$

allows us to reduce the general case to the case in which the span is equal to one, while the shift is equal to zero. It is therefore sufficient to state the following results in terms of integer valued random variables. From now on we assume $P_{i,n}$ has support on $\mathbb{Z}$.

The Bernoulli part decomposition of the random variables $\xi_{i,n}$ is expressed in terms of,

$$q(P_{i,n}) = \sum_{k} \left(P_{i,n}[k] \wedge P_{i,n}[k+1]\right) \ .$$

Define,

$$Q_n = \sum_{i=1}^{n} q(P_{i,n}) \ .$$

Theorem B.2. *Let $Z_n = \sum_{i=1}^{n} \xi_{i,n}$. Suppose there exist sequences $B_n > 0$ and A_n, $n \geq 1$, such that $B_n \to \infty$, $\limsup B_n/Q_n < \infty$, and, $(Z_n - A_n)/B_n$ converges in distribution to the standard normal. Then,*

$$\sup_k \left| B_n P[Z_n = k] - \phi\left(\frac{k - A_n}{B_n}\right) \right| \to 0 \quad as \quad n \to \infty \ , \tag{B.1}$$

where ϕ is the standard normal density.

We now give an alternative form of the local limit theorem, due to McDonald [99].

Theorem B.3. *Let $A_n = \sum_{i=1}^{n} \mathbb{E}[\xi_{i,n}]$, and $B_n^2 = \sum_{i=1}^{n} Var[\xi_{i,n}]$, and assume the following:*

(1) $\limsup_{n\to\infty} \frac{1}{n} \sum_{i=1}^{n} \mathbb{E}[e^{a|\xi_{i,n}|}] < \infty$ *for some positive constant a,*

(2) There exists a constant $c > 0$ such that

$$\liminf_{n\to\infty} \frac{1}{n} B_n^2 \geq c \ ,$$

(3) $\liminf_{n\to\infty} Q_n/n > 0$.

Then,

$$P[Z_n = k] = \frac{1}{B_n\sqrt{2\pi}} Exp\left(\frac{-(k - A_n)^2}{2B_n^2} + \frac{(k - A_n)^3}{n^2}\lambda_n\left(\frac{k - A_n}{n}\right)\right)\left(1 + o\left(\frac{k - A_n}{n}\right)\right) \ , \tag{B.2}$$

uniformly for k in $1 \leq |k - A_n| \leq n/w(n)$, where $\lim_{n\to\infty} w(n) = \infty$, and for each n, $\lambda_n(\tau)$ is a power series converging uniformly with respect to n for sufficiently small τ.

Appendix C

Large deviation methods

In the following we summarize some relevant aspects of large deviation principles. For proofs and more detailed information we refer the reader to [34],[35]. Throughout we assume that $\mathcal{X}$ is a Polish metric space with distance $d : \mathcal{X} \times \mathcal{X} \to [0, \infty)$ and P_n a sequence of probability measures on $(\mathcal{X}, \mathcal{B})$ where $\mathcal{B}$ contains the completed Borel σ-algebra.

Definition C.1 (Semi-continuity)**.** $f : \mathcal{X} \to [-\infty, \infty]$ is *lower semi-continuous* if it satisfies any of the following equivalent properties:

(i) $\liminf_{n\to\infty} f(x_n) \geq f(x)$ for all $x_n \to x \in \mathcal{X}$,

(ii) $\lim_{\epsilon \searrow 0} \inf_{y \in B_\epsilon(x)} f(y) = f(x)$ where $B_\epsilon(x) = \{y \in \mathcal{X} : d(x, y) < \epsilon\}$,

(iii) f has closed level sets, $f^{-1}([-\infty, c]) = \{x \in \mathcal{X} : f(x) \leq c\}$ is closed for all $c \in \mathbb{R}$.

$f : \mathcal{X} \to [-\infty, \infty]$ is *upper semi-continuous* if and only if $-f$ is lower semi-continuous.

Lemma C.1. *A lower (upper) semi-continuous function attains a minimum (maximum) on every non-empty compact set.*

Definition C.2 (Rate function)**.** $I : \mathcal{X} \to [0, \infty]$ is called a *rate function* if

(I1) $I \not\equiv \infty$,

(I2) I is lower semi-continuous,

(I3) I has compact level sets (implies lower semi-continuity).

Definition C.3 (Large deviation principle)**.** A sequence of probability measures (P_n) on $\mathcal{X}$ satisfy the *large deviation principle* with speed a_n and rate function I if

(D1) I is a rate function,

(D2) $\limsup_{n\to\infty} \frac{1}{a_n} \log P_n[C] \leq - \inf_{x \in C} I(x) \quad \forall C \subset X$ closed,

(D3) $\liminf_{n\to\infty} \frac{1}{a_n} \log P_n[O] \geq - \inf_{x \in O} I(x) \quad \forall O \subset X$ open.

A *weak* rate function satisfies (I1) and (I2) but not necessarily (I3). A *weak* large deviation principle holds with speed a_n and *weak* rate function I if,

(D1') I is a weak rate function,

(D2') $\limsup_{n\to\infty} \frac{1}{a_n} \log P_n[K] \leq -\inf_{x\in K} I(x) \quad \forall K \subset X$ compact ,

(D3) $\liminf_{n\to\infty} \frac{1}{a_n} \log P_n[O] \geq -\inf_{x\in O} I(x) \quad \forall O \subset X$ open.

Definition C.4 (Exponential tightness)**.** A family of probability measures P_n is *exponentially tight* if for every $M < \infty$, there exists a compact set K_M such that,

$$\limsup_{n\to\infty} \frac{1}{a_n} \log P_n[K_M^c] \leq -M \ .$$

If P_n satisfies the large deviation upper bound (D2) then the sequence of measures is exponentially tight. If P_n satisfies a weak large deviation principle and P_n is exponentially tight then P_n satisfies a large deviation principle.

Theorem C.2 (Varadhan's Lemma)**.** *Let (P_n) be a sequence of probability measures on $\mathcal{X}$ satisfying the large deviation principle with speed a_n and rate function I. Let $F : \mathcal{X} \to \mathbb{R}$ be a continuous function that is bounded above, then*

$$\lim_{n\to\infty} \frac{1}{a_n} \log \int_{\mathcal{X}} e^{nF(x)} \ P_n[dx] = \sup_{x\in\mathcal{X}} [F(x) - I(x)] \ . \tag{C.1}$$

Theorem C.3 (Contraction Principle)**.** *Let (P_n) be a sequence of probability measures on $\mathcal{X}$ satisfying the large deviation principle with speed a_n and rate function I. Let*

- *$\mathcal{Y}$ be a Polish space,*
- *$F : \mathcal{X} \to Y$ a continuous map,*
- *$Q_n = P_n \circ F^{-1}$ an image probability measure.*

The Q_n satisfies the large deviation principle on $\mathcal{Y}$ with rate n and rate function J given by

$$J(y) = \inf_{x\in\mathcal{X}:F(x)=y} I(x)$$

(By definition $\inf_\emptyset I = \infty$).

Definition C.5. Let $p : \mathbb{R}^d \to [-\infty, \infty]$ be an extended real valued function, then the Legendre-Fenchel transfrom of p is given by,

$$p^*(x) = \sup_{\mu\in\mathbb{R}} \{\langle x, \mu\rangle - p(\mu)\}, \quad \mu \in \mathbb{R}^d \tag{C.2}$$

where $\langle \cdot, \cdot \rangle$ is the usual inner product in $\mathbb{R}^d$.

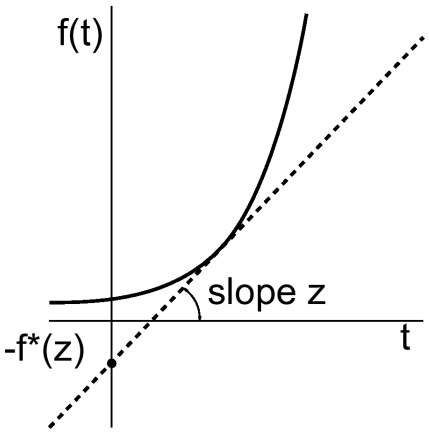

Figure C.1: Geometric interpretation of the Legendre-Fenchel transform.

Definition C.6. A point $x \in \mathbb{R}^d$ is called exposed for $f^* : \mathbb{R}^d \to [-\infty, \infty]$ if there exists a point $t \in \mathbb{R}^d$ such that

$$f^*(y) - f^*(x) > \langle y - x, t \rangle \quad \forall y \neq x \ .$$

Such a t is called an exposing hyperplane for x.

Notice f^* is convex, and at exposed points it is strictly convex. If f is differentiable and convex then,

$$f^*(x) = xt_x - f(t_x)$$

where t_x is found by inverting the derivative of f,

$$\partial_t f(t) = x \ .$$

Gärtner-Ellis Theorem

Given a sequence (Z_n) of random variables with law P_n. We make the following assumptions on the scaled generating function (pressure),

$$\lim_{n\to\infty} \frac{1}{n} \log P_n \left(e^{n\mu Z_n} \right) = p(\mu) \in [-\infty, \infty] \text{ exists}, \tag{C.3}$$

$$0 \in D_p^\circ, \text{ with } D_p = \{\mu \in \mathbb{R} : p(\mu) < \infty\} \ . \tag{C.4}$$

Theorem C.4 (Gätner-Ellis Theorem)**.** *Under the assumptions above (C.3,C.4) p^* is a rate function and,*

- $\limsup_{n\to\infty} \frac{1}{n} \log P_n[C] \leq - \inf_{x\in C} p^*(x) \quad \forall C \subset X$ *closed,*
- $\liminf_{n\to\infty} \frac{1}{n} \log P_n[O] \geq - \inf_{x\in O\cap E} p^*(x) \quad \forall O \subset X$ *open,*

where E is the set of points for which p^* is strictly convex and the exposing hyperplane belongs to D_p°. Suppose further that p satisfies,

(1) p is lower semi-continuous,

(2) p is differentiable on $\mathcal{D}_P^\circ$,

(3) Either $\mathcal{D}_p = \mathbb{R}^d$ or p is steep at its boundary, $\lim_{t\to\partial\mathcal{D}_p} |\partial_t p(t)| = \infty$.

Then $O \cap E$ can be replaced by O and (P_n) satisfies a large deviation principle with rate function p^*.

Concentration of probability

For details and proofs see [93] Chapter 2.

Definition C.7. Let (P_n) be a sequence of probability measures, we say that (P_n) is eventually concentrated on a set A if, for each measurable neighbourhood G of A, we have,

$$\lim_{n\to\infty} P_n[G] = 1 \ .$$

Theorem C.5. *Let (P_n) be a sequence of probability measures that satisfies a large deviation principle with rate function I, then*

a) the set

$$N_I = \{x \in \mathcal{X} : I(x) = 0\}$$

is non-empty and compact.

b) the sequence (P_n) is eventually concentrated on the set N_I, and for any measurable neighbourhood G of N_I, we have

$$\limsup_{n\to\infty} \frac{1}{a_n} \log P[N_I^c] < 0 \ .$$

Theorem C.6. *Let (P_n) be a sequence of probability measures, let $f : \mathcal{X} \to [-\infty, \infty]$, and let (B_n) be a sequence of measurable subsets of $\mathcal{X}$ such that,*

$$\lim_{n\to\infty} P_n[B_n] = 1 \ .$$

Suppose that (P_n) is eventually concentrated on a subset N of $\mathcal{X}$.

a) If f is lower semi-continuous and uniformly bounded below on B_n for n sufficiently large, then

$$\inf_{x\in N} f(x) \le \liminf_{n\to\infty} \int_{B_n} f(x) P_n[\,\mathrm{d}x] \ .$$

a) If f is upper semi-continuous and uniformly bounded above on B_n for n sufficiently large, then

$$\limsup_{n\to\infty} \int_{B_n} f(x) P_n[\,\mathrm{d}x] \le \sup_{x\in N} f(x) \ .$$

LD-regularity

For details and proofs see [93] Chapter 3.

Definition C.8. Let (P_n) be a sequence of probability measures satisfying the large deviation principle with speed a_L and rate function I. A sequence of sets (C_n) is *LD-regular* if,

(1) (C_n) is a decreasing sequence of measurable sets, and $0 < P_n[C_n] < \infty$ for all n sufficiently large;

(2) the closed set
$$C = \bigcap_n \bar{C}_n$$
is non-empty;

(3) the limit,
$$\lim_{n\to\infty} \frac{1}{a_L} \log P_n[C_n] = -\inf_{x\in C} I(x) \ .$$

Appendix D

Computational methods

D.1 Numerics

We state some properties of the canonical measures that we exploit to calculate exact numerics. These are a direct consequence of the product nature of the reference measure.

We consider a fixed lattice Λ_L of size L and local state space $\mathbb{N}$, the full state space is $\mathbb{N}^L$ (for details see Chapter 2). The reference measures are given by the product of L single site marginals,

$$\nu^L[\boldsymbol{\eta}] = \prod_{x=1}^{L} \nu[\eta_x] \ .$$

The canonical measures are defined by conditioning on the total number of particles in the system. Since we are not considering any limits here we can simplify the notation.

$$\begin{aligned} \pi_N^L[\boldsymbol{\eta}] &= \nu^L[\boldsymbol{\eta} \mid \sum_{x=1}^{L} \eta_x = N] \\ &= \frac{\nu^L[\boldsymbol{\eta}]}{Z(L,N)} \delta\left(\sum_{x=1}^{L} \eta_x - N\right) \end{aligned}$$

where δ is the Kronecker delta and $Z(L,N) = \nu^L\left[\sum_{x=1}^{L} \eta_x = N\right]$. Since ν^L is a product measure,

$$\begin{aligned} Z(L,N) &= \sum_{k=0}^{N} \nu^L\left[\sum_{x=1}^{L} \eta_x = N,\ \sum_{x=1}^{L-1} \eta_x = (N-k)\right] \\ &= \sum_{k=0}^{N} \nu[k] Z(L-1, N-k) \ . \end{aligned}$$

This can be used to calculate $Z(L,N)$ recursively, with initial condition $Z(1,k) = \nu[k]$. $Z(L,N)$ can always be divided into any such sub-systems in this manner. For large

system sizes it is therefore efficient to use the following form, for $L = 2^n$ for some $n \in \mathbb{N}$,

$$Z(L, N) = \sum_{k=0}^{N} Z(L/2, k) Z(L/2, N - k) \ .$$

Similar methods can be used to calculate the canonical distribution function for the maximum site occupation. We define,

$$Q(L, N, M) = \nu^L \left[\sum_{x=1}^{L} \eta_x = N, \ \max_{x \in \Lambda_L} \eta_x \leq M \right] \tag{D.1}$$

$$= \sum_{k=0}^{M} \nu[k] Q(L - 1, N - k, M) \ . \tag{D.2}$$

Again for $L = 2^n$ for some $n \in \mathbb{N}$ the most efficient recursion is given by

$$Q(L, N, M) = \sum_{k=0}^{N} Q(L/2, k, M) Q(L/2, N - k, M) \ ,$$

with initial condition $Q(1, k, M) = \nu[k]$ if $k \leq M$ and $Q(1, k, M) = 0$ if $k > M$. Q can be used to calculate the canonical (cumulative) distribution function of the maximum,

$$\pi_N^L \left[\max_{x \in \Lambda_L} \eta_x \leq M \right] = \frac{Q(L, N, M)}{Z(L, N)} \ .$$

The particular form of the single site weights for zero-range process (see Chapter 2 Section 2.2.1 allows us to calculate the average jump rate of a single site in terms of the partition functions above.

$$\nu[n] \propto \prod_{k=1}^{n} \frac{1}{g(k)} \ ,$$

therefore $g(k)\nu[k] = \nu[k - 1]$, so

$$\begin{aligned} \pi_N^L \left(g(\eta_1) \right) &= \frac{1}{Z(L, N)} \sum_{\boldsymbol{\eta}} g(\eta_1) \nu^L[\boldsymbol{\eta}] \delta \left(\sum_{x=1}^{L} \eta_x - N \right) \\ &= \frac{1}{Z(L, N)} \sum_{\boldsymbol{\eta}'} \nu^L[\boldsymbol{\eta}'] \delta \left(\sum_{x=1}^{L} \eta'_x - (N - 1) \right) \\ &= \frac{Z(L, N - 1)}{Z(L, N)} \ , \end{aligned}$$

where, on the second line, we have made the change of variables $\eta'_1 = (\eta_1 - 1)$ and $\eta'_x = \eta_x$ for $x \neq 1$. This also implies that the log of the canonical current is given by the derivative of the canonical entropy density since,

$$- \log \pi_N^L \left(g(\eta_1) \right) = \log Z(L, N) - \log Z(L, N - 1) \ .$$

D.2 Simulation methods

In this section we describe the Monte-Carlo methods of simulation that have been used throughout the thesis for the zero-range and inclusion processes. All pseudo random numbers were generated using the Fast Mersenne Twister [112].

D.2.1 Zero-range process: Random sequential update algorithm

Throughout the thesis simulation results for the zero-range process (2.12) are produced using a random sequential update algorithm described bellow. The state of the Markov process is given by $\boldsymbol{\eta}(t) = (\eta_x(t))_{x\in\Lambda_L}$ as described in Chapter 2.

Algorithm 1 Random sequential update algorithm for the ZRP with N particles on a lattice of L sites. The underlying homogeneous random walk q from (2.12) has range R.

Define: $g_{\max} = \max_{0\le n\le N} g(n)$
Define: $dt = 1/(L\ g_{\max})$
  { Choose a site uniformly }
  $x \leftarrow$ Uniform random integer from $\{1, 2, \ldots, L\}$
  $r \leftarrow$ Uniform random number on $[0, 1)$
  { Particle jumps with probability $g(\eta_x)/g_{\max}$ }
  if $r < g(\eta_x)/g_{\max}$ **then**
    $\eta_x \leftarrow \eta_x - 1$
    { Choose target site according to random walk q }
    $r \leftarrow$ Uniform random number on $[0, 1)$
    $S \leftarrow 0$ and $i \leftarrow -R$
    while $S \le r$ **do**
      $S \leftarrow S + q(i)$
      $i \leftarrow i + 1$
    end while
    $\eta_{x+i-1} \leftarrow \eta_{x+i-1} + 1$
  end if
  $t \leftarrow t + dt$

To save time at the expense of memory the $g(n)/g_{\max}$ are calculate for $n \in \{0, 1, \ldots, N\}$ and stored in memory at the beginning of the simulation. Algorithm 1 corresponds to a single update step, so that $O(L)$ steps are required for the simulation to reach a fixed time $t = T$.

This is an approximate algorithm since the time increment is fixed and not sampled from an exponential distribution. However, since the jump rates are bounded uniformly in L we know $dt \to 0$ as $L \to \infty$, and so, by the convergence of the (scaled) geometric distribution to the exponential distribution, the waiting times converge quickly to exponential waiting times as the system size increases. Therefore, this algorithm gives a good approximation of the true dynamics of the Markov process (2.12), provided $\sup_{L,n,m\in\mathbb{N}} |g_L(n) - g_L(m)|$ is not too large.

D.2.2 Inclusion process: Gillespie type algorithm

Throughout the thesis simulation results for the inclusion process are produced using a Gillespie type update algorithm described bellow (also known as the Bortz-Kalos-Lebowitz algorithm [14]). This is an exact algorithm in that it produces statistically correct trajectories of the Markov process. For the inclusion process (2.25) the jump rates are not bounded uniformly in L, and the difference between the slowest and fastest transitions are very large. So a random sequential update algorithm like the one described above would be very inefficient, due to a lot of rejected moves, and also would not give a good approximation of the Markov process.

Algorithm 2 Gillespie update algorithm for the inclusion process with N particles on a lattice of L sites. The underlying homogeneous random walk q has range R.

Requires: List of the L jump rates off each site in the current state $(c_i)_{i=1}^L$
Requires: The partial sums $C_n = \sum_{i=1}^n c_i$ and $C_0 = 0$
  { Sample time increment from $\mathrm{Exp}(C_L)$ }
  $dt \leftarrow$ Exponentially distributed random number with mean $1/C_L$
  $t \leftarrow t + dt$
  { Choose to move particle of site x with probability c_x/C_L }
  $r \leftarrow$ Uniform random number on $[0, C_L)$
  Perform a binary search for x such that $C_{x-1} \leq r < C_x$
  $\eta_x \leftarrow \eta_x - 1$
  { Choose target site according to random walk q }
  $r \leftarrow$ Uniform random number on $[0, 1)$
  $S \leftarrow 0$ and $i \leftarrow -R$
  while $S \leq r$ **do**
    $S \leftarrow S + q(i)$
    $i \leftarrow i + 1$
  end while
  $\eta_{x+i-1} \leftarrow \eta_{x+i-1} + 1$
  { Update transition rates and partial sums }
  Update rates c_x and c_{x+i-1}
  Update C_n for $n \in \{\min\{c_x, c_{x+i-1}\}, \ldots, L\}$

This update algorithm has computational complexity $O(L)$, since in each time step we must update each of the partial sums C_i for $i \in \{\min\{c_x, c_{x+i-1}\}, \ldots, L\}$. However the complexity can be reduced to $O(\log(L))$, at the expense of more memory usage, by storing a binary tree. In this case it is simplest to restrict to lattices of length $L = 2^n$ for $n \in \mathbb{N}$. Then the binary tree is defined recursively by $C_{i,j} = C_{i-1,2j-1} + C_{i-1,2j}$ for $i \in \{0, 1, \ldots, n\}$ and $j \in \{1, 2, \ldots, 2^{n-i}\}$ with initial conditions $C_{0,j} = c_j$ for $j \in \{1, 2 \ldots, 2^n{=}L\}$. In this case the updates to the rates can be done by retracing the path followed down the binary tree by the binary search, which selects the transition to make, which has a computational complexity of $O(\log L)$.

Bibliography

[1] S. Adams. Lectures on mathematical statistical mechanics. *Communications of the Dublin Institute for Advanced Studies (Series A) No. 30*, 2006.
2 citation(s) on 1 page(s): 4.

[2] E. D. Andjel. Invariant measures for the zero range process. *Ann. Probab.*, 10(3): 525–547, 1982.
5 citation(s) on 3 page(s): 7, 11, and 13.

[3] A. G. Angel, M. R. Evans, and D. Mukamel. Condensation transitions in a one-dimensional zero-range process with a single defect site. *J. Stat. Mech.*, 4:04001, 2004.
2 citation(s) on 2 page(s): 21 and 60.

[4] I. Armendáriz and M. Loulakis. Thermodynamic limit for the invariant measures in supercritical zero range processes. *Probab. Theory Relat. Fields*, 145(1):175–188, 2009.
5 citation(s) on 5 page(s): 22, 23, 52, 63, and 112.

[5] I. Armendáriz, S. Grosskinsky, and M. Loulakis. Zero range condensation at criticality. arXiv:0912.1793v1 [math.PR], 2009.
12 citation(s) on 9 page(s): 22, 24, 60, 83, 85, 87, 90, 92, and 112.

[6] H. Behringer and M. Pleimling. Continuous phase transitions with a convex dip in the microcanonical entropy. *Phys. Rev. E*, 74(1):011108, 2006.
1 citation(s) on 1 page(s): 89.

[7] J. Beltrán and C. Landim. Tunneling and metastability of continuous time markov chains. *J. Stat. Phys.*, 140(6):1065–1114, 2010.
2 citation(s) on 2 page(s): 27 and 90.

[8] J. Beltrán and C. Landim. Metastability of reversible condensed zero range processes on a finite set. *Probab. Theory Relat. Fields*, 2011.
7 citation(s) on 7 page(s): 22, 27, 86, 89, 90, 94, and 120.

[9] I. Benjamini, P.A. Ferrari, and C. Landim. Asymmetric conservative processes with random rates. *Stoch. Proc. Appl.*, 61(2):181 – 204, 1996.
1 citation(s) on 1 page(s): 21.

[10] A. Bianchi and A. Gaudilliere. Metastable states, quasi-stationary and soft measures, mixing time asymprtotics via variational principles. *arXiv:1103.1143v1 [math.PR]*, 2011.
1 citation(s) on 1 page(s): 27.

[11] M. Biskup, L. Chayes, and R. Kotecký. On the formation/dissolution of equilibrium droplets. *Europhys. Lett.*, 60(1):21, 2002.
2 citation(s) on 2 page(s): 29 and 90.

[12] M. Biskup, L. Chayes, and R. Kotecký. Critical region for droplet formation in the two-dimensional ising model. *Commun. Math. Phys.*, 242(1):137–183, 2003.
2 citation(s) on 2 page(s): 29 and 90.

[13] R. A. Blythe and A. J. McKane. Stochastic models of evolution in genetics, ecology and linguistics. *J. Stat. Mech-Theory E*, 2007(07):P07018, 2007.
1 citation(s) on 1 page(s): 147.

[14] A.B. Bortz, M.H. Kalos, and J.L. Lebowitz. A new algorithm for monte carlo simulation of ising spin systems. *J. Comput. Phys.*, 17:10, 1975.
1 citation(s) on 1 page(s): 164.

[15] A. Bovier. Metastability. In *Lectures given at the 5th Prague Summer School on Mathematical Statistical Physics*, 2006.
1 citation(s) on 1 page(s): 116.

[16] A. Bovier. Metastability: a potential theoretic approach. In *in Proceedings of the ICM 2006, Madrid, pp. 499-518*, 2006.
1 citation(s) on 1 page(s): 120.

[17] A. Bovier. Metastability, in methods of contemporary statistical mechanics. Lecture Notes in Mathematics 1970, 2009.
2 citation(s) on 2 page(s): 2 and 24.

[18] A. Bovier, M. Eckhoff, V. Gayrard, and M. Klein. Metastability and low lying spectra in reversible markov chains. *Commun. Math. Phys.*, 228:219–255, 2000.
1 citation(s) on 1 page(s): 27.

[19] A. Bovier, M. Eckhoff, V. Gayrard, and M. Klein. Metastability in stochastic dynamics of disordered mean-field models. *Prob. Th. Rel. Fields*, 119:99161, 2001.
1 citation(s) on 1 page(s): 27.

[20] A. Bovier, C F. den Hollander, and Spitoni. Homogeneous nucleation for glauber and kawasaki dynamics in large volumes at low temperatures. *Ann. Probab.*, 38(2): 661713, 2010.
1 citation(s) on 1 page(s): 27.

[21] W. Bryc. A remark on the connection between the large deviation principle and the central limit theorem. *Stat. Prob. Lett.*, 18 (4):253–256, 1993.
1 citation(s) on 1 page(s): 112.

[22] M. Samsonov C. Furtlehner, J.M. Lasgouttes. One-dimensional particle processes with acceleration/braking asymmetry. *arXiv:1109.1761v1 [cond-mat.stat-mech]*, 2011.
1 citation(s) on 1 page(s): 15.

[23] M. Cassandro, A. Galves, E. Olivieri, and M. E. Vares. Metastable behavior of stochastic dynamics: A pathwise approach. *J. Stat. Phys.*, 35:603–634, 1984.
1 citation(s) on 1 page(s): 27.

[24] P. Chleboun and S. Grosskinsky. Large deviations and metastability for condensation in stochastic particle systems. In preperation.
1 citation(s) on 1 page(s): 93.

[25] P. Chleboun and S. Grosskinsky. Finite size effects and metastability in zero-range condensation. *J. Stat. Phys.*, 140:846–872, 2010.
4 citation(s) on 4 page(s): v, 28, 67, and 94.

[26] C. Cocozza-Thivent. Processus des misanthropes. *Z. Wahrscheinlichkeit*, 70:509, 1985.
1 citation(s) on 1 page(s): 20.

[27] F. Coppex, M. Droz, and A. Lipowski. Dynamics of the breakdown of granular clusters. *Europhys. Lett. Phys. Rev. E*, 66:011305, 2001.
1 citation(s) on 1 page(s): 93.

[28] M. Costeniuc, R. S. Ellis, H. Touchette, and B. Turkington. The generalized canonical ensemble and its universal equivalence with the microcanonical ensemble. *J. Stat. Phys.*, 119(5):1283–1329, 2005.
2 citation(s) on 2 page(s): 29 and 48.

[29] M. Costeniuc, R. S. Ellis, and H. Touchette. Nonconcave entropies from generalized canonical ensembles. *Phys. Rev. E*, 74(1):010105, 2006.
2 citation(s) on 2 page(s): 29 and 48.

[30] M. Costeniuc, RS Ellis, H. Touchette, and B. Turkington. Generalized canonical ensembles and ensemble equivalence. *Phys. Rev. E*, 73:026105, 2006.
2 citation(s) on 2 page(s): 29 and 48.

[31] I. Csiszár. I-divergence geometry of probability distributions and minimization problems. *Ann. Probab.*, 3(1):146–158, 1975.
2 citation(s) on 2 page(s): 38 and 152.

[32] I. Csiszár and J. Körner. *Information Theory: Coding Theorems for Discrete Memoryless Systems.* Probability and Mathematical Statistics. Academic Press, New York, 1982.
1 citation(s) on 1 page(s): 152.

[33] B. Davis and D. McDonald. An elementary proof of the local central limit theorem. *J. Theor. Probab.*, 8(3):693–701, 1995.
4 citation(s) on 4 page(s): 42, 46, 47, and 154.

[34] A. Dembo and O. Zeitouni. *Large Deviations Techniques and Applications.* Springer, Application of Mathematics, vol. 38, 1998.
8 citation(s) on 8 page(s): 4, 40, 44, 46, 55, 75, 126, and 156.

[35] F. den Hollander. *Large Deviations.* American Mathematical Society, 2000.
6 citation(s) on 6 page(s): 40, 46, 55, 106, 126, and 156.

[36] F. den Hollander. Metastability under stochastic dynamics. *Stoch. Proc. Appl.*, 114:1–26, 2004.
1 citation(s) on 1 page(s): 24.

[37] D. Dhar and J. L. Lebowitz. Restricted equilibrium ensembles: Exact equation of state of a model glass. *Europhys. Lett.*, 92(2):20008, 2010.
2 citation(s) on 2 page(s): 28 and 33.

[38] R.L. Dobrushin, R. Kotecký, and S. Shlosman. *Wulff construction. A global shape from local interaction.* Providence, RI: Am. Math. Soc., 1992.
1 citation(s) on 1 page(s): 29.

[39] R. Durrett. *Probability: theory and examples.* Duxbury Press., 1995.
2 citation(s) on 2 page(s): 47 and 154.

[40] R.S. Ellis. *Entropy, Large Deviations, and Statistical Mechanics.* Springer, Classics in Mathemtaics, 1985.
1 citation(s) on 1 page(s): 4.

[41] R.S. Ellis, K. Haven, and B. Turkington. Large deviation principles and complete equivalence and nonequivalence results for pure and mixed ensembles. *J. Stat. Phys.*, 101:999–1064, 2000.
1 citation(s) on 1 page(s): 42.

[42] M. R. Evans. Phase transitions in one-dimensional nonequilibrium systems. *Braz. J. Phys.*, 30(1):42–57, 2000.
6 citation(s) on 6 page(s): 3, 13, 22, 59, 89, and 94.

[43] M. R. Evans and T. Hanney. Nonequilibrium statistical mechanics of the zero-range process and related models. *J. Phys. A: Math. Gen.*, 38(19):R195–R240, 2005.
2 citation(s) on 2 page(s): 3 and 11.

[44] M. R. Evans, S. N. Majumdar, and R. K. P. Zia. Canonical analysis of condensation in factorised steady states. *J. Stat. Phys.*, 123(2):357–390, 2006.
2 citation(s) on 2 page(s): 60 and 92.

[45] M.R. Evans. Bose-einstein condensation in disordered exclusion models and relation to traffic flow. *Europhys. Lett.*, 36(1):13, 1996.
1 citation(s) on 1 page(s): 21.

[46] M.R. Evans and T. Hanney. Phase transition in two species zero-range process. *J. Phys. A*, 36 (28):L441–L447, 2003.
2 citation(s) on 2 page(s): 19 and 20.

[47] M.R. Evans and S.N. Majumdar. Condensation and extreme value statistics. *J. Stat. Mech.: Theory Exp.*, 2008(05):P05004, 2008.
6 citation(s) on 4 page(s): 24, 57, 92, and 112.

[48] M.R. Evans, S.N. Majumdar, and R.K.P. Zia. Factorized steady states in mass transport models. *J. Phys. A-Math. Gen.*, 37(25):L275, 2004.
1 citation(s) on 1 page(s): 20.

[49] M.R. Evans, S.N. Majumdar, and R.K.P. Zia. Factorized steady states in mass transport models on an arbitrary graph. *J. Phys. A-Math. Gen.*, 39(18):4859, 2006.
3 citation(s) on 2 page(s): 21 and 58.

[50] P.A. Ferrari. The simple exclusion process as seen from a tagged particle. *Ann. Probab.*, 14(4):pp. 1277–1290, 1986.
1 citation(s) on 1 page(s): 15.

[51] P.A. Ferrari, H. Kesten, S. Martinez, and P. Picco. Existence of quasi-stationary distributions. a renewal dynamical approach. *Ann. Probab.*, 23(2):pp. 501–521, 1995.
1 citation(s) on 1 page(s): 27.

[52] P.A. Ferrari, C. Landim, and V.V. Sisko. Condensation for a fixed number of independent random variables. *J. Stat. Phys.*, 128(5):1153–1158, 2007.
3 citation(s) on 3 page(s): 22, 23, and 52.

[53] C. Furtlehner and J.M. Lasgouttes. A queueing theory approach for a multi-speed exclusion process. *Proceedings of Traffic and Granular Flow*, pages 129–138, 2007.
1 citation(s) on 1 page(s): 15.

[54] H.O. Georgii. *Canonical Gibbs Measures: Some Extensions of de Finetti's Representation Theorem for Interacting Particle Systems.* Springer: Lecture Notes in Mathematics, Vol. 760, 1979.
1 citation(s) on 1 page(s): 4.

[55] H.O. Georgii. *Gibbs Measures and Phase Transitions, volume 9 of Studies in Mathematics*. Walter de Gruyter, Berlin, 1988.
2 citation(s) on 2 page(s): 2 and 4.

[56] C. Giardinà, J. Kurchan, and F. Redig. Duality and exact correlations for a model of heat conduction. *J. Math. Phys.*, 48(3):033301, 2007.
2 citation(s) on 2 page(s): 17 and 58.

[57] C. Giardinà, J. Kurchan, F. Redig, and K. Vafayi. Duality and hidden symmetries in interacting particle systems. *J. Stat. Phys.*, 135:25–55, 2009.
5 citation(s) on 5 page(s): 4, 17, 21, 58, and 148.

[58] C. Giardinà, F. Redig, and K. Vafayi. Correlation inequalities for interacting particle systems with duality. *J. Stat. Phys.*, 141:242–263, 2010.
5 citation(s) on 3 page(s): 17, 122, and 148.

[59] C. Godrèche. Dynamics of condensation in zero-range processes. *J. Phys. A: Math. Gen.*, 36(23):6313–6328, 2003.
6 citation(s) on 6 page(s): 22, 24, 85, 89, 144, and 146.

[60] C. Godrèche. Nonequilibrium phase transition in a non-integrable zero-range process. *J. Phys. A.-Math. Gen.*, 39(29):9055, 2006.
1 citation(s) on 1 page(s): 94.

[61] C. Godrèche and J M Luck. Dynamics of the condensate in zero-range processes. *J. Phys. A: Math. Gen.*, 38(33):7215–7237, 2005.
8 citation(s) on 4 page(s): 22, 85, 89, and 91.

[62] C. Godrèche and J.M. Luck. Nonequilibrium dynamics of urn models. *J. Phys. Cond. Matter*, 14:1601, 2002.
1 citation(s) on 1 page(s): 20.

[63] R.L. Greenblatt and J.L. Lebowitz. Product measure steady states of generalized zero range processes. *J. Phys. A.-Math. Gen.*, 39(7):1565, 2006.
3 citation(s) on 2 page(s): 21 and 58.

[64] G. Grimmett and D. Stirzaker. *Probability and Random Processes*. Oxford University Press, 2001.
1 citation(s) on 1 page(s): 11.

[65] S. Grosskinsky. Equivalence of ensembles for two-species zero-range invariant measures. *Stoch. Proc. Appl.*, 118(8):1322 –1350, 2008.
3 citation(s) on 3 page(s): 19, 58, and 75.

[66] S. Grosskinsky and G.M. Schütz. Discontinuous condensation transition and nonequivalence of ensembles in a zero-range process. *J. Stat. Phys.*, 132(1):77–108, 2008.
11 citation(s) on 10 page(s): v, 28, 85, 89, 93, 94, 95, 103, 107, and 112.

[67] S. Grosskinsky and H. Spohn. Stationary measures and hydrodynamics of zero range processes with several species of particles. *Bull. Braz. Math. Soc.*, 34 (3): 1–19, 2003.
1 citation(s) on 1 page(s): 20.

[68] S. Grosskinsky, P. Chleboun, and G. M. Schütz. Instability of condensation in the zero-range process with random interaction. *Phys. Rev. E*, 78:030101, 1970.
1 citation(s) on 1 page(s): 59.

[69] S. Grosskinsky, G.M. Schütz, and H. Spohn. Condensation in the zero range process: Stationary and dynamical properties. *J. Stat. Phys.*, 113(3):389–410, 2003.
10 citation(s) on 7 page(s): 4, 22, 23, 29, 70, 85, and 149.

[70] S. Grosskinsky, F. Redig, and K. Vafayi. Condensation in the inclusion process and related models. *J. Stat. Phys.*, 142(5):952–974, 2010.
10 citation(s) on 7 page(s): 4, 17, 21, 28, 122, 125, and 148.

[71] S. Gupta, M. Barma, and S.N. Majumdar. Finite-size effects on the dynamics of the zero-range process. *Phys. Rev. E*, 76:4, 2007.
1 citation(s) on 1 page(s): 85.

[72] T. Hanney and M.R. Evans. Condensation transitions in a two-species zero-range process. *Phys. Rev. E*, 69, 016107, 2004.
1 citation(s) on 1 page(s): 19.

[73] J.-B. Hiriart-Urruty and C. Lemaréchal. *Fundamentals of Convex Analysis*. Springer Grundlehren Text Editions, 2001.
1 citation(s) on 1 page(s): 46.

[74] O. Hirschberg, D. Mukamel, and G.M. Schütz. Condensation in temporally correlated zero-range dynamics. *Phys. Rev. Lett.*, 103(9):090602, 2009.
1 citation(s) on 1 page(s): 12.

[75] R. Holley. A class of interactions in an infinite particle system. *Adv. Math.*, 5(2): 291 – 309, 1970.
1 citation(s) on 1 page(s): 13.

[76] K. Huang. *Statistical Mechanics*. John Wiley & Sons, New York, 2nd edition, 1987.
1 citation(s) on 1 page(s): 2.

[77] T. Huillet. On wright-fisher diffusion and its relatives. *J. Stat. Mech.-Theory E*, 2007(11):P11006, 2007.
2 citation(s) on 1 page(s): 147.

[78] A. Hüller. Finite size scaling at first order phase transition? *Z. Phys. B Condens. Matter*, 95:63–66, 1994.
1 citation(s) on 1 page(s): 89.

[79] I. Jeon. Phase transition for perfect condensation and instability under the perturbations on jump rates of the zero-range process. *J. Phys. A-Math. Theor.*, 43 (23):235002, 2010.
2 citation(s) on 2 page(s): 121 and 140.

[80] I. Jeon, P. March, and B. Pittel. Size of the largest cluster under zero-range invariant measures. *Ann. Probab.*, 28(3):1162–1194, 2000.
3 citation(s) on 3 page(s): 22, 23, and 24.

[81] Y. Kafri, E. Levine, D. Mukamel, G. M. Schütz, and J. Török. Criterion for phase separation in one-dimensional driven systems. *Phys. Rev. Lett.*, 89(3):035702, 2002.
3 citation(s) on 3 page(s): 12, 16, and 90.

[82] N.G. Van Kampen. *Stochastic processes in physics and chemistry*. Elsevier, 2007.
1 citation(s) on 1 page(s): 26.

[83] J. Kaupuzs, R. Mahnke, and R. J. Harris. Zero-range model of traffic flow. *Phys. Rev. E*, 72(5, Part 2):056125, 2005.
5 citation(s) on 5 page(s): 15, 16, 59, 73, and 90.

[84] S.-W. Kim, J. Lee, and J. D. Noh. Particle condensation in pair exclusion process. *Phys. Rev. E*, 81(5):051120, 2010.
1 citation(s) on 1 page(s): 12.

[85] C. Kipnis. Central limit theorems for infinite series of queues and applications to simple exclusion. *Ann. Probab.*, 14(2):pp. 397–408, 1986.
2 citation(s) on 2 page(s): 3 and 15.

[86] C. Kipnis and C. Landim. *Scaling limits of interacting particle systems*. Springer Verlag, 1999.
2 citation(s) on 2 page(s): 5 and 152.

[87] J. Krug and P.A. Ferrari. Phase transitions in driven diffusive systems with random rates. *J. Phys. A: Math. Gen.*, 29(18):L465–L471, 1996.
1 citation(s) on 1 page(s): 21.

[88] O. E. Lanford. *Entropy and equilibrium states in classical statistical mechanics*. (Lecture Notes in Physics vol 20) Berlin: Springer, 1973.
1 citation(s) on 1 page(s): 94.

[89] E. Levine, G. Ziv, L. Gray, and D. Mukamel. Traffic jams and ordering far from thermal equilibrium. *Physica A*, 340:636–646, 2004.
2 citation(s) on 2 page(s): 59 and 90.

[90] J. Lewis, C.-E. Pfister, and W. Sullivan. The equivalence of ensembles for lattice systems: Some examples and a counterexample. *J. Stat. Phys.*, 77:1/2(1):397–419, 1994.
3 citation(s) on 3 page(s): 28, 34, and 132.

[91] J.T. Lewis and C.-E. Pfister. Thermodynamic probability theory: some aspects of large deviations. *Russ. Math. Surv.*, 50(2):279, 1995.
5 citation(s) on 5 page(s): 28, 34, 39, 40, and 149.

[92] J.T. Lewis, C.-E. Pfister, and W.G. Sullivan. Large deviations and the thermodynamic formalism: a new proof of the equivalence of ensembles. Lecture notes, lectures by J. T. Lewis, 1994.
3 citation(s) on 3 page(s): 28, 34, and 40.

[93] J.T. Lewis, C.-E. Pfister, and W.G. Sullivan. Entropy, concentration of probability and conditional limit theorems. *Markov Proc. Rel. Fields*, 1(3):319–386, 1995.
9 citation(s) on 7 page(s): 4, 28, 34, 39, 46, 132, and 159.

[94] T. M. Liggett. *Stochastic Interacting systems: Contact, voter and exclusion processes*. Springer, 1999.
1 citation(s) on 1 page(s): 3.

[95] T.M. Liggett. *Interacting Particle Systems*. Springer. Classics in Mathematics, 1985.
8 citation(s) on 8 page(s): 3, 5, 6, 7, 8, 10, 17, and 21.

[96] T.M. Liggett and F. Spitzer. Ergodic theorems for coupled random walks and other systems with locally interacting components. *Probab. Theory Relat. Fields*, 56(4):443–468, 1981.
1 citation(s) on 1 page(s): 13.

[97] A. Lipowski and M. Droz. Urn model of separation of sand. *Phys. Rev. E*, 65(3): 031307, 2002.
1 citation(s) on 1 page(s): 93.

[98] S.N. Majumdar, M.R. Evans, and R.K.P. Zia. Nature of the condensate in mass transport models. *Phys. Rev. Lett.*, 94(18):180601, 2005.
2 citation(s) on 2 page(s): 60 and 92.

[99] D. McDonald. A local limit theorem for large deviations of sums of independent, nonidentically distributed random variables. *Ann. Probab.*, 7(3):pp. 526–531, 1979.
4 citation(s) on 4 page(s): 42, 133, 154, and 155.

[100] A.D. Wentzell M.I. Freidlin. Random perturbations of dynamical systems. *Springer, Berlin,*, 1984.
1 citation(s) on 1 page(s): 26.

[101] P.A.P. Moran. *The statistical processes of evolutionary theory.* Clarendon Press, Oxford, UK, 1962.
1 citation(s) on 1 page(s): 147.

[102] K.P.N. Murthy and K.W. Kehr. Mean first-passage time of random walks on a random lattice. *Phys. Rev. A*, 40(4):2082–2087, 1989.
1 citation(s) on 1 page(s): 88.

[103] A.V. Nagaev. Local limit theorems with regard to large deviations when cramér's condition is not satisfied. *Litovsk. Mat. Sb.*, 8:553–579, 1968.
3 citation(s) on 3 page(s): 92, 112, and 154.

[104] A.V. Nagaev. Limit theorems that take into account large deviations when cramér's condition is violated (in russian). *Izv. Akad. Nauk UzSSR Ser. Fiz.-Mat. Nauk*, 13(6):17–22, 1969.
2 citation(s) on 2 page(s): 112 and 154.

[105] S.V. Nagaev. Large deviations of sums of independent random variables. *Ann. Probab.*, 7:5:745–789., 1979.
2 citation(s) on 2 page(s): 112 and 154.

[106] J. R. Norris. *Markov Chains.* Cambridge University Press, 1998.
6 citation(s) on 5 page(s): 5, 7, 8, 10, and 34.

[107] E. Olivieri and M. E. Vares. *Large deviations and metastability.* Cambridge University Press, 2004.
8 citation(s) on 7 page(s): 2, 3, 24, 25, 28, 91, and 94.

[108] O. Penrose. Metastable decay rates, asymptotic expansions, and analytic continuation of thermodynamic functions. *J. Stat. Phys.*, 78:267–283, 1995.
3 citation(s) on 3 page(s): 27, 28, and 33.

[109] O. Penrose and J. Lebowitz. Rigorous treatment of metastable states in the van der waals-maxwell theory. *J. Stat. Phys.*, 3:211–236, 1971.
4 citation(s) on 4 page(s): 25, 27, 28, and 33.

[110] W. Rubin. *Real and complex analysis.* McGraw-Hill, 1987.
1 citation(s) on 1 page(s): 7.

[111] D. Ruelle. *Statistical Mechanics: Rigorous Results.* Amsterdam: Benjamin, 1969.
2 citation(s) on 2 page(s): 2 and 94.

[112] M. Saito and M. Matsumoto. Simd-oriented fast mersenne twister: a 128-bit pseudorandom number generator. *MCQMC*, 2:607, 2008.
1 citation(s) on 1 page(s): 163.

[113] G.M. Schütz. Critical phenomena and universal dynamics in one-dimensional driven diffusive systems with two species of particles. *J. Phys. A.-Math. Gen.*, 36 (36):R339, 2003.
2 citation(s) on 2 page(s): 3 and 19.

[114] Y. Schwarzkopf, M.R. Evans, and D. Mukamel. Zero-range processes with multiple condensates: statics and dynamics. *J. Phys. A: Math. Theor.*, 41(20):205001 (21pp), 2008.
2 citation(s) on 2 page(s): 12 and 57.

[115] F. Spitzer. Interaction of markov processes. *Adv. Math*, 5(246-290):2, 1970.
5 citation(s) on 4 page(s): 3, 11, 13, and 15.

[116] A.G. Thompson, J. Tailleur, M.E. Cates, and R.A. Blythe. Zero-range processes with saturated condensation: the steady state and dynamics. *J. Stat. Mech.: Theory Exp.*, 2010(02):P02013, 2010.
1 citation(s) on 1 page(s): 12.

[117] J. Török. Analytic study of clustering in shaken granular material using zero-range processes. *Physica A*, 355(2-4):374 – 382, 2005.
3 citation(s) on 3 page(s): 3, 90, and 93.

[118] H. Touchette. The large deviation approach to statistical mechanics. *Physics Reports*, 478(1-3):1 – 69, 2009.
1 citation(s) on 1 page(s): 4.

[119] H. Touchette. Methods for calculating nonconcave entropies. *J. Stat. Mech.-Theory E*, 2010(05):P05008, 2010.
4 citation(s) on 4 page(s): 27, 29, 48, and 94.

[120] H. Touchette. Ensemble equivalence for general many-body systems. *arXiv:1106.2979v2 [cond-mat.stat-mech]*, 2011.
1 citation(s) on 1 page(s): 42.

[121] A Traulsen, J. C. Claussen, and C. Hauert. Coevolutionary dynamics in large, but finite populations. *Phys. Rev. E*, 74:011901, 2006.
1 citation(s) on 1 page(s): 147.

[122] D. van der Meer, K. van der Weele, and D. Lohse. Sudden collapse of a granular cluster. *Phys. Rev. Lett.*, 88(17):174302, 2002.
3 citation(s) on 2 page(s): 90 and 93.

[123] D. van der Meer, K. van der Weele, P. Reimann, and D. Lohse. Compartmentalized granular gases: flux model results. *J. Stat. Mech.*, 07:P07021, 2007.
3 citation(s) on 3 page(s): 3, 90, and 93.

[124] K. van der Weele, D. van der Meer, M. Versluis, and D. Lohse. Hysteretic clustering in granular gas. *Europhys. Lett.*, 53(3):328–334, 2001.
4 citation(s) on 3 page(s): 59, 90, and 93.

[125] B. Waclaw and M.R. Evans. Explosive condensation in a mass transport model. *arXiv:1110.4330v1 [cond-mat.stat-mech]*, 2011.
1 citation(s) on 1 page(s): 144.

[126] B. Waclaw, J. Sopik, W. Janke, and H. Meyer-Ortmanns. Mass condensation in one dimension with pair-factorized steady states. *J. Stat. Mech.-Theory E*, 2009 (10):P10021, 2009.
2 citation(s) on 2 page(s): 58 and 151.

[127] B. Waclaw, J. Sopik, W. Janke, and H. Meyer-Ortmanns. Pair-factorized steady states on arbitrary graphs. *J. Phys. A-Math. Theor.*, 42(31):315003, 2009.
1 citation(s) on 1 page(s): 58.

[128] B. Waclaw, J. Sopik, W. Janke, and H. Meyer-Ortmanns. Tuning the shape of the condensate in spontaneous symmetry breaking. *Phys. Rev. Lett.*, 103:080602, 2009.
1 citation(s) on 1 page(s): 58.

[129] A. Wehrl. General properties of entropy. *Rev. Mod. Phys.*, 50:221–260, 1978.
1 citation(s) on 1 page(s): 152.

[130] R.E. Wilson. Mechanisms for spatio-temporal pattern formation in highway traffic models. *Phil. Trans. R. Soc. A.*, 366(1872):2017–2032, 2008.
2 citation(s) on 2 page(s): 90 and 91.

[131] S.L. Zabell. Mosco convergence in locally convex spaces. *J. Func. Anal.*, 110(1): 226 – 246, 1992.
1 citation(s) on 1 page(s): 44.

[132] R.K.P Zia, M.R. Evans, and S.N. Majumdar. Construction of the factorized steady state distribution in models of mass transport. *J. Stat. Mech-Theory E*, 2004(10): L10001, 2004.
3 citation(s) on 2 page(s): 21 and 58.

[133] F. Zielen and A. Schadschneider. Broken ergodicity in a stochastic model with condensation. *Phys. Rev. Lett.*, 89(9):090601, 2002.
1 citation(s) on 1 page(s): 58.

[134] F. Zielen and A. Schadschneider. Exact mean-field solutions of the asymmetric random average process. *J. Stat. Phys.*, 106(1):173–185, 2002.
1 citation(s) on 1 page(s): 58.